THE ANTIVIRAL EFFECTS OF ESTRADIOL ON HSV-2 INFECTION

TRANSCRIPTOMIC AND FUNCTIONAL ANALYSIS OF THE ANTIVIRAL EFFECTS OF ESTRADIOL ON HSV-2 INFECTION IN HUMAN VAGINAL EPITHELIAL CELLS

By TUSHAR DHAWAN, B.Sc.

A Thesis Submitted to the School of Graduate Studies in Partial Fulfillment of the Requirements

for the Degree of Master of Science

DESCRIPTIVE NOTE

MASTER OF SCIENCE (2021)

McMaster University, Hamilton, Ontario

Faculty of Health Science, Department of Medicine, Medical Sciences (Infection and Immunity)

TTITLE: Transcriptomic and Functional Analysis of the Antiviral Effects of Estradiol on HSV-2 Infection in Human Vaginal Epithelial Cells

AUTHOR: Tushar Dhawan, B.Sc. (McMaster University)

SUPERVISOR: Dr. Charu Kaushic

NUMBER OF PAGES: [xxi, 183]

ABSTRACT

Background:

Herpes simplex virus type 2 (HSV-2), the primary cause of genital herpes, is one of the most widespread, lifelong sexually transmitted infections (STIs). Incidence is disproportionately higher in women compared to men, so a better understanding of vaginal transmission, the primary mode for HSV-2 infection in women, is crucial for developing preventative strategies. Female sex hormone, estrogen (E2), has been shown to play a protective role against sexually transmitted viral infections and previous studies have shown that vaginal epithelial cells treated with E2 are protected against HSV-2 infection; however, the underlying mechanism of E2 protection remains unclear, so a transcriptome analysis followed by functional studies was performed.

Method of Study:

In this study, VK2/E6E7 (vaginal epithelial) cells were used to study HSV-2 entry, infection and replication. VK2s were grown in Air-Liquid-Interface (ALI) cultures, allowing for their proliferation and stratified layer formation in transwells; closely mimicking physiological conditions. Media was supplemented with no hormone (NH) or physiological concentrations of E2, P4 and MPA for 7 days. After 24 hours of HSV-2 infection in these cultures, VK2 cells were lysed and processed for RNA isolation. We performed a comprehensive genome-wide microarray to profile gene expression of VK2 cells pre-treated with and without E2, prior to, and following HSV-2 infection. For data analysis, “R” software was used to perform all pre-processing steps and normalization. Gene Set Enrichment Analysis (GSEA) was performed to identify potential cellular pathways regulated by E2 after infection using the Hallmark database, relative to NH conditions. Immunofluorescence staining was used for functional analysis to confirm transcriptomic data.

After selecting a pathway for investigation, small-molecule inhibitors and activators of this pathway were used in combination with NH or E2. Vero plaque assay and HSV-2-GFP infection were used to identify examine the protective effects of E2 and the selected pathway. In addition, we also used siRNA to specifically knockdown proteins part of the pathway and investigate the specific effects on protection against HSV-2.

Results:

Microarray analysis indicated that exposure to HSV-2 in the presence of E2 resulted in differential transcriptional profile compared to NH and P4. GSEA assigned one of the highest enrichment scores to the p53 pathway compared to other pathways under the influence of E2 compared to NH, following HSV-2 infection. Studies to correlate bioinformatic results with functional analysis showed significant increase in p53 protein expression after E2 treatment compared to NH. Vero plaque assay demonstrated 10-fold decrease in viral replication following E2 treatment as well as by direct activation of p53 in absence of E2. In contrast, p53 inhibition even in the presence of E2 resulted in 100-fold increased viral replication compared to E2 alone, suggesting that the p53 is involved in E2-mediated protection. We deduced that E2 particularly affects HSV-2 replication and not entry into VK2 cells. We also found that BST2 is strongly regulated by E2-mediated p53 and also contributes to protection against HSV-2. Lastly, we demonstrated that E2 demonstrates anti-inflammatory effects that correlate with its increase in barrier integrity seen with VK2s.

Conclusions:

With bioinformatic and functional analysis, we found that E2 provides protection through the p53 pathway, as well as through downstream BST2. Our data provides the first comprehensive

overview of host cellular responses to HSV-2 and female sex hormones at a transcriptional level and highlights the protective role of E2-mediated p53 pathway. This study is the first to deduce the antiviral mechanism of E2 against HSV-2 infection in human vaginal epithelial cells.

ACKNOWLEDGEMENTS

The journey towards this dissertation has been unforgettable, one that I'll cherish and remember for a lifetime. The credits of this accomplishment largely go to the special people who challenged and supported both me and my work along the way. Over the past three years at the McMaster Immunology Research Centre, I have been fortunate to have met such diversified students and scientists who have made my experience as enriching as possible.

First and foremost, I would like to thank Dr. Charu Kaushic, my supervisor, for providing me the opportunity to be part of the lab both for my undergraduate work and masters. She is someone who consistently challenged me while providing me with endless opportunities to grow. The leadership and skills you bring to work, are something one looks up to. Your astounding energy, knowledge and critical insight not only progressed my project to the level it is, but elicited a passion for scientific research that I hope to employ directly in the field of medicine some day. Lastly, your contributions and efforts in raising awareness of gender equality within and outside the field of science is admirable, and something I wish to contribute to in the future.

I would also like to thank Dr. Carl Richards and Dr. Chris Verschoor, my committee members, for their time, consistent and valuable advice, and guidance throughout this project. I would like to especially thank Dr. Chris Verschoor for taking time our from his schedule to guide me through the process of bioinformatics, a technique that was very intimidating and new to me. This project could not have even begun, if it weren't for Dr. Verschoor's support.

Dr. Aisha Nazli has been one of the closest people with whom I've spend the most time with at the lab. Aside from all the laughs, stories and food we have shared throughout my time here, Dr. Nazli never hesitated to share her strong scientific knowledge with me. Furthermore, Dr. Nazli has always been a helping hand, where she guided me through various protocols, sparked

various experimental ideas in my head and always went above and beyond to ensure the quality of work is at its best. Spending time with Dr. Nazli has been an unforgettable experience and I wish to cherish these moments forever, since researchers as brilliant and kind as her are hard to find.

Thank you to Dr. Denis Snider for assisting and guiding me throughout the process of writing manuscripts. With this process being new to me, Dr. Snider had been very supportive and a wonderful mentor whose scientific insight improved my approach in planning experiments.

To all past students of the Kaushic lab that I have been fortunate to work with, the times we have spend within or outside the lab have made the past two years pass by with ease. Ryan Chow, Ramtin Ghasemi, Haley Dupont, Dr. Puja Bhagri and Dr. Allison Felker, it has been a pleasure to work alongside you all. Ryan, you were the first person I met at the lab. I was fortunate to learn many experimental techniques through high efficiency whilst sharing many laughs together. Ramtin, I hear about this lab when back when you were my TA. Your guidance and mentorship within and outside the lab has been tremendously valuable. Puja, thank you for all the times you spent helping me become a better writer along with all the advice you consistently provided.

To all current members of the Kaushic lab, including Dr. Aisha Nazli, Dr. Christina Hayes, Sidney Pa, Nuzhat Rahman, Amanda Bakke and Ingrid Schwecht, the laughs and memories we made will be cherished forever. Sidney, we started our masters together in this lab and it has been a pleasure to work alongside with you, particularly with the plaque assays, which by now, we are professionals at. Nuzhat and Amanda, the one thing that I can't get enough of is all the times we have spend eating. Despite being the most recent lab students, it always felt like I've known you longer. Thank you for the motivation and support you've all provided.

To all my close friends who have been nothing but supportive. Raj, for always motivating me, being by my side through tough times, and going on taco trips with me. Harpreet, for believing in me more than I believe in myself. Adaviyyah, for being the crazy person that you are, I couldn't have pushed through this time without your presence. You made the toughest moments into the easiest, and the darkest days the brightest, and the "fijjiest" times the "chijjiest".

Last, but not least, my family, the most important people in my life. My mother and father, without whom I would not be where I am today. You came to this country with nothing but empty pockets yet managed to stand up and provide me with all the facilities that I am fortunate to have. Everything I do is with the motivation that I'll be able to repay you 10-fold back of what you've given me. No number of favors will ever be enough for the unsoliticaed support, selfless care and limitless motivation that you provide me on a daily basis. I believe I should thank my sister as well, who is one of the most supportive people in my life, and although very annoying, has always motivated me to push through.

And so, I would like to leave you with a final thought. Although the past two years of this masters have not been easy, especially with the COVID-19 pandemic that changed everything, I feel nothing but gratefulness with all I've accomplished. There will always be hardships and obstacles in life. You can cry over them, or face them with a smile, but you will have to deal with them one way or another, so, you might as well do it with a smile. "You can complain because roses have thorns, or rejoice because thorns have roses" – Alphonse Karr

DECLARATION OF ACADEMIC ACHIEVEMENT

All the experiments were conceived and designed by Tushar Dhawan, Dr. Aisha Nazli and Dr. Charu Kaushic. Tushar Dhawan performed all functional experiments. Dr. Aisha Nazli performed all confocal microscopy with the Nikon confocal microscope located at the Centre for Microbial Chemical Biology (CMCB). Dr. Chris Verschoor (Health Sciences North Research Institute) performed all microarray and bioinformatic normalizations, background corrections and organization of raw transcriptomic data, and supervised all subsequent bioinformatic analysis with this data. Tushar Dhawan wrote this dissertation with contributions from Dr. Charu Kaushic.

TABLE OF CONTENTS

LIST OF FIGURES AND TABLES

LIST OF ABBREVIATIONS

α-MEM	Alpha Minimum Essential Medium
ALI	Air Liquid Interface
ALOX15B	Arachidonate 15-Lipoxygenase Type B
AMP	Adenosine Monophosphate
ANOVA	Analysis of Variance
ARF	ADP-Ribosylation Factor
ATCC	American Type Culture Collection
ATP	Adenosine Triphosphate
BAX	BCL2 Associated X
BST2	Bone Marrow Stromal Cell Antigen 2
BTG2	B-cell Translocation Gene 2
CD4	Cluster of Differentiation 4
CD8	Cluster of Differentiation 8
cGAS	Cycling GMP-AMP Synthase
CNFN	Cornified Envelope Protein Cornefilin
CXCL14	C-X-C motif chemokine ligand 14
DAPI	4′,6-diamidino-2-phenylindole
DC	Dendritic Cell
DEG	Differentially Expressed Gene
DMEM/F12	Dulbecco's Modified Eagle Medium/Nutrient Mixture F-12
DNA	Deoxyribonucleic Acid
E2	Estradiol
EEA1	Early Endosomal Antigen 1
ELISA	Enzyme Linked Immunosorbent Assay
ER	Estrogen Receptor
ERα	Estrogen Receptor Alpha

ERβ	Estrogen Receptor Beta
FBS	Fetal Bovine Serum
FC	Fold Change
FDR	False Discovery Rate
FRT	Female Reproductive Tract
FSH	Follicle-Stimulating Hormone
GAPDH	Glyceraldehyde 3-phosphate dehydrogenase
gB	Envelope Glycoprotein B
gD	Envelope Glycoprotein D
GEC	Genital Epithelial Cell
GFP	Green Fluorescent Protein
GMP	Guanosine Monophosphate
GSEA	Gene Set
HBSS	Hanks' Balanced Salt Solution
HEPES	4-(2-hydroxyethyl)-1-piperazineethanesulfonic acid
HIV	Human Immunodeficiency Virus
HPV	Human Papillomavirus.
HSPG	Heparan Sulfate Proteoglycan
HSV-1	Herpes Simplex Virus type 1
HSV-2	Herpes Simplex Virus type 2
HVEM	Herpesvirus Entry Mediator
IAV	Influenza A Virus
ICP	Infected Cell Protein
ICP0	Infected Cell Protein 0
ICP4	Infected Cell Protein 4
ICP27	Infected Cell Protein 27
IE	Immediate Early

IER3	Immediate Early Response 3
IFI44L	Interferon Induced Protein 44 Like
IFIT1	Interferon Induced Protein With Tetratricopeptide Repeats 1
IFN-α	Interferon Alpha
IFN-β	Interferon Beta
IFN-γ	Interferon Gamma
IFN-λ1	Interferon Lambda 1
IFN-λ2	Interferon Lambda 2
IFNAR	Interferon Alpha And Beta Receptor
IL-1α	Interleukin 1 alpha
IL-1β	Interleukin 1 beta
IL-6	Interleukin 6
IL-8	Interleukin 8
ILV	Intralumenal Vesicle
IRF	Interferon Regulatory Factor
ISG	Interferon-Stimulated Gene
ISG15	Interferon-Stimulated Gene 15
JAK/STAT	Janus Kinase/Signal Transducer and Activator of Transcription
KD	Knockdown
KRAS	Kirsten Rat Sarcoma Viral Oncogene
KSFM	Keratinocyte Serum Free Media
LAMP3	Lysosomal Associated Membrane Protein 3
LCE1F	Late Cornified Envelope 1F
LCE3D	Late Cornified Envelope 3D
LCE3E	Late Cornified Envelope 3E
LDH	Lactate Dehydrogenase
LH	Luteinizing Hormone

LLI	Liquid-Liquid Interface
LOR	Loricrin Cornified Envelope Precursor Protein
LPS	Lipopolysaccharide
MCP-1	Monocyte Chemoattractant Protein 1
MDM2	Mouse Double Minute 2
MDS	Multidimensional Scaling
MEF	Mouse Embryonic Fibroblasts
MIF	Migration Inhibitory Factor
MOI	Multiplicity of Infection
MPA	Medroxyprogesterone Acetate
mRNA	Messenger Ribonucleic Acid
MVB	Multivesicular Bodies
NES	Normalized Enrichment Score
NFκB	Nuclear Factor kappa-light-chain-enhancer of activated B cells
NH	No hormone
NK	Natural Killer
OAS	2'-5'-Oligoadenylate Synthetase
OD	Optical Density
P4	Progesterone
PAMP	Pathogen-Associated Molecular Pattern
PBS	Phosphate Buffered Saline
PCNA	Proliferating Cell Nuclear Antigen
PFA	Paraformaldehyde
PFT-α	Pifithrin-α-HBr
PFU	Plaque Forming Unit
p.i	Post-infection
PRR	Pattern Recognition Receptor

RAB40C	Ras-Related Protein RAB-40C
RAP2B	Ras-Related Protein RAP-2B
RIG-I	Retinoic Acid-Inducible Gene I
RLR	RIG-I-Like Receptor
RNA	Ribonucleic Acid
RSAD2	Radical S-Adenosyl Methionine Domain Containing 2
RT-qPCR	Real Time Quantitative Polymerase Chain Reaction
SARS	Severe Acute Respiratory Syndrome
SEM	Standard Error of the Mean
siRNA	Small Interfering RNA
SIV	Simian Immunodeficiency Virus
SPHK1	Sphingosine Kinase 1
SPRR2B	Small Proline Rich Protein 2B
STAT	Signal Transducer and Activator of Transcription
STI	Sexually Transmitted Infection
STING	Stimulator of Interferon Genes
TER	Transepithelial Resistance
TGFβ1	Transforming Growth Factors Beta 1
TLR	Toll-like Receptor
TNF-α	Tumor Necrosis Factor alpha
TRAFD1	TNF Receptor Associated Factor - Type Zinc Finger Domain Containing 1
VAMP8	Vesicle Associated Membrane Protein 8
Vhs	Virion host shutoff
VSV	Vesicular Stomatitis Virus
WT	Wildtype
WHO	World Health Organization
ZO-1	Zona Occluden 1

CHAPTER 1: INTRODUCTION

1.1 Herpes Simplex Virus Type 2 (HSV-2)

1.1.1 Epidemiology and Clinical Manifestation of HSV-2

Sexually transmitted infections (STIs) account for a significant global health burden since they are responsible for high morbidity and mortality, particularly among women, in marginalized communities and those who engage in high-risk sexual behaviour. Herpes simplex virus type 2 (HSV-2), the virus that causes genital herpes, is a global health concern because it is one of the most prevalent STIs.[1] According to the World Health Organization, around 417 million people between the ages of 15 and 49 years are infected with HSV-2, with roughly 23 million new cases occurring each year.[1] In addition, around 65% of globally infected individuals are women.[1] The most serious burden of the disease is in Africa although places in South-East Asia and Western Pacific, despite their lower prevalence, contribute significantly.[1] HSV-2 increases risk of Human Immunodeficiency Virus (HIV) acquisition, especially in those recently infected with HSV-2.[1, 2] Increased HSV-2 seroprevalence is also associated with increased age and the number of sexual partners over one's lifetime, with sexual exposure as the predominant risk factor.[3]

The disease compromises the natural barrier of the skin by manifesting painful lesions in the genital area.[4] Dysuria, inflammation of the genital lymph nodes, cervicitis, and bilateral genital ulcers are some of the local genital symptoms that patients may suffer.[3] Following infection, HSV-2 establishes latency in neural tissue, expressing specific latent-associated transcripts, especially in the dorsal root and trigeminal ganglia.[3] The virus avoids immune detection during latency by keeping viral protein production at a minimum.[5] HSV-2 can be reactivated for lytic replication by being transported from sensory nerves to the genital mucosa or epithelial cells, resulting in genital ulcer disease.[3] Viral reactivation then leads to active induction of host immune responses or

internal cell signals that kill the infected cell.[5] Environmental stressors such as emotional stress, ultraviolet exposure, fever, and hormonal changes can trigger reactivation of the virus, although it is unclear whether these have direct or indirect effects on the neuron.[5] Currently available treatment options such as Acyclovir, Valacyclovir and Famcyclovir reduce viral replication and consequent symptom longevity and severity by inhibiting DNA polymerase; nonetheless, HSV-2 remains a lifelong condition with no known cure. To limit viral transmission, preventative strategies such as the use of condoms and avoidance of sexual activity are useful.[6] More therapeutic strategies to target different stages of the viral lifecycle are now being researched.[7-9]

1.1.2 HSV-2 structure, genome, and pathogenesis

Herpes simplex viruses (HSV) are members of the *Herpesviridae* family of viruses which includes viruses with double-stranded DNA genomes. Herpesviruses come in various forms, however, currently eight are known to cause disease in humans, particularly in those who are immunocompromised.[10] Herpesviruses can be further categorized into subfamilies (alpha, beta or gamma) based on their biological properties and sequence similarities.[10] HSV-2 is classified to be part of the alphaherpesvirus subfamily, with homology of up to 83% of its DNA with HSV-1.[11] This subfamily of viruses has a short replication cycle, infects a broad range of hosts, and is known to be neurotropic.[12]

HSV-2 virions are composed of a large DNA genome encased in the core of an icosahedral capsid, which is coated with the tegument (layer of proteins between envelope and capsid) and a lipid bilayer envelope composed of various viral membrane proteins and glycoproteins.[12, 13] Of the dozens of glycoproteins on the viral membrane, gB, gC, gD, gH and gL are most essential for the entry of the herpesvirus into the host; however, additional receptor-binding glycoproteins may also

play a role.[13] Each glycoprotein has a unique role that contributes to the attachment and fusion of the virus into host cells. The complete enveloped HSV-2 virion is 250nm in diameter and carries a linear double-stranded DNA genome approximately 155 kbp in length.[14] The viral genome is encased inside a 162-capsomer icosahedral capsid.[14] The viral genome is composed of two covalently linked sequences denoted L (long) and S (short), each with unique sequences designated U_L and U_S respectively.[15] Inverted repeats flank these areas, allowing for four distinct isomeric configurations of the viral genome.[15]

The HSV-2 lifecycle begins with attachment of glycoproteins, specifically gC and gD, binding to cellular receptors, followed by gB-mediated fusion of the viral envelope with the plasma membrane of the host cells such as epithelial cells. Viral gB is responsible for the virus's initial binding to the heparan sulfate proteoglycan (HSPG) on the surface cell.[4, 12, 13] Upon attachment of the virus to the cell, gD binds to any one of the three classes of HSV entry receptors: herpesvirus entry mediator (HVEM), a member of the tumor necrosis factor (TNF) receptor family; nectin-1 and/or nectin-2, members of the immunoglobulin superfamily; and specific sites in HSPG generated by isoforms of 3-*O*-sulfotransferases (3-O-S).[13] This interaction between gD and entry receptors mediates viral entry and results in a conformational change of gD itself, allowing for the interaction with gB or gH-gL to activate fusogenic activity between the virion envelope and cell membrane.[12, 13]

Following fusion, the tegument proteins and viral capsid are released into the cytoplasm and trafficked to the nucleus via microtubule transport.[16] This process is mediated by microtubule associated motor proteins such as dynein, an ATP-driven microtubule motor. While the most common mechanism of viral entry into the host cell is through membrane fusion, endocytosis is also an existent form of entry, as explained in section 1.1.3. [16] Once the virus docks to the nuclear

pores, viral DNA is released into the nucleus for subsequent transcription, genome replication and capsid assembly. Viral gene expression occurs in a sequential cascade: 1) immediate-early (IE) genes, which encode for regulatory proteins; 2) early (E) genes, which encode for enzymes involved in viral DNA replication; and 3) late (L) genes, which code for structural proteins.

Immediate-early genes, also known as alpha genes, can be transcribed by host-encoded factors once in the cell. Some IE-expressed viral proteins include infected cell proteins (ICPs) 0, 4, 22, 24 and 47, each with unique roles. For example, ICP0 is an IE gene encoded by the RL2 gene and is most extensively studied in HSV-2. ICP0 is a protein required for efficient viral propagation and functions as an E3 ubiquitin ligase, degrading cellular proteins involved in antiviral responses, allowing evasion of cellular antiviral defences. Recent literature suggests that ICP0 of HSV-1 targets IRF7 to limit induction of type I interferons that are key components of antiviral immune responses.[17] ICP0 has also been found to polyubiquitinate cellular proteins that are not well-known to have antiviral roles, such as p53, targeting them for proteasome-dependent degradation.[18] Some proteins derived from other IE genes will consequently induce expression of other viral genes in two sequential waves: the first being responsible for expression of early viral genes, or beta genes, followed by a wave of late viral genes, also known as gamma genes.[19] IE gene expression is known to peak between 2 and 4 hours after infection, whereas early genes reach peak rates of synthesis between 6 and 12 hours post infection (Figure 1). Early genes such as ICP6, ICP8 and UL30/UL42 are mainly responsible in supporting viral genome replication.[7, 20] For example, recent literature suggests that HSV-1 ICP8 mutant lacks annealing activity which results in the virus being deficient in viral DNA replication.[21]

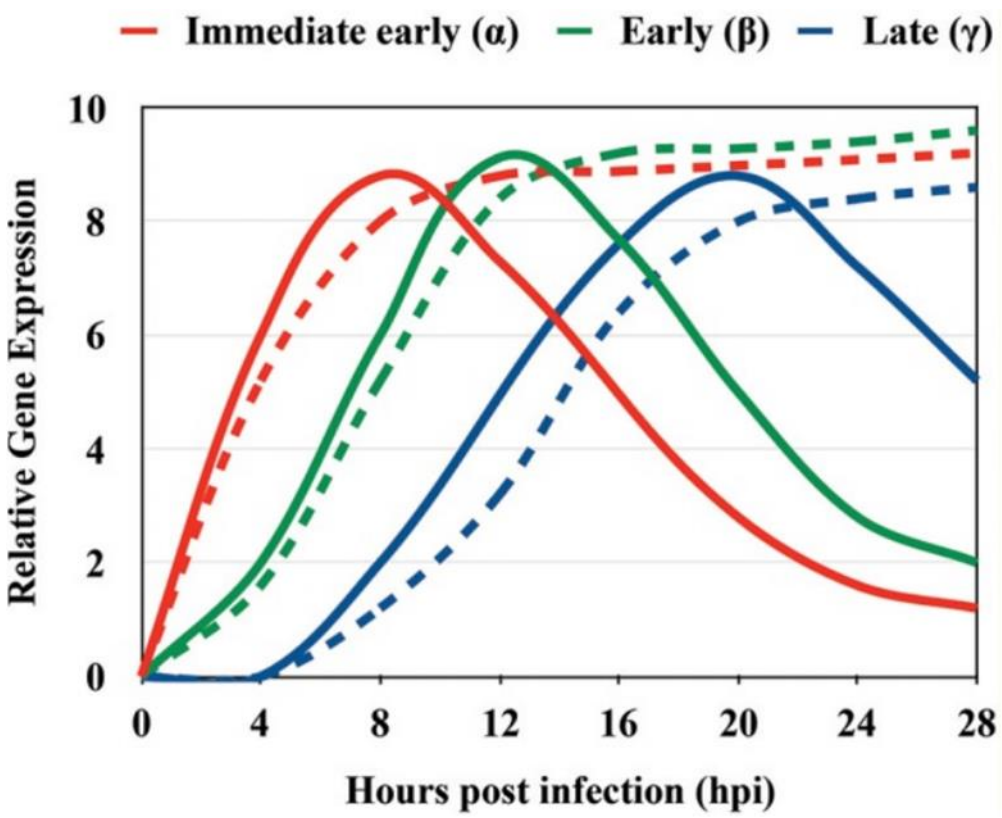

Figure 1: HSV-2 replication follows a typical pattern of expressing a set of genes in a time dependent manner. Gene expression kinetic analysis of immediate early (IE) (red), early (E) (green) and late (L) (blue) HSV genes. Solid lines represent characteristic expression patterns of HSV genes, whereas the dashed line indicated expression of genes that do not produce patterns typical of IE, E and L genes and continue to increase post infection. Figure extracted form Ibáñez et al.[7]

Viral DNA replication is mediated by the DNA polymerase complex in a unique process, with the linear genome circularized, where rolling circle motion synthesizes new DNA.[22] Following DNA replication, late genes begin to be transcribed and reach their peak expression between approximately 16 and 24 hours.[19, 23] These genes mainly encode for structural proteins and ultimately lead to viral assembly and packaging.[24] The newly synthesized circular genome is continuously cleaved into pieces as it unravels, and then packaged into capsids.[22] Various proteins communicate with each other to package the genome into capsids prior to the transport of nucleocapsids into the cytoplasm.[22] After virion assembly in the nucleus, the nucleocapsid coupled

with a matrix of tegument proteins is transported through the double membraned nuclear envelope into the cytoplasm by a mechanism called nuclear egress.[16] The virion envelope is thought to be acquired after being encased in a secondary vesicle through the trans-golgi network.[16] Tegument proteins then recruit molecular motor protein dystonin to mediate the transport of the virion to the cell surface, where either the progeny virions are released from the infected cell by lysis or the vesicle subsequently fuses with the plasma membrane of the cell, to thereby allow exocytosis of the virus.[10, 16, 25] The released viral progenies are then able to subsequently infect surrounding cells in the environment.

1.1.3 The role of the endocytic pathway in HSV-2 infection

It has recently been found that HSV viruses use endocytic machinery of epithelial cells for viral entry. Endocytosis is a cellular process by which molecules and substances are brought into cells. Various pathogens utilize the endocytic pathway to prevent detection from immune cells, however, some viruses such as HIV-1 enter cells through mechanisms such as membrane fusion. Entry through endocytosis can occur with viruses with or without envelopes. Depending on the type of virus, escape can occur from early endosomes, late endosomes, recycling endosomes or lysosomes.[26] Endocytic entry of viruses occurs by a stepwise process and starts by attachment of virus to cell surface followed by clustering of receptors and activation of signaling pathways that trigger the formation of endosomal vesicles for viral cargo to be delivered in. Fusion of mature endosomes with lysosomes can also occur, and is a process which generates endolysosomes where active degradation of endocytosed extracellular and intracellular components takes place.[27, 28] There is existing evidence that HSV-1 virions enter through endocytosis in epithelial cells.[29] Furthermore, endocytosis of HSV-2 in DCs has also been previously reported by virion uptake

into acidic endosomal compartments. Many pathogens hijack Rab protein function after invasion of hosts since Rab proteins are involved in multiple steps of the viral replication cycle, such as entry by endocytosis, viral glycoprotein trafficking, viral assembly and egress.[30] One study recently found that knocking down Rab9, which play roles in late endosomes, and knocking down Rab11, which is associated with transport along the recycling endosome to the cell surface, result in suppressed viral replication.[31, 32] Moreover, HSV-2 requires an intracellularly low pH for a successful endocytic infection.[33, 34]

1.2 Human Female Reproductive Tract

1.2.1 Morphology and function of the Female Reproductive Tract

Although the human female reproductive tract (FRT) engages in specific physiological events, such as menstruation, implantation, fertilization and pregnancy, it also plays a critical role in protection against STIs.[35] During heterosexual transmission, the FRT's epithelial cells and mucosal lining act as a physical barrier as the first line of defense against microbial, pathogenic and sexually transmitted infections such as HSV-2.[35] Epithelial cells and submucosal leukocytes, such as DCs and CD8 T cells, are one of the most important cell types with immune functions in the FRT. A dense stromal fibroblast layer provides structural tissue support underneath the epithelium, which serves as a barrier between the lumen and the tissue beneath.[35, 36] Although stromal fibroblasts underlying the epithelial cells are mostly for structural support, they have been shown to produce growth factors and cytokines which assist with innate immunity. Dynamic populations of leukocyte subsets remain dispersed throughout the stroma, with preferential distribution among different regions in the FRT.[37]

The FRT is divided into three sections: the upper part, the transitional cervix and the lower part, which are all lined with epithelial cells with different cellular morphologies.[35] The upper FRT is lined with a monolayer of columnar epithelial cells along the endocervix, uterus and fallopian tubes.[38] These columnar epithelial cells are connected by tight junctions, which are specialized intercellular connections between adjacent cells to restrict passage between apical (external environment) and basolateral (submucosa) compartments, and are responsible for maintaining mucosal barrier integrity.[38-40] The transitional compartment is the area between the upper and lower FRT where the columnar epithelium of the endocervix transition into a squamous epithelial layer of the ectocervix.[35] In contrast to the upper compartment, the vagina and ectocervix of the lower compartment are both lined with multiple layers of weakly-connected and non-keratinized stratified squamous epithelial cells, especially in superficial layers.[35, 37, 41] These cells are metabolically active and constantly proliferate, as opposed to the monolayer columnar cells in the upper compartment, eventually leading to terminal differentiation into superficial cornified layers of cells found in the squamous epithelium.[42]

Furthermore, the FRT is covered by a thin layer of mucus covering all luminal surfaces. In addition to the physically protective squamous epithelial cell layers lining the FRT, mucus secretions serve as a physical barrier, a viral trap, and a medium to strategically distribute various antimicrobial factors secreted by immune cells and epithelial cells.[43] Mucus is made up of mucins (glycoproteins that form the gel-like barrier which prevents pathogens from accessing the epithelium), electrolytes (nourish the environment) and proteins including lysozymes, immunoglobulins and lactoferrins, all of which work through unique mechanisms to defend against pathogens.[44] Moreover, the foreign pathogens and particles that become trapped in the vaginal

mucosa can also be ejected mechanically from the FRT by either renewal of mucosal layers or elimination by release during menstruation.[45]

1.2.2 Innate Immune response against HSV-2 in the Female Reproductive Tract

Following invasion of the genital epithelium by HSV-2, the mucosal immune system acts as the first line of defence where both the innate and adaptive immune system respond in the tissue.[46] The innate immune response is to limit viral spread and subsequently trigger the adaptive immune system's cellular and humoral-mediate immune response. Initial innate immune responses to HSV-2 are modulated by epithelial cells of the FRT, using various non-specific defence mechanisms, including release of chemokines and cytokines[47, 48], as well as antimicrobial secretions such as lysozymes and defensins.[49] The innate immune system primarily relies on the engagement of pathogen with pattern recognition receptors (PRRs) to trigger a cascade of signaling pathways involved in antiviral immunity. This initial response can lead to inflammation and cytokine production to recruit various innate immune cells, such as NK cells, DCs and inflammatory monocytes, to the site of infection.[46] PRRs recognize conserved pathogen-associated molecular patterns (PAMPs) of HSV-2 on various immune/non-immune cells, including toll-like receptors (TLRs), RIG-I-like receptors (RLRs), Nod-like receptors (NLRs) and DNA sensing systems which activate interferon regulatory factors (IRFs).[46, 50] A summary of viral genome recognition, including that of DNA viruses such as HSV-2, and the trigger of general downstream immune signaling pathways is shown in Figure 2.[51]

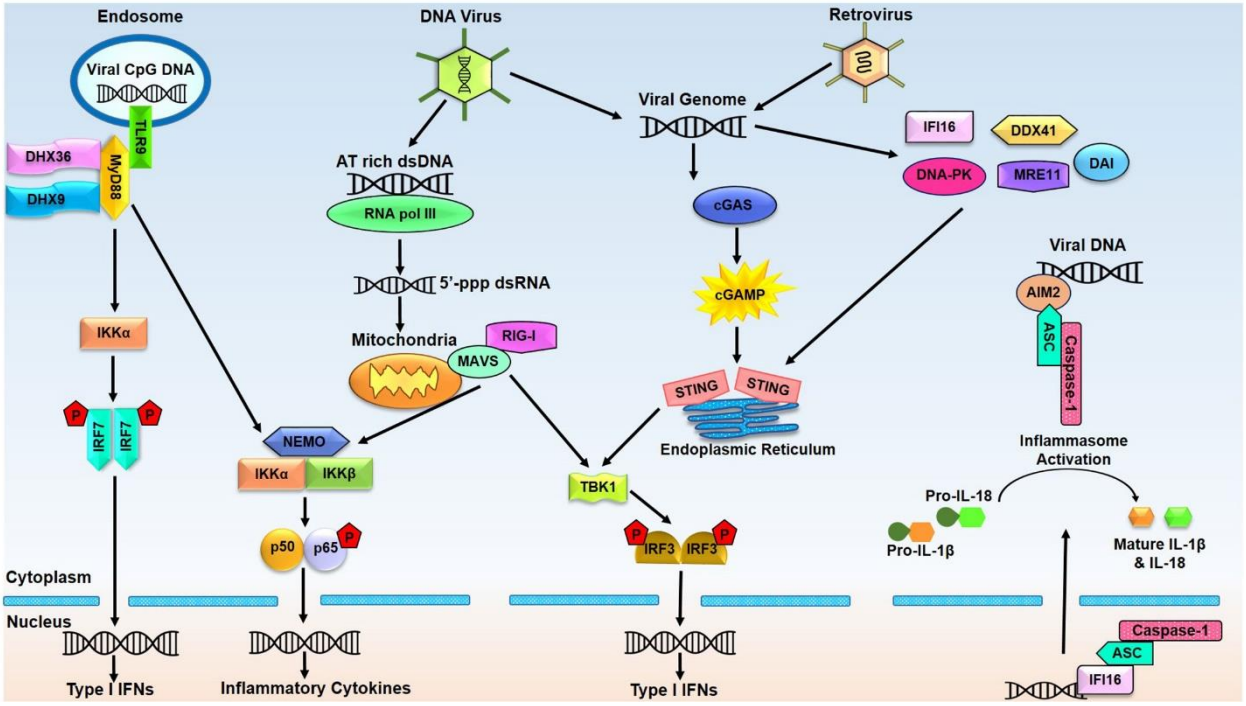

Figure 2: Innate immune signaling pathways induced by viral genome sensors. Recognition of viral DNA by cGAS (cyclic GMP-AMP synthase) DNA sensor triggers a signaling cascade that results in type I interferon production. Viral DNA can also be transcribed to 5' triphosphate double-stranded RNA, which induces NFκB (p65) phosphorylation and translocation to nucleus for the induction of proinflammatory cytokines. Entry of virus into endosomes can induce endosomal DNA sensors such as TLR9 to activate myD88 pathway and downstream type I interferon and proinflammatory cytokines production. This figure is retrieved from Zahid et al.[51]

More specifically, TLRs 2, 3 and 9 are known to recognize viral glycoproteins, double stranded RNA and viral CpG DNA, respectively, and act as initial innate immune responders to the virus.[10, 46] One study found that the human female reproductive tract expresses various TLRs such as TLR 1, 2, 3, 4, 5 and 6 among different regions.[52] Another study showed that HSV-2 infection in vaginal epithelial cells induces TLR4 expression, which is known to signal a cascade of downstream immune signaling pathways that may influence resistance against pathogens.[53] The importance of TLR-mediated protection has been demonstrated with *in vitro* studies which show

that following upregulation of TLR3, TLR5 and TLR9 via IFN-β, primary GECs inhibit replication of HSV-2.[54] Viral recognition by TLRs induces downstream intracellular pathways which lead to the activation of interferon regulatory factor (IRF), activator protein 1 (AP1) and nuclear factor-κB (NF-kB) transcription factors; subsequently leading to type I interferon (IFN) production and induction of proinflammatory cytokines and chemokines (CXCL9, IL-8, TNF-a, and MCP-1) via signal transducer and activator of transcription (STAT) factors.[10, 55]

Furthermore, various molecular pathways also exist where HSV-2 has been known to bind with cytosolic receptors, such as IFI16, and retinoic acid inducible gene I (RIG-I), by an RNA polymerase III-dependent manner.[46] Cyclic-GMP-AMP synthase (cGAS) is an enzyme part of a DNA sensing system that is characterized by binding of cytosolic DNA, subsequently triggering activation of stimulator of interferon genes (STING) by the production of a secondary messenger cGAMP.[46, 56, 57] Regardless of which cytosolic mechanism is triggered, many of these pathways converge towards the activation of Tank-binding Kinase 1 (TBK1), the mediator of IRF3 activation. TBK1 is known to phosphorylate and activate IRF3 and/or IRF7, resulting in type I interferon transcription.[57-59] To amplify type I IFN production, IFN-β generates positive feedback loops by binding to the interferon-α/β receptor (IFNAR) through a paracrine and autocrine process. Consequently, this leads to the activation of the JAK/STAT pathway, resulting in the induction of various interferon-stimulated genes (ISGs) which initiate IFN-α transcription, thus amplifying type I interferon expression.[60] Type I interferons, and their downstream ISGs, also activate crucial innate and adaptive immune system components, as well host resistance to viral infections.[50, 56] For example, Type I IFN production triggers cells in the surrounding environment to enter an antiviral state where antiviral molecules such as protein kinase R are upregulated, leading to the reduction or blocking of viral infection.[10, 60, 61]

Apoptosis, as well as other cell-death mechanisms, are also processes the host uses to induce cell death in response to viral infections, thus preventing further viral replication. Cellular mechanisms through which transmission of pro-apoptotic signals that respond to viral infections occurs includes protein kinase R, mitochondrial membrane potential and roles of various caspase proteins.[62]

1.2.3 Adaptive Immune response against HSV-2 in the Female Reproductive Tract

While the primary function of the innate immune system is to limit viral spread, it also subsequently triggers the adaptive immune system and its cellular and humoral-mediate immune responses which mediate clearance of infection. The adaptive immune system's role in antiviral defence against HSV-2 has been widely studied. Research has characterized the roles of both antibody-mediated immunity and cellular immunity against HSV-2, with recent research focusing more on the latter.

Cellular adaptive immune responses are mainly driven by T-cells, which constitute approximately 40 – 50% of the leukocytes in the FRT and have been demonstrated to be critical in the clearance of infections.[36, 55, 63] Interestingly, abundance of both $CD4^+$ and $CD8^+$ T cells is relatively similar in the lower FRT, whereas the $CD8^+$ T cells dominate the endometrium, suggesting tissue-specific constitution of different T cells.[64] One study reports that clusters of cells containing memory $CD4^+$ or $CD8^+$ T cells, as well as B cells, DCs and macrophages, form in the lower FRT in response to HSV-2 infection, and continue to persist up to years after viral clearance.[65] The formation of such cell clusters may be explained by a strategy for preserving T cell repertoire to prevent loss of memory T cells from shedding of the endometrial lining during menstruation. Earlier studies have shown that the HSV-2-specific $CD8^+$ cytotoxic T cells against

a particular epitope play a protective role against HSV-2, where depletion of $CD8^+$ T cells resulted in increased HSV-2 titres.[66] It has been suggested that this occurs through the ability of tissue resident $CD8^+$ T cells to produce IFN-γ which subsequently blocks viral replication, however, total clearance is only achieved through perforin or Fas-mediated cytolytic mechanisms that lead to apoptosis of infected cells.[67] However, recent studies have demonstrated that mice with $CD8^+$ knocked out continue to show protection after challenge with HSV-2, suggesting that $CD8^+$ T cells alone are not sufficient in providing protection.[68] Some studies indicate that mobilization of $CD8^+$ T cells to the vaginal epithelium is dependent on presence of $CD4^+$ T cells and their production of IFN-γ and downstream chemokines.[69] Interestingly, depletions in $CD4^+$ T cells have been reported to be correlated with higher viral load in vaginal tissues as compared to $CD8^+$ depletion.[66] Furthermore, it is the production of IFN-γ by Th1 cells that is attributed to the protective effects as mice with IFN-γ deficiency do not show protection against HSV-2 despite the presence of $CD4^+$ T cells.[66, 68]

$CD4^+$ helper T cells are also known to assist in humoral immunity by promoting maturation of B cells to plasma cells for antibody secretion. Although B cells constitute a minor population in the FRT, they make the reproductive tract unique in that both IgG- and IgA-producing plasma cells can be found.[70, 71] It has been reported that HSV-2 infection in the genital tract of humans primarily results in production HSV-2 specific immunoglobulin G (IgG) over IgA.[72] More specifically, a recent study with mice has found IgG2b and IgG2c as the primary isotypes secreted in response to HSV-2 infection.[73] Studies have shown that immunized mice deficient in B-cells and subsequently challenged with HSV-2 show higher levels of viral load in the vaginal epithelium and vaginal secretions.[74] However, many studies have also found that resistance to challenge by HSV-2 in immunized mice does not depend on presence of B-cells and their corresponding production of

antibodies.[68, 75] Overall, findings from literature regarding the role of B-cells needs further studies to establish a clear role. Although humoral immunity may play a role in primary HSV-2 infection, based on existing literature, it is mainly the cellular component that is required for its clearance and long-term protection.

1.3 Female Sex Hormones

1.3.1 Menstrual cycle and presence of female sex hormones

An important biological factor which influences the physiology of the FRT is the influence of female sex hormones, which vary with the phase of the menstrual cycle as shown in Figure 3. Female sex hormones, such as estrogen (E2) and progesterone (P4), have been known to impose effects on epithelial cells, fibroblasts and immune cells in the FRT to alter their functions and therefore a person's susceptibility to STIs through differential processes depending on the site of the FRT. [76-85] Balance between female sex hormones is crucial in maintaining an equilibrium between immune regulation against pathogens and tissue modeling for optimal conditions required for fertilization and implantation.[36, 37] In women of reproductive age, cyclic secretion of E2 and P4 is regulated by the hypothalamic-pituitary axis via the ovary throughout the menstrual cycle which is divided into four phases: i) menstrual phase; ii) proliferative phase; iii) mid-cycle phase; and iv) secretory phase. The first phase, menstruation, is triggered by a drop of E2 and P4 levels. The sharp reduction in these hormones causes the previous cycle's endometrial lining to shed out of the uterus, thus producing bleeding. During the initiation of the menstrual cycle, it is the follicle-stimulating hormone (FSH) which stimulates granulosa cells (with help from thecal cells) in the developing follicle in the ovary to produce E2. Under control of FSH and the luteinizing hormone (LH), E2 levels continue to rise during the proliferative phase, inducing the proliferation of a new endometrium, until they peak prior to ovulation.[36] Following the peak of E2 levels in the blood,

LH levels surge and are essential for ovulation, which occurs at the mid-cycle stage. This surge of LH from the anterior pituitary causes remnants of the follicle to become the corpus luteum which subsequently acts as the primary source of E2 and P4 during the secretory phase. Concentrations of progesterone, and to a reduced extent, estrogen, rise and peak near the mid-secretory phase, further increasing the development of the endometrium, including secretion of glycogen, lipids, and other material.[36] In absence of fertilization, degradation of the corpus luteum and a decline in E2 and P4 secretion trigger the onset of menstruation once again.

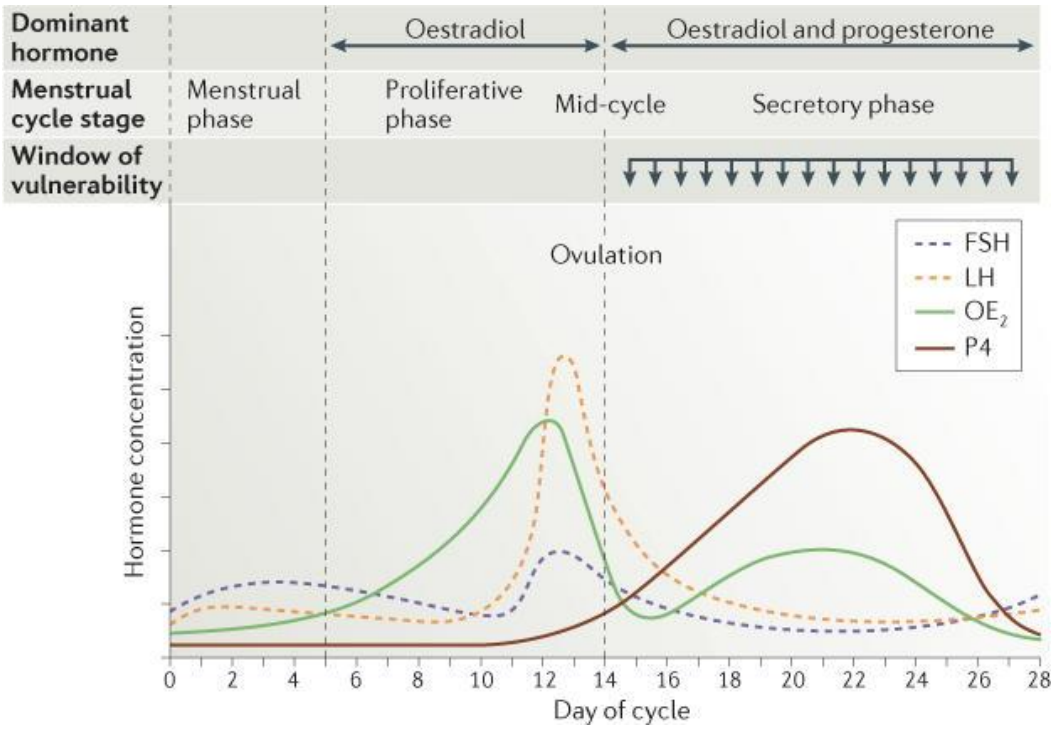

Figure 3: Cyclic female sex hormone levels throughout the 28-day menstrual cycle. The ovarian cycle is divided into four stages 1) menstrual phase (menstruation); 2) proliferative phase (follicular phase); 3) mid-cycle phase (ovulation); and 4) secretory phase (luteal phase). Graph plots the level of female sex hormone concentration based on the day of the menstrual cycle for up to 28 days. (FSH, follicular stimulating hormone; LH, luteinizing hormone; OE_2, oestradiol; P4, progesterone). Figure is retrieved from Wira et al.[36]

1.3.2 Estrogen

There are three major types of physiological estrogens found in females: estrone (E1), estradiol (E2, 17-β-estradiol), and estriol (E3). Each form of the estrogen is a different formulation derived from cholesterol and differ from each other by one step in a series reaction of estrogen biosynthesis. 17-β-estradiol, or E2, is the dominant estrogen found in women during the premenopausal process, whereas E1 primarily exerts its role post-menopause.[86] E3 is considered the weakest estrogen, synthesized by a hydroxylation on E1. It's found to have importance particularly during pregnancy since the placenta produces larger quantities.[86]

E2 is predominantly produced by granulosa cells of the ovaries, and plays a crucial role in sexual development, reproductive functions, sexual behaviour and differentiation of certain tissues. Estrogenic compounds exert their various complex physiological functions through interactions with intracellular estrogen receptors. There are two known subtypes of estrogen receptors: estrogen receptor alpha (ERα) and estrogen receptor beta (ERβ). Although these proteins are dispersed throughout the cell, they exert their role particularly in the cell nucleus by acting as transcription factors after binding to DNA regulatory sequences, thus regulating transcription of specific downstream target genes. ERα is located primarily female reproductive tract tissues, bone, liver, adipose tissue, testes, epididymis and stroma of the prostate, whereas ERβ is found mainly in the epithelium of prostate, bladder, granulosa cells of ovaries, colon and adipose tissue (Figure 4).[87, 88] These receptors are commonly expressed in non-immune cells such as genital epithelial cells, as well as by various immunocompetent cells such as T-lymphocytes, macrophages, NK cells, neutrophils, B-lymphocytes and DCs.[89]

A

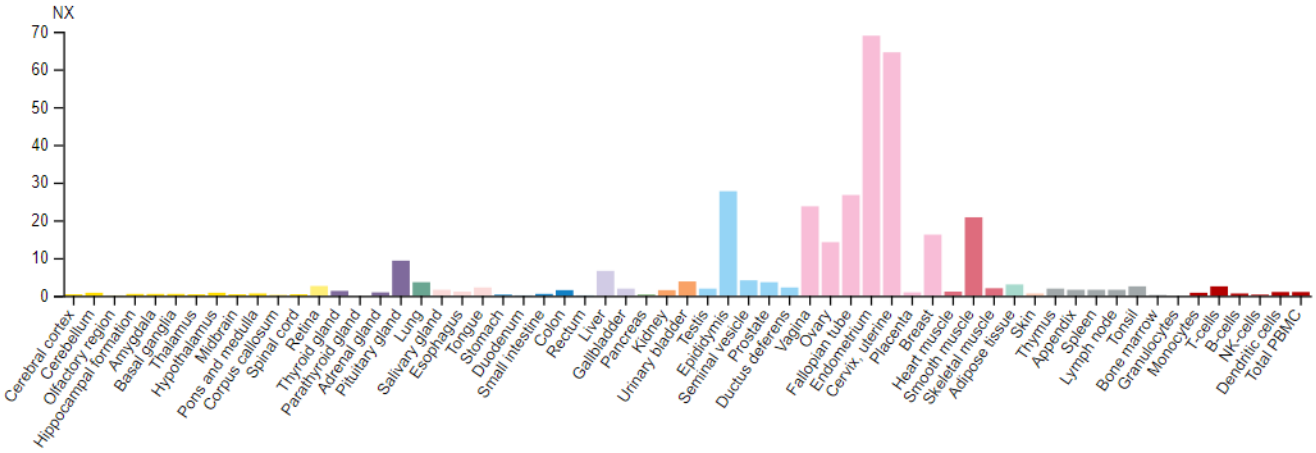
NX
70
60
50
40
30
20
10
0
Cerebral cortex
Cerebellum
Olfactory region
Hippocampal formation
Amygdala
Basal ganglia
Thalamus
Hypothalamus
Midbrain
Pons and medulla
Corpus callosum
Spinal cord
Retina
Thyroid gland
Parathyroid gland
Adrenal gland
Pituitary gland
Lung
Salivary gland
Esophagus
Tongue
Stomach
Duodenum
Small intestine
Colon
Rectum
Liver
Gallbladder
Pancreas
Kidney
Urinary bladder
Testis
Epididymis
Seminal vesicle
Prostate
Ductus deferens
Vagina
Ovary
Fallopian tube
Endometrium
Cervix, uterine
Placenta
Breast
Heart muscle
Smooth muscle
Skeletal muscle
Adipose tissue
Skin
Thymus
Appendix
Spleen
Lymph node
Tonsil
Bone marrow
Granulocytes
Monocytes
T-cells
B-cells
NK-cells
Dendritic cells
Total PBMC

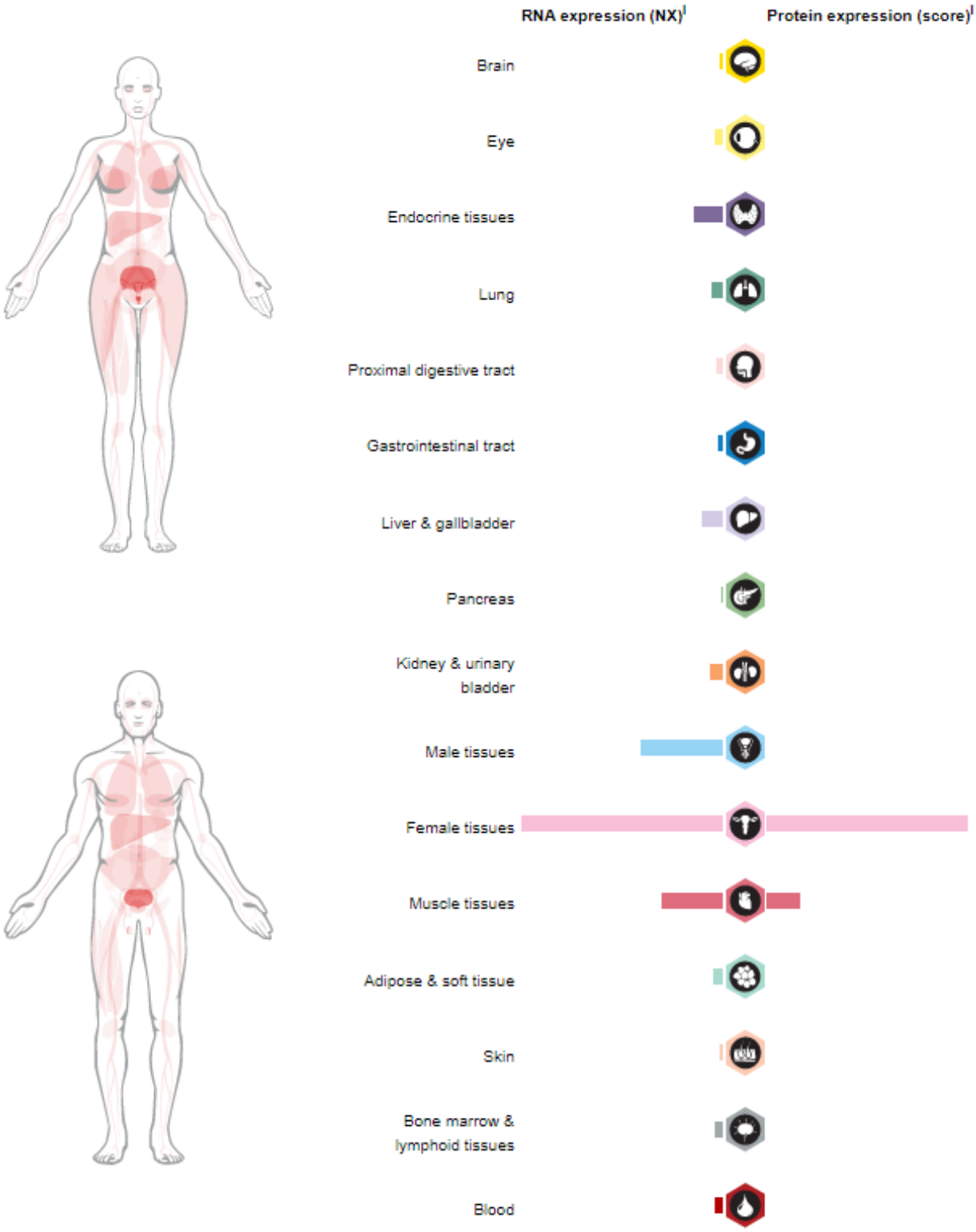

Figure 4: Female tissues show the highest expression of ERα in the human body. A) RNA expression of ERα in different parts of the body. B) Summary of protein and RNA expression of ERα RNA in various human tissues and organs. Figures are extracted from The Human Protein Atlas.[88]

1.3.3 Effect of female sex hormones on female reproductive tract

As sex hormones are secreted in systemic circulation, their influence varies throughout different compartments of the FRT. Epithelial cells that line the FRT not only respond to pathogenic stimuli, but to hormones as well. It is well known that E2 induces epithelial cell proliferation,[90, 91] whereas elevated P4 concentrations are linked with thinning of the vaginal epithelium in animal models.[79, 92, 93] This is important due to the absence of tight junctions in the superficial epithelium of the lower FRT result in loosely connected cells that may allow pathogens to penetrate and come in contact with immune cells in the basal epithelium and lamina propria. Estrogen plays an important, yet controversial role in the regulation of proteins involved in epithelium integrity. For example, one study showed the modulation of claudin and occludin protein expression by E2 results in relaxation of tight junctions and increased flux across the epithelium.[94, 95] However, researchers in a different *in vitro* study found that E2 treatment of vaginal epithelial cells leads to more pronounced cytokeratin expression, a cytoplasmic epithelial cell protein that interacts with desmosomes to assist in barrier integrity, relative to P4 conditions.[78]

Another physical component that is influenced by hormones is the mucus present in the FRT. Mucin, a glycoprotein secreted by endocervical epithelial cells, is a major component of mucus. Gene expression of mucin varies with the menstrual cycle, consequently causing variations in the properties of the mucus.[96] Water, being the major component of vaginal mucus, comprises about 85-98% of the mucus. During the proliferative phase, estrogenic mucus is very watery with a low viscosity and later becomes 95-98% water during peak E2 levels at ovulation. In contrast, progestational mucus, is about 85%-92% water, making it thick and viscous.[44, 97, 98] Estrogenic mucus, present at ovulation, facilitates sperm movement into the FRT, whereas progestational

mucus, present following ovulation and throughout the secretory phase, impedes the movement of substances from the lower to the upper FRT.[97]

Along with the unique immunomodulatory effects after PRR activation specific to different pathogens, PRR expression also tends to change with hormone exposure throughout the menstrual cycle.[36] In an *in vitro* study, it was found that E2 reduced expression of TLR2 and TLR6 in the VK2 vaginal epithelial cell line.[99] E2 has also been found to modulate signalling pathways downstream to PRRs. Studies on uterine epithelial cells have shown that E2 inhibits secretion of migration inhibitory factors (MIF), interleukin-6 (IL-6) and IL-8 by macrophages induced by polyinosinic-polycytidylic acid (poly(I:C)) and lipopolysaccharide (LPS), and reverses stimulatory effects of IL-1β on protein and mRNA expression of NF-κB, IL-8, human β-defensin 2, and tumour necrosis factor (TNF), suggesting that periods of high E2 levels in the menstrual cycle results in an anti-inflammatory environment in response to pathogens.[100, 101] More specifically, E2 has been reported to suppress the function of NF-κB through restricting NF-κB-inhibitor degradation, or inhibiting nuclear translocation of NF-κB, thus preventing downstream pro-inflammatory expression.[102, 103]

1.3.4 Role of sex hormones on susceptibility to sexually transmitted infections

E2 and P4 are produced endogenously by ovaries, but can also be released exogenously as main components of various hormonal contraceptives.[104] During menstruation, and in preparation for fertilization and implantation, release of E2 and P4 regulate immunity in the FRT to complement reproductive environments and processes.[36, 83] In preparation for fertilization, the body responds by suppressing innate and adaptive immune responses to prevent fetal rejection.[36]

This results in the phenomenon known as the window of vulnerability which increases women's risk of acquiring STI.[36, 105]

As discussed previously, hormones play an important role in the FRT and have various well-known roles in biological pathways such as cholesterol synthesis, innate immunity, cytokine signaling, cell division, cell cycle arrest, and many more. Viruses are intracellular obligate parasites dependent on host cell machinery, and so, vary in their ability to function depending on the presence of female sex hormones which alter many pathways required for their replication. Hence, the presence of female sex hormones may alter susceptibility or immune responses that play important roles against STIs.

Multiple studies in literature indicate that the window of vulnerability is applicable for other STIs. For example, studies have demonstrated that the secretory phase, which is progesterone dominant, is associated with higher HIV-1 transmission.[36, 105-107] One of the studies collected lavage samples characterized by follicular (proliferative) or luteal (secretory) phases and analyzed them via mass spectrometry.[106] Since luteal phase is dominated by progesterone, and found to enhance susceptibility to HIV when compared to the follicular phase, they investigated the genetic profiles of both phases and discovered each phase up/downregulates unique immune pathways.[106] Furthermore, *in vitro* studies have also shown that E2 treatment reduces HIV infection in macrophages and CD4+ T cells. [82, 108] Similarly, a study using the macaque animal model indicates that vaginal transmission of Simian Immunodeficiency Virus (SIV) increases during the secretory (luteal) phase of the menstrual cycle relative to the follicular phase.[109] Furthermore, estrogen treatment of macaques has been reported to significantly protect macaques against SIV infection with evidence of thickened and cornified vaginal epithelium.[84] Contrastingly, a study using

subcutaneous P4 implants to mimic hormone-based contraceptives demonstrated thinning of the vaginal epithelium along with a significant increase SIV vaginal transmission.[93]

For over a decade, our lab has been intensively studying effects of female sex hormones on HSV-2 infection using *in vivo* and *in vitro* models. Our studies, along with experimental evidence from others, has shown that E2 confers greater protection against STIs with no pathology, whereas P4 provides protection, but with increased immunopathology and inflammation.[76, 77] Interestingly, earlier studies in our lab also demonstrated that treatment of mice with saline suspension of progesterone or Depo, also known as medroxyprogesterone acetate (MPA), increased susceptibility to intravaginal HSV-2 infection by up to 10-fold and 100-fold, respectively.[80, 92] In the same way, our previous immunization studies have shown, using an ovariectomized model where endogenous source of hormones were removed and exogenous estradiol or progesterone were delivered in mice, that E2 treated mice confer protection from HSV-2 infection along with better outcomes on viral shedding and vaginal immunopathology. However, P4 treatment results in mice showing higher susceptibility to HSV-2 infection, higher viral shedding in vaginal secretions and chronic pathology.[76, 77] Another study from our lab interestingly shows that prolonged Depo exposure compromises immune responses against HSV-2 infection in immunized mice.[80] Furthermore, an *in vitro* study in our lab shows that VK2 cells grown under P4 treatment showed significantly higher HSV-2 infection and replication relative to E2 treatment.[78]

Based on the evidence of multiple studies, estrogen seems to overall have protective effects against various STIs, while progesterone appears to increase risk. It is important to consider that studies which show different patters in hormonal influence on susceptibility to pathogens most likely reflect variations among animal models, pathogen of interest and the consequent immune response against each pathogen.[36] Despite the fact that endocrine and hormonal conditions

responsible for differences in infection vary with cell culture and animal models, the idea of the window of vulnerability is an evidently useful concept which can be used to further examine how reproductive health of women can be compromised.[36] Moreover, due to the lack of understanding of the cellular mechanisms of E2 and its antiviral effects, further research is warranted to address this gap in understanding.

1.4 Vaginal Epithelial Cell Experimental Model

1.4.1 VK2/E6E7 cell line

Various *in vitro* studies that focus on vaginal physiology have previously utilized the vaginal epithelial cell line (VK2/E6E7) to study pathogen interactions, genetic alterations, and hormone influences.[53, 78, 110-112] The VK2 cell line was established in the mid-90s by isolation from fresh vaginal mucosal tissue obtained from a premenopausal women undergoing vaginal repair surgery.[113] These cells were immortalized using a retroviral vector containing the human papillomavirus (HPV) E6E7 antigen.[113] VK2 cells have characteristics that are similar to normal vaginal epithelial cells and are physiologically appropriate for studying the lower female genital tract. For example, the selective expression of certain cytokeratins in VK2s is similar to what is found in normal vaginal tissue.[113] The introduction of this cell line provides researchers with a better alternative and stronger representation of the vaginal tract than HeLa cells, which have been commonly used for vaginal studies in the past. However, most studies use liquid-liquid interface systems to grow these cells in a monolayer, which is not an accurate representation of the physiological conditions of the vaginal tract.[99, 114] As mentioned previously, the vaginal epithelium naturally exists with stratified layers of squamous epithelial cells. Therefore, our lab has recently

developed and optimized a multilayer culture method using VK2 cells that resembles the FRT more accurately.[78]

1.4.2 In-vitro air-liquid interface culture model

Our lab recently established and characterized an Air-Liquid-Interface (ALI) culture system which allows the vaginal epithelial cell line (VK2 cells) to proliferate in stratified layers in transwells, a state that more closely mimics the *in vivo* natural environment of the lower vaginal tract.[37, 78] This model allows us to study HSV-2 entry, infection and replication in a more realistic environment, since HSV-2 first infects vaginal epithelial cells, as compared to the traditional liquid-liquid interface (LLI) approach, as shown by a previous study in our lab by Lee et al.[78] Earlier culture models used the conventional LLI approach by providing growth medium to both apical and basolateral sides of cultures, resulting in monolayer growth of squamous epithelium. Instead, the vaginal epithelium absorbs nutrients from only its basolateral side while the apical side is in contact with air and mucus. This novel ALI culture system, which is supplemented with medium on only the basolateral side, better models the *in vivo* cells of the lower FRT (Figure 5).[78]

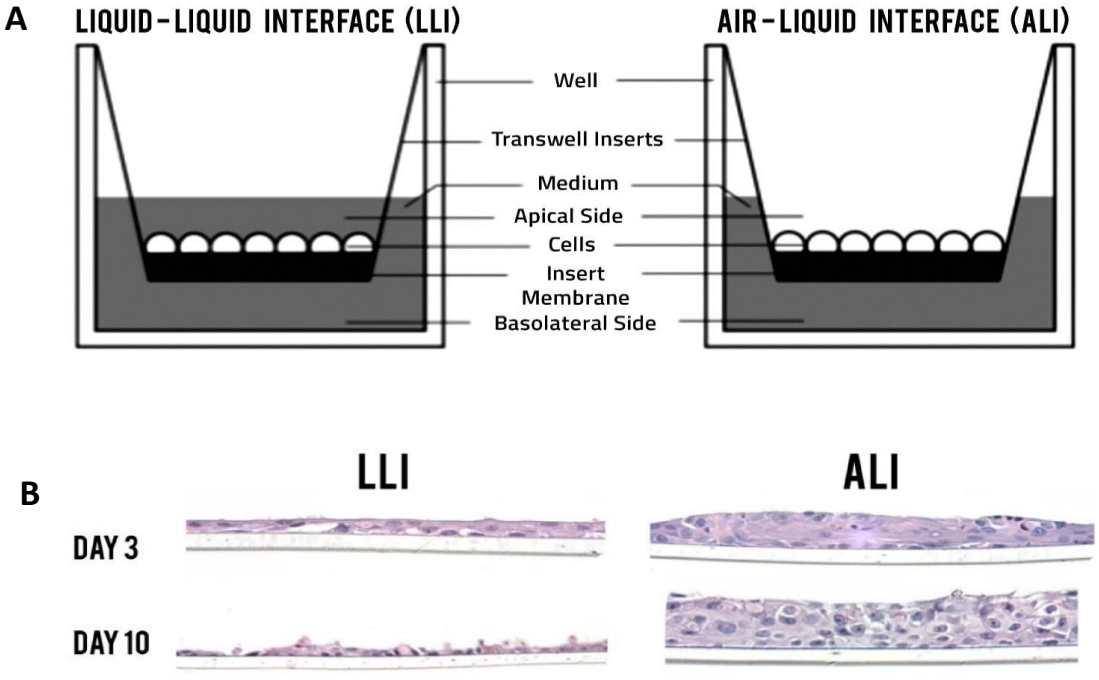

Figure 5: Air-liquid interface culture promotes multiple layers of stratified squamous epithelium mimicking physiological anatomy of lower female reproductive tract (A) Culture design comparison between the conventional Liquid-Liquid Interface (LLI) to the novel Air-Liquid Interface (ALI) VK2 culture systems. (B) Hematoxylin and eosin (H&E) staining LLI compared to ALI cultures after 10 days of VK2 culture growth. This figure demonstrates and highlights stratified squamous epithelial cell growth observed in ALI cultured VK2 cells, thus more closely mimicking physiological conditions found in the vagina in the lower FRT. Figures reproduced from Yung et al. 2016.[78]

1.5 The Role of p53 signaling pathway

1.5.1 The p53 Protein

The p53 pathway has previously been reported for its interactions with various viral infections, the immune system and hormones. p53 is a tumor suppressor protein that causes cell-cycle arrest and apoptosis when activated. Given its role, there have been multiple studies which have investigated its contribution in regulation of cell fate and tumour suppression.[115] Studies show that p53 prevents development of tumors by acting as a sensor for cellular stress and responding to various signals such as DNA damage, deprivation of nutrients, hypoxia, expression of oncogenes, and further limiting cell propagation under these unfavourable conditions.[115] As such, it is clear that p53 is an essential component of a vast network of host regulatory processes and factors that prevent tumor formation.

p53 functions as a transcription factor that accumulates in the nucleus to induce its downstream genes. It has also been reported that translocation of p53 is tightly regulated by the cell cycle: p53 has been found to accumulate in the cytoplasm during the G1 phase, enter the nucleus during the G1/S phase transition and return back to the cytoplasm shortly after the S phase.[116] The function of p53 protein is regulated post-translationally by interactions with signaling proteins including ubiquitin-like modifying enzymes (ubiquitination), methyl-transferases (methylation), acetyltransferases (acetylation) and protein kinases (phosphorylation),

which can not only alter the function of p53, but also affect its translocation between various compartments.[117] p53 can be phosphorylated at numerous sites in response to certain signals, thereby altering its biochemical functions, such as sequence-specific DNA binding and protein-protein interactions, required for increased activity as a transcription factor. Of the various phosphorylation sites reported on p53, only three (Ser15, Thr18, Ser20) are highly conserved. Despite evidence of p53 phosphorylation at various sites, their consequences on p53 function are poorly understood.

P53 employs its various effects through induction of key downstream regulatory factors which altogether make up the p53 pathway. These factors contribute to various outcomes such as growth arrest, apoptosis, DNA repair, senescence, autophagy, metabolism, and more.[118] For example, p21, the protein encoded by the cyclin-dependent kinase inhibitor 1A (CDKN1A), is p53-response gene and important mediator of cellular senescence.[119] Cellular p53 protein levels are under strict control of negative regulators such as MDM2, which in turn is a transcriptional target of p53, thus forming an auto-regulatory feedback loop. MDM2, together with its homolog MDM4, acts as an E3 ubiquitin ligase to ubiquitinate p53, resulting in its proteasomal degradation.[120] Various cellular signals, such as DNA damage, viral infection, or oncogene activation can induce p53 activation. DNA damage induces phosphorylation of p53, preventing its binding with MDM2, whereas activated oncogenes activate the ARF protein to prevent MDM-2 mediated degradation of p53.[120] Thus, designing of various compounds that employ their effects as inhibitors of the p53-MDM2 interaction is a favorable strategy for activating the p53 tumor-suppressor activity in tumours.

1.5.2 p53 and viral infections

Recent studies suggest that p53 is also involved in the life cycle of multiple viruses, including influenza virus, Zika virus, West Nile virus, Human Immunodeficiency Virus, HSV, and more.[121] Viruses are intracellular obligate pathogens that are unable to reproduce on their own, and thus require a host to use its signalling, metabolic and proteosynthetic pathways.[122] Interestingly, various viruses have been shown to have unique interactions with p53, where some activate p53 for sufficient viral replication, while others require inhibition of p53 activity.[121] For example, p53 is activated in response to influenza A virus (IAV) infection to inhibit viral replication.[123-125] As a transcription factor, p53 regulates expression of downstream responsive immune-related genes involved in IFN signaling and cytokine/chemokine production, suggesting a crucial role of p53 in regulation of inflammatory and antiviral responses against IAV.[125] Recent studies have also shown that p53 downregulates severe acute respiratory syndrome (SARS) coronavirus replication.[126, 127] In the context of herpesviruses, literature shows that p53 has a dual role in modulating HSV-1 replication depending on the stage of infection. While p53 increases HSV-1 replication by activating ICP17, a viral protein essential for early stage HSV replication, p53 also regulates the degradation of ICP0, a viral protein essential for replication of viral genome and repression of host immunity, and thus attenuates the replication of HSV-1.[121]

Overall, p53 has been shown to be an important contributor to the protective response against viruses, and its loss has been found to facilitate the ability of viruses to replicate. To counteract this protective response of p53, various viruses have evolved molecular mechanisms that hinder p53, often through viral proteins that can bind to and inhibit p53.

Multiple studies indicate that p53 has an important role in modulation of IFN-mediated antiviral immunity.[128-131] One study identified that p53 is able to activate the IFN pathway via

IRF9 activation, and subsequently, reduce viral replication early after infection.[128] On the other hand, recent studies also demonstrate that p53 is instead targeted and activated by type I IFNs post-infection.[131] Furthermore, studies show that various IFN-inducible genes such as IRF5, IRF9, TLR3, and ISG15 are transcriptional targets of p53.[131]

Overall, there seems to be a knowledge gap between p53 and HSV-2 with a paucity of existing research. However, there are a few studies which have investigated p53 and its role in the context of HSV-1, which is highly homologous with HSV-2. With p53 being highly expressed in female tissues (Figure 6), along with its ability to induce various immune functions and its role in interacting with various viruses, this makes it a potential candidate to further study its role against STIs such as HSV-2. Although studies have shown the important interaction between p53 and HSV-1 viral proteins,[121] there is minimal data on whether the antiviral responses induced by p53 and whether they are sufficient for suppressing HSV-2 replication.

A

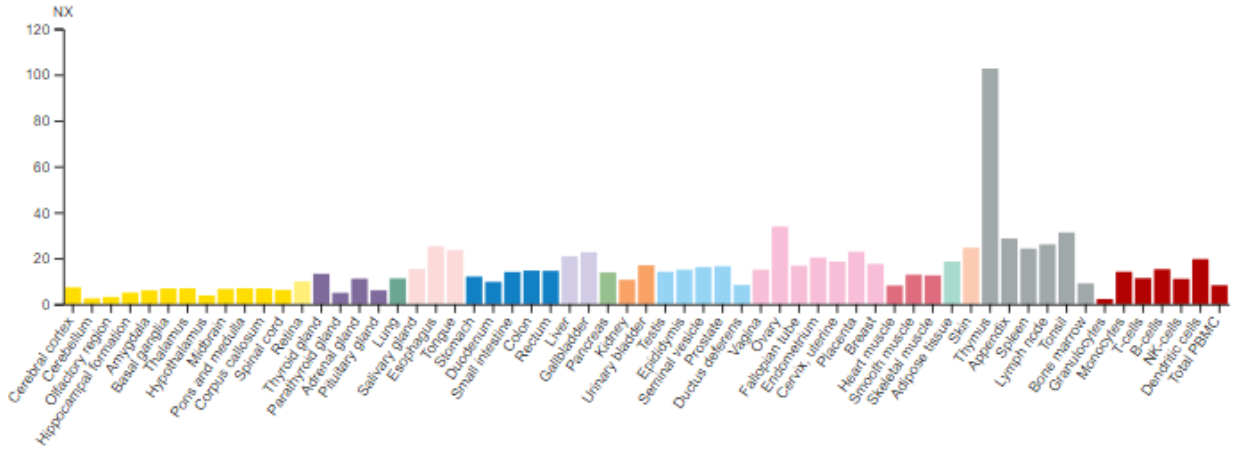

B

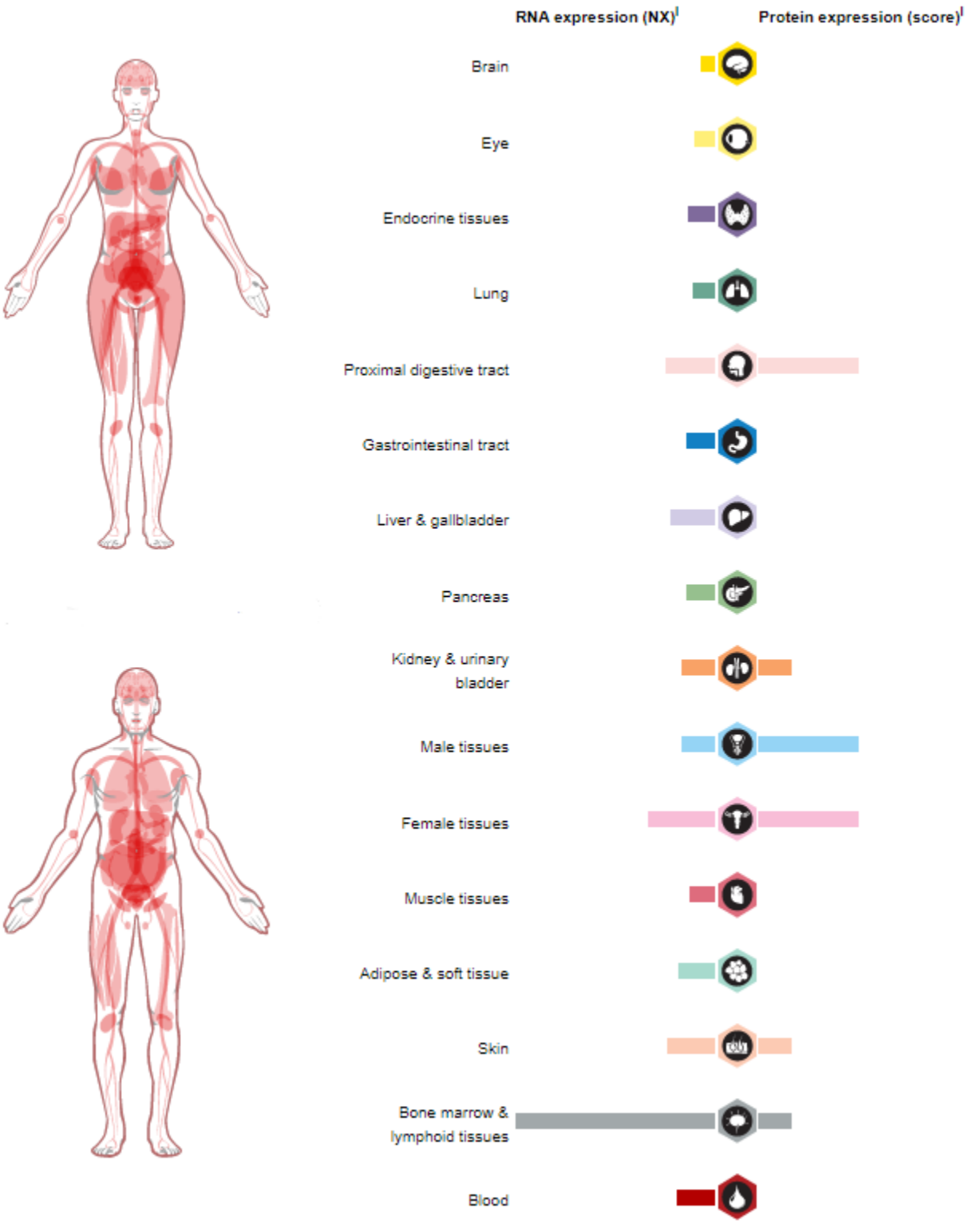
RNA expression (NX)
Protein expression (score)
Brain
Eye
Endocrine tissues
Lung
Proximal digestive tract
Gastrointestinal tract
Liver & gallbladder
Pancreas
Kidney & urinary bladder
Male tissues
Female tissues
Muscle tissues
Adipose & soft tissue
Skin
Bone marrow & lymphoid tissues
Blood

Figure 6: P53 expression and localization is found in various parts of the human body. A) Quantitative graph of RNA expression of p53 in fferent areas of the human body. B) Summary of p53 RNA and protein production in various tissues and organs. Figures are extracted from The Human Protein Atlas.[132]

1.5.3 Connection between p53 and estrogen signaling

Hormones and p53 have various interactions that lead to modulation of downstream cellular pathways. Multiple studies have demonstrated that estrogen plays an important role in altering p53 expression or its downstream targets.[133-137] One study found that treatment of T47D estrogen receptor (ER)-positive breast cancel cell line with ICI 164384, an antiestrogen, reduced cell count and p53 levels.[133] Conversely, when they cultured cells in hormone stripped medium, exogenous E2 treatment increased p53 expression and cell proliferation. Some reports demonstrate that estrogen can induce p53 gene transcription through multiple transcription factors such as NFκB or ERα, that bind to elements located upstream of the p53 transcriptional start site: NFκB-binding motifs or CCAAT-binding transcription factor 1,[138] c-Myc response element,[139] GC-rich Sp1 site[140] and estrogen response elements (EREs).[141] With the ER being heavily involved in transcriptional regulation of estrogen gene targets, its important to note that of the various functional domains located on ERα, a p53 binding region is located at domain D (dimerization/hinge domain) and E (ligand binding domain/activation function).[142]

1.6 Transcriptional profiling and Bioinformatics

1.6.1 Transcriptional Profiling of Female Reproductive Tract Epithelial Cells

Our lab has extensively investigated transcriptional profiles of different combinations of treatments, various epithelial cell types and viruses. We have published data that has exclusively looked at the effect of sex hormones on upper and lower FRT epithelial cells. One of the first transcriptional studies our lab looked at was the effect of MPA on human endometrial epithelial

cells, compared to E2 and P4.[143] Although MPA is a progestin-based contraceptive, the gene expression profile induced by it was distinct from P4. MPA resulted in the induction of a gene expression signature related to inflammation and cholesterol synthesis which were linked to innate immunity and HIV-1 susceptibility. Another study looked at comparing and characterizing the transcriptional profile of primary endometrial GECs in E2 and P4 conditions following acute exposure to HIV-1.[144] The findings indicated that acute exposure of HIV-1 to primary endometrial GECs results in various genes related to plasminogen activation, adhesion and diapedesis, interferon response, and inflammation. Interestingly, exposure to HIV-1 in the presence of sex hormones E2 and P4 resulted in unique gene signatures, suggesting that the response of the GECs to HIV-1 is modulated by female sex hormones. A more recent study evaluated the transcriptional response of ALI culture-grown vaginal epithelial cells to MPA treatment and compared it to E2 and P4.[145] Not only were unique transcriptional profiles seen in all conditions, but MPA treatment resulted in induction of genes related to cell-cell division and cell adhesion, results which were not seen under E2 or P4. It was further found that the gene signature under MPA treatment is also indicative of decreased barrier integrity, which was confirmed with functional analyses, and used to help explain why women using MPA as a hormonal contraceptive are more susceptible to HIV-1 infection.

1.6.2 Bioinformatic Analysis

Transcriptome analysis is a valuable tool as it provides a blueprint for the construction of gene interaction networks, which is the basis for functional characterization and annotation of genes and pathways.[146] Thus, the information gained can be used to: correlate the cellular functions of biological systems under specific conditions;[147] develop molecular techniques to pinpoint potential

targets for drug discovery and diagnostics of disease processes;[148] as well as provide an interface for studying the relationship between hosts and pathogens in order to develop novel prophylactic or therapeutic interventions.[149]

Although transcriptome analysis has various applications, there is no specific analytical method that can be optimally applied universally.[150] Usually when transcriptomic data is based on human-based, heavily annotated genomes, the transcriptome analysis can be performed on either existent annotated references or by identifying novel transcripts based on their differential regulation.[150] Both approaches can be helpful in answering hypotheses, and have unique advantages; while using existent annotated references is an approach that is reliable since information can be extracted from publication records, identifying novel transcripts with the researcher's retrieved transcriptomic logistics allows for reporting of novel data.

After hybridization of genetic material to the probes in the transcriptome array chip, transcriptome analyses often start off by performing essential *preprocessing* steps such as background correction and normalization.[150] The bias that results from non-specific RNA binding to the probes, which can fluctuate between runs, along with uneven background fluorescence, is removed by the process of background adjustment. Within a microarray chip, probes can also target intronic regions or have no target at all. Anything that binds to such probes is found to create background, along with the non-specific binding that occurs for targeted probes. Normalization is also needed for correcting for systematic errors which lead to undesired biological effects. Normalization allows for removal of technical noise caused by variances in the following factors: amount of RNA, efficiency of RNA extraction, efficiency of reverse transcription, DNA quality and the PCR yield associated with it, and many other factors. When performing experiments such as qPCRs, normalization is done with the use of housekeeping genes, whose expression does not

change by different conditions. With microarrays, methods such as introduction of spike-ins, where introduction of markers whose relative intensities are controllable can be used to calibrate intensities, can assist with normalization.[151] Furthermore, normalization is also relevant to the array type used and thus aims to eliminate variation across the chips.[150, 152] Methods such as scale normalization can be performed to normalize intensities between different replicate chips of the same treatments to reduce chip-to-chip variation, where intensities from one chip are multiplied and compared to summaries of another chip. [153]This allows exclusion of misinformation from the downstream analyses, and provision of fair and accurate comparison of biological effects.

Subsequent steps in transcriptomic processing include the *core analysis*. This step is composed of processes such as 1) transcriptome profiling, 2) differential gene expression and 3) functional profiling.[150] The mapping of data from these samples using microarrays as a convenient method of visualization is what is referred to as transcriptional profiling. Differential gene expression analysis allows for profiling of genes which visually show where differences occur, and the differential expression provides quantitative data to explain to what extent it occurs. The last step in transcriptome analyses includes *functional profiling*.[150] This includes analysis of single genes of interest based on the total data generated; the most traditional approach and also the final stage of most transcriptomic studies.[154] This is often supplemented by analyzing volcano plots or protein networks which indicate various pathways, and is followed by various types of functional analyses such as qPCRs, ELISAs, immunofluorescence staining and other methods to confirm functionally. Limitations of selecting a single gene for further analysis is that there is no natural value for thresholds, and so, different results are obtained with different cut-off values used, making the metrics arbitrary. Alternatively, when analyzing genes with statistical significance, a unifying theme isn't obvious depending on the number of changes observed, leading to difficulties in

interpretation of data depending on level of expertise in this field. Most importantly, analyzing single genes is not practical and does not often provide obvious context to how they relate to biological processes, hence why various bioinformaticians practice analysis of data networks and pathway analyses.[147]

CHAPTER 2: RATIONALE, HYPOTHESIS AND OBJECTIVES

HSV-2 remains a global burden with incidence of infection disproportionately higher in women compared to men. However, the disproportionality of HSV-2 infection between sexes during heterosexual transmission is not well understood. Further investigation and a better understanding of the FRT microenvironment is crucial for developing preventative strategies. The FRT is significantly influenced by the presence of female sex hormones, such as estrogen and progesterone, which vary across stages of the menstrual cycle.

Multiple studies, including those from our lab, have shown using both *in vivo* and *in vitro* models, that P4 increases susceptibility to HSV-2, while E2 plays a protective role (Figure 7).[76-81] Since the mechanisms through which these phenomena occur are still unknown, studying the protective effects of E2 on epithelial cells is an informative model since they primarily contact with HSV-2. To examine the mechanisms underlying differential susceptibility in the context of hormones at a cellular level, our lab recently established and characterized an Air-Liquid-Interface (ALI) culture system which allows the vaginal epithelial cell line (VK2 cells) to proliferate, and form stratified layers in transwells, in a state that more closely mimics the natural environment of the lower vaginal tract.[78] This model allows us to study HSV-2 entry, infection and replication, since HSV-2 first infects vaginal epithelial cells. In a study done using ALI cultures of VK2 cells, we showed that VK2 cells grown in the presence of E2 displayed significantly lower infection and viral replication of HSV-2 relative to NH conditions.[78] However, the underlying mechanism of how E2 modulates immunity and influence susceptibility to HSV-2 remains unclear.

Consequently, we are interested in studying genes and cellular pathways which are differentially regulated by E2, to specifically understand how genes/pathways are modulated to provide protection. In order to study the effects of hormones on modulation of differentially

expressed genes (DEGs), we recently performed a comprehensive genome-wide microarray to profile gene expression of HSV-2-infected VK2 cells and compared how this profile is altered based on the presence or absence of E2 and P4. Hormone treatments were conducted using concentrations of 10^{-9} M of E2 and 10^{-7} M P4, since this represents the peak physiological serum concentrations of these hormones found throughout the menstrual cycle.[155] The microarray results demonstrated that there is a distinct profile of host genes regulated by HSV-2 in the presence of E2, P4 and no hormone (NH) conditions. Although we initially planned to investigate both E2 and P4 effects on HSV-2-infected VK2 cells, we narrowed our focus to investigating the effect of E2 due to its the unique transcriptional profile it encompasses compared to NH.

Based on previous literature studies and the outcome of results from our transcriptome studies, ***I hypothesized that E2 will modulate host cellular pathways in VK2 cells that contribute to antiviral immunity, and thus are responsible for its protection compared to NH, against HSV-2 infection and a systematic analysis will be able to identify unique pathways initiated by E2. Furthermore, based on the subsequent transcriptome analysis, I also hypothesized that the E2-mediated antiviral protection against HSV-2 in VK2 cells is mediated through the p53 pathway.***

Part of this hypothesis was addressed by ensuring an efficient and accurate pathway analysis where an accurate and non-redundant analytic approach of bioinformatics was determined and utilized to identify signaling pathways differentially activated by E2, such as the p53 pathway. As the next step, functional analysis was performed to link this finding of E2-induced p53 pathway to antiviral effects and protection seen against HSV-2.

The hypothesis was addressed through the following objectives:

Objective 1: Conducting bioinformatic pathway analysis to identify the differentially regulated genes and cellular pathways modulated in E2-treated HSV-2-infected VK2 cells

Objective 2: Conducting a functional analysis to determine whether

a) the p53 pathway is activated by E2 and b) if activation of p53 confers protection against HSV-2 in vaginal epithelial cells

Objective 3: Determining the mechanism of E2-mediated p53 protection against HSV-2 infection in VK2s

A

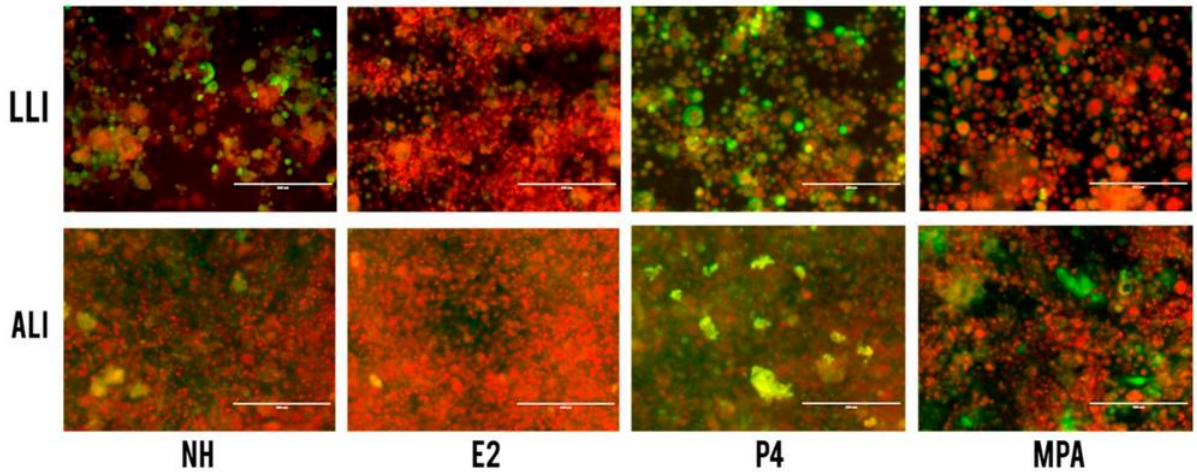

B

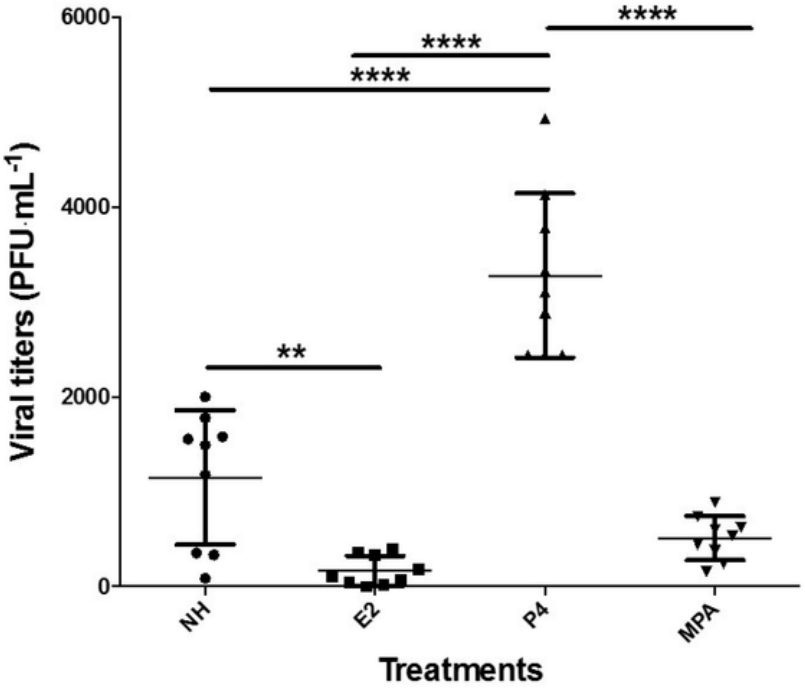

Figure 7: Female sex hormones and MPA influence HSV-2 infection and replication. (A) HSV-2-GFP (green) infection in NH/E2/P4/MPA-treated VK2 cells. Nuclei (red) counter-stained using propidium iodide. (B) Differences in HSV-2 viral shedding by VK2 cells treated exposed to different female sex hormones and MPA in ALI cultures. Figures were reproduced from Yung et al. 2016.[78]

RESULTS

CHAPTER 3: BIOINFORMATIC ANALYSIS AND IDENTIFICATION OF GENES AND PATHWAYS

Objective 1: Conducting bioinformatic pathway analysis to identify the differentially regulated genes and cellular pathways modulated in E2-treated HSV-2-infected VK2 cells

3.1 Performing bioinformatic analysis of differentially expressed genes from the transcriptomic data at a single-gene level

In order to investigate the effects of female sex hormones on vaginal epithelial cells and the response to HSV-2 infection, we isolated RNA from VK2 cells grown in various conditions. The experimental design consisted of four treatment groups: VK2 cells in ALI cultures without hormones or treated with E2 (10^{-9} M), P4 (10^{-7} M) or MPA (10^{-7} M) for 7 days followed by HSV-2 infection at a multiplicity of infection (MOI) of one for 24 hours. Following RNA isolation, an Affymetrix Human Genome 2.0 array was performed to obtain the transcriptome data. In addition to the data from these treatments, we also have data based on similar hormone treatments without HSV-2 infection (mock). Combination of these data has allowed us to generate many hypotheses. For example, an ongoing study compares HSV-2-infected and uninfected NH-/E2-/P4-/MPA-treated VK2 cells, allowing us to investigate the role of HSV-2 in modulating the transcriptional profile under different hormonal conditions. (Dhawan, Zahoor et al., in progress). While the above study focuses on the effect of virus on hormone-treated cells, the study outlined in this thesis, focuses on the effects that hormones have on host cellular pathways against the virus, specifically looking at how E2-/P4-/MPA-treatments modulate genes and pathways in response to HSV-2-infection in VK2 cells compared to untreated HSV-2 infected cells. Previous studies in our lab have also assessed the response of hormones against other viruses such as HIV-1, but in the context of endometrial GECs.[144]

Prior to performing core analyses, it was essential to determine the question of interest. As outlined previously, we planned to investigate the role of hormones in modulating the gene expression profile of the lower FRT, using VK2 cells, in the context of HSV-2 infection. Since our transcriptomic data was heavily annotated and contained large amounts of data, we decided to briefly look into identify novel transcripts by comparing conditions of SE2 (estradiol-treated VK2 cells infected with HSV-2 for 24 hours) with SNH (untreated VK2s cells infected with HSV-2 for 24 hours), SP4 (progesterone-treated VK2 cells infected with HSV-2 for 24 hours) and SMPA (MPA-treated VK2 cells infected with HSV-2 for 24 hours), as well as by comparing SP4 to SNH. A heatmap of all genes of the transcriptome data under NH, E2 and P4 conditions after infection with HSV-2 were plotted (Figure 8). This heatmap indicates a very quiet profile of E2, where most genes show low intensity of gene expression while P4 shows higher intensity relatively.

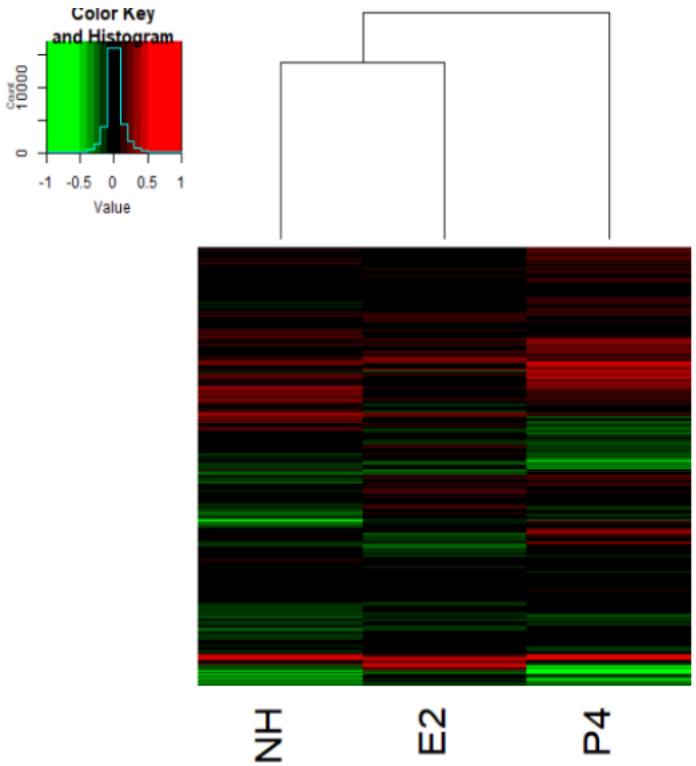

Figure 8: Vaginal epithelial cells infected with HSV-2 in presence of female sex hormones show differential expression of genes (A) Hierarchal clustering of all genes from the transcriptomic profile regulated by VK2 cells infected with HSV-2 are shown in the heatmap. The intensity of red and green indicate the magnitude of upregulated and downregulated gene expression, respectively, represented by the color key histogram. HSV-2-infected cells were grown in the presence of E2, P4 or NH were compared to uninfected cells grown in the presence of E2, P4, or NH, respectively.

To identify the differences and determine whether hormonal treatment results in a unique transcriptional profile, gene expression patterns of differentially expressed genes (DEGs) between HSV-2-infected VK2 cells grown under E2 vs P4 conditions were plotted with a heatmap using hierarchal clustering, where treatments with similar expression patterns are grouped together and connected by a series of branches (Figure 9A). First, a comparison of E2 vs P4 in the context of HSV-2 was performed to identify only significant DEGs between the two conditions. Then, gene expression values were plotted with a heatmap to visualize the expression patterns. The NH condition was also included to examine which treatment it is more similar to. The results indicated that the DEGs show similar expression patterns between P4 and NH treatments. Moreover, the heatmap also shows that various clusters of genes on the coloured panel to the left of the heatmap are clearly oppositely regulated by E2 compared to NH and P4. Overall, this suggests that E2 plays a more unique role in altering the transcriptomic profile of HSV-2-infected VK2s, compared to P4, hence we focused on investigating the E2 response in this project. With the hierarchal trees of P4 and NH columns, it is clear that they show closer resemblance in gene expression; however, some differences still exist and would be important to explore further.

After seeing distinct differences between all treatment groups, we performed differential gene expression analysis to investigate key genes ($p<0.05$). The analysis is shown by a Venn diagram (Figure 9B). Results indicate that E2 differentially regulates 624 unique genes (89% of all genes regulated by E2), which is 7.6 times more significant DEGs ($p<0.05$) than P4 (82 genes;

51.6% of all genes regulated by P4), when compared to NH conditions in the context of HSV-2 infection. The 77 that overlap between these conditions represent 9.83% of all significant DEGs between E2 and P4. Investigation of the unique DEGs belonging to each treatment, however, would be valuable in providing gene-specific roles of hormonal treatments. These results suggest female sex hormones differentially impact gene expression in HSV-2 infected VK2 cells, particularly under the influence of E2.

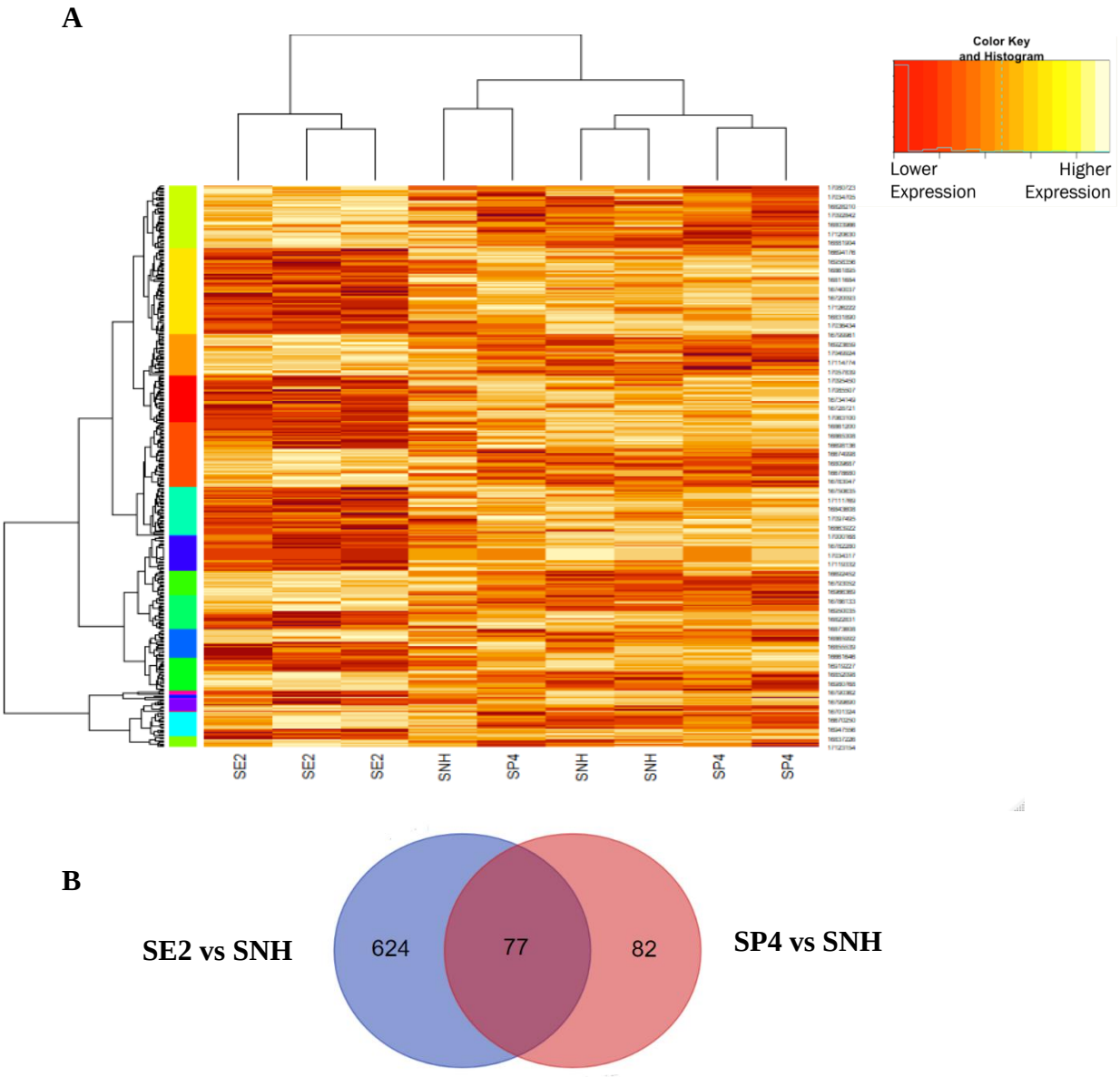

Figure 9: Estrogen treatment induces a distinct transcriptional profile in VK2 cells infected with HSV-2 (A) VK2 cells were grown in ALI cultures and treated with E2 (estrogen) (10^{-9} M), P4 (progesterone) (10^{-7} M), or no hormone (NH) controls. Extracted RNA from each treatment of each experiment (n=3) was analyzed, as indicated by three columns per treatment. Significantly differentially expressed genes between SE2 and SP4 comparison were selected, and their gene expression values plotted with a heatmap. No hormone (NH) condition was also included in addition to E2 and P4 to examine which treatment it resembles. Each row represents a gene and each column a treatment. The hierarchal tree of the columns (at the top) depicts the correlation of treatments. The hierarchal tree of the rows (at the left) depicts the correlation of certain genes, grouping them into clusters that distinguished by different colours with the bar on the left. Treatments and genes with similar expression profiles are presented in proximity of each other and connected by a series of branches. (B) Venn diagram showing significant differentially expressed genes in E2 vs NH and P4 vs NH comparisons of VK2 cells infected with HSV-2 ($p < 0.05$).

Since our transcriptomic data was heavily annotated and contained a large amount of data, we first decided to briefly look into identifying novel transcripts by investigating E2 vs NH, P4 vs NH, E2 vs P4 and MPA vs P4 comparisons for any highly significantly upregulated or downregulated genes. In order to further visualize differences of differentially expressed single genes, volcano plots depicting log fold change (FC) of all genes comparing E2 vs NH, P4 vs NH, E2 vs P4, and E2 vs MPA were generated (Figure 10). Results from the volcano plots indicate that genes such as late cornified envelope 3D (LCE3D), C-X-C motif chemokine ligand 14 (CXCL14) and cornified envelope protein cornefilin (CNFN) are affected by E2; not only do they show high significance and high logFC (fold change) compared to SP4 (Figure 10B), but the differential expression is also observed when compared to SNH (Figure 10A). Expression of these genes, however, is not significantly altered by P4 (Figure 10C). This suggests that the increased expression of these two genes is unique to E2-treated vaginal epithelial cells in the context of HSV-2 infection. Since MPA is a progestin-based compound, we compared E2 to MPA as well, similar as what was done with P4, to confirm the differences between estrogen and progestin compounds. When comparing SE2 vs SMPA (Figure 10D), late cornified envelope genes such as LCE3E and LCE1F, along with LCE3D, are significantly upregulated. Moreover, loricrin cornified envelope

precursor protein (LOR), as well as Small Proline Rich Protein 2B (SPRR2B) which is involved in keratinization, are both upregulated in SE2 vs SMPA comparison as well (Figure 10D). Therefore, the family of late cornified proteins is likely an important one regulated by E2 hormonal response in VK2 cells, particularly in comparison to progesterone-based treatments (P4 and MPA).

Despite the provision of high-throughput data, single gene analyses have various limitations as described before. Since looking at single genes is not as effective and does not provide a broader view of how the host cells respond to treatments, we decided to investigate the role of important contributing biological signaling pathways as well.

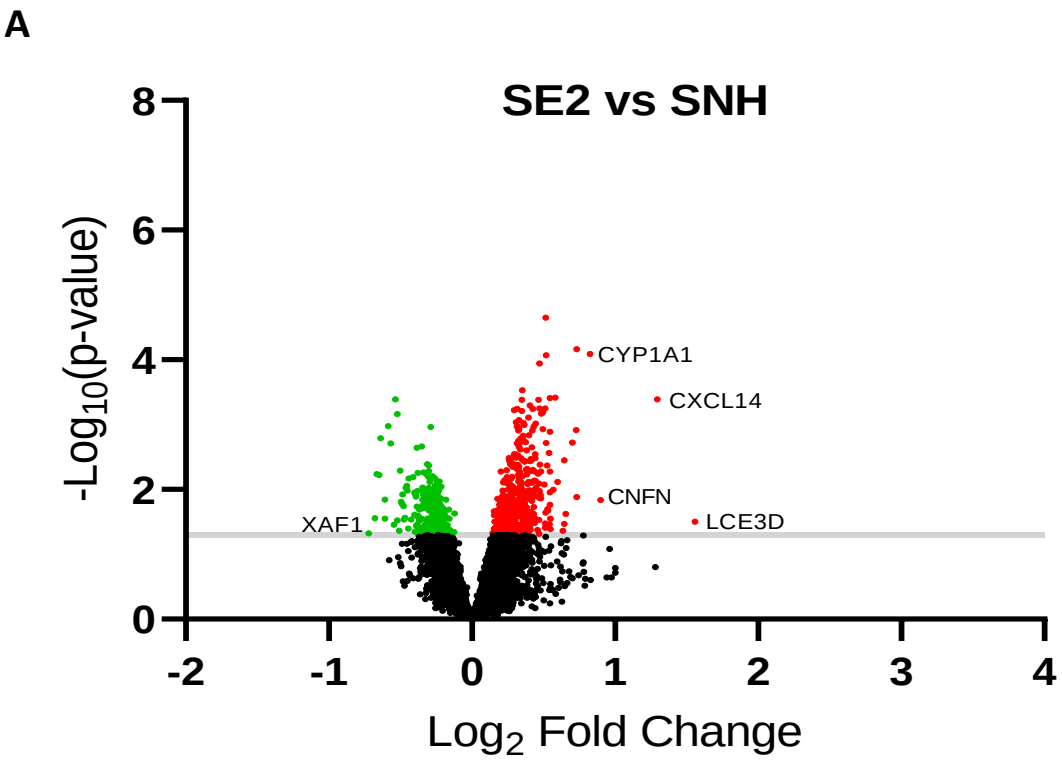

B

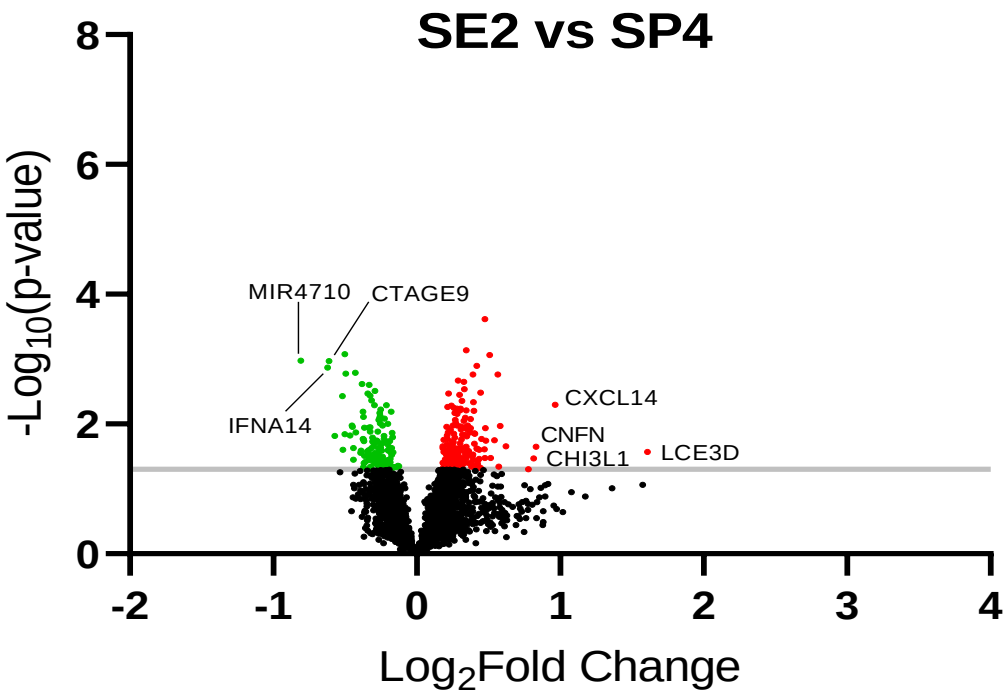
SE2 vs SP4
-Log10(p-value)
Log2Fold Change
MIR4710
CTAGE9
IFNA14
CXCL14
CNFN
CHI3L1
LCE3D
8
6
4
2
0
-2
-1
0
1
2
3
4

C

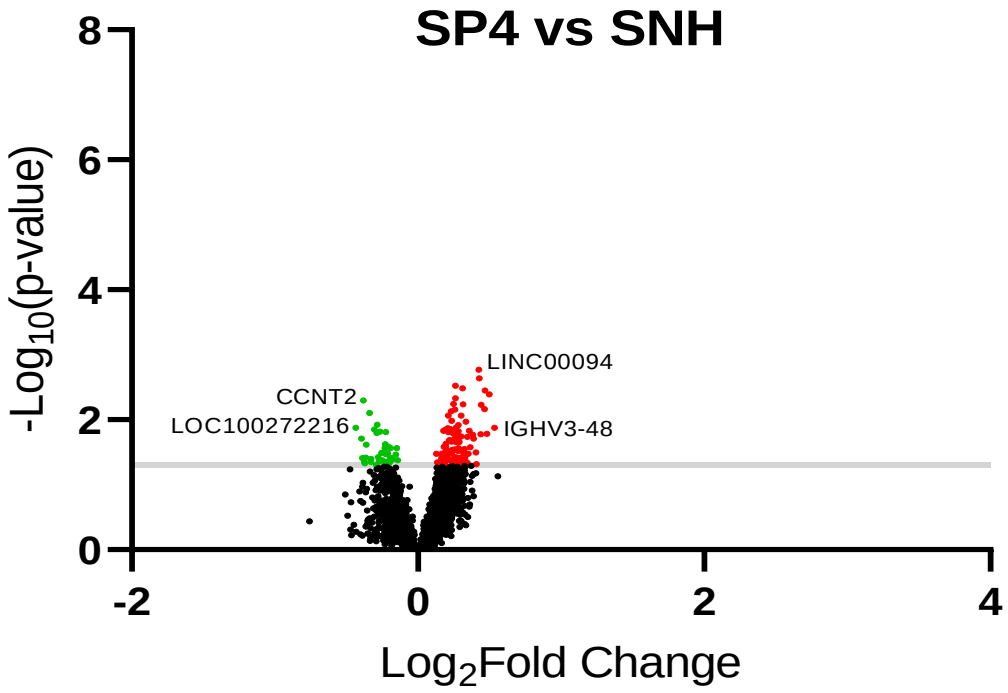
SP4 vs SNH
-Log10(p-value)
Log2Fold Change
LINC00094
CCNT2
LOC100272216
IGHV3-48
8
6
4
2
0
-2
0
2
4

D

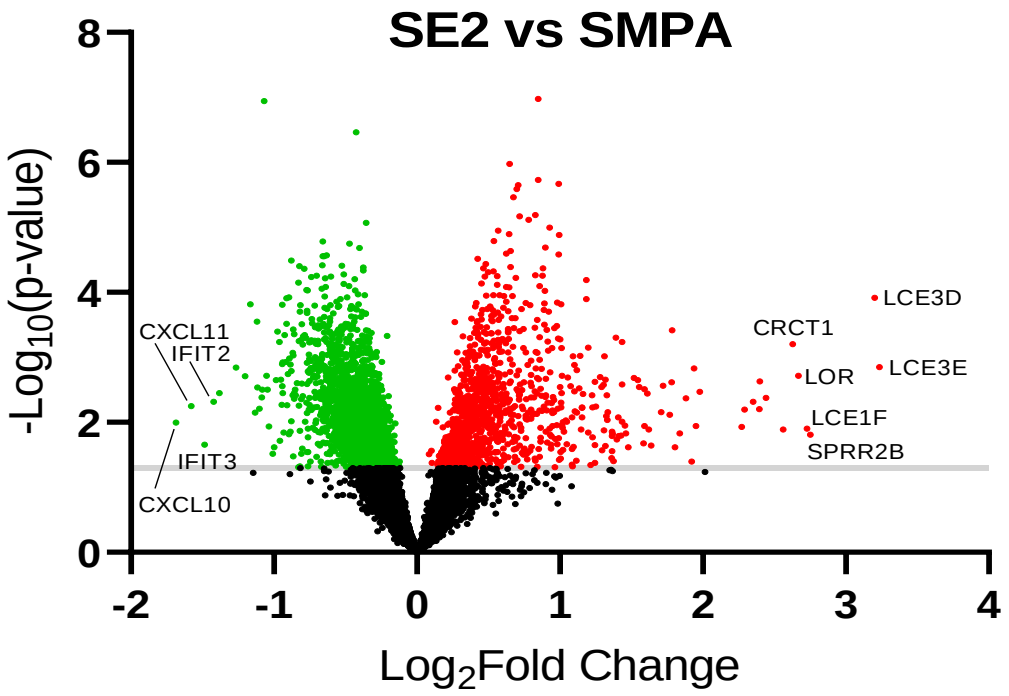

Figure 10: Volcano plots of differentially expressed of genes after HSV-2 infection in vaginal epithelial cells. HSV-2-infected cells grown in the absence or presence of E2, P4 or MPA were compared to show upregulated (red) and downregulated (green) genes. Volcano plots depict the computational fold change and p-values of DEGs between. (A) SE2 (HSV-2-infected VK2s treated with estrogen) vs SNH (HSV-2-infected VK2s treated without no hormones), (B) SE2 vs SP4 (HSV-2-infected VK2s treated with progesterone), (C) SP4 vs SNH and (D) SE2 vs SMPA (HSV-2-infected VK2s treated with MPA). Grey line represents p value cut-off of 0.05.

3.2 Perform gene set enrichment analysis (GSEA) of transcriptome data and analysis of corresponding differentially expressed genes

GSEA of transcriptomic data identifies pathways and determines their significance based on the magnitude of transcripts, and identifies the direction of the effect as upregulated and downregulated. A functional pathway is identified when it obtains enough enrichment of various genes from the transcriptomic profile. They are subsequently scored with normalized enrichment scores (NES), which indicates the abundance of genes enriched from the entire profile. GSEA comparing NH vs E2, NH vs P4, E2 vs P4 and E2 vs MPA conditions was performed (Figure 11). Comparison of E2 with progesterone-based treatments P4 and MPA helps highlight the difference in induced pathways, since E2 has opposite effects on susceptibility to infection against pathogens relative to P4 and MPA.[76, 77, 80] Since the GSEA identified various pathways, we focused on pathways with the lowest FDR values (FDR < 0.05) as they are more likely to be a true difference.

Enrichment analysis of DEGs between SE2 and SNH shows that genes altered by E2 treatment in HSV-2-infected VK2 cells fall into a total of 28 pathways (FDR < 0.25), of which 23 are upregulated and 5 are downregulated (Figure 11A). The top ten most significant and enriched pathways from the GSEA comparing E2 vs NH are epithelial mesenchymal transition with a normalized enrichment score (NES) of 2.03, myogenesis (2.01), hypoxia (1.99), coagulation (1.99), mitotic spindle (-1.90), p53 pathway (1.78), cholesterol homeostasis (1.74), interferon alpha response (-1.73), glycolysis (1.71) and apical junction (1.69) Enrichment analysis of DEGs between SP4 and SNH shows that genes altered after P4 treatment in HSV-2-infected VK2 cells fall into 15 pathways, all of which are upregulated (Figure 11B). The top ten most significant and enriched pathways from the GSEA comparing P4 vs NH are epithelial mesenchymal transition (1.99), hypoxia (1.93), cholesterol homeostasis (1.73), coagulation (1.74), myogenesis (1.59),

apical junction (1.55), peroxisome (1.43), apoptosis (1.43), pancreas beta cells (1.38), and angiogenesis (1.36).

Since E2 and P4 are both steroid hormones, it is expected that they may share some similar effects on pathways. However, we were most interested in studying pathways which are differentially affected to study the specific role of how E2 and P4 confer protection and susceptibility towards HSV-2, respectively. While comparing the pathways between E2 vs NH and P4 vs NH, the only pathways with an FDR < 0.05 which were unique to E2 were: p53 pathway, xenobiotic metabolism, estrogen response early and estrogen response late.

We wanted to ensure that these pathways maintain their significance when GSEA is performed on DEGs in E2 vs P4. As a result, we observed that in the context of HSV-2 infection, E2 treatment upregulates 17 pathways compared to P4, whereas P4 upregulates only 2 pathways relative to E2 (Figure 11C). The top ten most significant and enriched pathways from the GSEA comparing E2 and P4 are Myc targets V1 (-2.02), KRAS signaling down (1.95), myogenesis (1.89), mitotic spindle (-2.02), hypoxia (1.77), heme metabolism (1.67), coagulation (1.66), p53 pathway (1.63), xenobiotic metabolism (1.57) and estrogen response late (1.57).

We were interested in studying pathways which were upregulated in both SE2 vs SP4 and SE2 vs SNH, since these would demonstrate that E2 modulates these pathways significantly when compared to NH treatment as well as P4, thus potentially identifying unique pathways through which E2 provides protection against HSV-2. The pathways KRAS signaling down, myogenesis, hypoxia, and p53 pathway were all upregulated in both E2 vs P4 and E2 vs NH comparisons, whilst maintaining an FDR < 0.05. KRAS signaling down, myogenesis and hypoxia pathways appeared in P4 vs NH, thus indicating that they are not unique to the E2 response. P53 was the

only pathway that appeared to unique to E2 vs P4 and not enriched under P4 vs NH, yet common among both E2 vs NH and E2 vs P4. Therefore, we hypothesized that p53 may be an important contributor to E2-mediated protection against HSV-2.

Since MPA is a progestin-based contraceptive, we performed an enrichment analysis of E2 vs MPA to validate whether E2-based pathways are regulated when compared to MPA conditions as well (Figure 11D). Surprisingly, multiple pathways that were present in E2 vs P4 were more significantly upregulated and enriched by E2 in the comparison of E2 vs MPA. The top ten most significant and enriched pathways from the GSEA comparing E2 and MPA are hypoxia (2.92), KRAS signaling down (2.22), interferon alpha response (-2.14), mitotic spindle (-1.93), TNFa signaling via NFκB (1.85), G2M checkpoint (-1.84), Interferon gamma response (-1.84), cholesterol homeostasis (-1.81), p53 pathway (1.76), Myc targets V1 (-1.78). The p53 pathway was once again upregulated in E2 compared to MPA conditions.

A

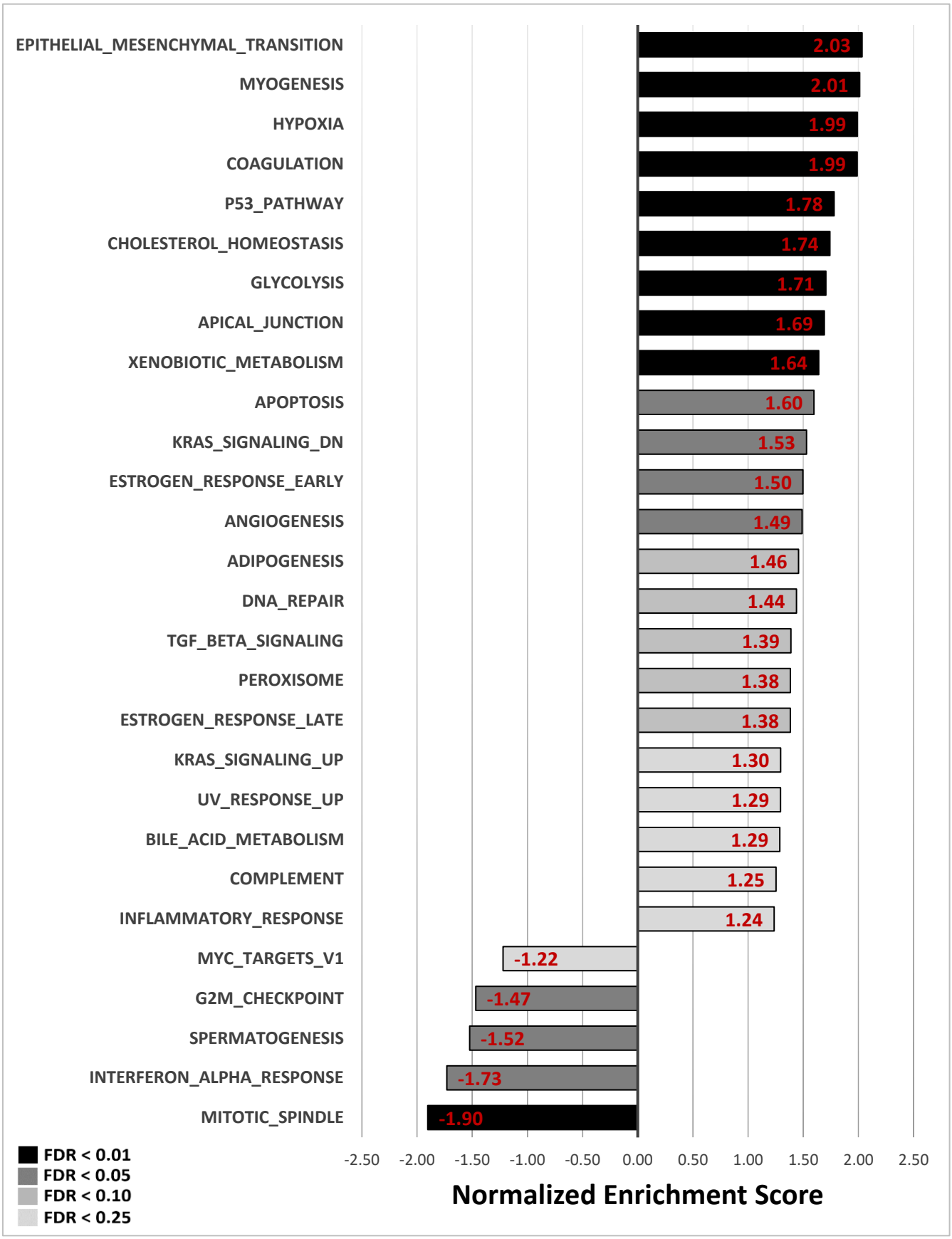
EPITHELIAL_MESENCHYMAL_TRANSITION 2.03
MYOGENESIS 2.01
HYPOXIA 1.99
COAGULATION 1.99
P53_PATHWAY 1.78
CHOLESTEROL_HOMEOSTASIS 1.74
GLYCOLYSIS 1.71
APICAL_JUNCTION 1.69
XENOBIOTIC_METABOLISM 1.64
APOPTOSIS 1.60
KRAS_SIGNALING_DN 1.53
ESTROGEN_RESPONSE_EARLY 1.50
ANGIOGENESIS 1.49
ADIPOGENESIS 1.46
DNA_REPAIR 1.44
TGF_BETA_SIGNALING 1.39
PEROXISOME 1.38
ESTROGEN_RESPONSE_LATE 1.38
KRAS_SIGNALING_UP 1.30
UV_RESPONSE_UP 1.29
BILE_ACID_METABOLISM 1.29
COMPLEMENT 1.25
INFLAMMATORY_RESPONSE 1.24
MYC_TARGETS_V1 -1.22
G2M_CHECKPOINT -1.47
SPERMATOGENESIS -1.52
INTERFERON_ALPHA_RESPONSE -1.73
MITOTIC_SPINDLE -1.90
FDR < 0.01
FDR < 0.05
FDR < 0.10
FDR < 0.25
-2.50 -2.00 -1.50 -1.00 -0.50 0.00 0.50 1.00 1.50 2.00 2.50
Normalized Enrichment Score

B

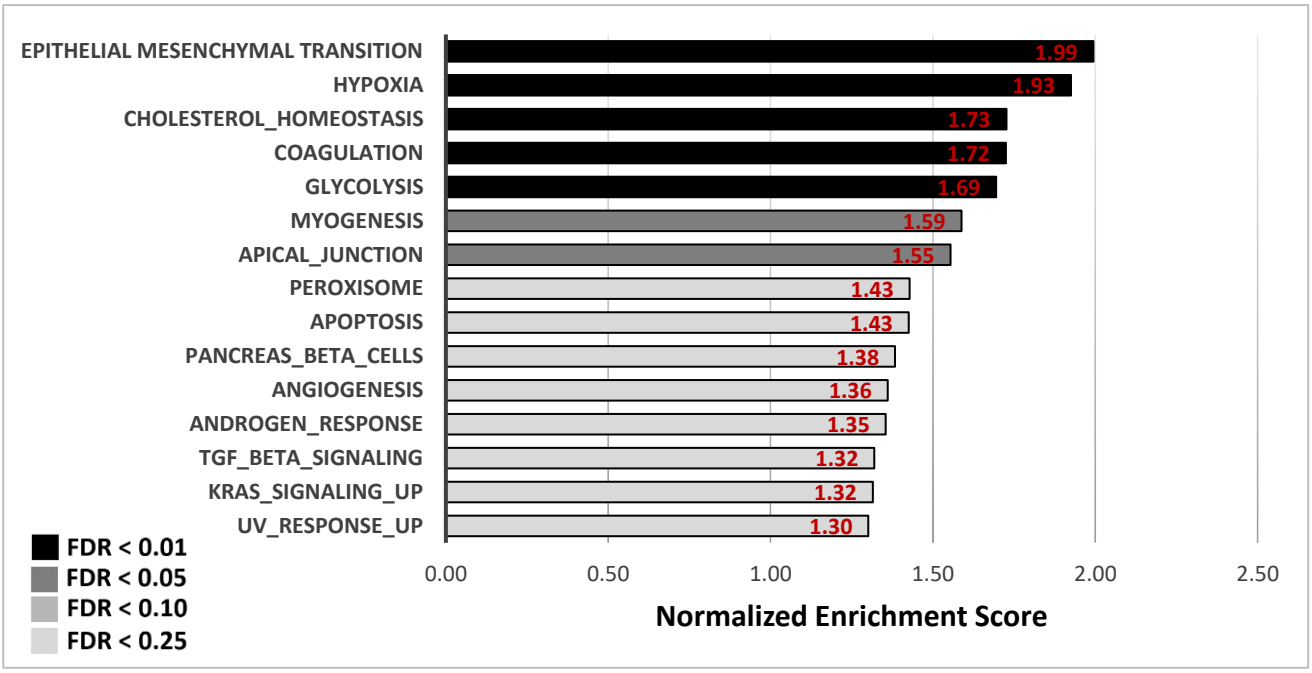
EPITHELIAL MESENCHYMAL TRANSITION 1.99
HYPOXIA 1.93
CHOLESTEROL_HOMEOSTASIS 1.73
COAGULATION 1.72
GLYCOLYSIS 1.69
MYOGENESIS 1.59
APICAL_JUNCTION 1.55
PEROXISOME 1.43
APOPTOSIS 1.43
PANCREAS_BETA_CELLS 1.38
ANGIOGENESIS 1.36
ANDROGEN_RESPONSE 1.35
TGF_BETA_SIGNALING 1.32
KRAS_SIGNALING_UP 1.32
UV_RESPONSE_UP 1.30
FDR < 0.01
FDR < 0.05
FDR < 0.10
FDR < 0.25
0.00 0.50 1.00 1.50 2.00 2.50
Normalized Enrichment Score

C

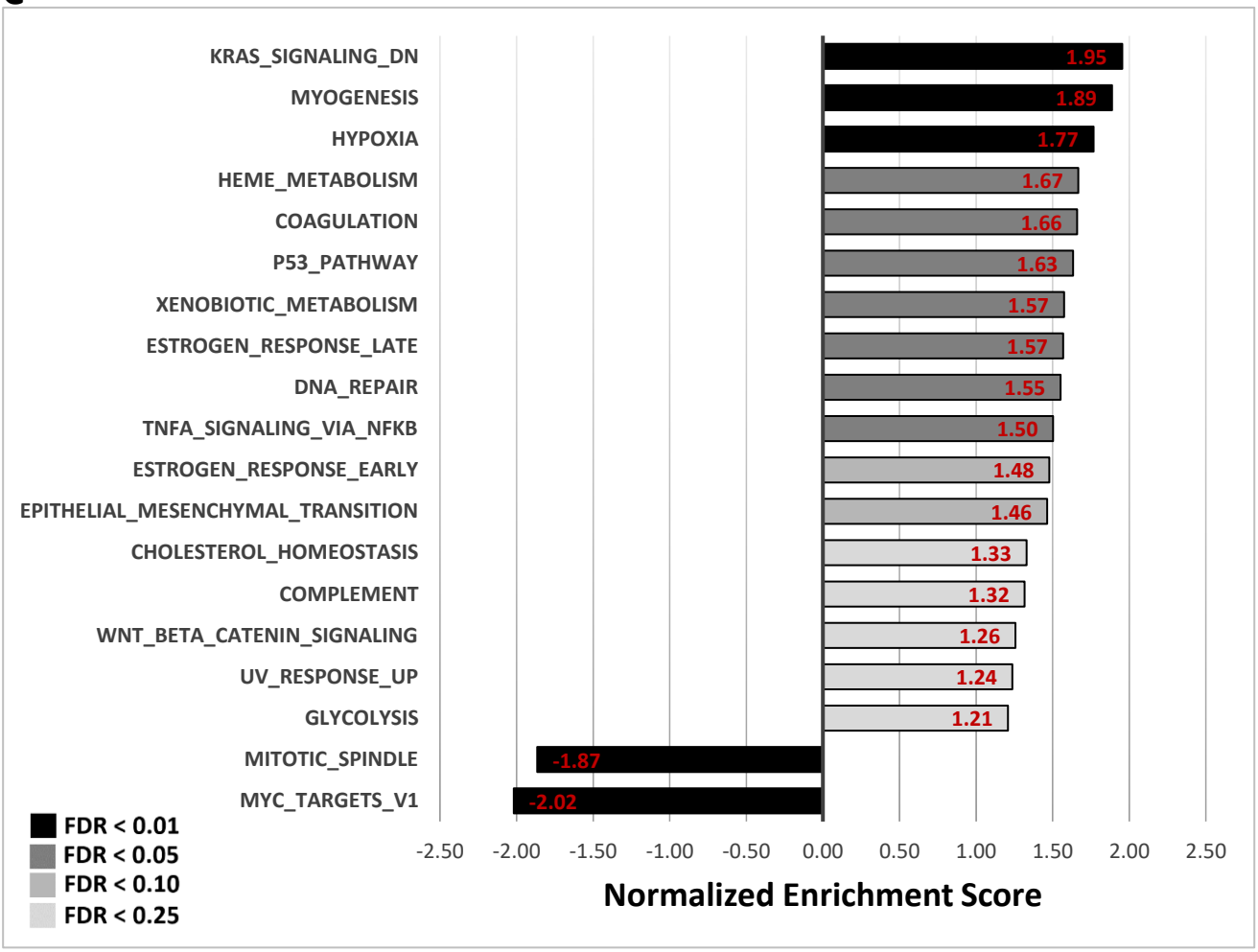
KRAS_SIGNALING_DN 1.95
MYOGENESIS 1.89
HYPOXIA 1.77
HEME_METABOLISM 1.67
COAGULATION 1.66
P53_PATHWAY 1.63
XENOBIOTIC_METABOLISM 1.57
ESTROGEN_RESPONSE_LATE 1.57
DNA_REPAIR 1.55
TNFA_SIGNALING_VIA_NFKB 1.50
ESTROGEN_RESPONSE_EARLY 1.48
EPITHELIAL_MESENCHYMAL_TRANSITION 1.46
CHOLESTEROL_HOMEOSTASIS 1.33
COMPLEMENT 1.32
WNT_BETA_CATENIN_SIGNALING 1.26
UV_RESPONSE_UP 1.24
GLYCOLYSIS 1.21
MITOTIC_SPINDLE -1.87
MYC_TARGETS_V1 -2.02
FDR < 0.01
FDR < 0.05
FDR < 0.10
FDR < 0.25
-2.50 -2.00 -1.50 -1.00 -0.50 0.00 0.50 1.00 1.50 2.00 2.50
Normalized Enrichment Score

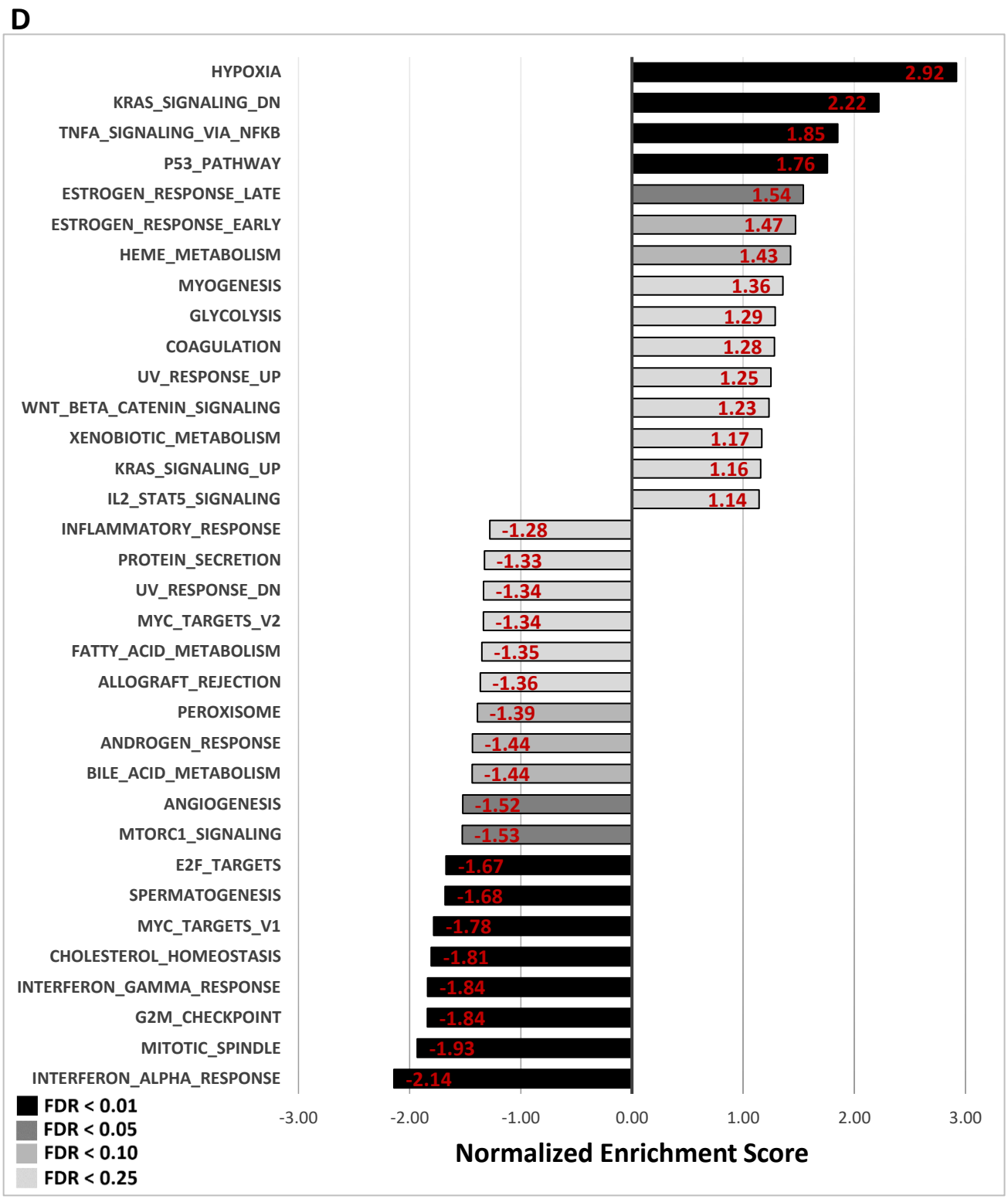

Figure 11: Gene set enrichment analysis (GSEA) with the Hallmark database. List of all significantly upregulated and downregulated pathways when comparing (A) SE2 vs SNH; (B) SP4 vs SNH; (C) SE2 vs SP4; and (D) SE2 vs SMPA transcriptomic profiles. Pathways are sorted by normalized enrichment score as well as false discovery rate values, as described in the legend.

Since the p53 pathway was upregulated in HSV-2-infected VK2 cells treated with E2 specifically, compared to all other experimental treatments (NH, P4 and MPA), and has previously been associated with innate immune functions, viral infection, and antiviral processes[121, 125, 128-131]; it was selected for further investigation. Figure 12 shows the distribution of genes from our dataset that contributed to the p53 pathway identified by GSEA. Most p53 pathway genes were found to be upregulated by E2 in comparison to NH and P4, demonstrated by the green peak towards the positive (left) side of the graph, indicating that the p53 pathway is being upregulated under E2 conditions. Additionally, we also performed a second order protein-protein network analysis of the genes under the E2 condition and found that the p53 pathway was a large contributor to this response, as indicated by the multitude of interacting proteins (Figure 13).

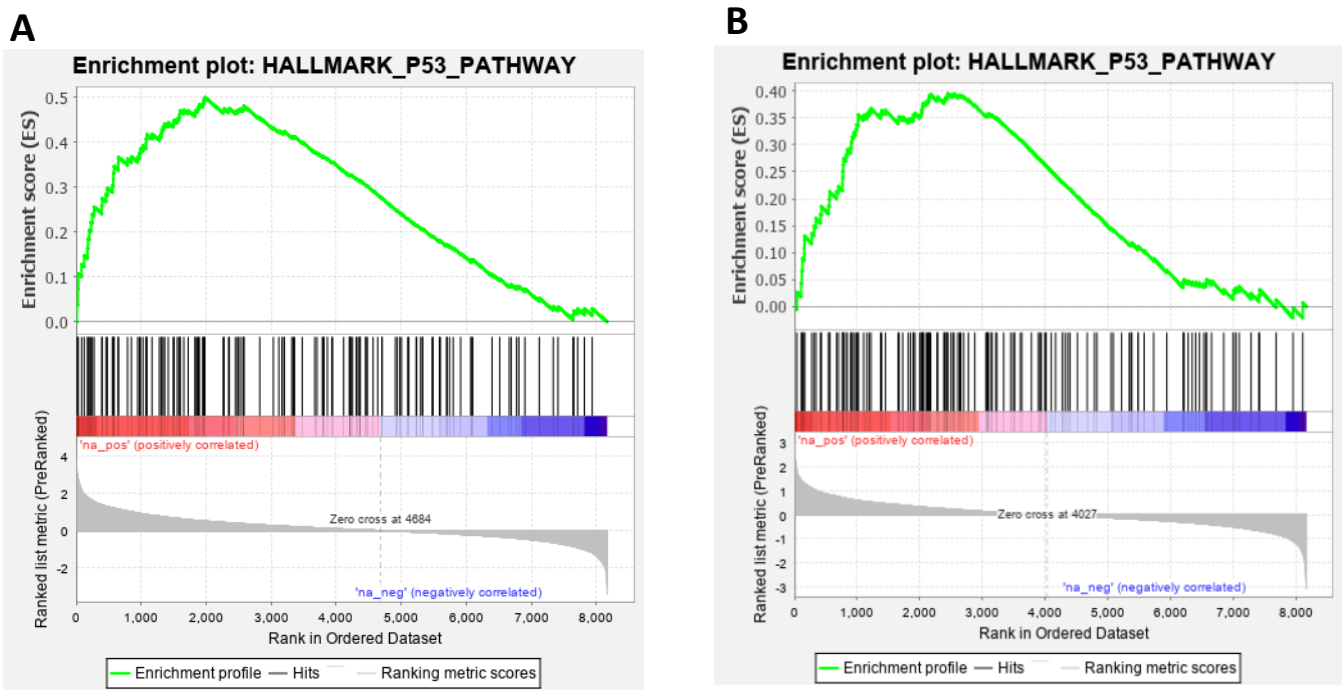

Figure 12: E2 treatment results in enrichment of p53 pathway genes in HSV-2 infected VK2 cells. GSEA enrichment plots of the p53 pathway genes identified using the Hallmark database between (A) SE2 vs SNH and (B) SE2 vs SP4.

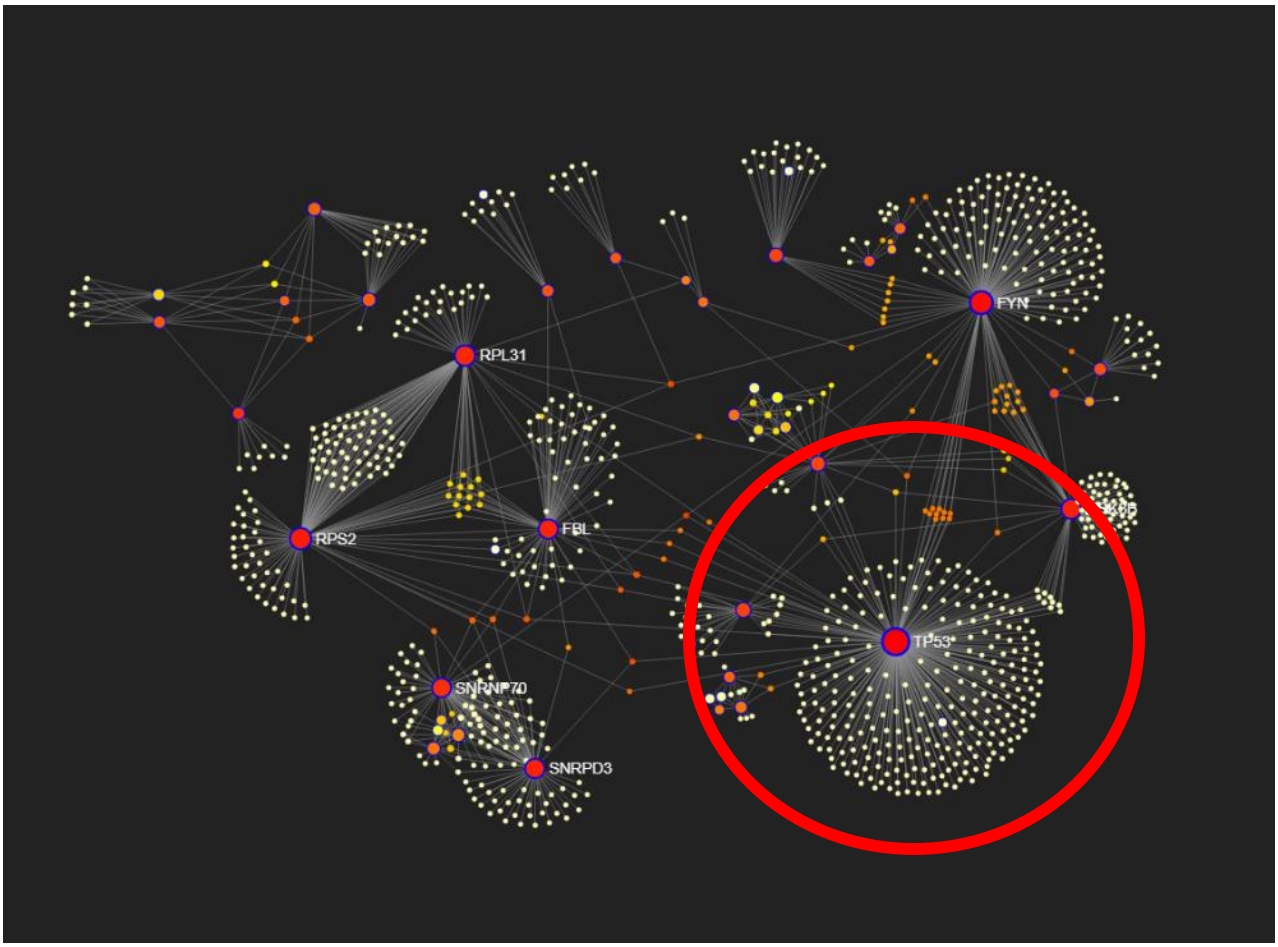

Figure 13: Protein network analysis of differentially expressed genes in estrogen-treated VK2s infected with HSV-2 indicate p53 as a major protein node hub. Second-order protein network showing differentially expressed genes ($P < 0.05$) in vaginal epithelial cells cultured in E2 hormone and infected with HSV-2. The p53 protein hub is identified with a red circle along with associated proteins linked to this hub.

Overall, our analysis suggested that p53 is a unique and potentially important contributor to the E2 response. Literature analysis further validated that p53 is associated with estradiol pathways, which may be the potential link E2's regulation of viral infections.[133-136, 138] After gaining strong consensus between our GSEA analysis and literature review, we decided to move forward with further investigating the p53 pathway and its contribution to E2-mediated protection against HSV-2.

CHAPTER 4: FUNCTIONAL ANALYSIS TO EXAMINE THE ROLE OF P53 IN E2 MEDIATED ANTI-VIRAL EFFECTS IN HUMAN VAGINAL EPITHELIAL CELLS

Objective 2: Conducting a functional analysis to determine whether

a) the p53 pathway is activated by E2 and b) if activation of p53 confers protection against HSV-2 in vaginal epithelial cells

4.1 Estrogen regulation of the p53 signaling pathway

4.1.1 Estrogen treatment induces expression of p53 in VK2 cells

As an initial step to connect the bioinformatics results with functional analysis, we conducted *in vitro* assays to test the hypothesis that the p53 pathway would be modulated in VK2 cells treated with E2. Therefore, we performed immunofluorescent staining on VK2 cells grown in E2 conditions to assess whether p53 is activated by E2. VK2 cells were grown in liquid-liquid interface (LLI) cultures for 7 days with either NH or E2 (10^{-9} M). As controls, cells were treated with Nutlin-3 (5 µM), an activator of the p53 pathway, and Pifithrin-α-HBr (PFT-α) (10 µM), an inhibitor of the p53 pathway, based on various studies in literature.[156-160] More information about these compounds can be found in section 7.2 of Material and Methods.

Effects of estradiol are exerted in cells through estrogen receptors (ERs). While there are two forms of ERs, ERα and ERβ, we analyzed the expression of ERα since it is the predominant form found in female reproductive tract tissues. With the high prevalence of ERα known to be present in female genital tissues,[88] it is expected that VK2 cells will be able to consequently express high levels of this receptor as well. Treatment with E2 is expected to further increase ERα levels, form a homodimer complex and induce downstream pathways of ER signaling by interacting with estrogen response elements.[161] Moreover, some studies report that ERα interacts with p53 through and that interaction at residues beyond amino acid 103 may be involved in this protein-protein interaction.[162] Furthermore, one study shows that ER-positive MCF-7 breast cancer cells to

respond to E2 by an increase in p53 levels.[163] Therefore, we performed examined the effect of estradiol on ERα to confirm the effect of estradiol on VK2 cells, as well as p53 to examine its association with E2, by performing immunofluorescent staining of ERα and p53 (Figure 14A). VK2 cells were grown in LLI conditions under various treatments: no hormone (NH) treatment served as background control to the effects of E2. Nutlin-3 (5 μM) was added to NH to examine upregulation of p53 in absence of E2 and PFT-α (10 μM) was added alone or to E2-treated cells to examine the effect of inhibition of p53. Immunofluorescence intensity of p53 was also quantified in the respective conditions, as seen in Figure 14B. We observed a significant increase in p53 protein expression after E2 treatment when compared to NH ($p<0.001$) (Fig 12 A and B). The addition of Nutlin-3 in no hormone conditions resulted in significant upregulation of p53 immunofluorescence compared to NH alone ($p<0.01$), but not as potently as E2. Therefore, the increase in p53 expression observed in the E2-treated group indicates that the p53 pathway is an important contributor to E2 hormone response. In this experiment, we decided to add PFT-α after E2 treatment and used this condition for multiple experiments later for two main reasons. First, it should be noted that since the basal level of p53 is low in NH conditions, it can be difficult to confirm whether PFT-α is functioning efficiently in these conditions. Thus, addition of the p53 inhibitor to E2 would better show whether the inhibitor is truly reducing p53 levels with a more noticeable difference since E2 induces higher levels of p53 than what we see in NH. Second, it can help distinguish E2-mediated results that are dependent on p53 activation, since PFT-α inhibits p53 downstream of E2. We would therefore be able to deduce the importance of the p53 pathway in contributing to E2-mediated protection that is observed against HSV-2 infection.

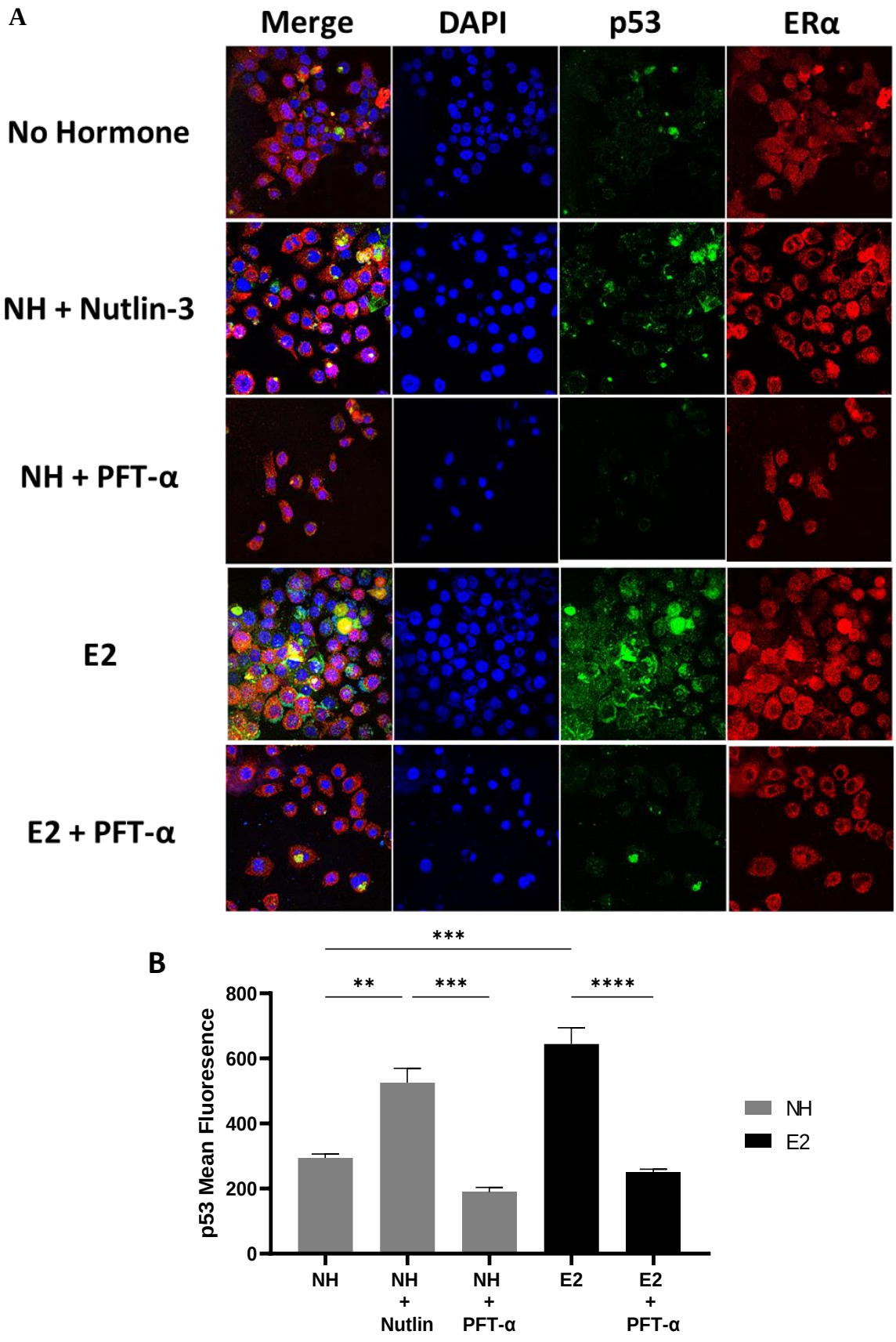
A
Merge
DAPI
p53
ERα
No Hormone
NH + Nutlin-3
NH + PFT-α
E2
E2 + PFT-α
B
***
**
***
****
p53 Mean Fluoresence
800
600
400
200
0
NH
NH + Nutlin
NH + PFT-α
E2
E2 + PFT-α
NH
E2

Figure 14: Estrogen treatment induces expression of p53 in VK2 cells (A) VK2 cells grown in LLI culture were treated with no hormone, E2, NH + PFT-α (10 µM), NH + Nultin-3 (5 µM) or E2 + PFT-α (10 µM) and subsequently fixed and stained with DAPI (blue), p53 (green) and ERα (red) using antigen-specific antibodies. Occasional yellow stain indicates colocalization of p53 (green) and ERα (red). Images were captured on confocal microscope at x600 magnification. Representative images are shown. (B) Quantification of p53 fluorescent intensity under respective conditions with ImageJ software with mean fluorescence measurements presented. Data shown represents mean ± SEM (n=3) with conditions done in duplicates. Statistical significance: **p <0.01, ***p < 0.001, ****p < 0.0001.

We further investigated the modulation of p53 and ERα mRNA gene expression under these treatments. VK2 cells were grown in ALI cultures treated with no hormone, E2, NH + Nultin-3 (5 µM) or E2 + PFT-α (10 µM) up until day 7, as described in section 7.2 – 7.3 of Materials and Methods. Cultures were then left uninfected or overlayed with HSV-2 on ice for 2 hours, washed and finally incubated for 2, 8 or 24 hours prior to RNA extraction. The extracted RNA was used for cDNA synthesis and RT-qPCR of p53 and ERα, as described in section 7.12 of Materials and Methods. Interestingly, we observed that p53 gene expression was significantly increased by E2 treatment, compared to NH in uninfected mock conditions, as well as after HSV-2 infection for 2 and 8 hours (Figure 15A). Gene expression of ERα, however, was not significantly affected by E2, p53 activation or p53 inhibition at all time points before and after HSV-2 infection (Figure 15B).

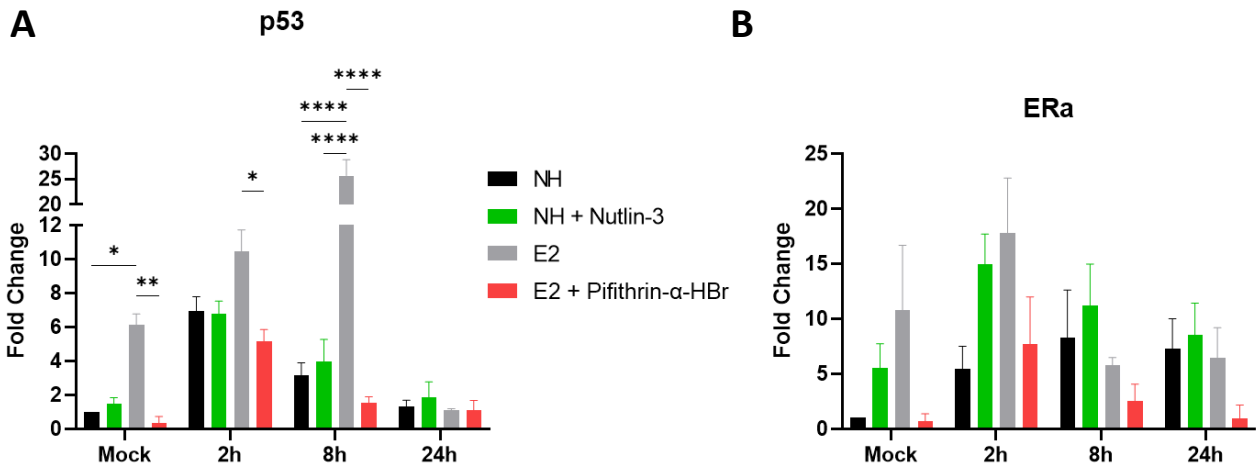

Figure 15: E2 upregulates p53 mRNA expression in VK2 cells prior to and after HSV-2 infection. VK2 cells were grown in ALI cultures under various treatments up until 7 days: no hormone, E2 (10^{-9} M), NH + Nultin-3 (5 µM) or E2 + PFT-α (10 µM) prior to being infected with HSV-2 for 2, 8 or 24 hours or left uninfected. VK2s were subsequently lysed after each time point for RNA collection. (A) p53 and (B) ERα mRNA eexpression was assessed in VK2s by RT-qPCR before and after 2, 8 and 24 hours of HSV-2 infection. Data shown represent mean ± SEM (n=3) with conditions done in duplicates. Data was analyzed using two-way ANOVA, with Bonferroni test to correct for multiple comparisons. Statistical significance: *p<0.05, **p <0.01, ****p < 0.0001.

Nutlin-3 and PFT-α reagents failed to alter gene expression of p53. One limitation of using PFT-α is that it is a reagent that may have other unreported off-target effects. Moreover, PFT-α is known to inhibit p53 post-translationally through a mechanism that is still unknown. This may be one of the reasons why differences in mRNA expression of p53 are not seen after PFT-α treatment. A recent study analyzing the specific effects of PFT-α on p53 modulation shows that PFT-α treatment degrades p53 which has been phosphorylated at Ser15 and Ser33 sites, which are types of post-translational modifications.[164]

To address whether PFT-α is behaving as it should with its post-translational effect on p53, we performed immunofluorescent staining of Ser15 phosphorylated p53 (p-p53). VK2 cells were grown in LLI cultures supplemented with no hormone or E2, in combination with either no treatment, Nultin-3 (5 µM) or PFT-α (10 µM) as described in materials and methods. Cell cultures were then fixed, stained for p-p53 and visualized with confocal microscopy (Figure 16A). Fluorescent intensity of p-p53 was also quantified with ImageJ software (Figure 16B). Since p-p53 results in nuclear translocation and subsequent activation, this experiment also addressed whether E2 treatment plays a role in promoting p53 activation. Results showed that Nutlin-3 treatment showed similar pattern as E2, where p-p53 expression was significantly elevated relative to NH conditions (Figure 16 A and B). Interestingly, NH treatment alone showed minimal p-p53 expression, hence why comparing NH + PFT-α to NH alone is not the best way to deduce PFT-α

function. However, when E2 + PFT-α is compared to E2 alone, a significant reduction in p-p53 is seen. Overall, results from this immunofluorescent staining indicate that PFT-α treatment is indeed able to inhibit p53 post-translationally, thus confirming that the PFT-α is functioning efficiently to inhibit p53. These findings also indicate that E2 not only increases total p53 expression, but also plays a role in promoting its activation.

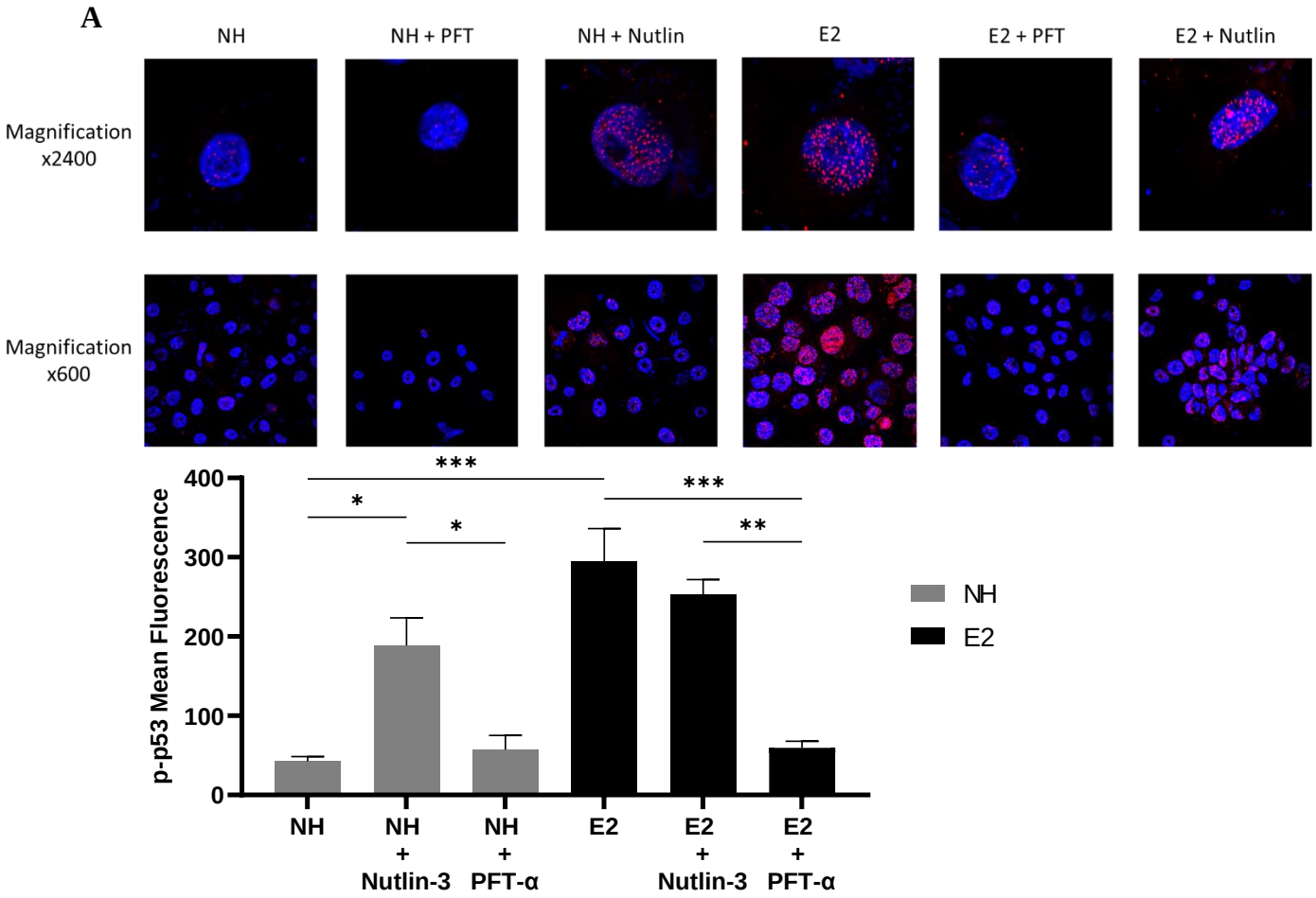

Figure 16: Estrogen treatment induces p-p53 in VK2 cells A) VK2 cells were grown in LLI cultures under NH or E2 (10^{-9} M) in combination with or without PFT-α (10 µM) or Nutlin-3 (5 µM) and subsequently fixed and stained with DAPI (blue) and Ser 15 phosphorylated p53 (red). Images were captured on confocal microscope at x2400 magnification. Representative images are shown. B) Quantification of p-p53 fluorescent intensity under respective conditions with ImageJ software with mean fluorescence measurements presented. Data shown represents mean ± SEM (n=2) with conditions done in duplicates. Statistical significance: *p < 0.05, **p <0.01, ***p < 0.001.

4.1.2 Nutlin-3 treatment upregulates p53 and Pifithrin treatment inhibits p53 in a dose dependent manner

To confirm we are used optimal concentrations of p53 activator and inhibitor, we performed a dose response curve analysis of both Nutlin-3 and PFT-α reagents in combination with either NH or E2 treatment conditions. Since most studies that have used Nutlin-3 have reported to use working concentrations ranging between 0.5 µM and 10 µM, we decided to investigate this range.[156, 158, 165, 166] To see whether higher doses would further activate p53, we also decided to try 50 µM, a dose that is 10-fold and 100-fold higher than our selected 5 and 0.5 µM doses, respectively. To determine the optimal dose range of Nutlin-3 in VK2 cells, we first experimented with these four different doses 0.5µM, 5 µM, 10 µM and 50µM, all provided for 48 hours of treatment. The effect of increasing doses of Nutlin-3 treatment on p53 expression in presence of NH or in combination of E2 was examined (Figure 17). Nutlin-3 treatment at 5µM and 10µM demonstrated the highest fluorescence of p53 protein in NH conditions (Figure 17A and C). We also performed a similar dose response curve of Nutlin-3 with E2 conditions (Figure 17 B and D). However, results indicated that Nutlin-3 has no additional effect on the p53 expression with E2, suggesting two things: 1) Nutlin-3 may function through similar pathways as E2; 2) E2 highly induces p53 expression to a level which Nutlin-3 cannot surpass. Surprisingly, the highest dose of 50µM in addition to E2 treatment (Figure 17 B and D) significantly reduced p53 fluorescence back to basal levels seen in NH conditions in Figure 17 A and C, and may also be killing the cells based on minimal cell counts observed during confocal imaging. This may indicate that Nutlin-3 may have an optimal curve in VK2s which peaks at approximately 10µM. This observation is similar to how many drugs have been found to behave, where under high doses the effect may no longer be discernible or may actually have opposite effects.[167]

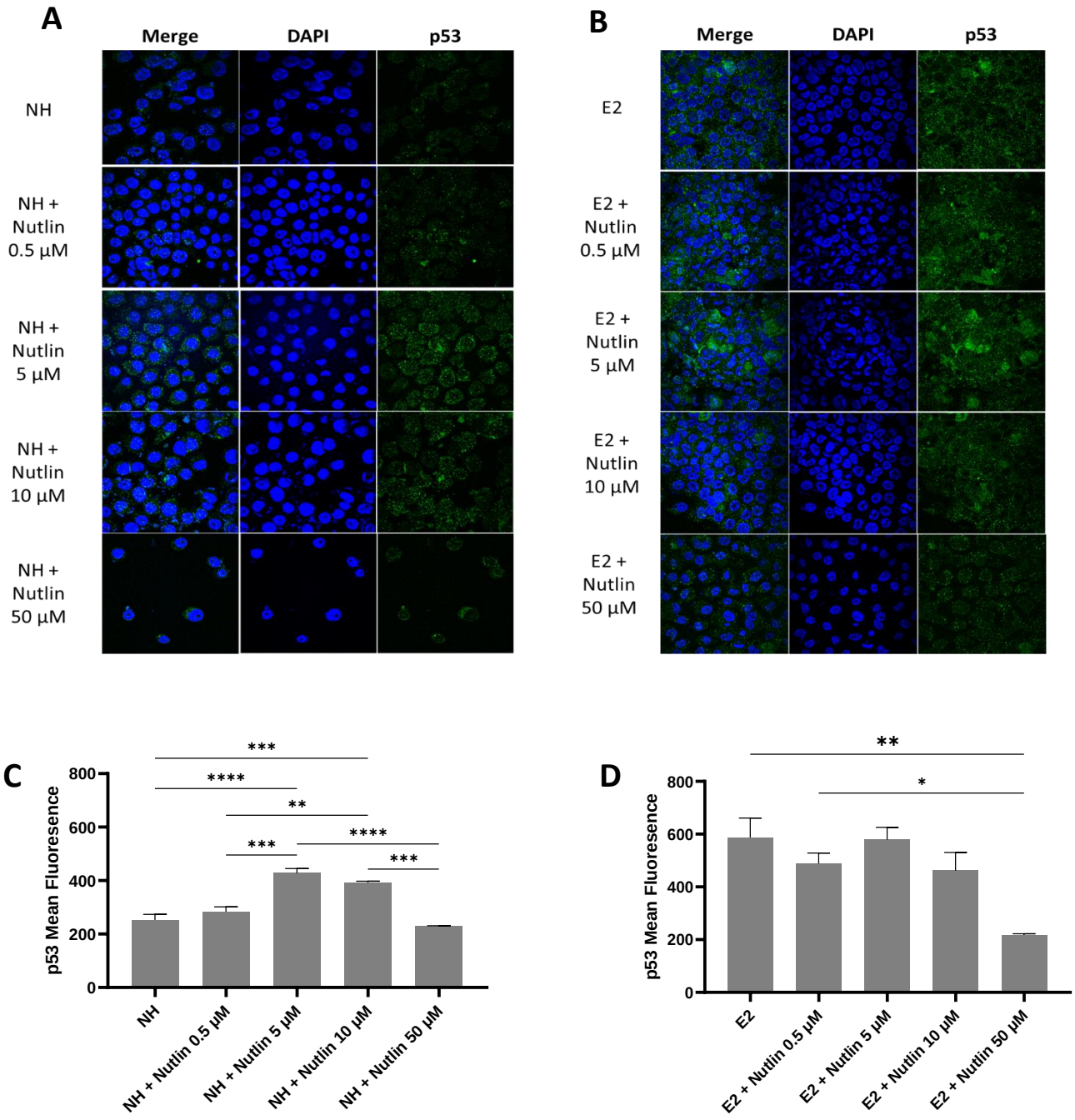

Figure 17: Nutlin-3 treatment upregulates p53 in a dose-dependent manner. VK2 cells were grown in LLI cultures in NH or E2 (10^{-9} M) conditions, and either left untreated or treated with various concentrations of Nutlin-3 (0.5 µM, 5 µM, 10 µM, 50 µM). Immunofluorescent staining of p53 was performed to visualize the dose response of Nutlin-3 in (A) no hormone or (B) E2 conditions. Images were captured on confocal microscope (n=3) at x600 magnification. Representative images are shown. Fluorescence intensity of p53 in VK2s was measured after Nutlin-3 treatment in (C) No hormone and (D) E2 conditions using ImageJ software with mean fluorescence presented. Data shown represents mean ± SEM (n=2) with conditions done in duplicates. Statistical significance: *p<0.05, **p <0.01, ***p < 0.001, ****p < 0.0001.

A similar process to assess the dose response curve of PFT-α was performed in VK2s. A short literature review was conducted to identify that most studies that have used PFT-α have reported to use working concentrations of 10 µM.[158-160]We decided to investigate this concentration, as well as doses that are 10-fold lower since high levels of PFT-α can be toxic to cells. Nevertheless, we decided to try 50 µM as well to see whether it can reduce the dose further. Therefore, to determine the optimal dose range of PFT-α in VK2 cells, we first experimented with four different doses 0.1 µM, 1 µM, 10 µM and 50µM, all provided for 1 hours of treatment. We experimented with four different doses ranging from 0.1µM to 50µM, all provided for 1 hour of treatment. VK2 cells were grown with or without hormones for 7 days of LLI culture as described in material and methods, and the effect of increasing doses of PFT-α treatment on p53 expression in the presence of NH or in combination with E2 was examined (Figure 18). LLI cultures were fixed and stained for DAPI and p53, prior to visualization with confocal microscopy. PFT-α treatment at in all doses demonstrated the significant reduction in p53 fluorescence in NH conditions when compared to NH alone (Figure 18 A and C). We also performed a similar dose response curve of PFT-α with E2 conditions. A similar effect in reduction of p53 was observed in E2-treated cells, as observed in the NH condition (Figure 18B and D). Since our previous working concentration of 10µM shows similar efficiency in reducing p53 expression as the highest dose of 50µM of PFT-α, we continued to work with 10 µM.

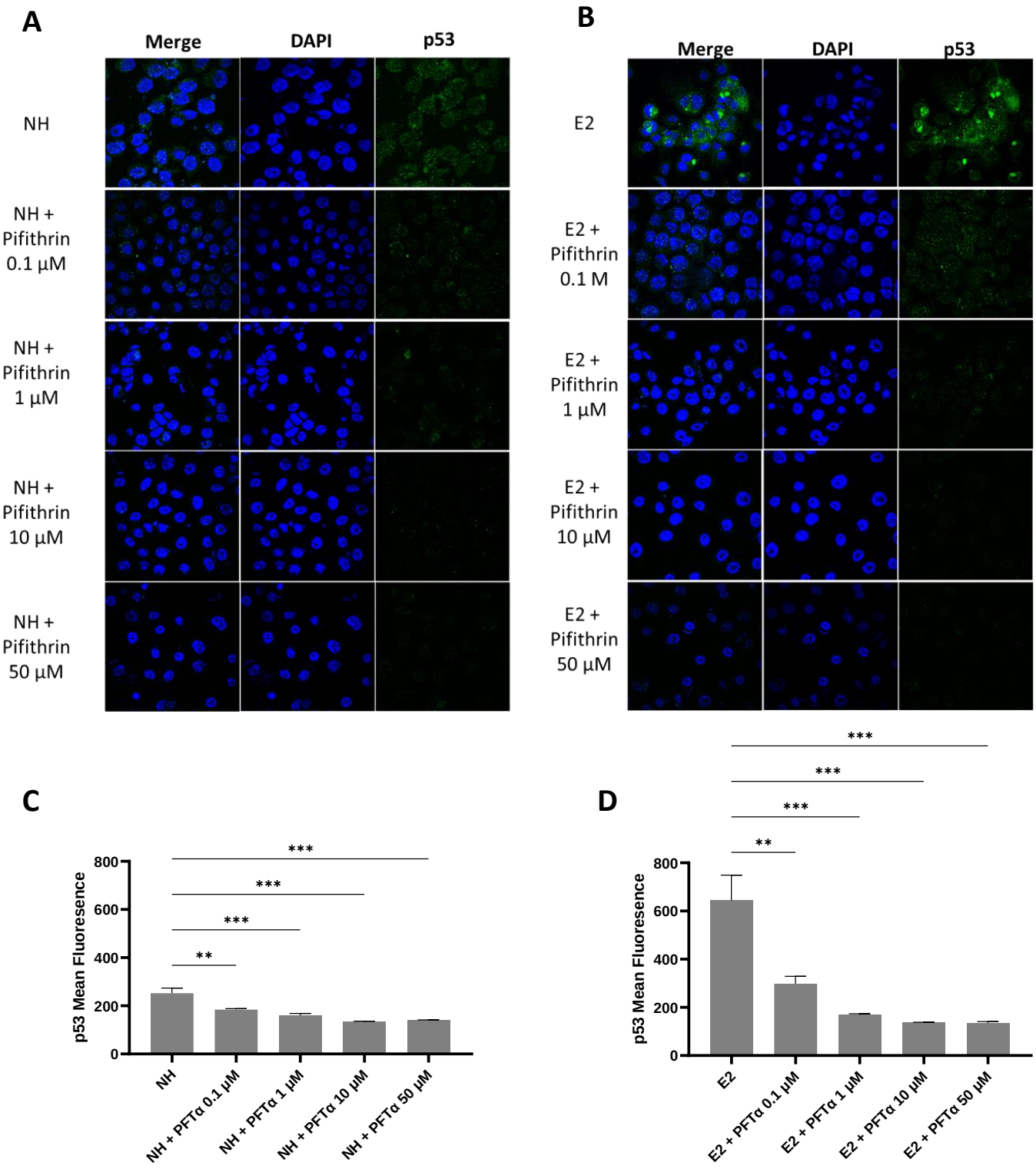

Figure 18: PFT-α treatment inhibits expression of p53 in a dose-dependent manner. VK2 cells were grown in LLI cultures in NH or E2 (10^{-9} M) conditions, and either left untreated or treated with various concentrations of PFT-α (0.1 µM, 1 µM, 10 µM, 50 µM). Immunofluorescent staining of p53 was performed to visualize the dose response of PFT-α in A) no hormone or (B)

E2 conditions. prior to being fixed for immunofluorescent staining of p53. Images were captured on confocal microscope (n=3) at x600 magnification. Representative images are shown. Fluorescence intensity of p53 in VK2s was measured after PFT-α treatment in (C) No hormone and (D) E2 conditions using ImageJ software with mean fluorescence presented. Data shown represents mean ± SEM (n=3) with conditions done in duplicates. Statistical significance: **p <0.01, ***p < 0.001.

Moreover, previous studies have also established that the maximum non-toxic concentration of PFT-α concentration is 10μM, while the maximum usable concentration is 30μM.[168] However, this may differ with various variables such as the type of cell line used, the duration that the reagent is provided, the media reagent is provided in, etc. Therefore, this led us to investigate the effects of our reagents and their selected doses on survival of VK2 cells.

Once optimal concentrations were confirmed, we analyzed the cytotoxic effect on VK2 cells at these concentrations of activator and inhibitors to ensure that cell viability is not negatively affected by these treatments. VK2 cells were seeded in ALI cultures with various experimental conditions over 8 days. We decided to investigate this timeline because E2 treatment is given for 7 days, and it is vital to determine whether it has effects on cell viability over this time-period. The eight day is essential since HSV-2 infection is performed during that day; it would be important see whether any differences in cell viability occur during this day in with absence of virus. If differences are seen, then this may be a factor which contributes to differences seen in HSV-2 infection/replication in experiments we execute later, since less cells would result in less viral shedding. A trypan blue exclusion assay (Figure 19A) was first performed, where cells from each condition were trypsinized, neutralized and collected for cell counting and cell viability every day for 8 days to monitor the effect. No significant differences in cell viability were observed among NH+ Nutlin-3, E2 or E2 + PFT-α when compared to NH alone. Similarly, cells were grown in ALI cultures in similar conditions for 8 days, and media was added on the apical side for 1 hour each

day, and subsequently collected, as described in material and methods. Using these supernatants, Lactate Dehydrogenase (LDH) cell viability assay (Figure 19B) was performed to verify results of the trypan blue exclusion assay. In this assay, lysis buffer was used to perform 100% lysis of one transwell of VK2 ALI cell culture to serve as a positive control**.** The LDH activity of different treatments resulted similar results and no differences in cell viability were seen by the various treatments when compared to NH alone and were minimal compared to the positive control. This confirmed that the selected concentrations for use in our experiments will not interfere with the functional analysis we planned to conduct.

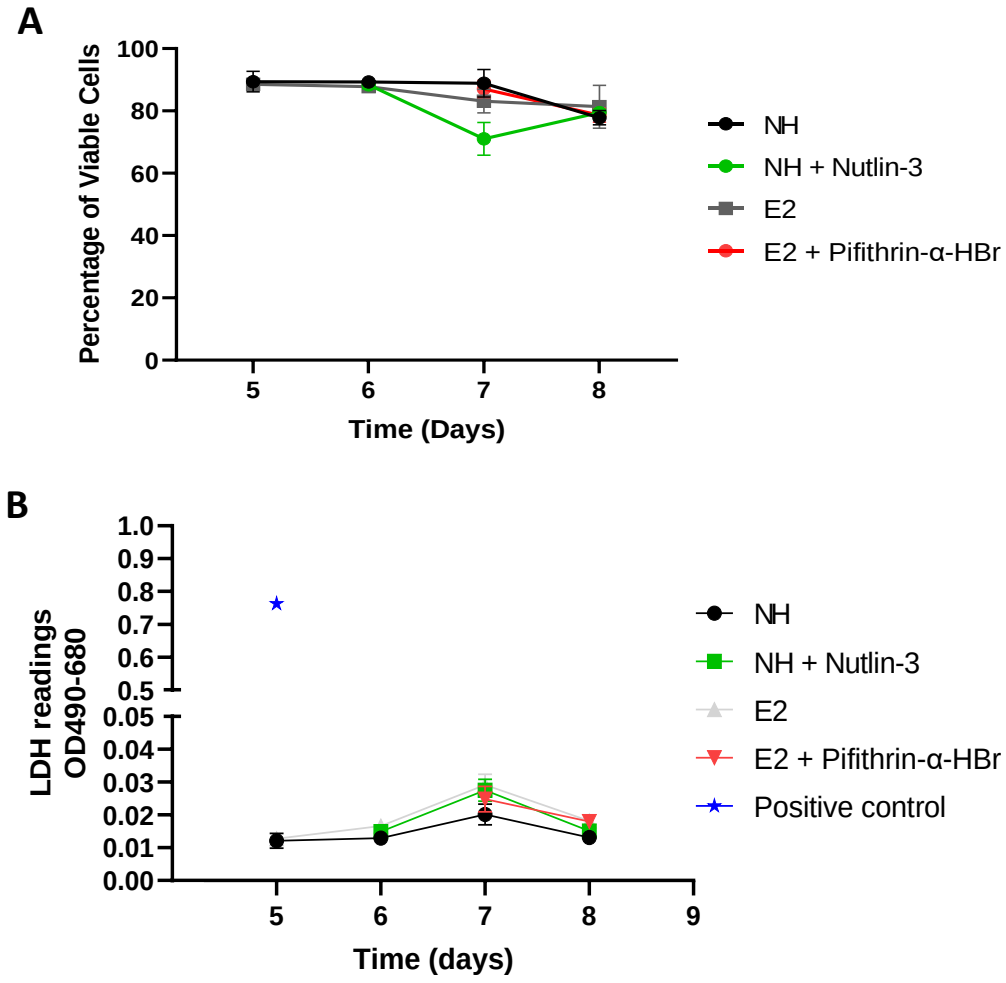

Figure 19: Cell viability of VK2 cells is not affected by E2, Nutlin-3 or PFT-α treatments. VK2 cells were grown under various treatments up until 7 days: no hormone, E2 (10^{-9} M), NH + Nultin-3 (5 µM) or E2 + PFT-α (10 µM), and washed on the 7th day. (A) Trypan blue dye exclusion test was used to quantify percent viable cells each day over a period of 8 days. (B) Media was added on apical side of ALI culture for 1 hour and collected each day for 8 days, and used for lactate dehydrogenase (LDH) assay. 100% lysis of one transwell of VK2 cells acted as the positive control. Data are mean ± SEM for (n = 3) with conditions done in triplicates

4.2 Effects of E2 on the p53 signaling pathway in ectocervical and endometrial primary epithelial cells

One limitation of using the VK2 cell line is that they are immortalized with the addition of E6/E7 sequences from Human papillomavirus (HPV). The E6 protein has been known to associate with p53 as a mechanism by which HPV induces tumors.[169] The E6 protein also has been known to target p53 for proteosome-dependent degradation, contributing to virus-induced cellular transformation.[169] To address this limitation and confirm whether the effects we see are not due to E6/E7 interference, we performed immunofluorescent staining of p53 and ER-α in primary epithelial cells, which are not under the influence of E6/E7 genes.

We investigated the effects of E2 and the p53 inhibitor and activator in primary ectocervical cells, which are part of the lower FRT and form a stratified non-keratinizing squamous epithelium similar to vaginal cells. Since primary vaginal cells are difficult to obtain, ectocervical cells are the next best representation of how vaginal cells would behave due to their similarity in morphology and growth. Ectocervical tissues were obtained surgically from women who were undergoing hysterectomy, and subsequently digested with enzymes for ectocervical cell extraction, as described in section 7.6 of Materials and Methods. Ectocervical cells were seeded sparsely in LLI culture conditions for 7 days in various combinations of treatments similar to those done in VK2s. No hormone (NH) treatment served as background control to the effects of E2. Nutlin-3 (5 μM) was added to NH to examine upregulation of p53 in absence or presence of E2, and PFT-α (10 μM) was added alone to E2-treated cells to examine the effect of inhibition of p53. After completion of 7 days since initial seeding, cells were fixed and immunofluorescent staining of p53 and ERα was performed (Figure 20A), as described in section 7.17 of Material and Methods. Fluorescence intensity of p53 protein levels in the respective conditions was quantified, as seen in

Figure 20B. Results were similar to those observed in VK2 cells. The addition of Nutlin-3 to NH, E2 alone, and addition of Nutlin-3 to E2 all resulted in increased p53 fluorescence as compared to NH alone. Addition of PFT-α to E2 resulted in reduction of p53 expression compared to E2 alone, resulting in reduction to a similar level seen in NH.

A

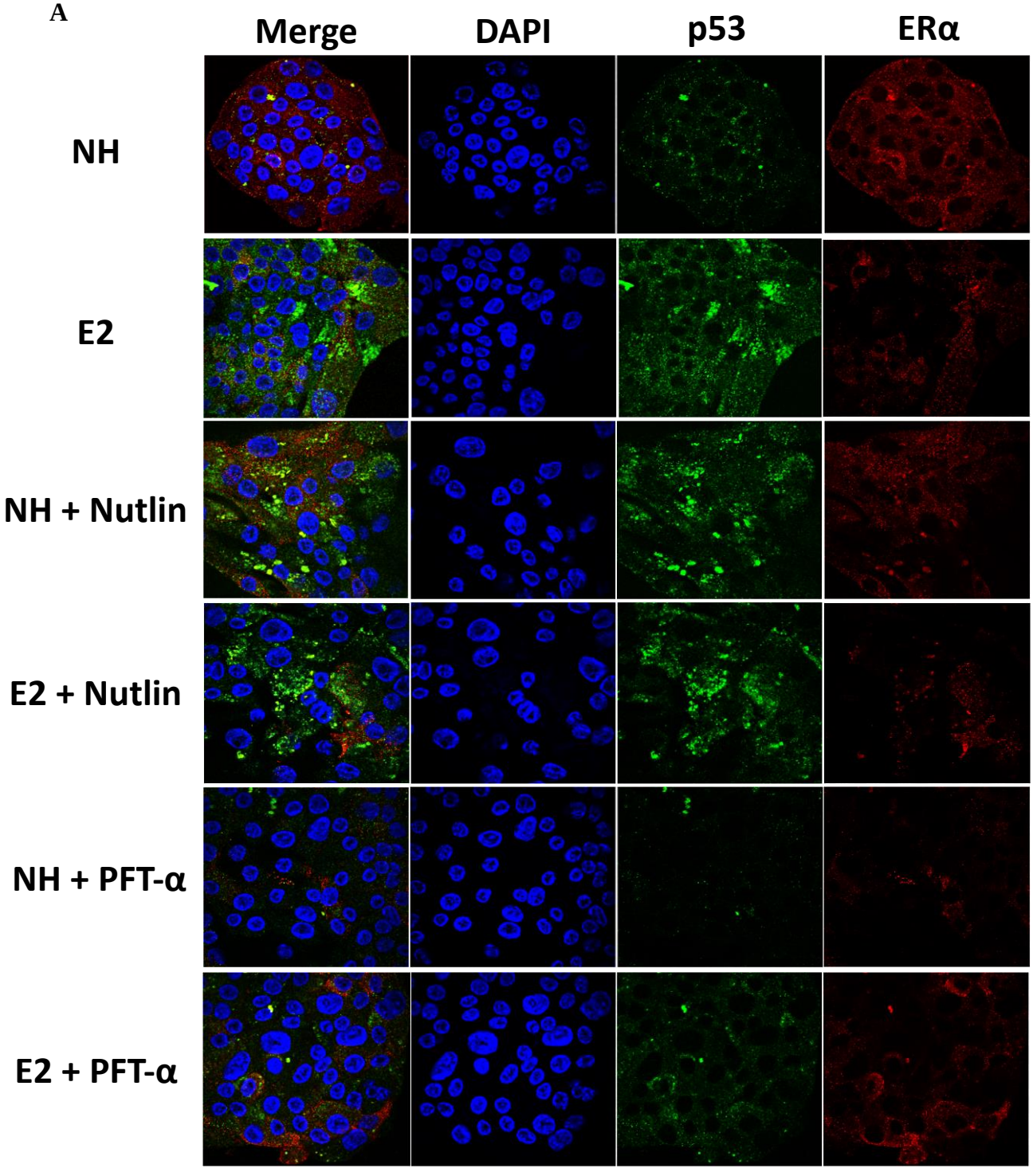

B

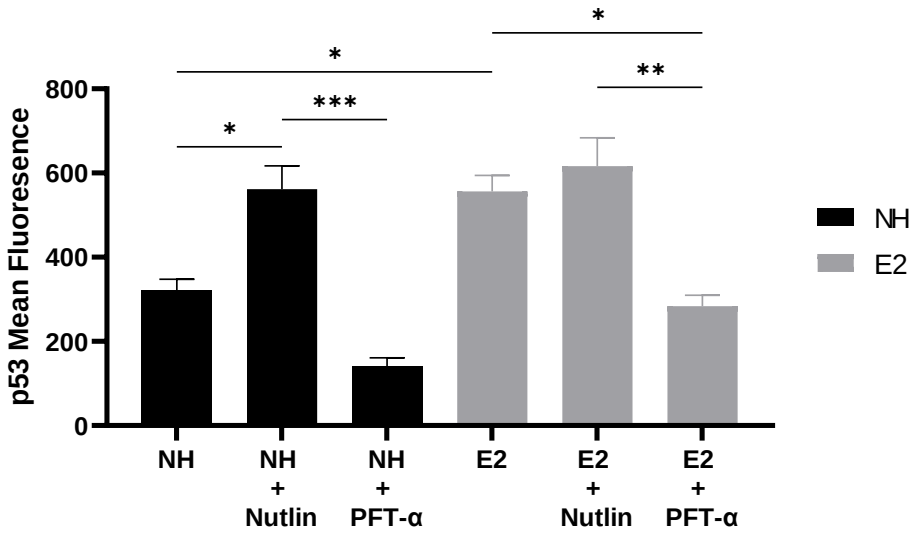

Figure 20: Estrogen treatment induces expression of p53 in primary ectocervical cells (A) Primary ectocervical cells were isolated from human ectocervical tissues as described in material and methods. Cells were plated and grown in LLI cultures and treated with either no hormone or E2 (10^{-9} M), with addition of Nutlin-3 (5 µM), PFT-α (10 µM) or left untreated. Cells were subsequently fixed and stained with DAPI (blue), p53 (green) and ERα (red). Occasional colocalization stain (yellow) in nuclei indicates p53 and ERα are colocalized. Images were captured on confocal microscope (n=2) at x600 magnification. Representative images are shown. (B) Quantification of p53 fluorescent intensity under respective conditions was performed with ImageJ software with mean fluorescence presented. Data shown represents mean ± SEM (n=2) with conditions done in duplicates. Statistical significance: *p<0.05, **p <0.01, ****p < 0.0001.

We were also interested in investigating whether the upper and lower FRT respond similarly or differently to E2 treatment. The endometrium is highly dynamic and its growth, regeneration and differentiation in response to the menstrual cycle is highly and specifically influenced by ovarian hormones. Similar to ectocervical tissues, endocervical tissues were obtained surgically from uteruses of women who recently underwent hysterectomies, and subsequently digested with enzymes for endocervical cell extraction, as described in materials and methods. Endocervical cells were seeded sparsely in LLI culture conditions for 7 days in various combinations of treatments, as described above. No hormone (NH) treatment served as

background control to the effects of E2. Nutlin-3 (5 μM) was added to NH to examine upregulation of p53 in absence of E2 and PFT-α (10 μM) was added to E2-treated cells to examine the effect of inhibition of p53. After 7 days, cells were fixed and immunofluorescent staining of p53 and ERα was performed (Figure 21A), as described in material and methods. Fluorescence intensity of p53 protein levels in the respective conditions was quantified, as seen in Figure 21B. Immunofluorescent staining of primary endometrial cells showed similar results as those seen in ectocervical cells and VK2 cells, where E2 alone or addition of Nutlin-3 to NH results in increased p53 expression, compared to NH alone. Addition of PFT-α, however, suppresses expression of p53 compared to E2, as well as compared to NH. Interestingly, significantly higher colocalization of p53 and ERα is seen in endometrial cells treated with E2 or NH + Nutlin-3 (Figure 21A), compared to similar conditions in ectocervical (Figure 20A) and VK2 (Figure 14A) cells.

Overall, results from these primary genital epithelial cells indicate that the E6/E7 genes do not interfere as a variable in the modulation of p53 in response to E2 treatment, as well as p53 inhibitor and activator reagents. Moreover, we can also conclude that E2-mediated p53 induction is not specific to just the lower FRT, but rather, similar in various cell types of the FRT.

A

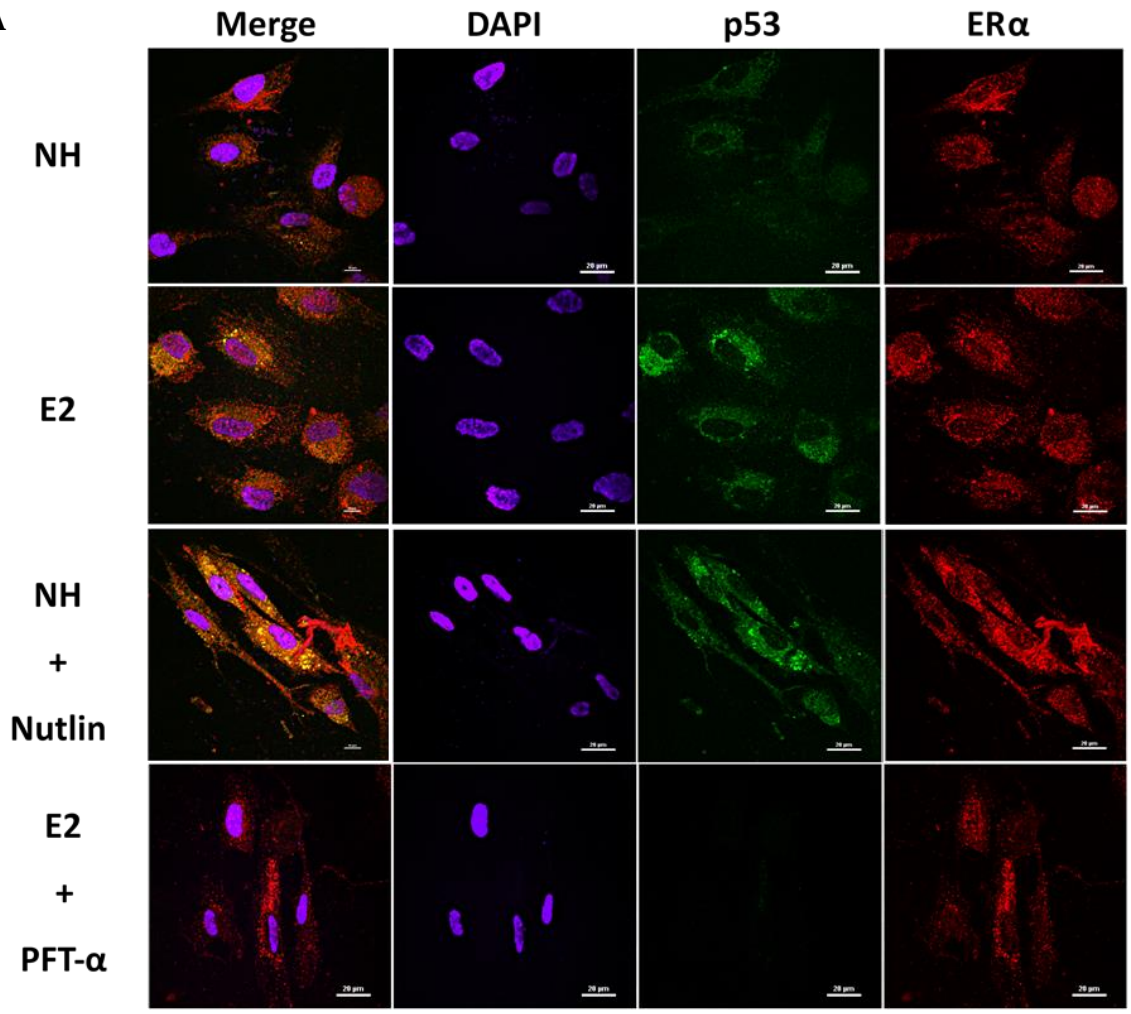
Merge
DAPI
p53
ERα
NH
E2
NH + Nutlin
E2 + PFT-α

B

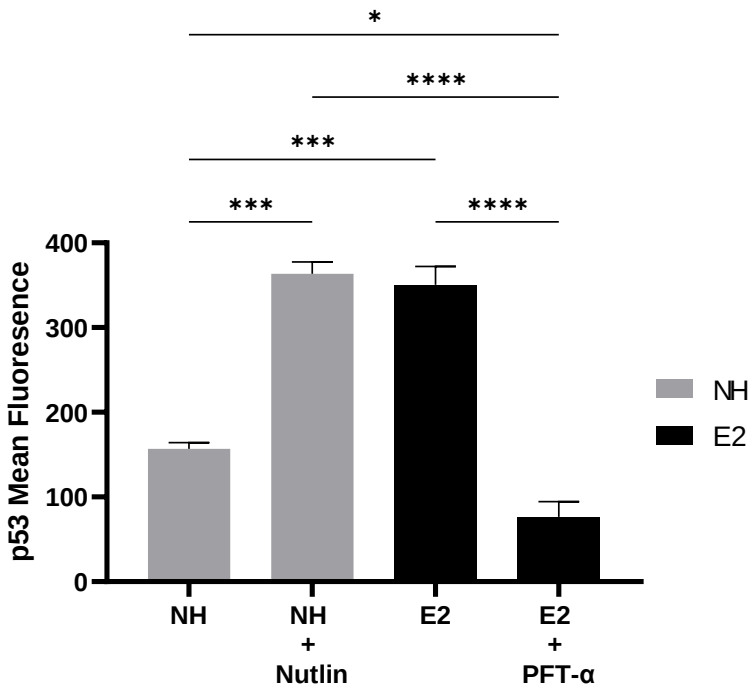
*
****
***
***
****
p53 Mean Fluorescence
400
300
200
100
0
NH
NH + Nutlin
E2
E2 + PFT-α
NH
E2

Figure 21: Estrogen treatment induces expression of p53 in primary endometrial cells (A) Primary endometrial cells were treated with either no hormone, E2 (10^{-9} M), NH + Nultin-3 (5 μM) or E2 + PFT-α (10 μM) and subsequently fixed and stained with DAPI (blue), p53 (green) and ERα (red). Occasional yellow fluorescence indicates p53 and ERα colocalization. Images were captured on confocal microscope (n=2) at x1200 magnification. Representative images are shown. (B) Quantification of p53 fluorescent intensity under respective conditions was performed with ImageJ software with mean fluorescence presented. Data shown represents mean ± SEM (n=2) with conditions done in duplicates. Statistical significance: *$p<0.05$, ***$p < 0.001$, ****$p < 0.0001$.

4.3 E2 confers protection against HSV-2 through a p53-mediated mechanism

4.3.1 E2 exerts anti-viral effect through p53 mediated pathway

Since we were able to show that p53 pathway is upregulated by E2 treatment, we next investigated the role of E2 and p53 in conferring protection against HSV-2. With strong existing evidence of the p53 pathway and its role in attenuating the replication of viruses such as HSV-1 and influenza A virus (IAV),[123-125] we expect to see similar results in the context of HSV-2. However, the link between E2 exerting anti-viral effect through p53 has not been reported before. To investigate this phenomenon, we first assessed viral shedding, a measure of viral replication, by quantifying plaques generated by a Vero plaque assay using supernatants collected from HSV-2-infected VK2 cells. Cells were first grown in ALI cultures for 7 days in the presence of NH or E2 alone. Nutlin-3 (5 μM) was added for 48 hours in NH-treated cells on day 5, allowing cells to be ready for infection by day 7. PFT-α (10 μM) was added to cells with E2 pre-treatment one hour prior to infection on day 7. On day 7, VK2 cells in ALI cultures were inoculated with HSV-2 at a multiplicity of infection (MOI) of one, removed after 2 hours, and overlayed with media to allow viral shedding, as described in material and methods. We decided to exclude the condition where Nutlin-3 is added to E2 treatment, since we previously saw no significant difference compared to E2 alone. We also did not investigate PFT-α treatment in NH-treated cells since addition of 10 μM of PFT-α to E2 results in similar outcome of p53 expression as 10 μM of PFT-α to NH. Moreover, we later address how suppression of p53 with either siRNA or PFT-α affects viral replication. Therefore, we focused on only the four aforementioned conditions: NH, E2, NH + Nutlin-3 (5 μM), and E2 + PFT-α (10 μM). The supernatants were then collected on ice 24 hours after inoculation and overlayed onto Vero cells for 48 hours to measure the viral titres that were present

in the supernatants. The plaques that formed in Vero cells were later quantified to calculate viral titres, as an indicator of viral replication.

We hypothesized that if the anti-viral effect of E2 was mediated through p53, then suppressing the p53 pathway will make the cells more susceptible to HSV-2 infection in E2-treated cells compared to NH alone, and result in greater HSV-2 infection and viral shedding. Interestingly, the results aligned with our expectations: we saw a 10-fold decrease in viral titres (PFU/mL) following E2 treatment as well as by direct activation of p53 (Nutlin-3) in absence of E2 (Figure 22A). In contrast, p53 inhibition, even in the presence of E2, resulted in a 10-fold increase in viral replication, suggesting that the p53 pathway is involved in E2-mediated anti-viral protection. We also performed a 16-hour HSV-2-GFP infection experiment to confirm these results. VK2s were grown in monolayers in 24 well plates treated with either NH or E2. Similar to as mentioned previously, Nutlin-3 (5 μM) treatment was provided on the 5^{th} day, while PFT-α (10 μM) treatment was given 1 hour prior to infection. On day 7, VK2 cells were inoculated with HSV-2-GFP for 2 hours, washed with PBS, and then overlayed with media, as explained in material and methods. When VK2 cells were visualized under an EVOS microscope at the 16-hour time point, which is the approximate peak of HSV-2 replication, we observed a similar pattern of results as before: the E2-induced p53 pathway was able to protect cells from HSV-2 infection (Figure 22B). These results confirm not only the ability of p53 to provide protection against HSV-2 infection, but also that the E2 response in the absence of p53 signaling is unable to provide protection against HSV-2, thus indicating that E2-mediated protection may be dependent on the induction of the p53 pathway.

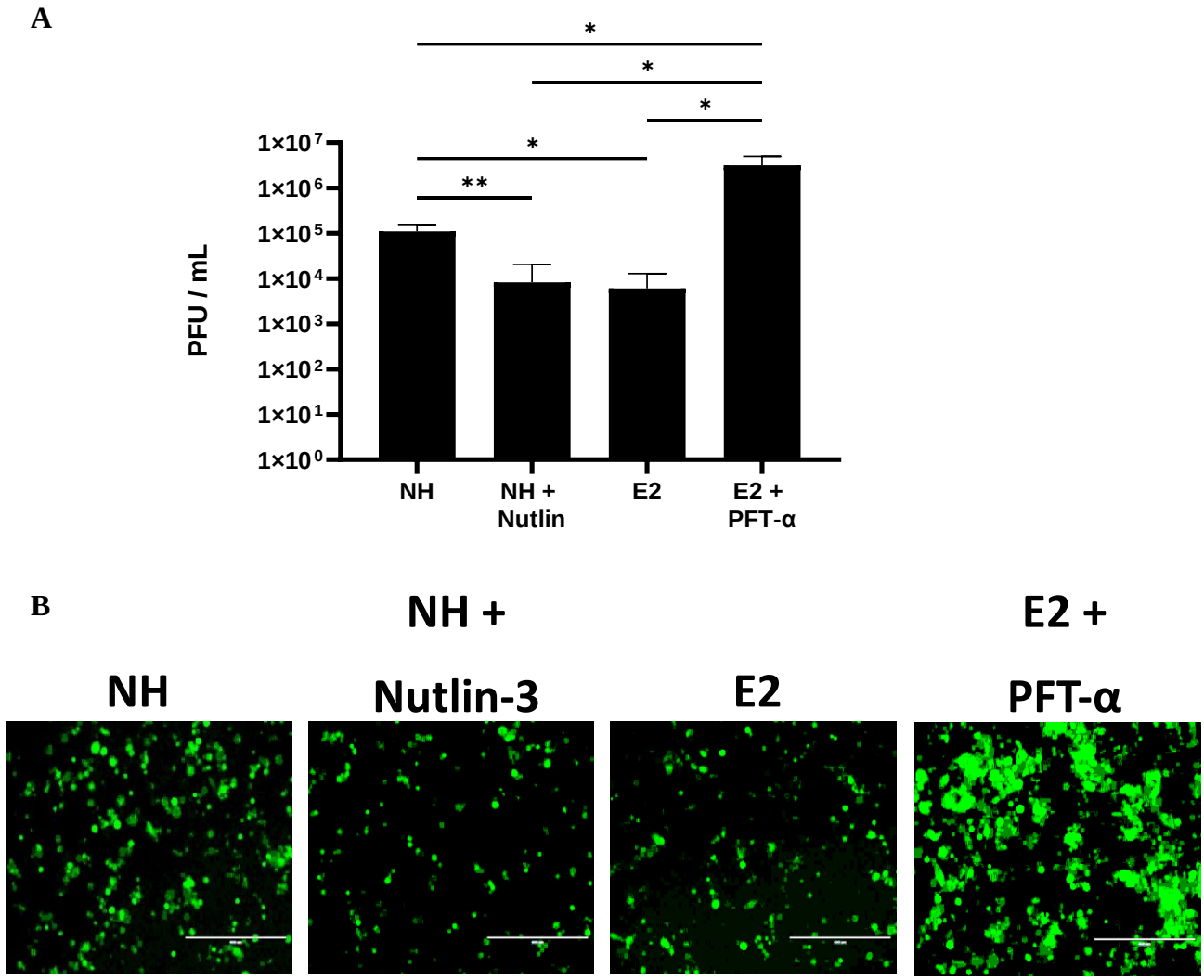

Figure 22: Estrogen treatment provides p53-mediated protection against HSV-2 infection and replication in VK2 cells. (A) VK2 cells were grown in ALI cultures up until 7 days in NH, E2 (10^{-9} M), NH + Nutlin-3 (5 µM) or E2 + PFT-α (10 µM) conditions. Cultures were inoculated with HSV-2 strain 333 at a multiplicity of infection (MOI) of one on day 7 for 2 hours before being washed with PBS and overlayed with media for 24 hours, as described in material and methods. HSV-2 viral titrations were performed with supernatants collected 24 h post infection. Data is shown as mean ± SEM (n = 6) with conditions done in triplicates. Statistical significance: *$p<0.05$, **$p<0.01$. (B) VK2s were grown in monolayers in 24 well plates treated with either NH, E2 (10^{-9} M), NH + Nutlin-3 (5 µM) or E2 + PFT-α (10 µM) prior to infection. On day 7, VK2 cells were inoculated with HSV-2-GFP at an MOI of one for 2 hours, washed, and incubated to allow viral replication. Infected cells showing HSV-2-GFP expression were visualized using an EVOS fluorescent microscope after 16 hours of infection under low magnification (10 × objective). Experiment has been done three times with each condition done in duplicates. Representative images are shown for each treatment. White line indicates 400 µm scale bar.

4.3.2 Knockdown of p53 increases HSV-2 replication

To address the concern that the inhibitor used in previous experiments may have off-target effects, we decided to confirm our results by specifically knocking down p53 with siRNA. We decided to first optimize our siRNA doses prior to performing further experiments. VK2 cells were grown in LLI cultures in transwells under NH conditions in the absence or presence of Nutlin-3 (5 μM) for 48 hours. Once confirming that cells are at approximately 30-60% confluence, cultures were treated transfected with p53 siRNA or scrambled siRNA (negative control) at various doses (1 nM, 10 nM, 30 nM and 50 nM). VK2 cells with NH alone or Nutlin-3 with NH were examined without siRNA transfection to determine baseline levels of p53 expression. Effects of siRNA doses are shown in either NH (Figure 23A) or Nutlin-3 (Figure 23B) treatment conditions. Using Nutlin-3 allowed us to visualize the true effects of the siRNA since basal levels of p53 in NH conditions are quite low. We used two different siRNAs targeting different exon sequences of p53, to ensure we were able to choose an siRNA which exerted maximum silencing effect on p53 gene.

Figure 23 shows that both siRNAs reduce p53 expression in a dose-dependent manner in both NH and Nutlin-3-treated VK2 cells. However, siRNA 2 seemed to reduce p53 better at lower concentrations than siRNA 1, so we decided to use siRNA 2 in subsequent experiments. Since both 30 nM and 50 nM of siRNA provide equivalent knockdown of p53, we decided to use the lower concentration of 30 nM as the optimal dose for future experiments.

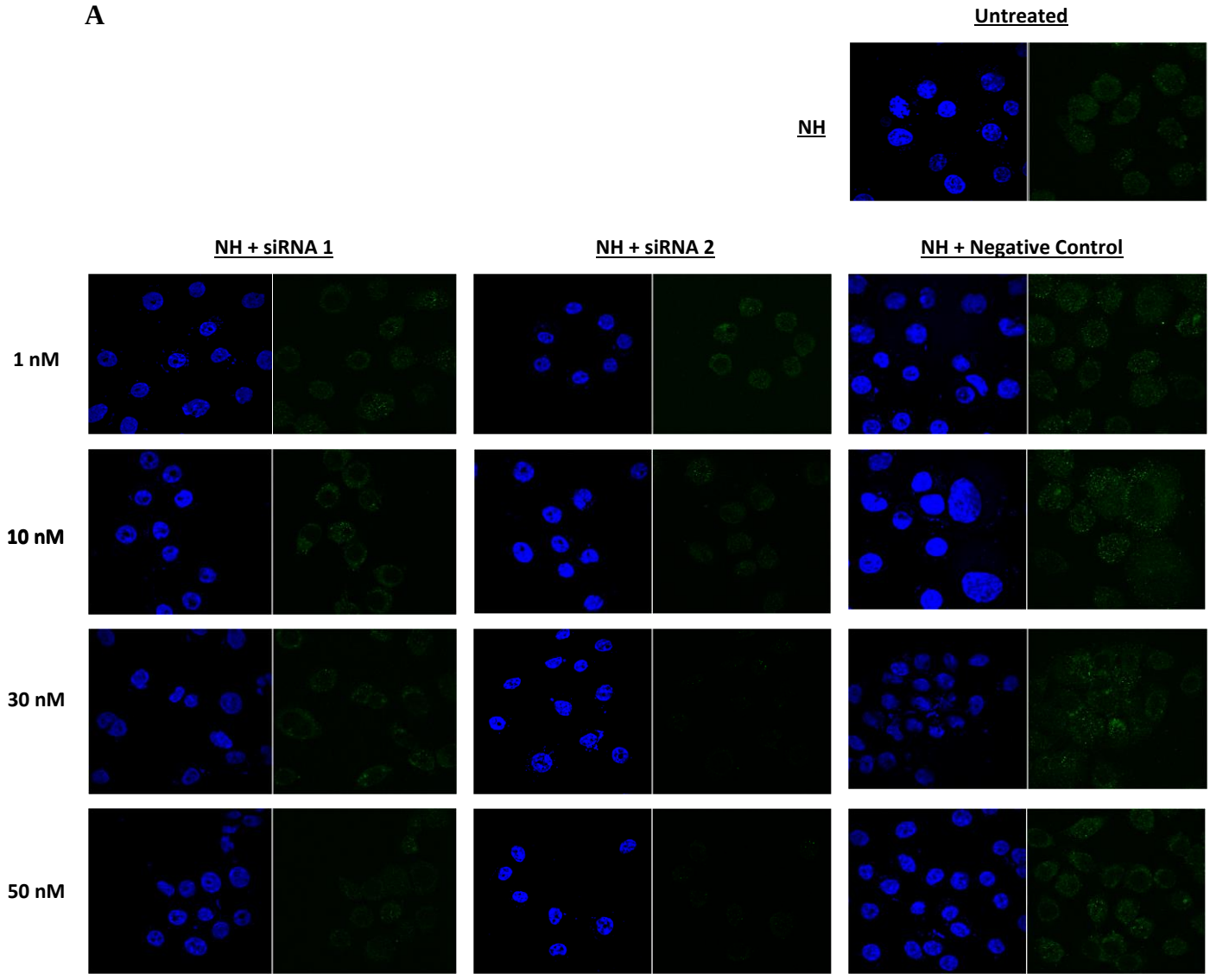
A
Untreated
NH
NH + siRNA 1
NH + siRNA 2
NH + Negative Control
1 nM
10 nM
30 nM
50 nM

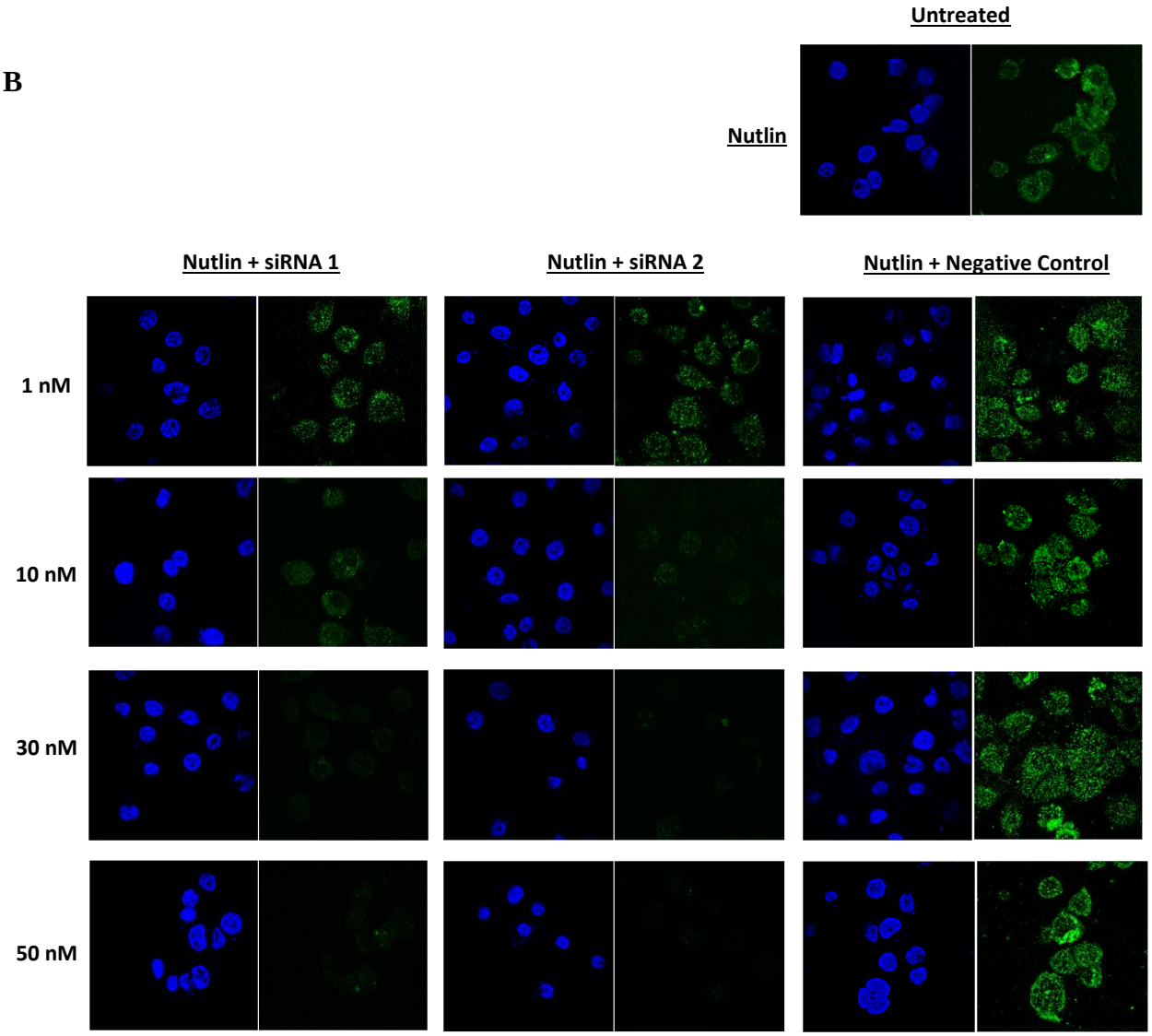

Figure 23: Knockdown of p53 with siRNA shows reduced p53 expression in VK2 cells in a dose-dependent manner. VK2 cells were grown in LLI cultures in NH conditions alone or with Nutlin-3 (5 µM) until 30 – 60 % confluency, and subsequently transfected with two p53 siRNAs (siRNA1 and siRNA2) targeting different exons, or with scrambled siRNA as a negative control, at various concentrations (1, 10, 30 and 50 nM). VK2 cells without transfection were used to see baseline levels, as seen at the top of VK2s treated with (A) NH and (B) NH + Nutlin-3. Cells were fixed, stained for p53 and visualized for immunofluorescent microscopy using a confocal microscope at x600 magnification. Experiment has been done once with each condition done in triplicates. Representative images are shown.

After determination of the optimal concentration, VK2 cells were grown in monolayers in 24 well plates under NH, Nutlin-3 (5 µM) with NH or E2 alone for 7 days until 30-60% confluency. Cultures were subsequently provided with no treatment, transfected with p53 siRNA for 24 hours, trasnfected with scrambled siRNA (negative control) for 24 hours, or provided PFT-α treatment for 1 hour. prior to inoculation with HSV-2-GFP, as described in material and methods. Cells were washed after 2 hours and overlayed with media until visualization with the EVOS microscope at the 16-hour timepoint. Results show that knockdown of p53 in either NH, NH + Nutlin-3 (5 µM), or E2 (10^{-9} M) conditions resulted in increased HSV-2-GFP expression (Figure 24). However, p53 knockdown in E2 shows less HSV-2-GFP expression than NH and Nutlin-3 conditions. Addition of PFT-α (10 µM) to NH, Nutlin-3, or E2-treated VK2s also results in increased HSV-2-GFP expression compared to respective conditions with no treatment, however, not to the same extent as p53 siRNA. Since knocking down p53 with the use of siRNA in E2-treated VK2 cells did not restore HSV-2 infection levels comparable to NH condition, this indicates that there must be other mechanisms that E2 is still able to provide its effects through. Treatment of VK2s with scrambled RNA resulted in no differences in HSV-2-GFP expression when compared to respective conditions with no treatment, indicating that transfection with RNA nucleotides induces no anti-viral signaling pathways, and that effects seen with p53 siRNA are truly attributed to knockdown of p53. Nevertheless, suppression of p53 with E2 still results in increased infection compared to E2 alone, indicating that p53 still has some protective role against HSV-2.

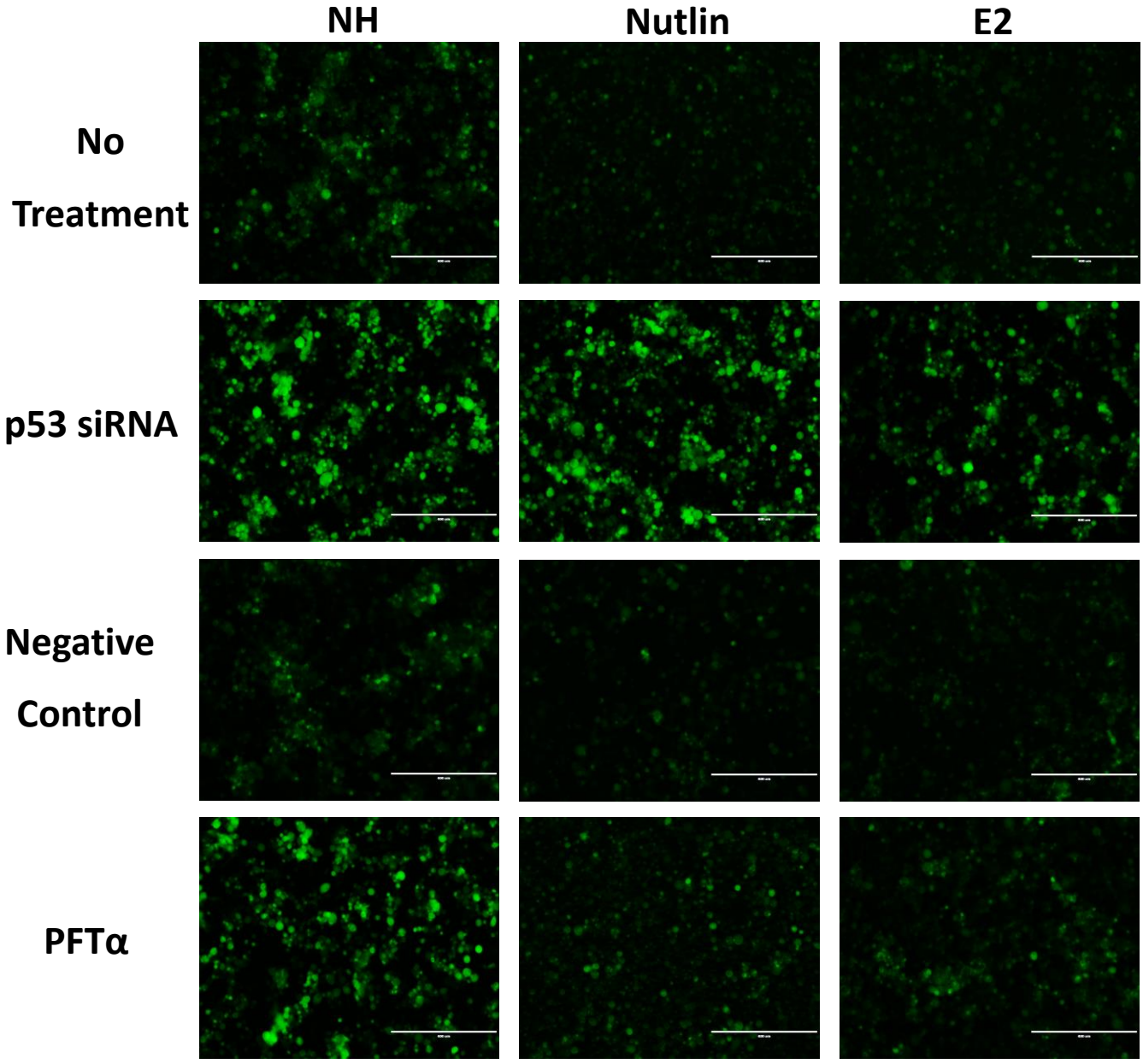

Figure 24: Blocking expression of p53 enhances HSV-2-GFP infection confirming the role of P53 in providing protection from HSV-2 infection. VK2 cells were grown in 24-well plates in either NH, NH + Nutlin (5 μM) or E2 (10^{-9} M) conditions. Once 30 – 60 % confluent, they were then transfected with 30 nM of p53 siRNA or 30 nM of scrambled siRNA as negative control. After 24 hours of transfection, cell cultures were infected with HSV-2-GFP (MOI = 1) for 16 hours. Infected cells showing HSV-2-GFP expression were visualized using an EVOS fluorescent microspore under low magnification (10 x objective). Experiment has been done once with each condition done in triplicates. Representative images are shown for each treatment. While line indicates 400 μm scale bar.

Objective 3: Determining the mechanism of E2-mediated p53 protection against HSV-2 infection in VK2s

In Objective 1, we examined the transcriptomic data with bioinformatic tools and based on the analysis, hypothesized that the p53 pathway may be involved in antiviral protection exerted by estradiol. In Objective 2, we conducted a functional analysis that demonstrated that E2 treatment upregulates p53 expression in VK2 cells and found this was correlated with anti-viral protection against HSV-2. In Objective 3, I summarize the experiments that were conducted to examine the underlying mechanism by which p53 exerted its anti-viral effect under the influence of E2. In an attempt to determine the mechanism through which E2 acts to provide its protective effects, we decided to investigate various different pathways and protective factors, as well as our bioinformatics data. We first examined how E2 mediates its protection through the p53 pathway against HSV-2 infection, by investigating different steps of the viral cycle: virus entry and viral replication. To examine which host cellular mechanisms are involved in protection, we first resorted to our GSEA bioinformatic data by examining the leading genes from our transcriptomic profile that contributed to the p53 pathway. We further examined other mechanisms such as antiviral factors. This examination led us to further evaluate the ISG BST2, which we later hypothesized to play an important role due to its significance from our data and known role in literature. The mechanism of BST2 as an antiviral factor against HSV-2 was further investigated to confirm whether it is mediated through p53, and whether it contributes to protection.

4.4 Examination of viral uptake and replication under the influence of E2 and role of p53

We further investigated whether the differences seen in viral infection and viral shedding are due to E2's influence on the ability of HSV-2 to initially enter the cells or its ability to replicate. Endosomal uptake is one of the mechanisms that various viruses have been shown to utilize for viral entry. For example, HIV has been shown to utilize endocytosis as a method of crossing epithelial cells, however, there is still a lack of understanding regarding its early transmission in the lower FRT.[170, 171] There is also evidence that HSV-1 preferably enters through endocytosis in epithelial cells; however, the signals and factors which determine the preference of herpesviruses to use endocytic pathways for entry or membrane fusion remains to be elucidated.[29, 33, 172] Previous research in our lab has shown that lysosome-associated membrane glycoprotein 3 (LAMP3), a gene induced by HSV-2 infection is involved in playing a role in mediating HSV-2 entry through early endosomes (Chow et al, unpublished). To confirm that HSV-2 uses the endosomal pathway for entry into VK2s, we also performed immunofluorescent staining of HSV-2 and early endosome antigen 1 (EEA1) in VK2 LLI cultures after infection for 1 hour (Figure 25A) and 3 hours (Figure 25B). Results show that there is indeed uptake of HSV-2 through the early endosome at both 1 and 3 hours, but more at 3 hours, as seen by the yellow color as an indicator of colocalization of HSV-2 and EEA1.

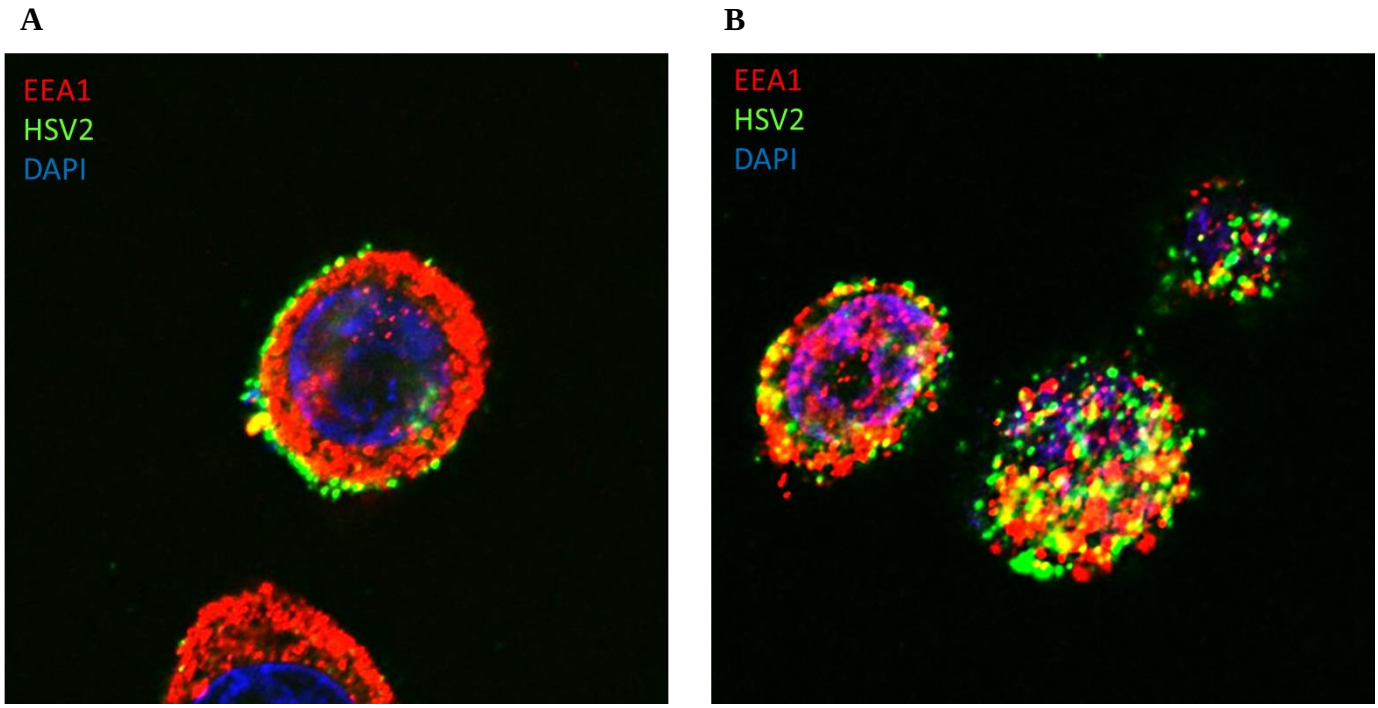

Figure 25: HSV-2 endocytosis into vaginal epithelial cells occurs through early endosomes. VK2 were grown in LLI cultures and infected with HSV-2 strain 333 (MOI=1) for (A) 1 hour or (B) 3 hours and subsequently fixed and stained for HSV-2 (green) and early endosomal marker EEA1 (red) using specific antibodies. The yellow colour is indicative of HSV-2 and EEA1 colocalization. Images were taken with a confocal microscope at x2400 magnification. Experiment has been done twice with each condition done in triplicates. Representative images are shown.

Since we were able to observe the uptake of HSV-2 into VK2 cells through the early endosome, we continued with our investigation of whether E2-mediated p53 signaling has an effect on this HSV-2 uptake into early endosomes. We did this by performing immunofluorescence staining of HSV-2 at 2 hours after infection (Figure 26A) as an indicator of viral entry, as well as at 16 hours which is when HSV-2 is completing its replicative phase (Figure 26B). In case there were differences seen in viral entry at 2 hours, we wanted to examine whether this could be attributed to the modulation of endosomal pathways by E2 and p53. Thus, we also stained for EEA1, a marker of the early endosome.

We first grew VK2 cells for 7 days in LLI cultures under conditions with either NH, NH+Nutlin-3 (5 μM), E2 (10^{-9} M) alone or E2 + PFT-α (10 μM), as described in section 7.2 – 7.3 of Materials and Methods, and overlayed with HSV-2 for 2 hours on ice. Addition of HSV-2 on ice allows for the virions to settle down on the cells without being uptaken.[34] This allows for consistency of results among different cells at a single cell level, thus providing uniform results. VK2s were then incubated for either 2 hours or 16 hours, allowing uptake of the virus, and finally fixed with 4% PFA. Confocal microscopy was performed by imaging Z-stacks of each cell and then examining fluorescence of EEA1 and HSV-2 (Figure 26). Results were further validated by quantification of fluorescence intensity of 20 slices (Z-stacks) of 3-dimensional cells under each condition (Figure 26 D-G).

Interestingly, we saw that at 2 hours after infection there seem to be similar levels in HSV-2 fluorescence when visualizing single slices (Figure 26A), as well as EEA1 fluorescence (Figure 26B). To determine the fluorescence throughout the cell, we plotted the fluorescence intensity of HSV-2 (Figure 26D) and EEA1 (Figure 26F) belonging to each slice from Z-stacks of cells within each treatment. Since there are no major differences in fluorescence intensity of HSV-2 and EEA1 between the treatments, these results indicate that there is no role of E2 or p53 in viral entry (Figure 26D) or early endosome expression (Figure 26F) after 2 hours of infection However, E2 treatment, as well as direct activation of p53 by Nutlin-3 in absence of E2, at 16 hours post HSV-2 infection shows significantly reduced HSV-2 as seen with green fluorescence, compared to NH (Figure 26B and 24E). When the p53 pathway was inhibited with PFT-a in E2 treated VK2 cells, this effect was reversed, and HSV-2 infection was significantly increased compared to NH. These results further expand on previous data as we see E2-mediated protection correlated with induction of p53 pathway, particularly at the 16-hour time point, which is close to completion of replication cycle

of HSV-2. At this late time point in replication cycle, we also see differences in EEA1 expression among the different treatments, with E2 and NH+ Nutlin-3 conditions showing reduced EEA1 expression, while PFTα treatment of VK2 cells treated with E2 reduced its level of expression similar to those seen under NH conditions (Figure 26B and G). It may be possible that early endosome may be playing a role other than uptake of virus, which may account for its persistent expression even after 16 hours post infection. We also noticed that there was colocalization of EEA1 and HSV-2 observed at 16 hours, particularly in the E2 + PFT-α treatment as compared to NH, as indicated by the white arrows (Figure 26C). Interestingly, E2 treatment as well as NH+ Nutlin-3 did not show any colocalization of HSV-2 and EEA1, compared to NH which showed some.

Since the protective effects E2-mediated p53 pathway were seen at late stages of HSV-2 replication at 16 hours, instead of early time point at 2 hours where we saw similar amount of viral uptake in all conditions, this suggests that the protection may be exerted by suppressing replication of the HSV-2 virus rather than influencing viral entry.

A

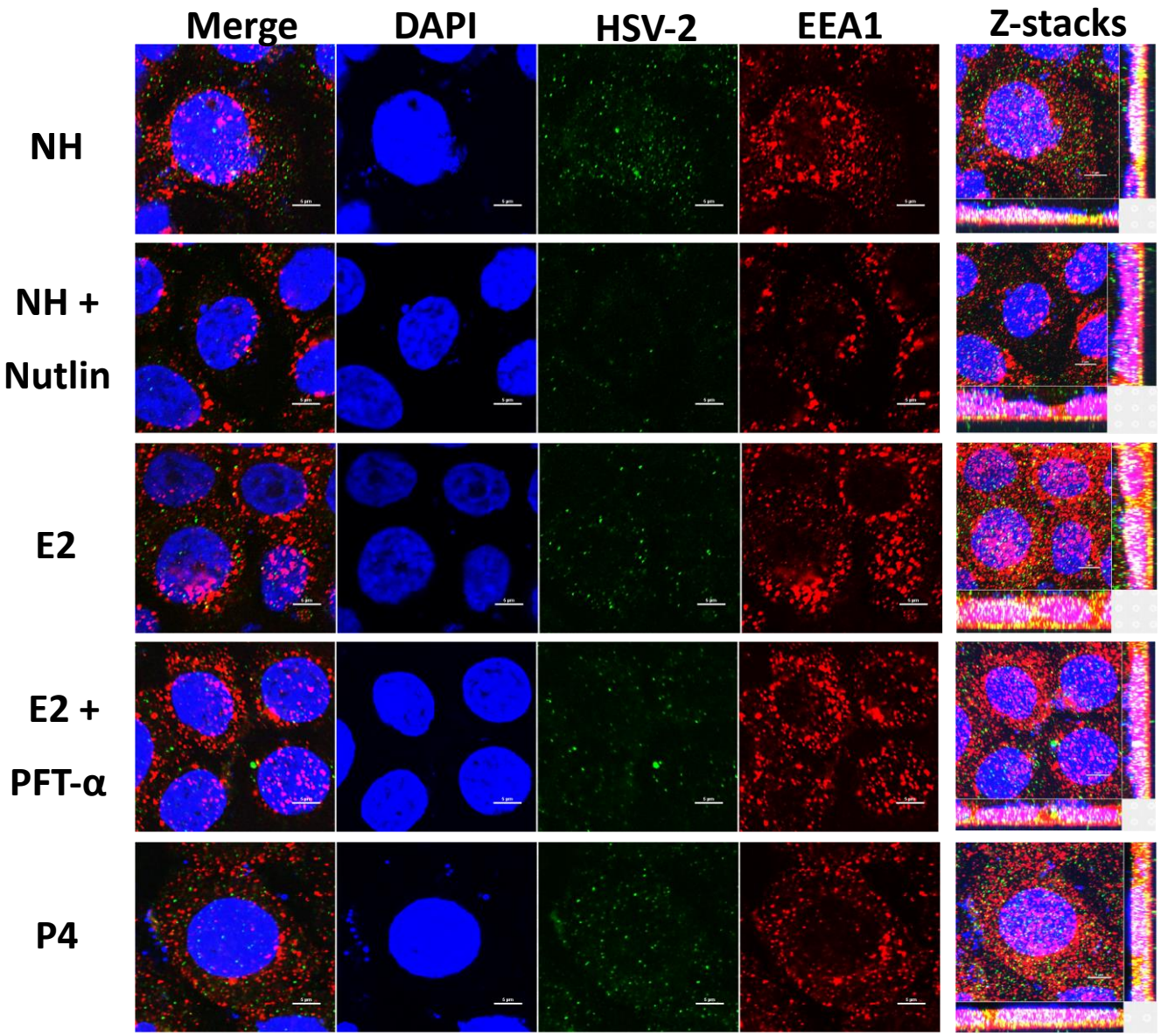

B

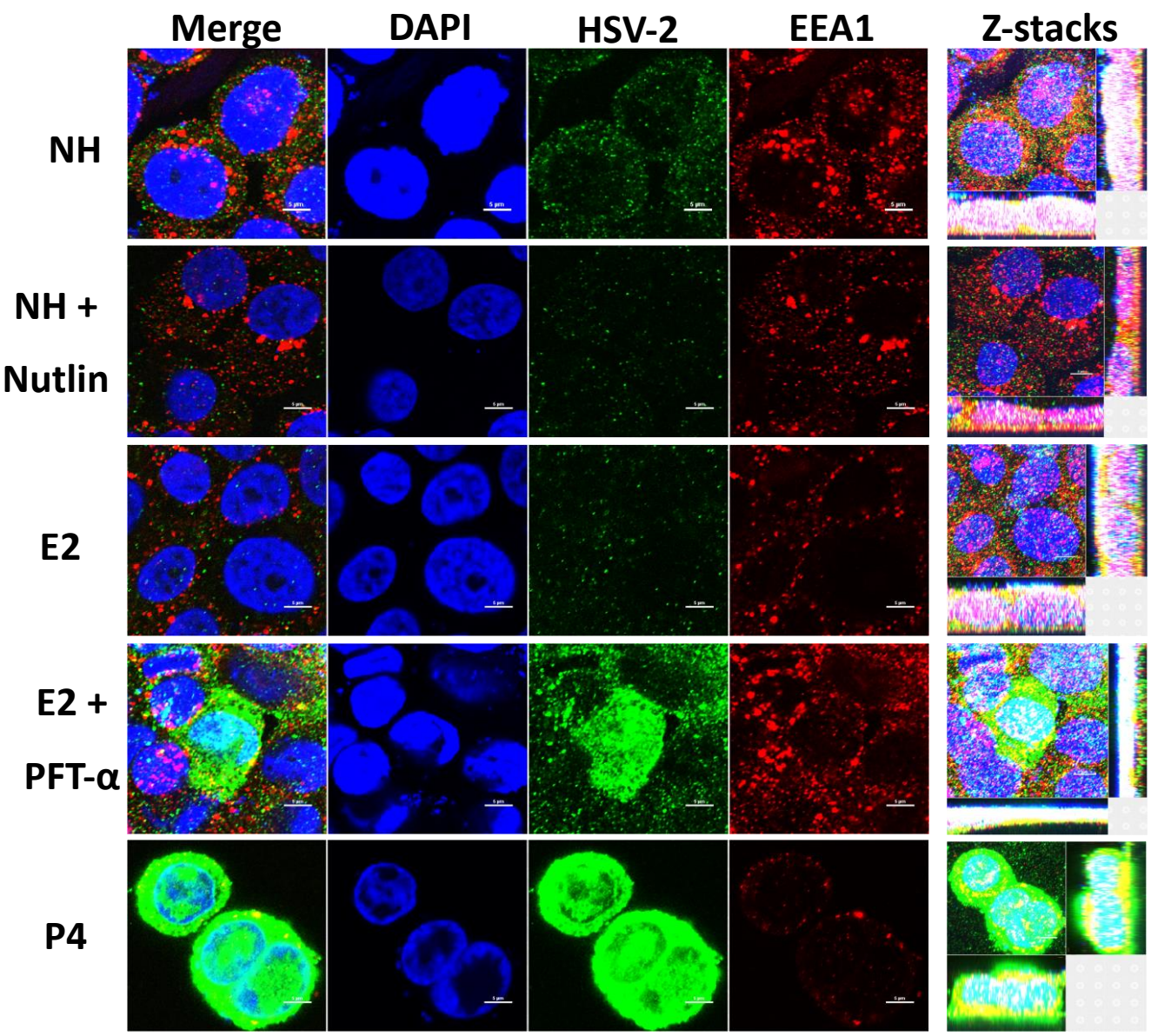

C

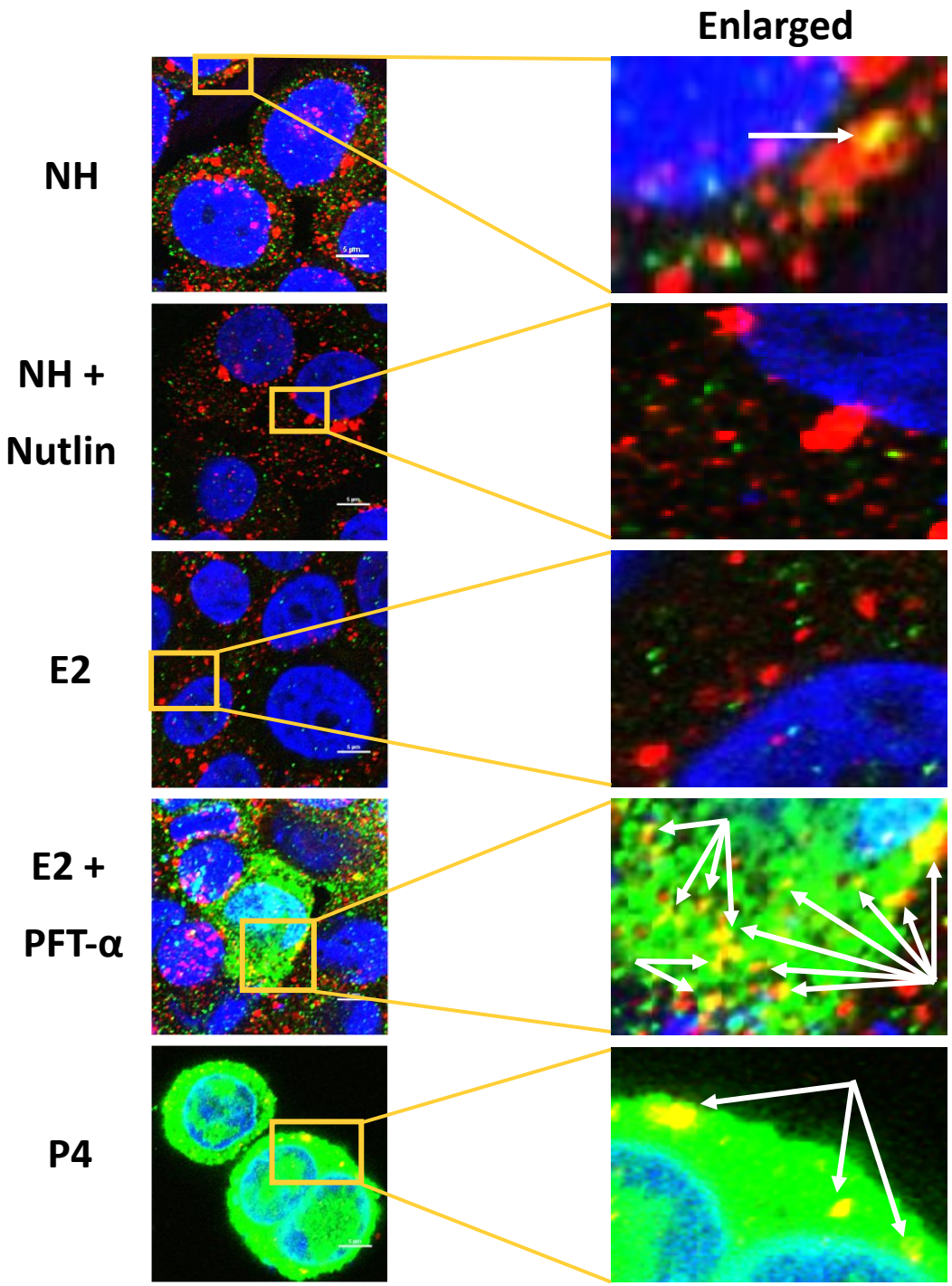

D

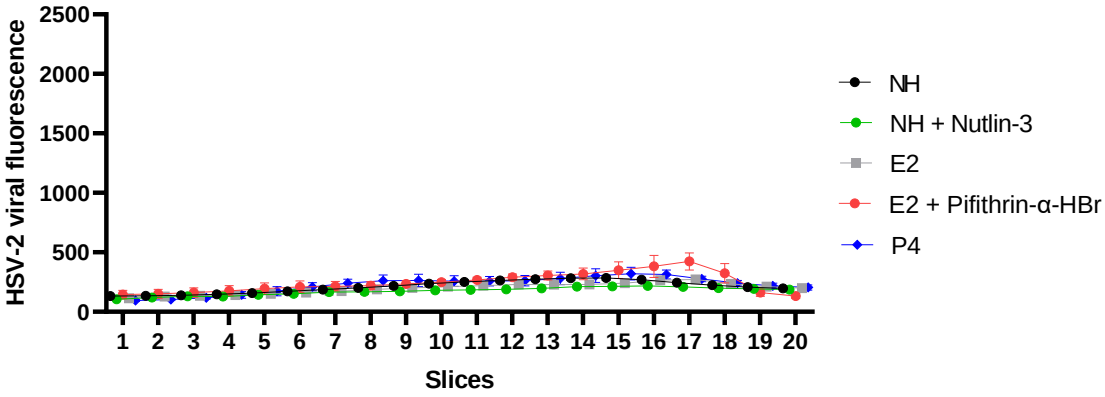
HSV-2 viral fluorescence
2500
2000
1500
1000
500
0
1 2 3 4 5 6 7 8 9 10 11 12 13 14 15 16 17 18 19 20
Slices
NH
NH + Nutlin-3
E2
E2 + Pifithrin-α-HBr
P4

E

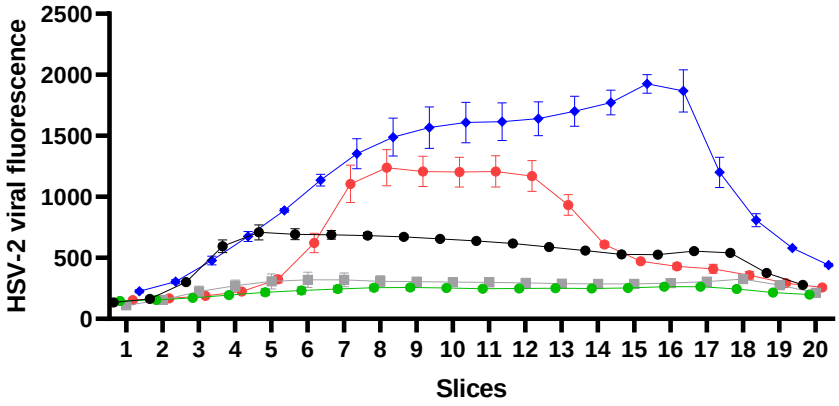
HSV-2 viral fluorescence
2500
2000
1500
1000
500
0
1 2 3 4 5 6 7 8 9 10 11 12 13 14 15 16 17 18 19 20
Slices

F

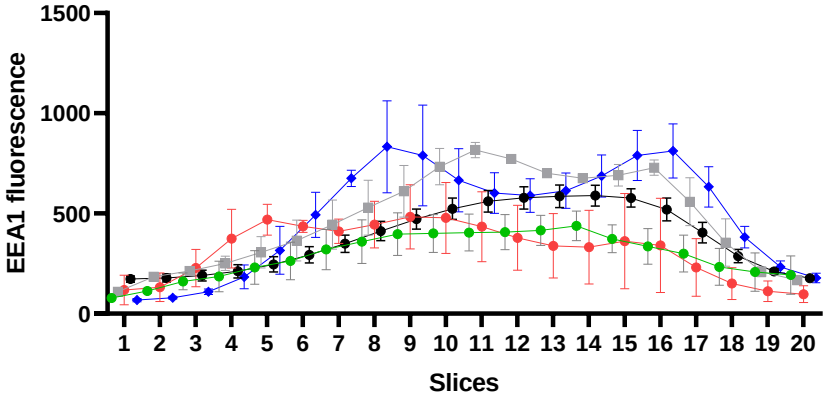
EEA1 fluorescence
1500
1000
500
0
1 2 3 4 5 6 7 8 9 10 11 12 13 14 15 16 17 18 19 20
Slices

G

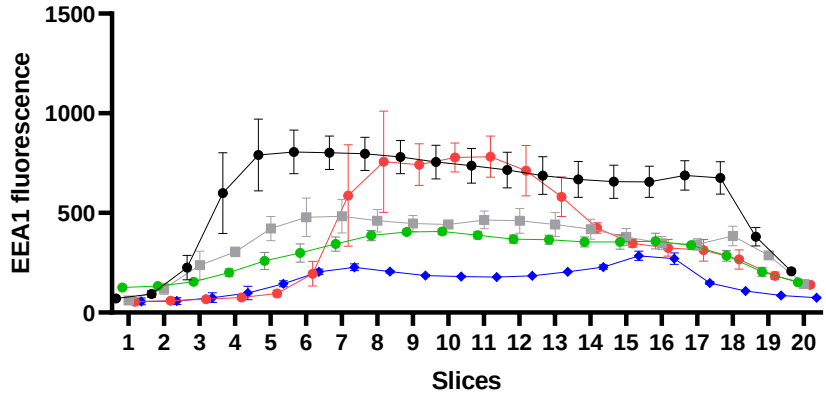
EEA1 fluorescence
1500
1000
500
0
1 2 3 4 5 6 7 8 9 10 11 12 13 14 15 16 17 18 19 20
Slices

Figure 26: p53 pathway contributes to modulation of HSV-2 replication, but not viral entry. VK2 cells were grown in LLI cultures in NH, E2 (10^{-9} M), NH + Nutlin-3 (5 μM) or E2 + PFT-α (10 μM) conditions up the 7th day, as explained in M&M. Cultures were then overlayed with HSV-2 strain 333 (MOI=1) for 2 h at 4 °C and then incubated for (A) 2 h and (B) 16 h at 37 °C. The cells were fixed and stained for HSV-2 (green), EEA1 (red) and nuclei were stained with DAPI (blue). Images were visualized by confocal microscopy (magnification x2400). Merge of all signals through the cells are shown by Z-stack overlap. (C) Enlarged images of merge channels at 16 hours post infection are shown with white arrows pointing to yellow areas of colocalization between HSV-2 and EEA1. Quantification of HSV-2 fluorescence (y-axis) was performed for each Z-stack slice (x-axis) from representative single cells after (D) 2h and (E) 16 hours of infection. EEA1 fluorescence was also quantified in all Z-stack slices after (F) 2h and (G) 16h of HSV-2 infection. Quantification of fluorescent intensity under respective conditions was performed with ImageJ software with mean fluorescence presented. Experiment has been done three times with each condition done in duplicates.

To confirm that p53 particularly influences the ability of HSV-2 to replicate, we next quantified expression of various HSV-2 genes at multiple time points as an indicator of HSV-2 replication. We used a panel of immediate early (VP16, ICP0, ICP4, ICP27) and late (gD) genes to investigate this phenomenon. VK2 cells were grown in ALI cultures in either NH or E2 for 7 days. Nutlin-3 (5 μM) treatment was added on the 5th day for 48 hours, allowing the treatment to finish at the same time as the 7-day E2 treatment, while PFT-α (10 μM) was added for 1 hour in E2-treated cells. After completion of treatments, VK2 cells were then overlayed with HSV-2 on ice for 2 hours, washed, and then incubated for 15 minutes, 2 hours, 8 hours or 24 hours prior to RNA extraction, as explained in material and methods. We observed that E2 treatment, as well as p53 activation (NH+ Nutlin-3), resulted in significantly reduced expression of ICP0, ICP27 and gD compared to NH treatment at the 24-hour time point (Figure 27). Interestingly, p53 inhibition in VK2 cells grown in E2 prevented this downregulation and allowed expression of HSV-2 genes to return to NH levels. These results confirmed the role of E2-mediated p53 pathway at preventing replication of HSV-2 and that this effect is exerted in the later stages of HSV-2 replication cycle rather than due to decreased viral uptake.

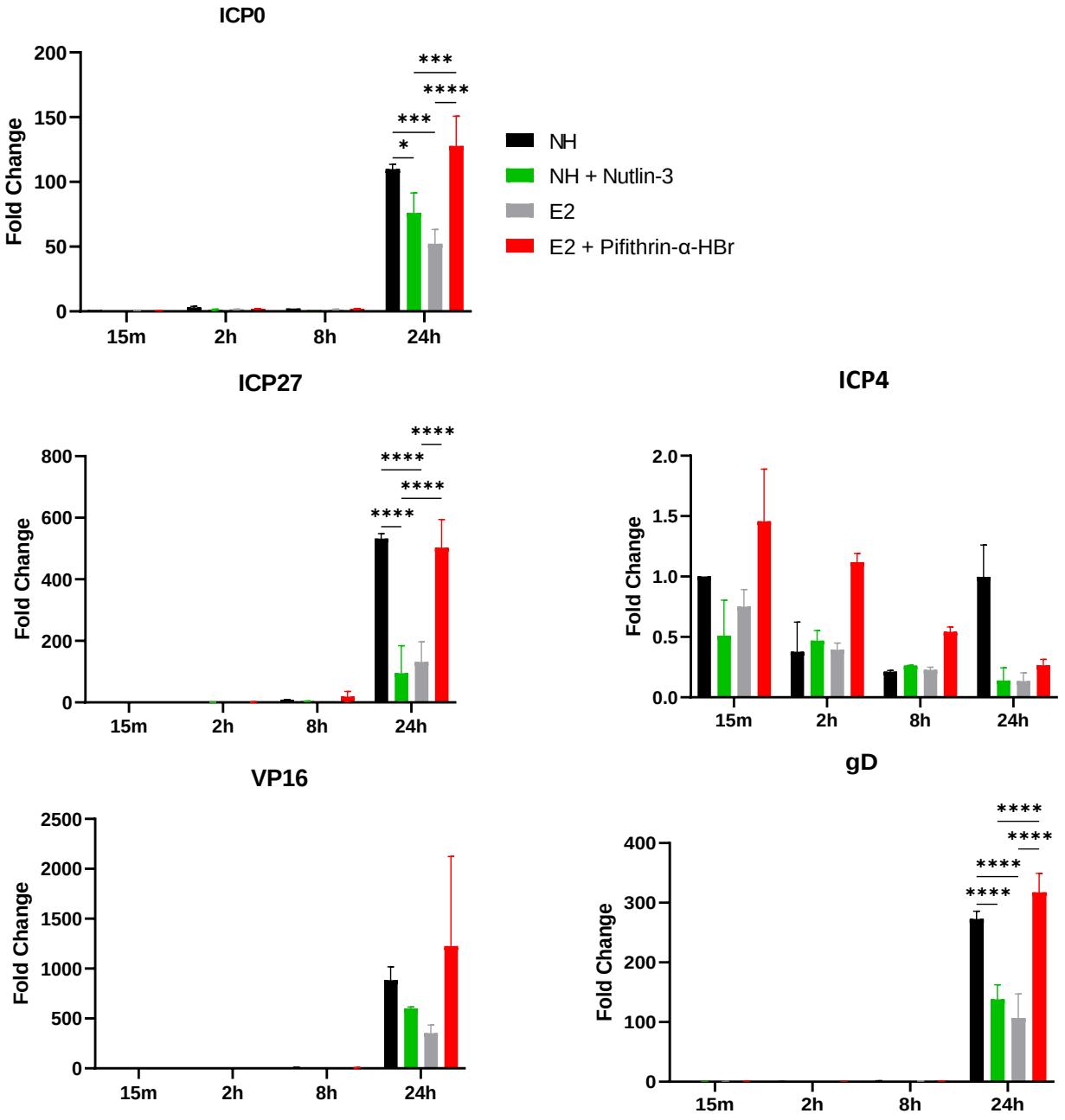

Figure 27: E2 treatment attenuates HSV-2 viral replication. VK2 cells were grown in LLI cultures in duplicates of NH, E2 (10^{-9} M), NH + Nutlin-3 (5 µM) or E2 + PFT-α (10 µM) conditions up the 7th day, as explained in M&M. Cultures were then overlayed with HSV-2 strain 333 (MOI=1) for 2 h at 4 °C and then incubated for 15 minutes, 2 hours, 8 hours or 24 hours. Cell culture replicates were lysed and combined and then used for RNA extraction. Replication of HSV-2 was assessed in VK2s by RT-qPCR of immediate early (ICP0, ICP4, ICP27 and VP16) and late (gD) genes after 15 minutes, 2, 8 and 24 hours of HSV-2 infection. The fold change in viral gene expression at 2, 8 and 24h was determined using the 15-minute time point in NH-treated VK2s as baseline. Data is shown as mean ± SEM (n = 2) with each condition done in duplicates. Statistical significance: *p<0.05, ***p <0.001 and ****p < 0.0001.

4.5 Analyze leading-edge subset analysis of the p53 pathway

We posited that the transcriptomics analysis through may provide more clues regarding the involvement of genes that correlate with p53 expression. In an attempt to examine which host cellular mechanisms are involved in protection, we first resorted to our GSEA bioinformatic data that initially indicated the contribution of p53 pathway to the E2 transcriptomic profile (Figure 11). To determine the mechanism through which E2 and the p53 pathway mediate protection, we investigated the leading genes that contribute to the p53 pathway provided by the GSEA leading-edge subset. These are genes contribute significantly to the overall normalized enrichment score (NES) since they are found on the left of the peak NES on the positive end of the transcriptomic profile, hence why they are named leading-edge subset genes (Figure 12). Although this set of genes was identified from our initial transcriptomic analysis which was at 24 hours post-HSV-2 infection in VK2 cells grown in E2, which may be a late time point for identifying p53 related genes that could play a role in anti-viral effect of E2, we decided to examine the expression of these genes between 2-24 hrs post-HSV-2 infection, since this correlates with the viral replication cycle.

To address this, VK2 cells were grown in ALI cultures in either NH alone, NH + Nutlin-3 (5 μM), E2 alone, or E2 + PFT-α (10 μM) up until 7 days as described in material and methods. After completion of treatments, VK2 cells were then overlayed with or without HSV-2 on ice for 2 hours, washed with PBS, and then incubated for 2 hours, 8 hours or 24 hours prior to RNA extraction, as explained in material and methods. We then performed qRT-PCR of RNA extracted from VK2s before and after HSV-2 infection at various time points (2, 8 and 24 hours). A closer examination showed that groups of genes display noticeably similar patterns at particular stages of infection. For example, VAMP8 and RAP2B showed a reduced expression pattern with E2

treatment as well as p53 activation 2 hours post-HSV-2 infection. TRAFD1, TGFB1, and BAX, however, showed an increased, but non-significant, expression pattern in E2 and NH+ Nutlin-3 treatments after 2 hours of infection (Figure 28). These genes showed no differences at any other time points after HSV-2 infection.

We were expecting that VK2 cells treated with E2 would show similar patterns of gene induction or repression as VK2s treated with NH+Nutlin-3. Moreover, we also expected that addition of PFT-α to E2 pre-treatment, would show differences in some genes compared to E2 alone. Nevertheless, no statistically significant differences were seen in almost all genes when comparing between different treatments with or without infection at any timepoints. VAMP8, however, was the only gene that showed significantly higher mRNA expression in E2 + PFT-α conditions compared to E2 alone. Keeping VAMP8 in mind, we decided to also examine the canonical antiviral pathways to try to find a connection between p53 activation and decreased HSV-2 infection to determine how this protective response may be occurring.

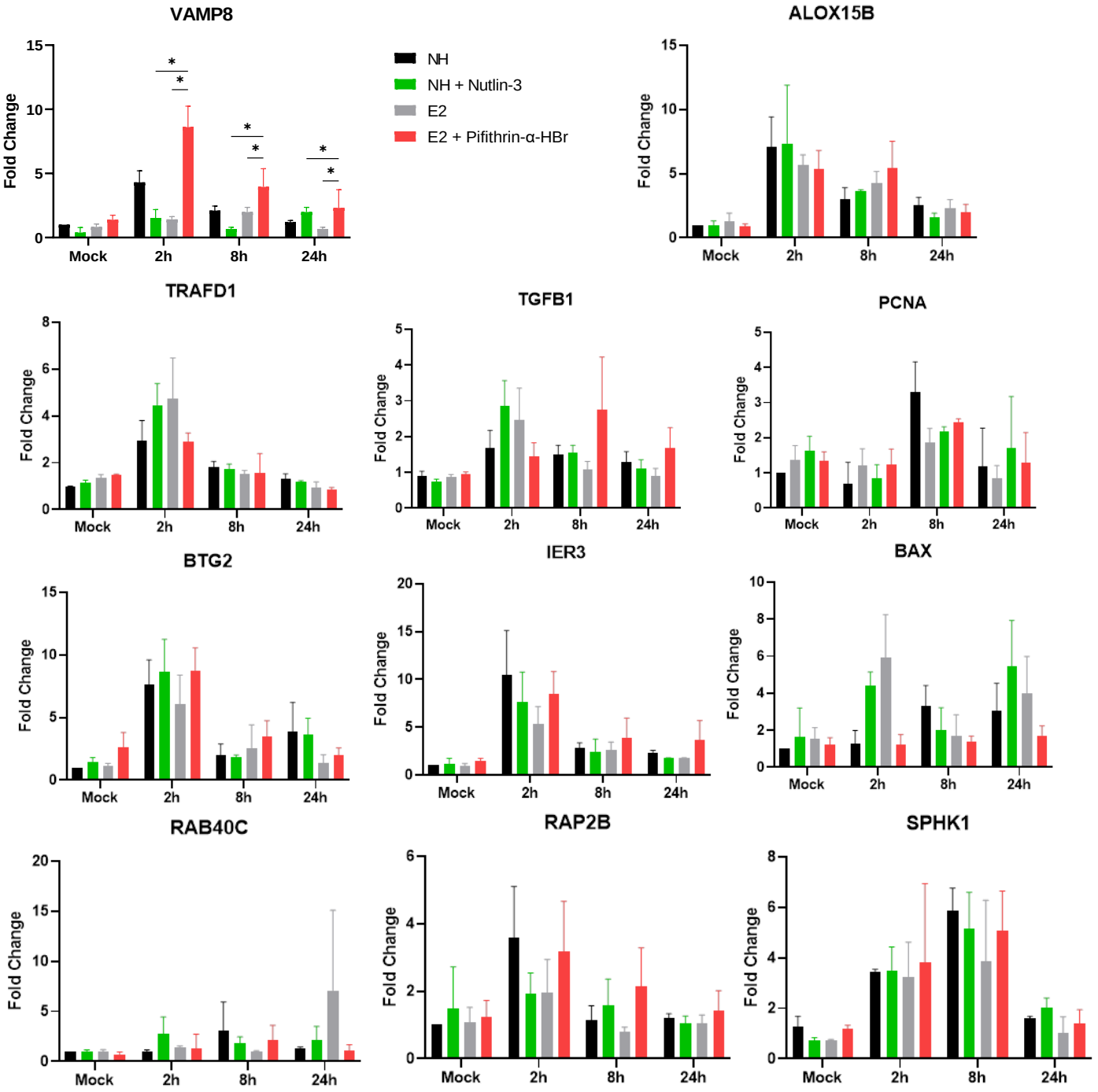

Figure 28: Contribution of GSEA leading edge subset genes to the E2-induced p53 mechanism. VK2 cells were grown in ALI cultures with NH or E2 (10^{-9} M) treatment. Cultures were treated with Nutlin-3 (5 µM) in NH conditions or left untreated. Cultures grown in E2 (10^{-9} M) were either treated with PFT-α (10 µM) or left untreated, as explained in M&M. The VK2 ALI cultures were either left uninfected or overlayed with HSV-2 strain 333 (MOI=1) for 2 h at 4°C, washed with PBS, and subsequently incubated for 2 hours, 8 hours or 24 hours at 37°C. Cell culture replicates were lysed and combined and then used for RNA extraction. RT-qPCR of leading-edge subset genes of the p53 pathway was then performed. Data shown are mean ± SEM (n = 2) with each condition done in duplicates. Statistical significance: *p < 0.05.

4.6 Investigate antiviral responses of E2 and the p53 pathway against HSV-2 infection

Based on the highly protective role observed under the E2-induced p53 mechanism against HSV-2, we decided to investigate whether this protection was mediated through antiviral innate immune responses such as interferon signaling and ISG responses. Since BST2 was one of the highly expressed ISGs in response to Nutlin-3 treatment in the context of HSV-2 infection, we further investigated the role of this ISG in the context of E2 and p53 signaling, and whether it mediates protection against HSV-2.

4.6.1 Examination of E2 and the p53 pathway in interferon signaling

As previously discussed, a key mechanism which may influence HSV-2 susceptibility in the lower FRT is the induction of innate immune-related signaling pathways that generate antiviral responses. Moreover, p53 has previously been known to regulate expression of responsive immune-related genes involved in IFN signaling.[125, 128-131] Indeed, a previous study in our lab has found that blocking IFN-β signaling in primary genital epithelial cells resulted in increased viral shedding, indicating that antiviral responses such as those of IFN-β signaling likely play a role in reducing viral burden associated with HSV-2.[48] Thus, we investigated the effects of estrogen and p53 on induction of various interferons, IFNα, IFN-β, IFN-γ and IFN-λ, as well as type I IFN receptor (IFNAR). VK2 cells were grown in ALI cultures from RNA isolated from uninfected and HSV-2 infected VK2s under various treatments over a time course of infection. VK2 cells were grown in ALI cultures in either NH alone, NH + Nutlin-3 (5 μM), E2 alone, or E2 + PFT-α (10 μM) up until 7 days as described in section 7.2 – 7.3 of Material and Methods. After completion of treatments, VK2 cells were then overlayed with or without HSV-2 on ice for 2 hours, washed, and then incubated for 2 hours, 8 hours or 24 hours prior to RNA extraction, as explained in material and methods.

We also measured secretion of IFN-β released into apical supernatants of VK2s grown in ALI conditions. VK2 cell ALI cultures were grown in NH alone, NH + Nutlin-3 (5 μM), E2 alone, or E2 + PFT-α (10 μM), as well as in P4. VK2 cells were either uninfected (mock) or infected with HSV-2 for 2, 4, 8, 16 and 24 hours. Supernatants were collected from apical sides of the ALI cultures at the respective time points after infection, and used measure release of IFN-β with the use of an IFN-β ELISA kit.

Interestingly, we observed that VK2 cells grown in E2 in the absence of HSV-2 infection (mock) showed significantly higher expression of IFN-λ2 compared to VK2 cells grown in NH in absence of HSV-2 infection (Figure 28F). Activation of p53 with Nutlin-3in absence of infection did not show differential expression of IFN-λ2 compared to NH. However, inhibition of p53 with PFT-α in after E2 treatment significantly reduced IFN-λ2 expression compared to E2 alone. Results from IFN-β (Figure 29A) show an increased, but non-significant, pattern of gene expression after E2 or Nutlin-3 treatment relative to NH conditions after 2 hours of HSV-2 infection. Similarly, IFN-λ1 gene (Figure 29E) shows an increased non-significant pattern under Nutlin-3 treatment or E2 alone, relative to NH; however, in uninfected mock conditions rather than after infection. Furthermore, production of IFN- β protein was not significantly different amongst the various treatments and when compared to NH in all time points before and after infection (Figure 29G). Therefore, it appeared that the protective effects seen by the p53 pathway against HSV-2 were likely not mediated through IFN signaling.

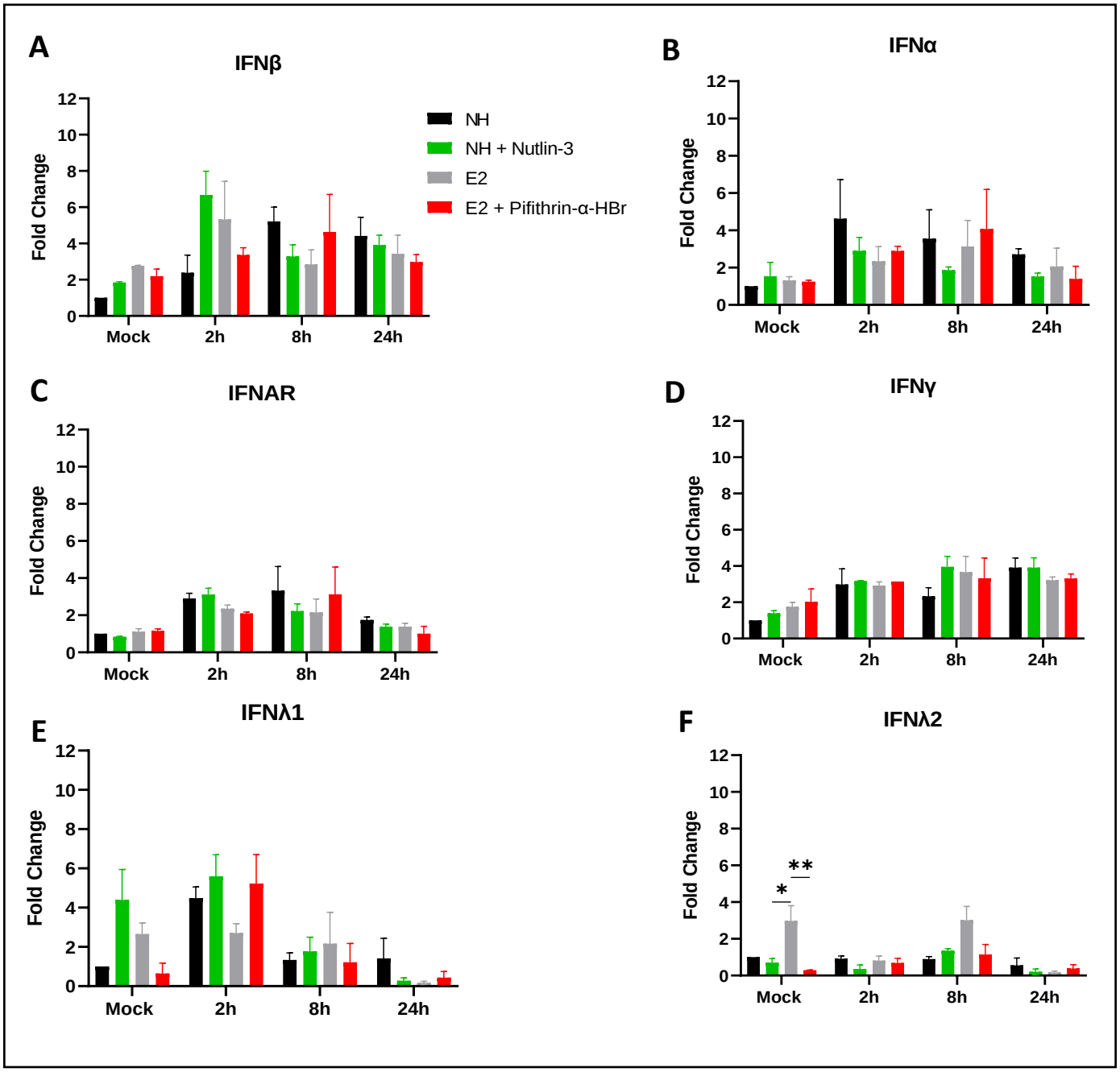
A
IFNβ
Fold Change
NH
NH + Nutlin-3
E2
E2 + Pifithrin-α-HBr
Mock
2h
8h
24h
B
IFNα
C
IFNAR
D
IFNγ
E
IFNλ1
F
IFNλ2
*
**

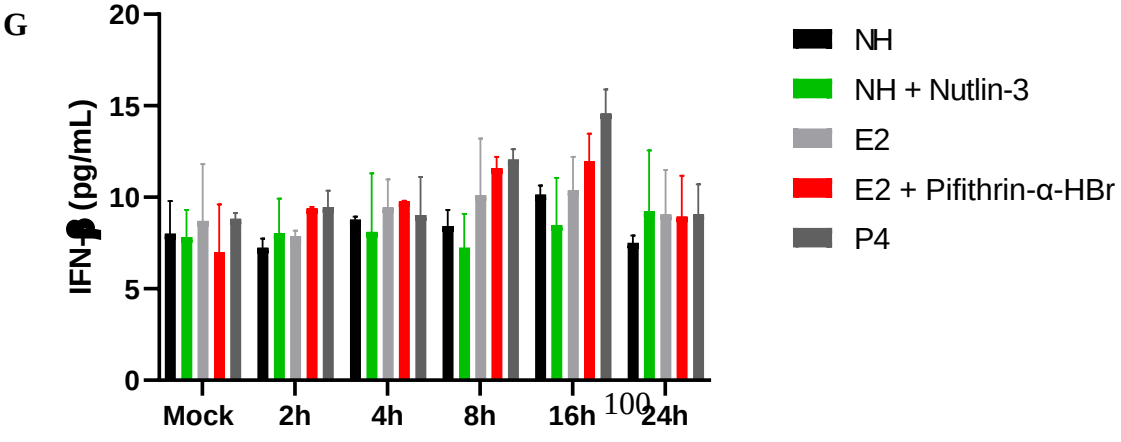
G
IFN-β (pg/mL)
Mock
2h
4h
8h
16h
24h
NH
NH + Nutlin-3
E2
E2 + Pifithrin-α-HBr
P4

Figure 29: E2 treatment and effect of p53 modulation on IFN signaling pathways. VK2 cells were grown in ALI cultures in either NH alone, NH + Nutlin-3 (5 μM), E2 alone (10^{-9} M), or E2 + PFT-α (10 μM) up until 7 days as described in material and methods. After completion of treatments, VK2 cells were then overlayed with or without HSV-2 strain 333 (MOI=1) on ice for 2 hours, washed with PBS, and then incubated for 2 hours, 8 hours or 24 hours. Cultures were lysed and subjected to RNA extraction for RT-qPCR to detect mRNA of (A) IFN-β, (B) IFNα, (C) IFNAR, (D) IFN-γ, (E) IFN-λ1 and (F) IFN-λ2. Data shown are mean ± SEM (n = 2) with each condition done in duplicates. Data was analyzed using two-way ANOVA, with Bonferroni test to correct for multiple comparisons. Statistical significance: *$p < 0.05$, **$p < 0.01$. (G) VK2 cell ALI cultures were grown in NH alone, NH + Nutlin-3 (5 μM), E2 alone (10^{-9} M), or E2 + PFT-α (10 μM), as well as in P4. Cultures were either left uninfected (mock) or infected with HSV-2 strain 333 at an MOI of one for 2, 4, 8, 16 and 24 hours. Supernatants were collected from apical sides of the ALI cultures for measurement of secreted IFN-β with an ELISA. Data shown are mean ± SEM (n = 2) with each condition done in triplicates. Data was analyzed using two-way ANOVA, with Bonferroni test to correct for multiple comparisons

4.6.2 Examination of E2 and the p53 pathway in regulation of interferon-stimulated genes

Although no differences were seen in IFN induction, we were still interested in investigating other antiviral responses that may play a role. Since there is existing evidence of IFN-independent ISG production,[173, 174] we continued our investigation by examining expression of various ISGs We selected and quantified various ISGs including MX1, RSAD2, ISG15, OAS1, OAS2, OAS3, IFIT1, IFI44L, and BST2 based on their previously identified roles with various herpesviruses.[175-177] Moreover, a recent microarray analysis of genes altered by HSV-2 infection shows differential expression of many of these ISGs.[178] VK2 cell ALI cultures were first grown in NH alone, NH + Nutlin-3 (5 µM), E2 alone, or E2 + PFT-α (10 µM) as described in material and methods. Cultures were either uninfected (mock) or overlayed with HSV-2 virus for 2 hours on ice prior to incubation for 2, 8, and 24 hours, as described in material and methods. RNA was extracted from VK2 cells in duplicate cultures, combined, converted to cDNA, and subjected to RT-qPCR, as described in section 7.12 in Material and Methods. Of the nine ISGs analyzed, MX1 and BST2 were the only ones which showed significantly increased expression with p53 activation using Nutlin-3 treatment after 2 hours of HSV-2 infection compared to NH treatment after 2 hours of infection (Figure 30). However, a nonsignificant increase in BST2 expression was also seen under E2 conditions at the same time point. Moreover, gene expression of BST was also the highest quantitively, with fold change values reaching up to approximately 15 and 7.5 under Nutlin-3 and E2 treatments, respectively. OAS2, OAS3 and IFIT1 showed significantly lower expression in E2 + PFT-α compared to Nutlin-3, and only in uninfected conditions., while other treatments show no difference (Figure 30). IFI44L, however, shows significance with various treatment comparisons: there is significantly higher expression of IFI44L in VK2 cells grown under NH + Nutlin-3 treatment, compared to NH alone, along with significant reduction in its expression after

E2 + PFT-α treatment compared to both E2 or Nutlin-3 alone. Overall, many of the ISGs showed significant expression at mock conditions, but were counteracted and reduced after viral infection. However, BST2 was a potential candidate for further examination based on its increase in expression after p53 activation even after infection.

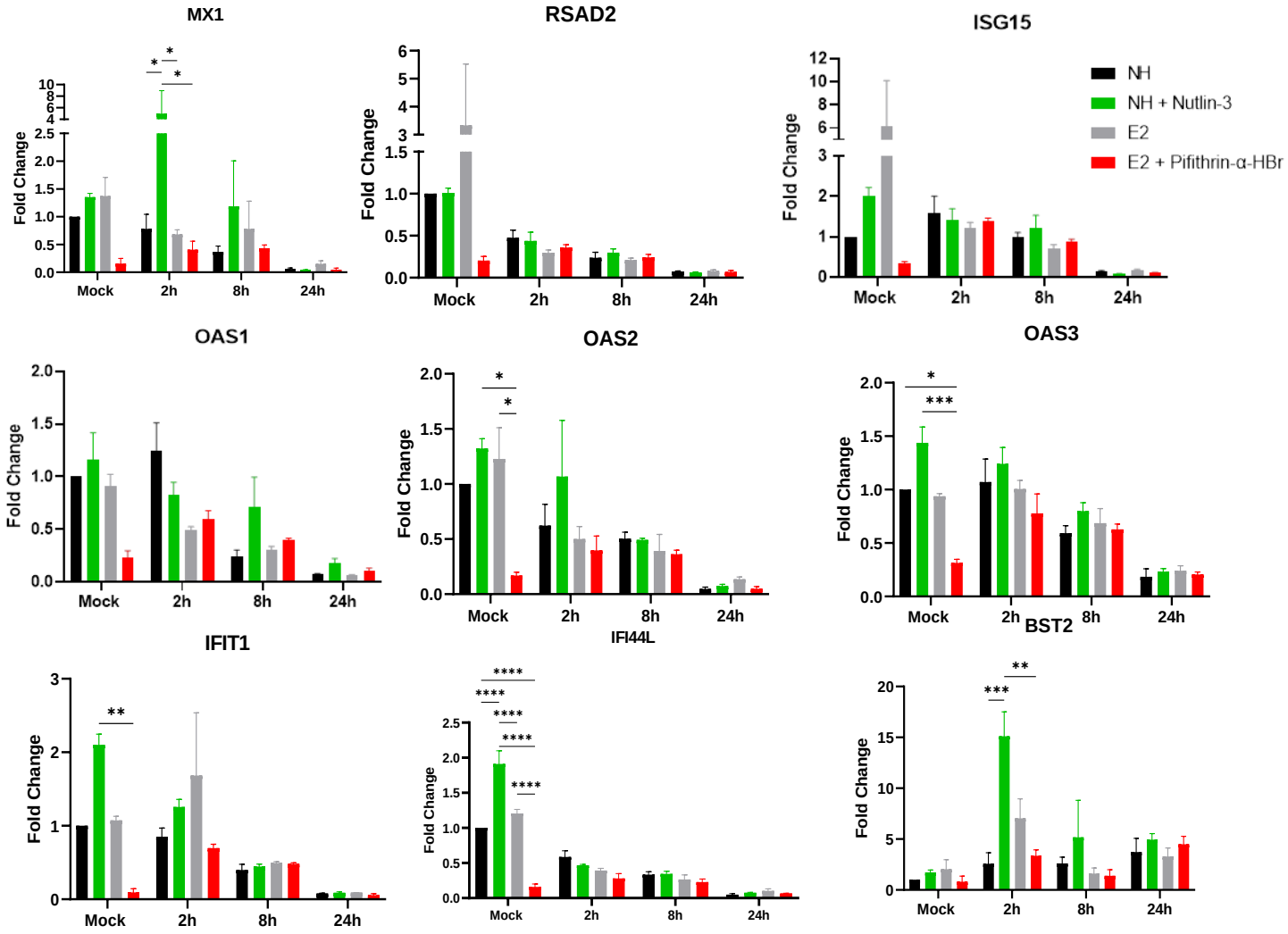

Figure 30: E2 treatment and p53 response shows differential expression of various ISGs before and after HSV-2 infection in VK2s. VK2 cell ALI cultures were first grown in NH alone, NH + Nutlin-3 (5 µM), E2 alone, or E2 + PFT-α (10 µM) and either left uninfected (mock) or infected with HSV-2 strain 333 (MOI=1) for 2, 8 or 24 hours. RNA was extracted and used for RT-qPCR to detect mRNA of various ISGs. Data shown are mean ± SEM (n = 2) with each condition done in duplicates. Data was analyzed using two-way ANOVA, with Bonferroni test to correct for multiple comparisons. Statistical significance: *p < 0.05, **p < 0.01, ***p < 0.001, **** p < 0.0001.

4.6.3 Examination of E2 and the p53 pathway in regulating BST2

Based on results obtained from investigation of ISGs, we decided to investigate the role of BST2 since it was the most highly expressed ISG and one of only two genes to show increased expression after HSV-2-infection, as well as a slight, but nonsignificant, increase under E2 conditions by RT-qPCR. VK2 cells were grown in LLI cultures with NH, E2, NH + Nutlin-3 (5 μM) and E2 + PFT-α (10 μM) treatments, as described in material and methods, and subsequently left either uninfected or infected with HSV-2 for 2 hours or 16 hours, prior to performing immunofluorescence staining with BST2, also known as tetherin (Figure 31). We decided to investigate BST2 expression in uninfected conditions, as well as after 2 hours after HSV-2 infection as an indictor of viral entry, and 16 hours infection since HSV-2 is in its replicative phase. Results show that E2 as well as Nutlin-3 treatment result in upregulation of tetherin protein expression in both uninfected and HSV-2 infected VK2 cells, as compared to NH (Figure 31). However, an interesting observation that we noted was that BST2 showed localization towards the periphery of the cell in E2-treated cells after 2 hours of HSV-2 infection as seen by the outline of red, however, p53 activation resulted in BST-2 localization towards the periphery after 16 hours of infection. It is known that BST2's antiviral effects are based on its ability to be integrated into nascent budding virions, thus bridging virions and cellular membranes.[179] PFT-α treatment after E2 pre-treatment resulted in significantly downregulated BST2 expression compared to E2 alone in uninfected cells and also after HSV-2 infection. Tetherin expression was most upregulated by E2 in uninfected mock conditions, and reduced after 2 hours and 16 hours of HSV-2 infection. Nutlin-3 treatment, however, resulted in increased tetherin protein expression in cells after 16 hours of HSV-2 infection, as compared to Nutlin-3 treatment in mock and 2-hour HSV-2-infected cells.

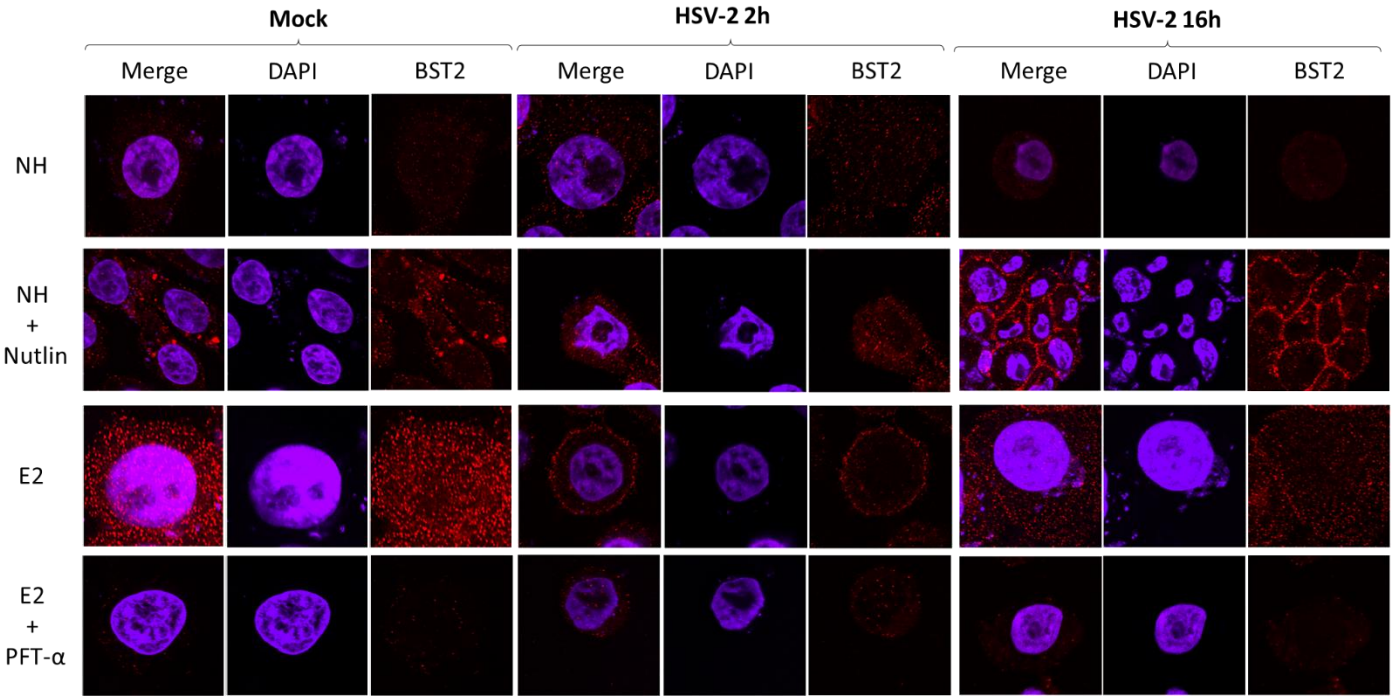

Figure 31: E2 and Nutlin-3 treatment upregulates BST2 protei n expression in VK2 cells. VK2 cells were grown in LLI cultures in NH, E2 (10^{-9} M), NH + Nutlin-3 (5 µM) or E2 + PFT-α (10 µM) conditions up the 7th day, as explained in M&M. Cultures were then either left uninfected or overlayed with HSV-2 (MOI=1) for 2 h at 4 °C, washed with PBS and then incubated for 2 hours or 16 hours at 37 °C. The cells were fixed and stained for BST2 (red) and nuclei were stained with DAPI (blue). Images were visualized by confocal microscopy at x2400 magnification. Experiment has been done twice with each condition done in duplicates. Representative images are shown.

To validate that p53 plays a role in modulating BST2, we knocked down p53 using a p53 specific siRNA, as described in section 7.16 in Materials and Methods, and investigated the effects on BST2 protein expression. VK2 cells were grown in LLI cultures in NH with or without Nutlin-3 (5 µM) treatment, and subsequently transfected with 30 nM of p53 siRNA for 24 hours. Cultures with fixed for immunofluorescent staining of p-p53 and BST2, and then visualized with confocal microscopy (Figure 32). P-p53 was used since the host for the p53 antibody was the same as the BST2 antibody. Results show that VK2 cells with p53 knocked down express significantly less

BST2 in both NH or Nutlin-3 conditions, as compared to untreated VK2s in the respective conditions. This suggests that p53 plays a role in regulating BST2 expression.

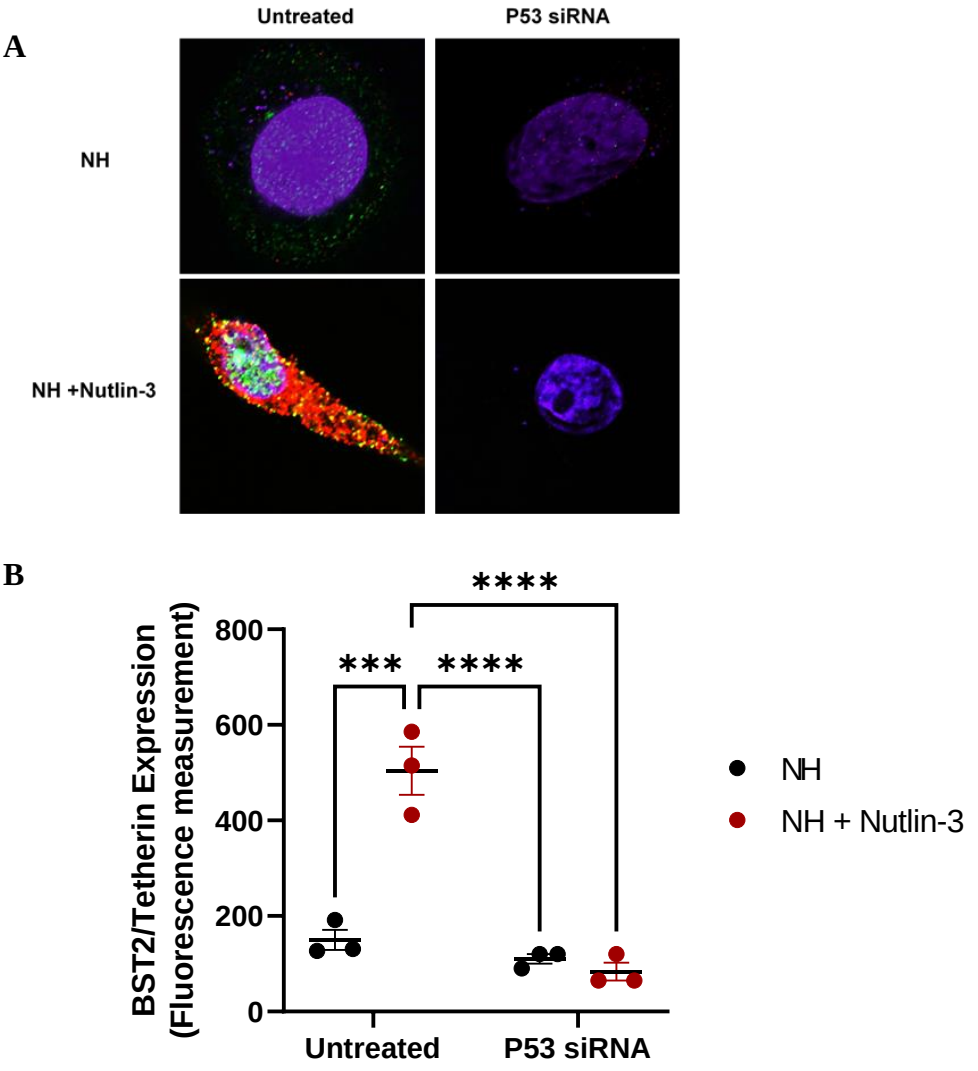

Figure 32: Knockdown of p53 reduces BST2 protein expression

VK2 cells were grown in LLI cultures in NH conditions alone or with Nutlin-3 (5 µM) until 30 – 60 % confluency, and subsequently transfected with two 30 nM of p53 siRNA for 24 hours. (A) Cultures were then fixed and stained with p-p53 (green) and BST2 (red) and visualized for immunofluorescent microscopy using a confocal microscope at x2400 magnification. (B) Fluorescence intensity of BST was quantified with ImageJ software with mean fluorescence presented. Experiment had been done once with duplicates. Data was analyzed using two-way ANOVA, with Bonferroni test to correct for multiple comparisons. Representative images are shown.

Sine we have shown that E2 induces BST2 expression in a p53-dependent manner (Figure 31), and that p53 strongly regulates BST2 (Figure 32), we were interested in analyzing whether modulation of BST2 can affect HSV-2 replication. We did this by using siRNA against BST-2 and performing an HSV-2-GFP infection in cells after 16 hours of infection. VK2 cells were grown in NH, NH + Nutlin-3 (5 μM), or E2 (10^{-9} M) conditions in 24-well plates as described in material and methods. Cultures were then left untreated or treated with three different doses of BST2 siRNA (10 nM, 30 nM, and 50 nM) for 24 hours as seen in Figure 33. We also used scrambled siRNA as a negative control to ensure that addition of RNA sequence had no effect. Cultures were then inoculated with HSV-2 and visualized under the EVOS microscope as described in materials and methods.

Results indicate that knockdown of BST2 under all siRNA dose conditions results in increased HSV-2-GFP expression in all of NH, NH+Nutlin-3, and E2 treatments. However, knockdown of BST2 in VK2s treated with E2 or Nutlin-3 resulted in slightly less HSV-2-GFP expression as compared to knockdown of BST2 in NH conditions under all BST2 siRNA doses. This finding suggests either of two things: 1) the residual BST2 protein levels after siRNA knockdown may be contributing to the antiviral activity, or 2) E2 may have other protective effects aside from BST2 induction which may contribute to reducing HSV-2 replication even when p53 is blocked following induction by E2 or Nutlin-3.

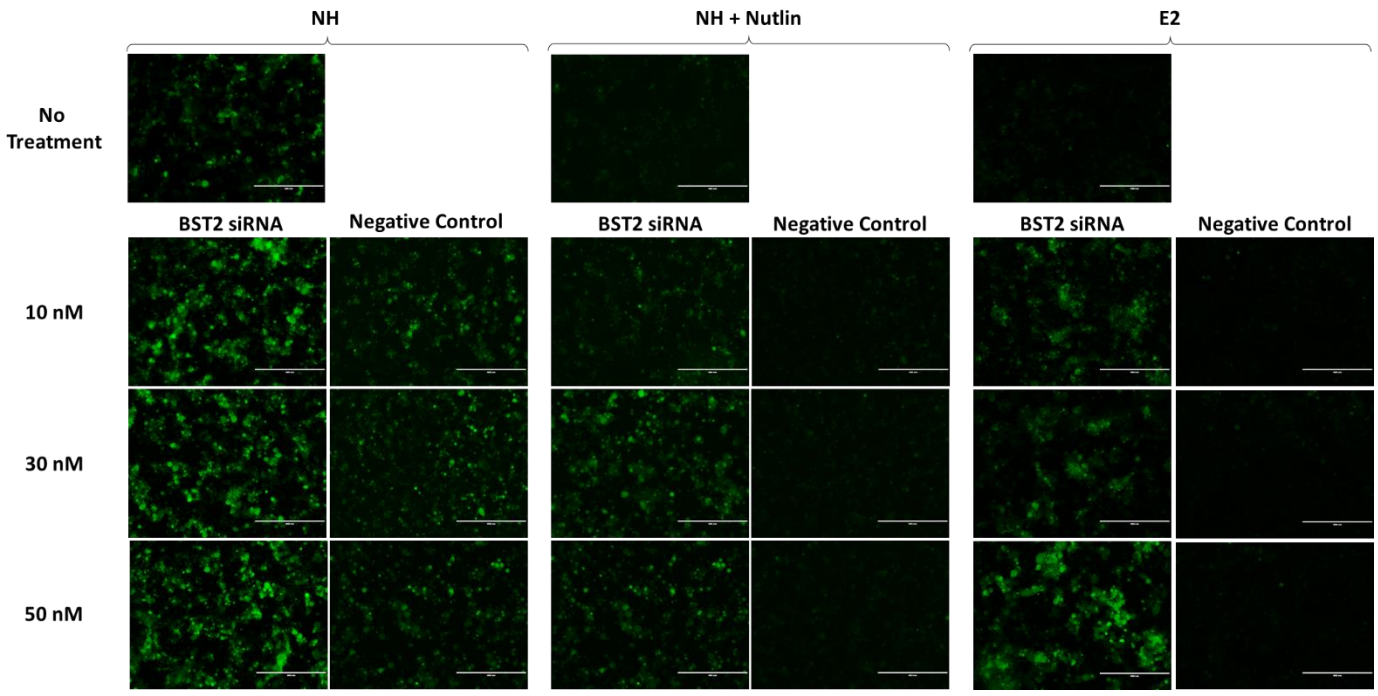

Figure 33: Blocking expression of BST2 increases the rate of infection by HSV-2. VK2 cells were grown in 24-well plates in under NH, NH + Nutlin-3 (5 μM) or E2 (10^{-9} M) until 30-60% confluence. Cultures were then left either untreated or transfected with various doses of BST2 siRNA (10, 30 and 50 nM) or scrambled siRNA (negative control). 24 hours after transfection with BST2 siRNA, cells were infected with HSV-2-GFP at an MOI of one. Images were captured 16 hours after HSV-2-GFP infection with EVOS microscope where green fluorescence of GFP indicates infected cells. Scale bar is represented by the white 400 μm line.

Since we have found that knockdown of p53 results in reduced BST2 expression and that knockdown of BST2 results in increased replication, we decided to perform immunofluorescence staining of both BST2 and HSV-2 simultaneously under the conditions NH, NH + Nutlin-3 (5 μM), E2 or E2 + PFT-α (10 μM), after 16 hours of infection during the replication phase of HSV-2 (Figure 34). We wanted to examine how BST2 and HSV-2 expression is altered after modulation of p53 signaling, as well as visually negatively correlate their expressions. VK2 cells were grown in the aforementioned conditions and subsequently infected with HSV-2 for 16 hours prior to being

fixed, as described in material and methods. We decided to focus on this time point since we previously showed in section 3.1 that the E2-mediated p53 response provides protection particularly at this time point of viral replication (Figure 26). Since we have shown that p53 provides protection against HSV-2 and that p53 modulates BST2 expression, we hypothesize that p53 may be providing its protective effects through BST2. Interestingly, results show that the increased expression of tetherin under E2 or Nutlin-3 conditions after 16 hours of HSV-2 infection correlates with the reduced HSV-2 protein expression (Figure 34). NH and addition of PFTα to E2-treated cells results in lower BST2 expression compared to E2 and correlated with increased HSV-2 fluorescence. The lack of BST2 expression seen in NH conditions may be due to the ability of virus to suppress the antiviral response. These results are consistent with results observed previously where we saw reduced HSV-2 replication after 16 hours of infection (Figure 26), however, we now show its correlation with BST2.

A

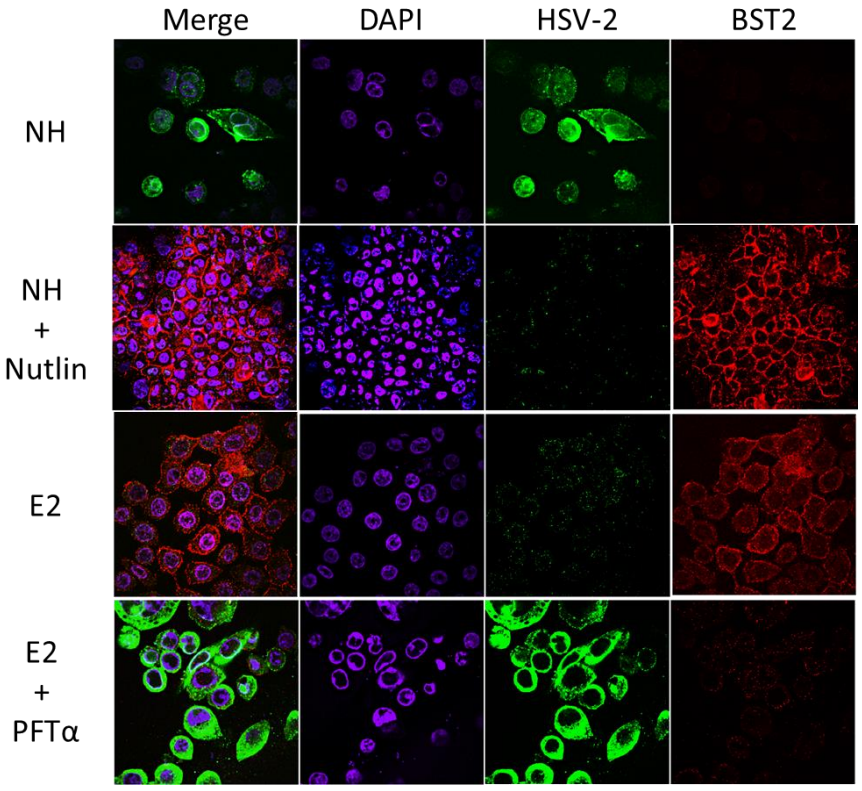

Figure 34: E2 increases BST2 expression and suppresses HSV-2 after 16 hours of infection through p53-mediated effects. VK2 cells were grown in LLI cultures in NH, E2 (10^{-9} M), NH + Nutlin-3 (5 μM) or E2 + PFT-α (10 μM) conditions up the 7th day, as explained in M&M. Cultures were then infected with HSV-2 strain 333 (MOI=1) for 2 h, washed with PBS and then incubated at 37 °C until 16 hours post infection. The cells were fixed and stained for BST2 (red), HSV-2 (green) and nuclei were stained with DAPI (blue). Images were visualized by confocal microscopy at x600 magnification. Experiment has been done once with each condition done in triplicates. Representative images are shown.

Since BST2 is known for its role in tethering onto viruses to prevent their release and exocytosis into the extracellular environment, we decided to investigate its expression during a later time point. VK2 cells were grown in the LLI cultures in NH, NH + Nutlin-3 (5 μM), E2 or E2 + PFT-α (10 μM) conditions, and subsequently infected with HSV-2 for 24 hours prior to being fixed, as described in material and methods. Since we have shown that BST2 has protective effects, we hypothesize that it may be possible for E2 to prevent exocytosis of HSV-2 from host cells through BST2.p53. Interestingly, we observed that E2 not only showed significant upregulation of BST2 at 24 hours of infection, but that it formed clear colocalization of BST2 and HSV-2 around the periphery of the cell, as seen by the yellow colour (Figure 35). Moreover, this colocalization observed in E2 was significantly higher compared to NH. Although Nutlin-3 treatment did not show as increased BST2 expression as E2 after 24 hours of HSV-2 infection, colocalization of BST2 with HSV-2 was still observed. Interestingly, treatment of PFT-α with E2 showed no BST2 expression, and thus no colocalization with HSV-2, compared to E2 alone.

Based on these experiments, we believe that p53 is a regulator of BST2 expression, and that BST2 may play antiviral roles such as preventing viral release, and thus viral replication. Overall, our results show that E2-mediated p53 signaling pathway provides antiviral effects through BST2 signaling.

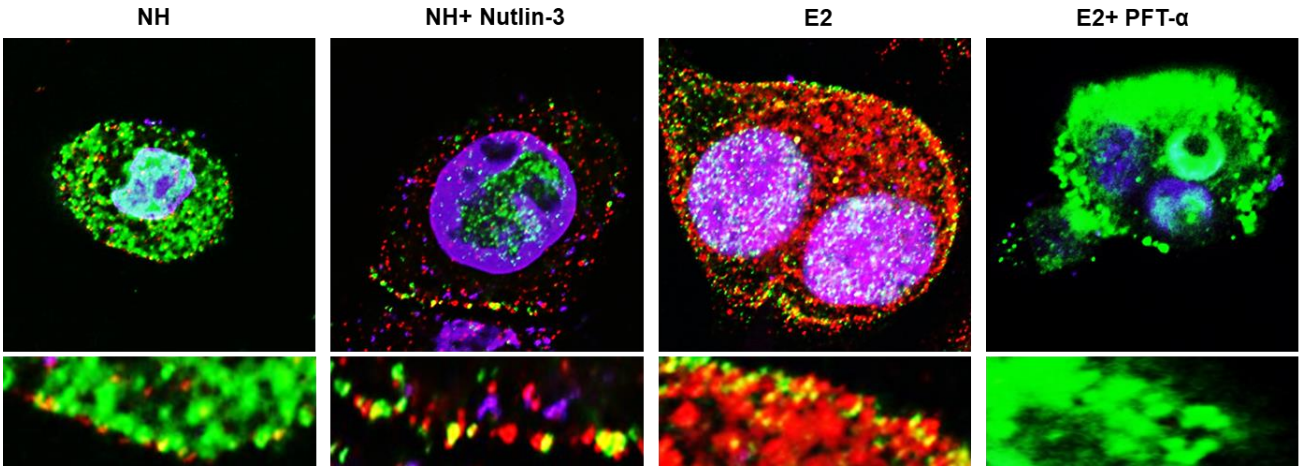

Figure 35: E2 upregulates BST2 expression through a p53-mediated mechanism to physically tether HSV-2 on the cell surface. VK2 cells were grown in LLI cultures in NH, E2 (10^{-9} M), NH + Nutlin-3 (5 µM) or E2 + PFT-α (10 µM) conditions up the 7th day, as explained in M&M. Cultures were then infected with HSV-2 strain 333 (MOI=1) for 2 h, washed with PBS and then incubated at 37 °C until 24 hours post infection. The cells were fixed and stained for BST2 (red), HSV-2 (green) and nuclei were stained with DAPI (blue). Images were visualized by confocal microscopy at x2400 magnification. Lower panel showed enlarged images of cell surface. Experiment has been done twice with each condition done in duplicates. Representative images are shown.

Literature also suggests that suggests BST2 is able to localize in endosomes which have been known to play roles in viral entry.[26, 28, 180] Since we have shown that HSV-2 is able to use the endosomal pathway to enter VK2 cells, we wanted to see where tetherin is located inside the cell. We previously performed EEA1 and HSV-2 staining (Figure 26) after HSV-2 infection and saw minimal colocalization after 2 hours of infection. However, we have indeed shown that EEA1 and HSV-2 are able to colocalize during the early phases of infection (Figure 25). Since BST2 expression is particularly higher under E2 treatment prior to infection, we decided to investigate whether it colocalizes with EEA1 during uninfected mock conditions. We did this to examine whether tetherin is found to localize with endosomes. To address this speculation, we performed an immunofluorescent staining experiment with BST2 and EEA1 in mock conditions (Figure 36). VK2s were grown in LLI cultures in NH, NH + Nutlin-3, E2 and E2 + PFT-α

conditions prior to being fixed, as described in material and methods. Interestingly, we saw that E2 is the only treatment which resulted in colocalization of BST2 and EEA1, as seen with the yellow colour.

Overall, since we see increased expression of BST2 after Nutlin-3 or E2 treatment compared to NH, and reduced BST2 expression after addition of PFT-α to E2 compared to E2 alone; these results suggests that E2 has a p53-dependent effect on tetherin expression.

In conclusion, the p53 pathway is unable to induce interferon signaling and has minimal effect on downstream antiviral pathways to protect against HSV-2 infection. However, one of the antiviral genes BST2, responsible for tetherin protein expression, is modulated by E2 through a -p53-mediated mechanism. Suppression of BST2 results in increased HSV-2 replication, indicating that BST2 has an important antiviral role in the context of HSV-2. Therefore, the results suggest that E2-mediated p53 pathway may be providing protection against HSV-2 infection through modulation of BST2 as its mechanism.

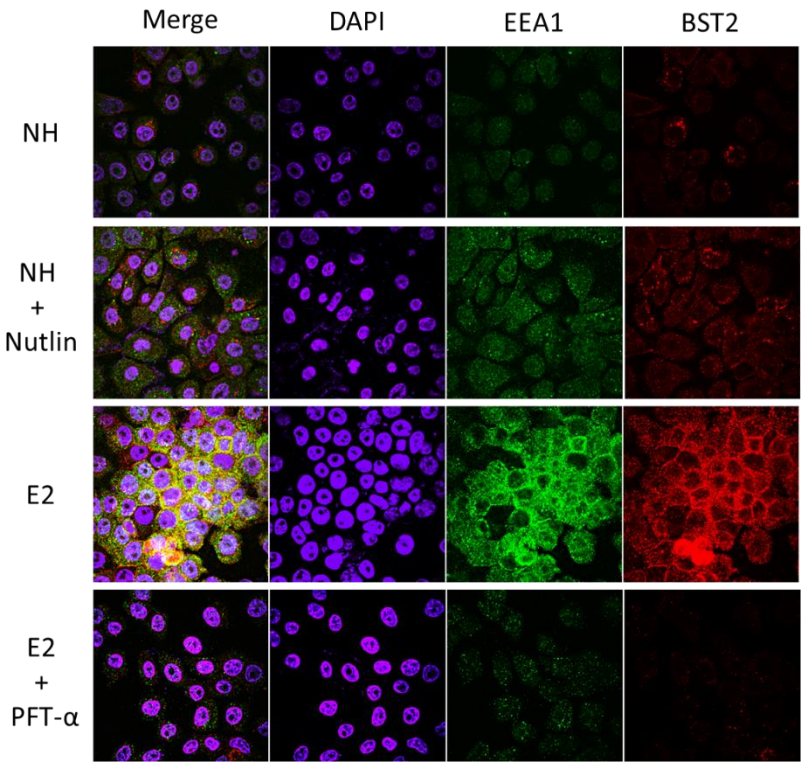

Figure 36: E2 treatment increases endosomal uptake of BST2. VK2 cells were grown in LLI cultures in NH, E2 (10^{-9} M), NH + Nutlin-3 (5 μM) or E2 + PFT-α (10 μM) conditions up the 7th day, as explained in M&M. Cultures were then fixed and stained for BST2 (red), EEA1 (green) and nuclei were stained with DAPI (blue). Yellow expression is indicative of colocalization of BST2 and EEA1. Images were visualized by confocal microscopy at x600 magnification. Experiment has been done once with each condition done in duplicates. Representative images are shown.

4.7 Examination of inflammatory response of E2-induced p53 pathway upon HSV-2 infection in VK2s

Our lab has previously shown that E2 treatment increases barrier integrity and decreases pro-inflammatory cytokine response in primary upper genital epithelial cells.[181] Since we have shown that the upper and lower FRT responded similarly to activators and inhibitors that alter p53, as well as E2 treatment and its effects on p53 expression (Figure 14, 18, 19), we therefore hypothesized that E2 treatment will promote increased barrier integrity and decreased inflammation. Thus, we decided to investigate the role of E2 in modulating the inflammatory state in the host cell through the p53 pathway.

4.7.1 Investigation of the role of E2 and p53 in modulating NF-κB

Infection with viruses can elicit protective responses, where host cells are inclined to undergo apoptosis or restrict the cell cycle as pre-emptive measures to prevent viral replication and subsequent production of infectious viral particles. Due to the protective effects we have shown with E2 through the p53 pathway along with the connection of p53 to inflammation found in literature, we expect to see a dampened inflammatory environment in these conditions as a potential mechanism to prevent viral pathogenicity. Various studies in literature have reported the role of NF-κB as a crucial regulator that links infections and chronic inflammation.[182, 183] Moreover, there is long known opposing relationship that exists between NF-κB and p53 in scientific literature.[184-186]. Interestingly, E2 has also been reported to regulate the function of NF-κB through restricting NF-κB-inhibitor degradation, or inhibiting nuclear translocation of NF-κB, thus preventing downstream pro-inflammatory expression.[102, 103] Since we have reported that E2

treatment decreases viral replication, we hypothesized that E2 achieves this protection by suppressing inflammatory pathways through a p53 mediated mechanism.

Based on literature findings that suggest the connection between E2, p53 and NF-κB, as well as the role of NF-κB in inducing inflammatory cytokines, we first performed immunofluorescent staining of NF-κB. VK2 cells were grown in LLI cultures in NH, NH + Nutlin-3 (5 μM), E2 or E2 + PFT-α (10 μM) until day 7, and subsequently infected with HSV-2 as described in material and methods. Cultures were either fixed without infection or after 2 and 16 hours of HSV-2 infection to investigate the modulation of NF-κB during times of viral entry and virus replication, respectively. Results indicate that NF-κB protein expression was significantly lower under the influence of E2 treatment compared to NH treatment in VK2s infected for 2 hours and 16 hours, but not in uninfected mock conditions (Figure 37). Comparison between NH, NH+Nutlin-3, and E2 + PFT-α panels showed no significant difference in NF-κB expression in uninfected and 2- or 16-hour HSV-2-infected VK2s. This suggests that NF-kB expression was not altered by p53 activation. However, E2 + PFT-α treatment shows higher NF-kB expression when compared to E2 alone before and after infection. Interestingly, NF-κB expression in NH, NH + Nutlin-3 and E2 + PFT-α conditions was visually higher after infection compared to uninfected cells in respective treatments. However, expression of NF-κB under the influence of E2 treatment did not increase after infection when compared to uninfected E2-treated cells, suggesting that E2 prevents HSV-2-mediated induction of NF-κB in VK2s. Since NF-κB is involved in inflammation, this finding supports our speculation of E2 having an anti-inflammatory role. However, these results also indicate that modulation of NF-κB expression by E2 is possibly through the p53 pathway.

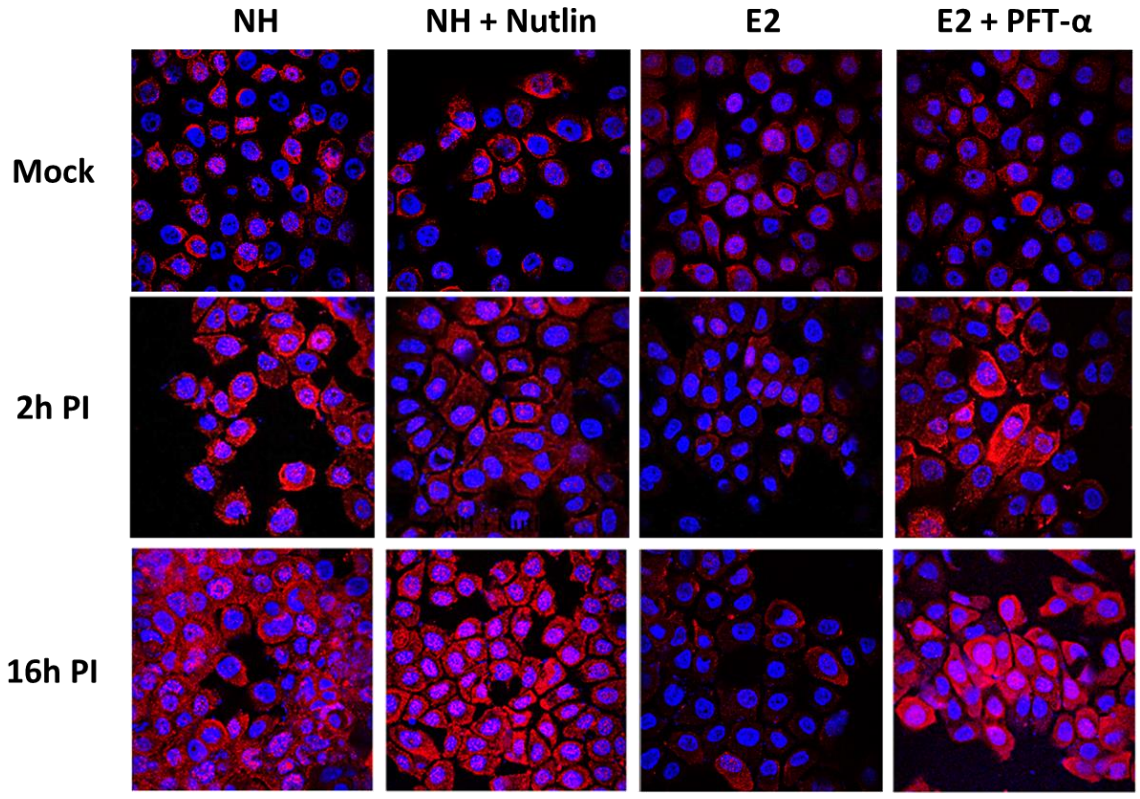

Figure 37: E2 treatment prevents HSV-2 induced NFκB expression. VK2 cells were grown in LLI cultures in NH, E2 (10^{-9} M), NH + Nutlin-3 (5 μM) or E2 + PFT-α (10 μM) conditions up to the 7th day, as explained in M&M. Cultures were then infected with HSV-2 strain 333 (MOI=1) for 2 h, washed with PBS and then incubated at 37 °C for 2 hours and 16 hours. The cells were fixed and stained for total NFκB (red) and nuclei were stained with DAPI (blue). Images were visualized by confocal microscopy at x600 magnification. Experiment has been done once with each condition done in triplicates. Representative images are shown.

4.7.2 Determining the role of E2 and p53 in modulating cytokines and chemokines downstream of NF-κB

We further investigated mRNA expression of cytokines/chemokines which are activated downstream of NF-κB, including cytokines TNF-α andIL-1β, as well as chemokineIL-8, to validate the effect of E2 on suppressing inflammation. VK2 cells were grown in ALI cultures in conditions of NH, NH + Nutlin-3 (5 μM), E2 or E2 + PFT-α (10 μM) up until 7 days, as described in material and methods. Cultures were either left uninfected or inoculated with HSV-2 for 2, 16 and 24 hours prior to RNA extraction, as described in material and methods. We then performed RT-qPCR of the genes TNF-α, IL-1β and IL-8 and reported their fold change relative to expression in NH mock conditions (Figure 38). Of the three genes analyzed, TNFα was the only gene found to be reduced under E2 treatment, particularly at 2 hours and 16 hours after HSV-2 infection (Figure 38A). However, no significant difference is seen when compared to NH during mock and 24 hours after HSV-2 infection. These results indicate that E2 does induce some anti-inflammatory effect as seen by suppression of TNF-α. Moreover, this appears to be through a p53-dependent mechanism since inhibition of p53 in E2-treated VK2s significantly reduced TNF-α gene expression compared to VK2s treated with E2 alone.

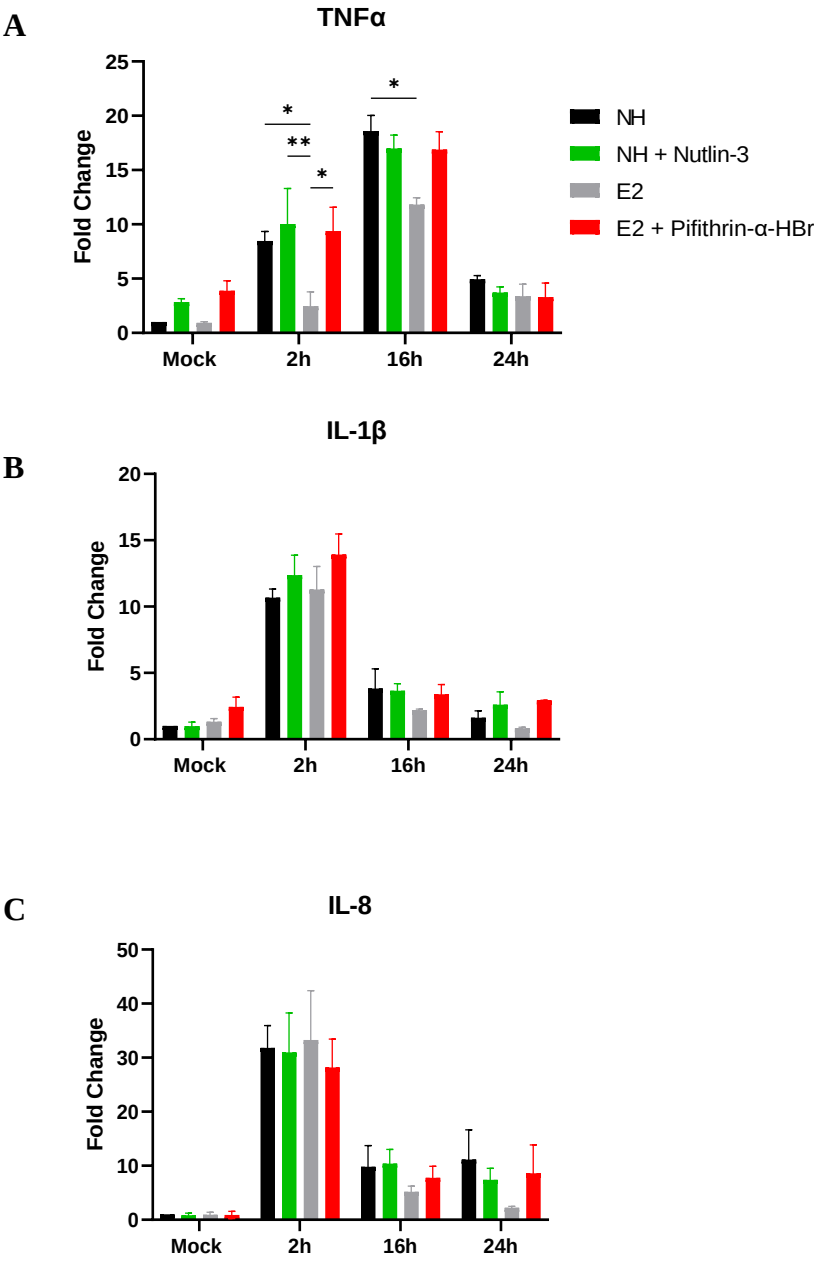

Figure 38: E2 treatment significantly downregulates TNF-α expression in VK2 cells after 2 and 16 hours post HSV-2 infection. VK2 cell ALI cultures were first grown in NH alone, NH + Nutlin-3 (5 µM), E2 alone (10^{-9} M), or E2 + PFT-α (10 µM) and either left uninfected (mock) or infected with HSV-2 strain 333 (MOI=1) for 2, 16 or 24 hours. RNA was extracted and used for RT-qPCR to measure mRNA expression of A) TNF-α, B) IL-1β and C) IL-8. Data shown are mean ± SEM (n = 2) with each condition done in duplicates Data was analyzed using two-way ANOVA, with Bonferroni test to correct for multiple comparisons. Statistical significance: *p < 0.05, **p < 0.01, ***p < 0.001, **** p < 0.0001.

4.7.3 Investigating the role of E2 and p53 in barrier integrity of VK2s

Next, we decided to investigate whether E2 influences barrier integrity of VK2s in relation to anti-inflammatory effect. Transepithelial resistance (TER) was measured to assess growth and barrier function of VK2s grown in ALI conditions under NH, NH + Nutlin-3 (5 μM), E2 (10^{-9} M), E2 + PFT-α (10 μM) or P4 (10^{-7} M) conditions, as described in materials and methods. Cultures were grown up till the 7th day and TER measurements were subsequently recorded. E2 and P4 treatment both resulted in significantly higher TER measurements as compared to NH conditions, while activation or inhibition of p53 did not alter TER values (Figure 39).

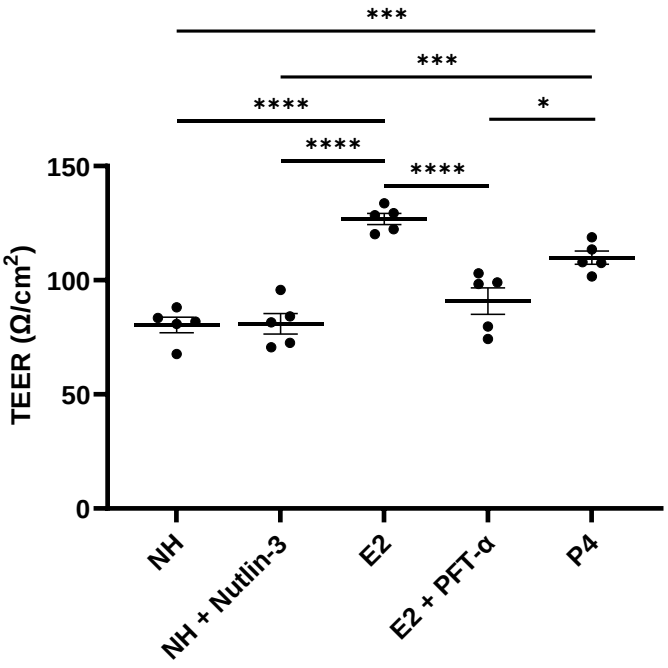

Figure 39: E2 treatment improves epithelial barrier function in VK2 cells. VK2 cells were grown in LLI cultures in NH, E2 (10^{-9} M), NH + Nutlin-3 (5 μM) or E2 + PFT-α (10 μM) conditions until the 7th day. Transepithelial resistance (TER) was measured with a chop-stick electrode and presented as raw measurements. Data shown are mean ± SEM (n = 3) with each condition done in triplicates. Data was analyzed using two-way ANOVA, with Bonferroni test to correct for multiple comparisons. Statistical significance: *p < 0.05, ***p < 0.001, **** p < 0.0001.

Interestingly, pro-inflammatory cytokines such as TNF-α and IL-1β are known to promote disruption of tight junction barriers, thus resulting in decreased barrier integrity.[187] Since E2 resulted in increased barrier integrity along with suppressed TNFα expression levels, we decided to investigate the effect of E2 on tight junction proteins. ZO-1 is a multi-domain polypeptide that acts as a scaffolding protein and is required for the assembly of tight junctions.[188] Consequently, we performed an immunofluorescent staining assay of ZO-1 on VK2s grown in NH or E2 and subsequently treated with either no treatment, Nutlin-3 (5 μM) or PFT-α (10 μM) prior to finishing the 7th day of culture, as described in materials and methods. This was done in both LLI and ALI cultures because tight junctions behave differently in stratified layers of cells, as they form junctions vertically above and below, as well as horizontally across the plane. Results show that E2 resulted in significant induction of ZO-1 protein expression compared to NH in both LLI (Figure 40A) and ALI (Figure 40B) cultures. Interestingly, addition of PFT-α to E2 resulted in significant reduction in ZO-1 expression when compared to E2 alone in both ALI and LLI cultures, suggesting that blocking p53 in addition to E2 reduces barrier integrity. However, addition of PFT-α to NH showed no reduction in ZO-1 expression when compared to NH alone, possibly because the basal levels are too low for a difference to be noticeable. Nutlin-3 treatment in addition to NH, however, displayed no significant difference in ZO-1 expression in both LLI and ALI cultures compared to NH alone. Similarly, addition of Nutlin-3 to E2 also showed no difference in ZO-1 expression when compared to NH + Nutlin-3.

In summary, the results suggest that E2 likely plays an anti-inflammatory role as indicated by suppression of NF-κB, and its downstream cytokines such as TNF-α. This may result in beneficial effects to the cells, enabling stronger barrier integrity with upregulation of tight junction proteins such as ZO-1.

A

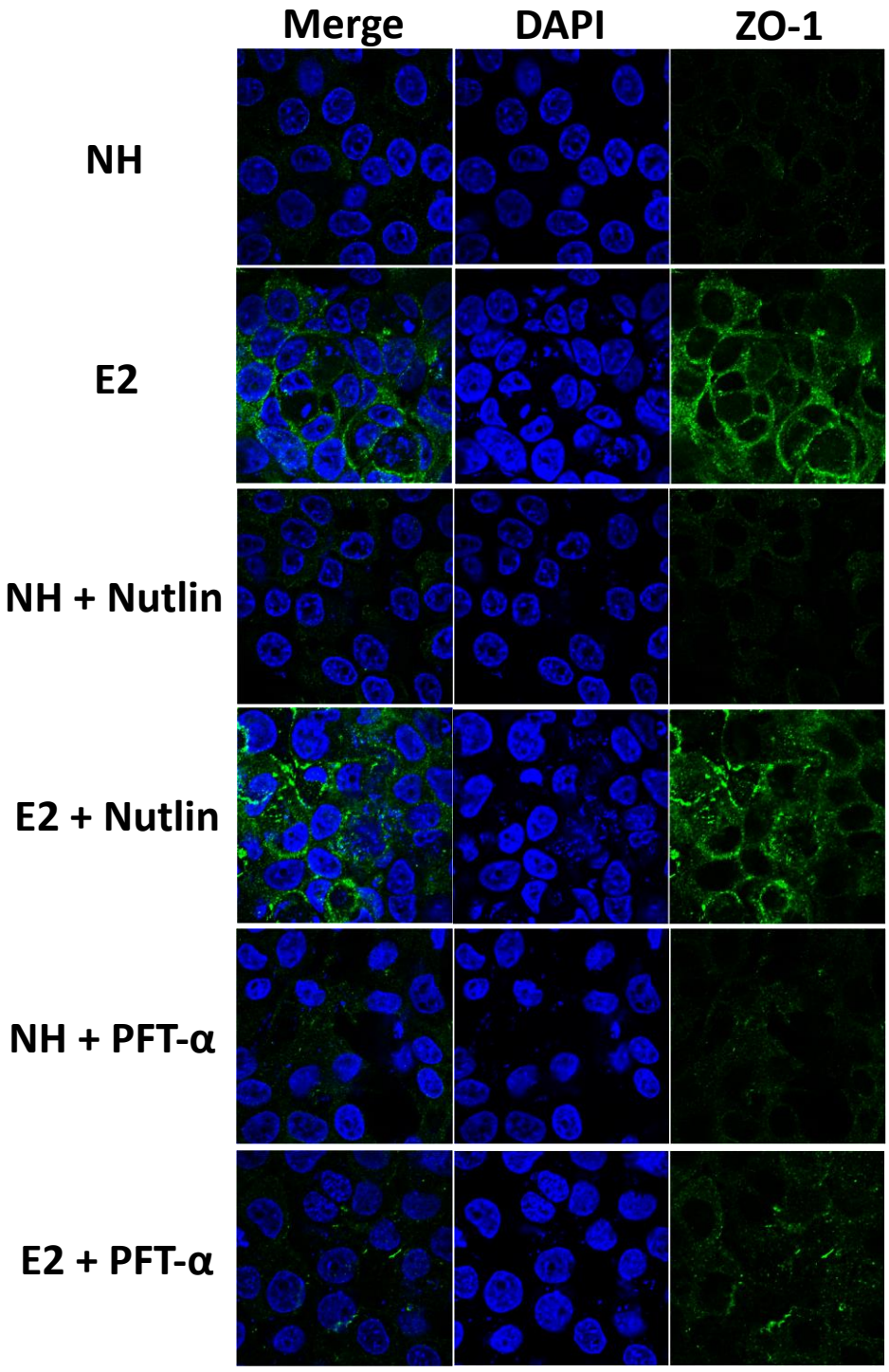

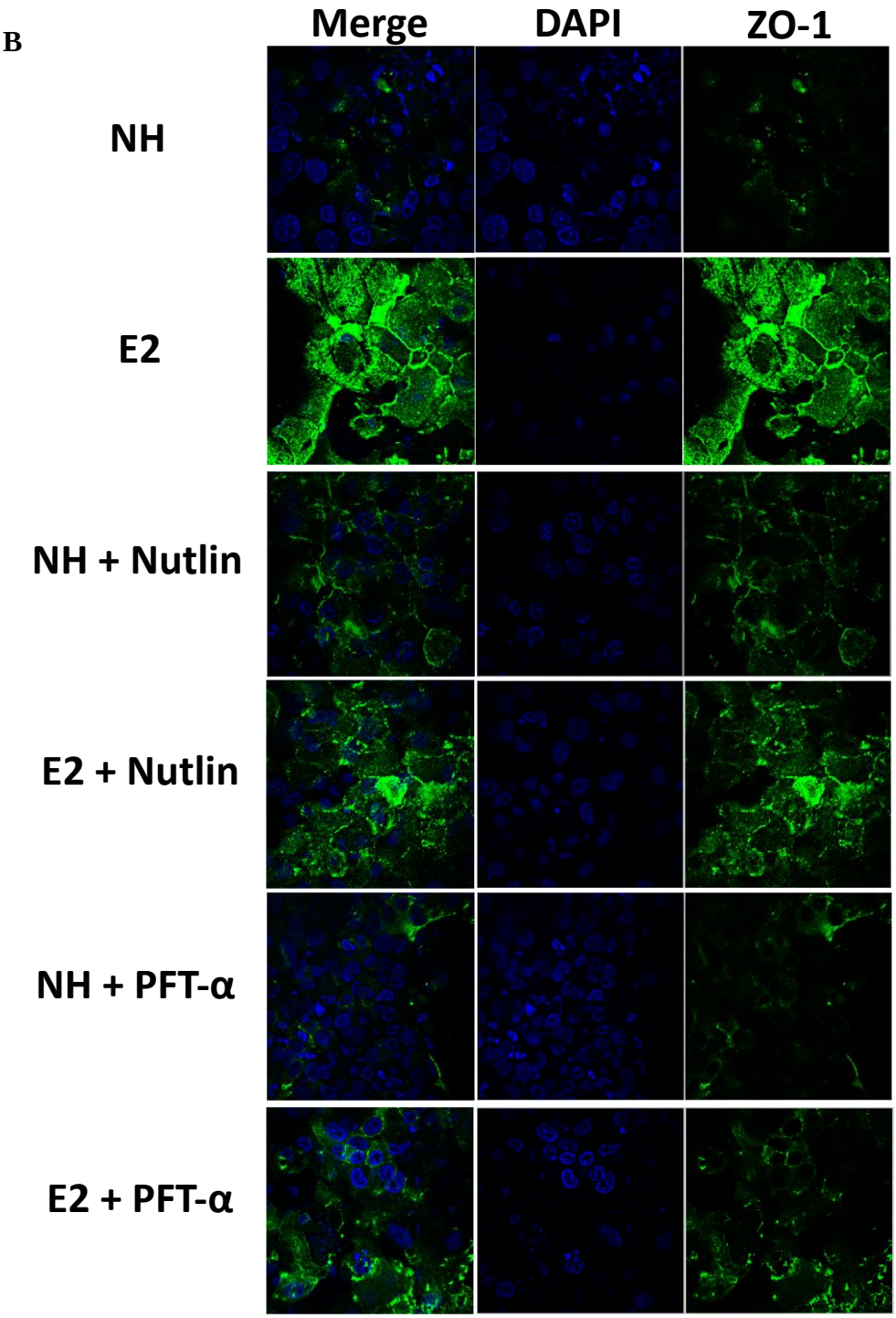

Figure 40: E**2 upregulates ZO-1 tight junction in VK2 cells.** VK2 cells were grown in (A) LLI or (B) ALI cultures treated with either no hormone or E2 (10^{-9} M), with addition of Nutlin-3 (5 µM), PFT-α (10 µM) or left untreated. Cells were subsequently fixed and stained with ZO-1 (green) and nuclei stained with DAPI (blue). Images were captured on confocal microscope (n=2) at (A) x1200 magnification and (B) x600 magnification. Experiment has been done once with each condition done in duplicates. Representative images are shown.

CHAPTER 5: DISCUSSION

5.1 Summary

Many studies have consistently found that women are at a significantly greater risk of acquiring sexually transmitted infections relative to men.[105, 189] For example, prevalence of genital herpes is reported to be higher in women than men, with Western European men showing the lowest prevalence rates of around 13% and sub-Saharan African women associated with the highest prevalence rates of >70%.[1] Similarly, women are also more likely to contract HIV infections which continues to be a serious health issue globally.[190]

A key factor which has consistently been shown to alter STI susceptibility in the FRT is the presence of female sex hormones.[36, 37, 76-81, 83] During the menstrual cycle, women in estrogen-high phases are less susceptible to STIs, including HIV-1 and HSV-2.[78, 79, 81, 82] When progesterone levels peak during the cycle, women show increased susceptibility instead.[79, 92] Interestingly, there is also substantial evidence showing that progestin-based contraceptives, such as MPA, increase susceptibility as well.[92, 191] A meta-analysis study also demonstrated that the use of MPA by women is associated with increased susceptibility to HIV.[192] Although there are many epidemiological studies as well as *in vivo* studies which have demonstrated the effects of hormones on susceptibility to infections, a recent study has shown similar findings at an *in vitro* level when investigating vaginal epithelial cells, which are one of the first cells to interact with pathogens.[78] However, no study has investigated the mechanism responsible for the direct effects of hormones on epithelial cells of the vaginal tract. Since estrogen has been shown to have protective effects on vaginal epithelial cells, the initial aim of our study was to use a bioinformatic approach to determine how this hormone, at a cellular level, modulates cellular pathways to alter susceptibility against HSV-2.

Overall, the first part of our study constituted a bioinformatic approach that was used to identify a potential pathway that contributes to E2-related protection. Results from the transcriptomic analysis found the p53 pathway to be an important part of the E2 response. The second part of our study used functional analyses to confirm the bioinformatic hypothesis and prove whether it can contribute to antiviral effects and thus, protection against HSV-2. E2 was found to increase p53 expression, thus confirming our hypothesis from our bioinformatic analysis. Furthermore, we discovered that E2-mediated p53 plays an important role in suppressing viral replication. It was found that E2 also modulates BST2, an interferon stimulated gene reported to have antiviral roles, which depends on p53 expression Examination of the antiviral effects of BST2 prove that it too is important in suppressing HSV-2 replication. Finally, this study also demonstrated that E2 has anti-inflammatory effects on VK2 cells which correlates with enhanced barrier integrity as seen by increased tight junction protein expression. Therefore, this study elucidates the mechanism of some of the cellular pathways through which estradiol provides protection against HSV-2 infection in human vaginal epithelial cells. Although the role of E2 in providing protective effects against infections has been reported multiple times in literature, this study is the first to demonstrate the novel findings of antiviral effects that E2 modulates in vaginal epithelial cells. A summary of the results from this study is shown in Figure 41.

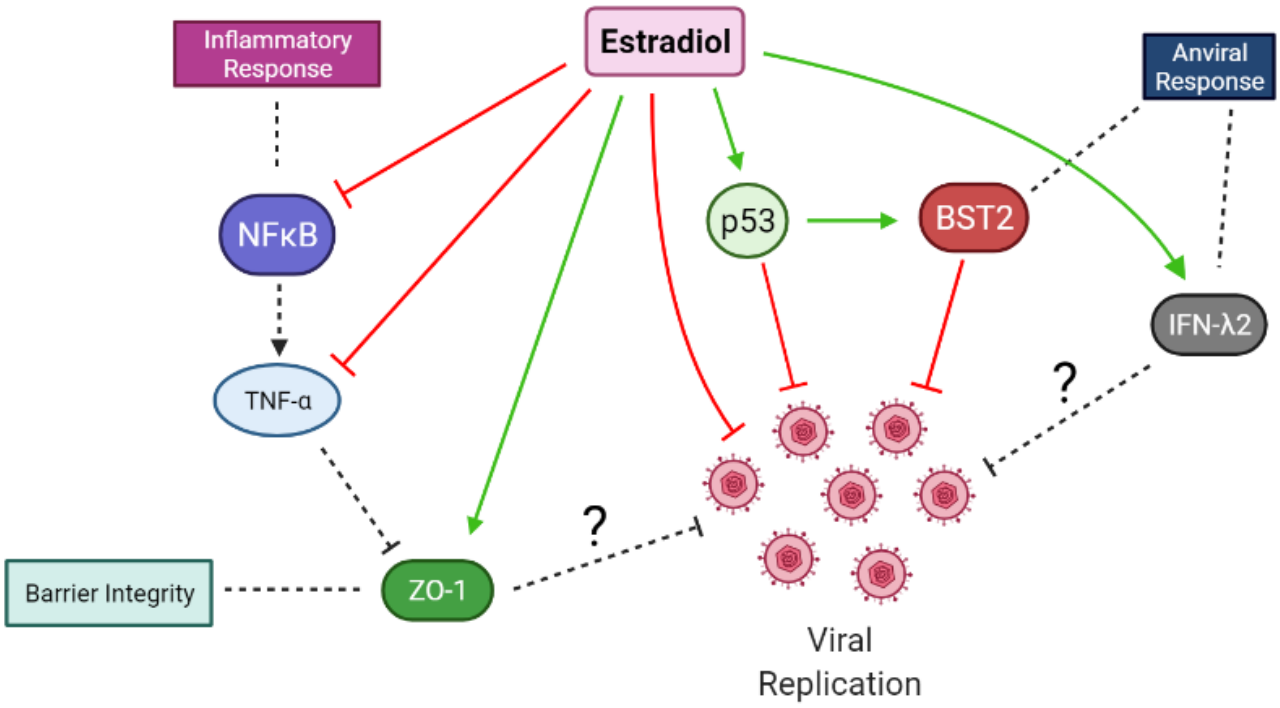

Figure 41: Summary of study. Results from this study show estradiol is a key factor in providing protective effects against HSV-2, and primarily does this through the p53 pathway. Estradiol directly promotes p53 activation which consequently reduces HSV-2 replication. Moreover, results also imply that the E2-mediated p53 pathway is able to induce BST2, an interferon stimulated gene, as an anti-viral mechanism that contributes to suppression of HSV-2 replication. We also showed that E2 induces IFN-λ2 gene expression, an anti-viral interferon previously shown to have inhibitory effects on HSV-2. Estradiol was also found to suppress inflammation by inhibiting NFκB and its known downstream cytokine TNF-α. With literature suggesting a negative correlation between inflammation and barrier integrity, our results strengthen this phenomenon with results of estradiol-dependent ZO-1 upregulation. We can only speculate that this upregulation of ZO-1 and increase in barrier integrity plays a role in HSV-2 infection, however, further studies are needed to confirm. Dotted lines indicate correlations between proteins implied by literature. Green arrows indicate activation or upregulation, whereas red lines indicate inhibition or suppression.

Prior to this study, our lab had developed a well-established and optimized *in vitro* ALI cell culture system. This ALI culture system is a method used to grow vaginal epithelial cell cultures to examine how HSV-2 infects in a physiologically similar environment to the lower FRT. Using these ALI cultures, our lab grew VK2 cells under the absence or presence of hormones E2 and P4 under physiological concentrations, as well as MPA, and infected them with HSV-2 for 24 hours prior to RNA extraction. RNA was sent for analysis of raw expression values of a full transcriptome of genes and the relevant data obtained was what I used to begin the transcriptomic analysis, the first step of this study. We first determined all differentially expressed genes between E2 and P4 to determine which treatment showed the most unique profile compared to NH (Figure 9A). Interestingly, we discovered that E2 had a distinct transcriptomic profile, compared to P4 which showed a similar heatmap gene pattern to NH conditions. This discovery suggested that indeed E2 had unique effects not seen in other experimental conditions, which further strengthened the importance of investigating effects of estradiol on modulation of cellular pathways that contribute to protection seen in VK2 cells in response to HSV-2 infection.

To address the first objective outlined in thesis, which is to conduct bioinformatic pathway analysis to identify the differentially regulated genes and cellular pathways modulated in E2-treated HSV-2-infected VK2 cells, we begun by looking at the effect of hormonal treatments at a single-gene level and performed a volcano-plot analysis (Figure 10). We found that LCE3D and CNFN, which are known to play roles in envelope cornification and epithelial cell keratinization whilst providing structural stability to the epithelium,[193] were upregulated by E2 conditions when compared to either NH or P4 (Figure 10A and B). Interestingly, a recent study investigated the effects of estrogen treatment on vaginal epithelial responses following uropathogenic *E. coli*

challenge.[85] They performed a microarray analysis and found that estradiol (4nM) upregulates LCE3D and CNFN as well, thus strengthening our findings.[85] It is notable that DEG analysis with P4, compared with E2 or NH, shows reduced number of genes with significance while E2 comparison with MPA shows an extremely active profile relative to E2 compared to NH. Although MPA is progestin-based contraceptive that exerts its effects through the progesterone receptor, MPA has been reported to bind with glucocorticoid receptors as well which are ubiquitously expressed in VK2s.[194, 195] This is likely the reason why comparison with MPA shows a much more potent effect compared relative to comparison of E2 to P4 volcano plots. More specifically, volcano plot analysis comparing E2 and MPA indicate significant upregulation of LCE3D, LCE3E and LCE1F, an entire cluster of genes belonging to the late cornified envelope family, as well as LOR and SPRR2B, which are involved in cornification and keratinization (Figure 10D). The epithelium in the lower FRT differentiates continuously, culminating in an actively dividing basal layer and terminally differentiated superficial layer with cornified epithelial cells which contribute to preventing infection by STIs such as HIV.[196] Since the top layers of multilayered vaginal squamous epithelium are devoid of tight junctions,[41] disruptions in the lower protective corneum barrier are likely to be more permeable to entry of various pathogens.[196, 197] Late cornified envelope proteins are involved in the keratinization process and provides structural stability as well as barrier function to the epithelium.[198] This not only suggests that E2 has a role in inducing stronger barrier integrity in response to HSV-2, but also that P4 and MPA may have decreased barrier integrity of VK2s relative to E2. In support of this, a recent transcriptional study by our lab also found the transcriptional response of VK2s to MPA treatment correlated to decreased barrier integrity.[145] Despite the intriguing clues obtained from single-gene analysis, we decided to focus

on the entire transcriptional profile to better gauge which cellular pathways are altered under E2 treatment.

We next performed a pathway analysis rather than utilizing results from the single-gene approach. Gene-set enrichment analysis of DEGs between various hormone comparisons was done using the Hallmark database (Figure 11). Results from our GSEA, as well as from a protein-protein network analysis (Figure 13), suggested the p53 pathway as a major contributor to the E2 transcriptomic profile. Modulation of the p53 pathway was not found under P4 treatment when compared to NH, suggesting that this is a E2-specific observation.

p53 is often described as the "guardian of the genome", as it is often involved in cell cycle checkpoint to allow DNA repair before the cell continues to replicate. It's often given the description as a tumor suppressor protein because without its presence, the cell proceeds through the cell cycle unregulated with various mutations and high level of proliferation, thus leading to tumors.[115] P53 employs its various effects through induction of key downstream regulatory factors which altogether make up the p53 pathway. These factors contribute to various outcomes such as growth arrest, apoptosis, DNA repair, senescence, autophagy, metabolism, and more.[118] The p53 pathway has previously been reported for its interactions with various viral infections, the immune system and hormones. Multiple studies have demonstrated that estrogen plays an important role in altering p53 and its downstream targets.[133-137] Since the estrogen receptor is an important factor of estrogen-mediated signaling of downstream response genes, it is important to note that out of the various functional domains located on ERα, a p53 binding region is located at domain D (dimerization/hinge domain) and E (ligand binding domain/activation function), thus suggesting the link between p53 and estrogen signaling.[142] p53 has also been reported to regulate downstream responsive immune-related genes involved in IFN signaling and cytokine/chemokine production,

suggesting a crucial role of p53 in regulation of inflammatory and antiviral responses.[125, 128-131] Interestingly, p53 has also been known to play an important role in the context of HSV-1 infection, where it has been shown to interact with different HSV-1 viral proteins.[121] With the paucity of research of the role of p53 in the context of viral infection, as well as the link between estrogen and p53 signaling, the p53 pathway was a strong and interesting candidate pathway for further studies. Although studies have shown the important interaction between p53 and other viruses, including HSV-1 and its viral proteins,[121] there is minimal data on the link between p53 and HSV-2, and the corresponding antiviral responses. By using our bioinformatic results, our next goal was to perform functional analyses to confirm that that E2 modulates the p53 pathway to subsequently induce antiviral effects, as well as suppress inflammation, to protect against HSV-2 replication.

To confirm the bioinformatic pathway analysis and address our second objective which was to conduct a functional analysis to determine whether a) the p53 pathway is activated by E2 and b) if activation of p53 confers protection against HSV-2 in vaginal epithelial cells. We first performed a functional analysis to assess whether E2 can induce p53 protein expression and compared this to a commonly used p53 activator, Nutlin-3, as our positive control (Figure 14). Nutlin-3 activates p53 expression by displacing p53 from MDM2, a negative regulator of p53. By occupying the p53-binding pocket of MDM2, Nutlin-3 is able to prevent a MDM2-p53 interaction, thus leading to p53 stabilization and activation of the p53 pathway, one of the most common methods of activating p53.[199, 200] This suggests that Nutlin-3 activates p53 through an indirect mechanism which explains why there were no differences seen in p53 gene expression with Nutlin-3 treatment. We also used a p53 inhibitor, PFT-α, to show that it is able to suppress p53 since we used it in various experiments henceforth. PFT-α, on the other hand, is known to inhibit p53 post-translationally. However, the mechanism through which this occurs is still

unknown. A recent study shows that PFT-α treatment results in inhibition of total p53 protein suppression after Nutlin-3 induction, as well as suppression of various phosphorylated forms of p53, however; this effect is not observed consistently among different cell lines.[164] Moreover, the same study found that PFT-α had a differential inhibitory effect on various genes downstream of p53, where some were partially inhibited, while others were not inhibited at all, suggesting that PFT-α does not function as a complete inhibitor of the p53 pathway and that it may have other unknown effects.

We performed immunofluorescent staining of p53 in LLI cultures for confocal assessment since ALI cultures grow in stratified cell layers and resulted in unclear images. We confirmed that indeed, E2 was able to induce p53 very potently even when compared to the positive control. The effect of physiological concentrations of E2 on inducing p53 expression has been also reported previously.[133] Interestingly, another study has shown that treatment with E2 not only increases p53 expression, but when cells are treated with E2 and the pure estrogen receptor antagonist ICI 182,780, the increase in p53 is reversed back to levels similar to that of the control.[201] We then confirmed our transcriptome results by performing RT-qPCR of p53 to prove that E2 acts as an inducer on the p53 gene at a transcriptional level (Figure 15). Literature suggests that the estrogen receptor is heavily involved in the transcriptional regulation of estrogen gene targets, and so, we analyzed ERα as well, since it is the receptor that is highly expressed in female genital tissues. Interestingly, there is presence of a p53 binding region located on the functional domains of ERα, suggesting an interaction between these two factors.[142] Results indicated that E2 significantly upregulates p53 gene expression as compared to NH during mock conditions, as well as after HSV-2 infection. This suggests that E2 results in an initial high level of p53 expression, and that it may be responding to infection by further increasing p53 levels as a mechanism of protection, as

discussed later. Treatment with either the p53 activator or inhibitor did not alter p53 gene expression levels as compared to NH before and after HSV-2 infection, which may be attributed to the mechanisms of these small-molecule compounds. Nutlin-3's induction of p53 through an indirect mechanism where it binds to its negative regulator MDM2 may help explain why there were no differences seen in p53 gene expression with Nutlin-3 treatment. The p53 inhibitor, PFT-α, on the other hand, is known to inhibit p53 post-translationally. A recent study shows that PFT-α treatment suppressed p53 which has been phosphorylated at either Ser15 or Ser33 sites, which are post-translational modifications, suggesting that PFT-α may be inhibiting p53 post-translationally, which may explain why we did not see differences in mRNA expression of p53 after PFT-α treatment.[164]

To confirm whether PFT-α is functioning the way it has been reported, we analyzed the level of Ser15 phosphorylated p53 after PFT-α treatment. We found that it reduced p-p53 levels despite E2 pre-treatment, thus strengthening our speculation of why we don't see differences in p53 gene expression (Figure 16). Interestingly, we also found that E2 was able to induce significantly high levels of phosphorylated p53 (p-p53) compared to NH which showed minimal expression. Therefore, since phosphorylation is an important event that contributes to nuclear translocation, it is inferred that E2 plays a role in promoting p53 activation in VK2s.

Prior to further investigation, we performed experiments to establish and confirm the optimal dose of our p53 activator and inhibitor reagents (Figure 17 and 16). After deciding on the optimal dose with least affect on cell viability, we continued with our investigation. Since the VK2 cell line is immortalized due to addition of E6/E7 sequences from Human papillomavirus (HPV), it raises concerns whether this could interfere with the effects we saw on p53 upregulation. For example, the E6 protein has been found to associate with p53 as a mechanism by which HPV

induces tumors, and in some cases target p53 for proteosome-dependent degradation.[169] Thus, to address this concern and to confirm that the effects of treatments seen in VK2s are not affected by E6/E7 interference, we performed immunofluorescent staining of p53 and ER-α in primary genital epithelial cells, particularly endometrial and ectocervical cells, which are not under the influence of E6/E7 genes (Figure 20F and 19). Although endometrial cells are from the upper FRT, ectocervical cells are closest representation of how vaginal cells would behave due to their similarity in morphology. Results showed that primary GECs also showed upregulation of p53 after estrogen as well as Nutlin-3 treatment, thus confirming that E6/E7 genes do not interfere as a variable. Moreover, these results also suggest that the E2-mediated induction of p53 may not be specific to just the lower FRT, but rather, similar in both upper and lower FRT epithelial cells.

Once we confirmed that E2 is indeed able to induce p53 expression, we investigated whether this is the mechanism through which protection is mediated. Interestingly, E2 treatment was able to significantly suppress viral replication compared to NH conditions, similar to the results seen after p53 activation alone (Figure 22). However, when p53 was suppressed after E2 treatment, HSV-2 replication was substantially increased, resulting in significantly higher replication as compared to NH. This suggests that the p53 pathway is a major contributor to the E2-mediated protection we see in VK2s in response to HSV-2 infection. To confirm these results, we decided to also investigate whether knocking down p53 through siRNA resulted in similar effects, since using small molecular inhibitors such as PFT-α can have off-target effects. Using siRNA treatment for gene silencing has been shown to be an efficient method, and an important complimentary technique to use of traditional inhibitors. Once the p53 siRNA concentrations were validated (Figure 23), we showed that knock down (KD) of p53 in NH, Nutlin-3, or E2 conditions result in significantly higher HSV-2 replication as compared to no treatment in respective

conditions (Figure 24). Since p53 KD in E2 resulted in lower HSV-2 replication as compared to the level seen after p53 KD in Nutlin-3, this implies that E2 may have other antiviral effects aside from the p53 pathway which contribute to its protective effects. Previous studies have shown that the p53 pathway could contribute to attenuation of replication of viruses such as HSV-1 and influenza A virus, so the concept of p53 involvement in protection against viruses is not completely new. [121, 123-125] One study that investigated the antiviral role of p53 showed that viral infection with either VSV, or vaccinia virus, in primary mouse embryonic fibroblast cells (MEF) from p53 knockout mice resulted in 10-fold higher virus yield compared to WT-infected cells, whereas MEFs from 'super p53 mice' with p53 overexpressed showed 10-fold lower yield compared to WT-infected cells.[202] Although the antiviral effect of p53 has been reported, this is the first time that a link between E2 exerting antiviral effects through p53 is being reported.

Once we had confirmed the functional pathway, we addressed our third objective which was to determine the mechanism of E2-mediated p53 protection against HSV-2 infection in VK2s. We decided to investigate at what stage of the HSV-2 life cycle did E2 exert the anti-viral influence. HSV-2 virus begins by first attaching to host cells for initial uptake/infection, replicates itself to form more virions, and lastly exists the cells to infect neighbouring host cells. Studies in literature report evidence of HSV-1 entering through endosomal compartments in epithelial cells; however, the signals and factors which determine the preference of herpesviruses to use these endocytic pathways for entry or membrane fusion remains to be elucidated.[29, 33, 172] Our results also confirm the entry of HSV-2 into VK2 cells through endosomal uptake, due to the colocalization seen between EEA1 and HSV-2 at early hours post-infection (Figure 26). Results from our analysis showed that E2 mainly affected HSV-2 levels at 16 hours post infection through modulation of p53, but not after 2 hours of infection (Figure 26A and B). This suggests that E2

suppresses viral replication of HSV-2, but not viral entry, through the p53 pathway. Results also showed that E2, through p53, was able to modulate EEA1 expression after 16 hours of infection, with less expression of the early endosome seen after E2 treatment or p53 activation compared to NH. It is interesting to note that although P4 has the most potent effect on increasing viral replication, it shows the lowest levels of EEA1 expression at 16 hours. This is an opposite correlation from what is seen under E2, where lower EEA1 expression correlates with low viral replication, as compared to NH. This indicates that the early endosomal uptake of HSV-2 may not be involved in influencing the level of viral replication under P4 treatment.

These results demonstrate the complexity of hormone-influenced signaling pathways and the extent to which E2 and P4 differ in their effects on viral susceptibility despite some similarities in regulation of factors. If we look closely, there was minimal colocalization seen between early endosomes and HSV-2 during onset of HSV-2 infection. Interestingly, results during the replicative phase show that HSV-2 is rarely found in the early endosome of VK2s treated with E2, as well as with p53 activator, when compared to NH, whereas inhibiting p53 by PFT-α with E2 pre-treatment shows a significantly higher amount of colocalization (Figure 26C). It may be possible that early endosomes have a role other than viral entry which may be contributing to its colocalization with HSV-2 during its replication and the differences seen in the replication of HSV-2. It is well established that endosomes deliver viruses to specific intercellular sites which are crucial for their replication. A recent study has shown that EEA1 vesicles serve as a platform for rapidly obtaining excesses of the plasma membrane from the cell surface that can be used to subsequently form intraluminal vesicles (ILVs) and multivesicular bodies (MVBs), which are a considered late endosomes formed as a result of maturation.[203] It known that the sorting of receptors in the early endosomes is done by transfer to the ILVs, and this process starts in hybrid

EEA1-positive endosomes. Moreover, this suggests that ILVs and MVBs cannot be identified solely as late endosomes as long as there are EEA1 domains in the membrane.[203] These novel findings from this study may help address why EEA1 is found to be localized with HSV-2 during the replicative phase, and suggests that HSV-2 may still be part of the endocytic pathway after entry into host cells such that it affects its replication, a speculation that requires further research. Moreover, these complexities of the endocytic pathway are most definitely modulated by E2 through a p53-dependent mechanism, however, further investigation is needed to determine exactly how this occurs and the effects it has on viral replication.

After looking at the effect of E2 on viral replication, we focused our attention to our search for antiviral mechanisms downstream of p53. Initial GSEA results were analyzed in more detail where genes that were part of the leading-edge subset of the p53 pathway were further evaluated. Results showed that there were no obvious or significant leading edge subset contributors to the p53 for us to investigate, particularly since E2 was not able to induce expression of any of these genes compared to NH. The reason for the lack of gene expression seen from this subset could be because our transcriptomic analysis was done at 24 hours after infection. Looking back at the transcriptomic gene fold changes, most genes were upregulated less than 2 log-fold under E2 conditions as compared to NH. This was another reason why it was more beneficial to perform a pathway analysis rather than focus on single genes; analyzing single genes may have showed no discovery in a mechanism since there is no major significant upregulated gene, whereas the pathways constitute a subset of multiple genes that are upregulated and better represent the entire profile. Nevertheless, vesicle associated membrane 8 (VAMP8) was the only gene that showed significantly higher gene expression E2-treated VK2s with p53 inhibited compared to VK2s with E2 treatment alone. VAMP8 is a soluble N-ethylmaleimide-sensitive factor-attachment protein

receptor (SNARE) protein, a family of proteins essential of fusion of cellular membranes and has been known to be involved in molecular control of exocytosis.[204] One study found that VAMP8 plays an important role in mucus secretion by coordinating mucin exocytosis from goblet cells.[205] With our results showing suppression of VAMP8 by E2, and induction of VAMP8 after inhibiting p53, we speculate that E2 could potentially play a role in exocytosis by preventing the amount of virus released from the host cell, thus reducing viral infection and replication in neighbouring cells. However, further functional studies are needed to investigate whether this finding is relevant.

Since there were no obvious candidate genes for examining the anti-viral mechanism, we decided to examine the canonical cellular pathways associated with innate anti-viral mechanisms. Therefore, we analyzed whether protection by E2-mediated p53 occurs through interferon signaling and ISG responses. We investigated gene expression of various interferons, as well as a type I interferon receptor before and after infection. We observed that no IFN gene, except for IFN-λ2, showed significantly altered expression after E2 treatment or by modulating p53, as compared to NH. IFN-λ2 was the only gene to be upregulated after E2 treatment in mock conditions, and its expression was significantly reduced after inhibiting p53. However, this effect was not seen after infection, which may be due to the ability of the virus to overcome interferon-mediated effects. These results suggest that IFN-λ2 may have a play a role in the context of E2-induced p53 signaling in mock conditions, but further investigation is required to confirm. Interestingly, one study has also shown that IFN-λ is able to protect the female reproductive tract against zika virus.[206] Another study reports that lambda interferons are able to inhibit HSV-2 replication in human cervical epithelial cells.[207] If E2 induces IFN-λ gene expression which can suppress HSV-2 replication, this may possibly be a connection since we have shown the same effects by E2. Nevertheless, since we did not see differences in IFN-λ expression during the course

of HSV-2 infection, and the biggest decrease in HSV-2 was observed 16-18 hours after infection, we decided to continue our investigation for something more significant. Although we only saw regulation of one of the interferons, there is still a possibility of interferon independent ISG production. To rule out ISGs as an antiviral mechanism against HSV-2 infection, we analyzed expression of various ISGs and how they are altered in response to E2 treatment or modulation of p53. Out of all ISGs analyzed, MX1 and BST2/tetherin were the only ones showing upregulation in response to HSV-2 infection after p53 activation (Figure 30). While there are two types of Mx proteins, MX1 is responsible for antiviral activity against various viruses by binding to essential viral components to inhibit their function.[208] One study even shows that disruption of the MX1 gene results in complete loss of innate immunity against IAV in mice, resulting in increased infection and death.[209] BST2 expression showed an increased pattern under Nutlin-3 and E2 conditions at an early phase of infection with fold change in expression being the highest among all ISGs and reaching up to approximately 15 and 7.5, respectively. BST2, also known as tetherin, has previously been reported to restrict HSV-1.[210] Furthermore, another study suggests that overexpression of human BST2/tetherin decreases the release of HSV-2 progeny virions.[211]

Based on our results from analyzing ISGs, as well as promising literature of effect of BST2 on herpesviruses, we decided to investigate the role of BST2 since it was most highly expressed ISG from our analysis and one of only two genes to be induced by p53 activation after HSV-2 infection. We examined the effect of E2 treatment and p53 modulation on BST2 expression before and after HSV-2 infection (Figure 31). Results showed that both E2 and p53 activation showed significantly higher expression of BST2 compared to NH in mock conditions. This difference was seen after 2 hours of infection as well, but not to the same level as the difference seen in mock. This may be due to the fact that HSV-2 is able to counteract BST2 expression after infection.

Indeed, previous studies have shown that HSV-1 is able to counteract the effects of tetherin while HSV-2 targets tetherin for degradation through the lysosomal pathway.[212, 213] This aligns with our results since we also see that BST2 expression notably decreased after HSV-2 infection. One of these study shows that it is particularly the gD glycoprotein of HSV-2 that interacts with BST2 to promote its degradation.[212] Looking back at our previous results, we showed that gD expression is decreased by E2 treatment or p53 activation, while inhibiting p53 in addition to E2 treatment causes gD expression to return to NH levels. If it is reported that gD plays a role in promoting BST2 degradation, and if we have shown that E2 resulted in reduced gD expression (Figure 27) as well as increased BST2 expression after infection (Figure 31, 32 and 33), this suggests that E2 may have also have suppressive effect on gD which subsequently allows BST2 expression to remain increased. Thus, although E2 has a direct effect on increasing BST2 expression, it is intriguing and worthy of further investigation to examine how VK2s treated with E2 are able to dodge gD-mediated BST-2 degradation. We also showed that inhibition of p53 in E2-treated VK2s significantly suppressed BST2 expression to levels similar to NH conditions, compared to E2 alone, suggesting that E2 induction of BST2 occurs through the p53 pathway. Interestingly, we also saw that gD levels were similar in VK2s treated with either NH or PFT-α with E2 treatment. These results suggest that it is possible that p53 may also play a role in dodging gD-mediated degradation of BST2. However, since there is a possibility that the use of PFT-α may have off-target effects, we confirmed the specific effects of suppressing p53 on BST2 expression by siRNA experiments. Results show that knockdown of p53 in VK2s by siRNA resulted in significant inhibition of BST2, thus confirming that BST2 expression is dependent on the p53 pathway (Figure 32).

Literature also suggests that BST2/tetherin has various antiviral effects. [212-215] For example, BST2 is well known in its ability to anchor onto HIV-1 virions and prevent their release, and also lower the infectivity of progeny virions.[216] Based on the antiviral role of this ISG, we further investigated the E2-mediated and p53-dependent effects of BST2 on HSV-2 infection. We showed that knocking down BST2 resulted in significantly increased HSV-2 infection in VK2s that were untreated, p53-activated, or E2 treated (Figure 33). Since there is less HSV-2 infection after knockdown of BST2 in VK2 cells with either E2 treatment or p53 activation compared to VK2s cells with knockdown of BST in NH conditions, this suggests that E2, as well as the p53 pathway, may induce other protective effects aside from BST2 induction which may be contributing to inhibiting HSV-2 replication. However, this cannot be concluded since there may be a possibility that there is residual amount of BST2 protein that remains despite BST2 knockdown with siRNA. Effects of BST2 siRNA on protein expression of BST2 should have been analyzed at various doses to confirm this effect, which may have helped confirm this finding.

Since effects of E2-mediated protection through the p53 pathway have been shown to impact HSV-2 replication, and not entry, (Figure 26) we investigated the expression of HSV-2 and BST2 simultaneously after 16 hours of infection to show their negative correlation (Figure 34). Results confirmed our expectation and we observed significantly lower HSV-2 expression correlated with increased BST2 expression in VK2s with p53 activated or with E2 treatment, compared to NH. Inhibiting p53 in E2-treated VK2s, however, reversed this effect and showed suppressed BST2 expression correlated with significantly increased HSV-2 replication compared to VK2 cells treated with E2 alone. This confirms that BST2 is an important contributor to the protective effect seen by E2-mediated p53 against viral replication of HSV-2.

Although BST2 is known to have various immunomodulatory effects, it has been reported to have antiviral effects due to its role in tethering onto various lipid enveloped viruses to prevent their release and exocytosis into the extracellular environment[217-225] After HSV-2 replication, the virus progeny migrate towards the cell membrane and exocytose into the extracellular environment to infect other neighbouring cells. With BST2 being a host restriction factor of virus multiplication through its ability to physically tether budding virions and subsequently restrict viral spread, it would be interesting to examine whether this effect is seen under the context of E2 and p53. We examined the effect of E2 and p53 modulation on BST2 and HSV-2 expression after 24 hours of infection to show what happens during the late phase of the viral life cycle. We found that E2 continues to show significant upregulation of BST2 as compared to NH (Figure 35). Interestingly, we observed clear colocalization between BST2 and HSV-2 around the periphery of the cell after E2 treatment, as compared to NH. This effect was also seen after p53 activation, but not to the same extent of that seen with E2. Inhibiting p53 resulted in significant increase in HSV-2 expression, with minimal expression of BST2. Overall, these results indicate that BST2 may play a role in tethering the virus on the plasma membrane through the E2-dependent p53 pathway. One study has reported that knockdown of BST2 resulted in small clusters of virions to be associated with the cell membrane, as compared to the large-scale surface clustering seen in the control, and resulting in a higher number of virion particles released into the medium by BST2 KD cells.[211] These findings suggest that upregulation of BST2 by E2, along with the higher level of HSV-2 tethering seen after 24 hours of infection, may be a method by which E2 prevents viral release and subsequent infection and replication in neighbouring cells. In addition, there may be a connection with E2-mediated suppression of VAMP8, thus affecting exocytosis. It is intriguing to imagine that E2 could be suppressing exocytosis of vesicles containing virus, in synergy with BST2

mediated budding of virus to the cell membrane, to prevent viral release and subsequently reduce viral infection and replication in neighbouring cells.

We previously showed that knocking down BST2 in E2-treated cells results in less HSV-2 infection as compared to the level of infection seen after BST2 KD in NH-treated cells, suggesting that E2 may have other roles that contribute to protection. Since our lab has previously shown that E2 treatment increases barrier integrity and decreases pro-inflammatory cytokines in upper GECs, we examined these factors in response to E2 and p53 modulation in VK2s.[181] Many studies have reported the role of NF-κB as a crucial regulator that links infections and chronic inflammation.[182, 183] Some studies have also shown that E2 can indirectly suppress NF-κB or prevent its nuclear translocation, thus preventing downstream pro-inflammatory expression.[102, 103] We found that expression of NF-κB under the influence of E2 did not increase in response to infection when compared to E2-treated cells, whereas NF-κB showed an increasing pattern of expression after infection in NH conditions. This suggests that E2 prevents HSV-2 mediated induction of NF-κB in VK2s. Since NF-κB is needed for HSV-2 replication, its inhibition would have a dampening effect on HSV-2. A study from our lab has shown this phenomenon with the use of curcumin activity which specifically inhibits NF-κB, and subsequently results in reduced HSV-2 replication.[226] Overall, they show that it is the anti-inflammatory activity of curcumin which blocks the replication of HSV-2, as well as HIV-1. Nevertheless, although we did not see differences in NF-κB expression after p53 activation as compared to NH, we noticed that inhibiting p53 with PFT-α in E2-treated VK2s resulted in similar NF-κB expression as what is seen under NH conditions before and after infection. Studies in literature have also report that there is a long known opposing relationship that exists between NF-κB and p53.[184-186] Since an opposite pattern is not seen after p53 activation, it may once again be possible that PFT-α has an off-target

inflammatory effect which increases NF-κB. We further investigated expression of cytokines and chemokines downstream of NF-κB to validate the anti-inflammatory effect of E2 (Figure 38). Results showed that E2 treatment suppressed TNFα gene expression after HSV-2 infection, however, inhibition of p53 in E2-treated VK2 cells resulted in increased TNFα expression compared to E2 alone, which aligns with the pattern seen with NF-Kb expression. Another explanation attributed to the reduced TNF-α could be due to the fact that it depends on viral replication of HSV-2, as previously reported in primary GECs.[48] It is also well established that higher levels of pro-inflammatory cytokines/chemokines, such as IL-1α, IL-1β, IL-6, IL-8 and TNF-α in the female genital tract increases susceptibility to viral infections such as HIV.[227] Overall, these results suggest that E2 may be modulating NF-κB and its downstream TNFα gene through the p53 pathway, however, examination after specifically knocking down p53 with siRNA is crucial to confirm this speculation. Regardless, these results suggest that E2 has anti-inflammatory effects on VK2s in response to HSV-2 infection. It can also be speculated that E2 achieves suppressed inflammation due to the lack of viral replication that occurs under this condition.

Our lab has previously shown that increased levels of pro-inflammatory cytokines can result in impairment of barrier function in primary GECs.[228, 229] One of the studies in our lab has also shown that it is the anti-inflammatory activity of curcumin which protects the GEC epithelial barrier from disruption.[226] Although one of the postulated mechanisms of E2-mediated protection against HSV-2 is by enhancement of vaginal epithelial cell barrier integrity, there haven't been any studies that have demonstrated this. As a final investigation, we sought to examine the effect of E2 treatment on barrier integrity of VK2s and whether it is mediated through the p53 pathway. Our lab has also previously shown that E2 is indeed able to increase

barrier function of primary GECs as seen with higher transepithelial resistance measurements (TER) compared to no hormone conditions.[181] Another study has also reported that estradiol treatment led to increased TERs in Vk2 cells, however, this was in monolayers of VK2s which may not be an accurate representation of what occurs *in vivo*, compare to the physiologically relevant ALI culture model system we use.[99] Similarly, we examined TER of ALI culture-grown VK2 cells and found that E2 treatment results in significantly higher barrier integrity compared to NH, while activating p53 does not alter TER measurements (Figure 39). It may be possible that increased barrier function seen under E2 conditions is attributed by the E2 induction of genes related to cornification and keratinization that we reported (Figure 10). Interestingly, inhibiting p53 after E2 pre-treatment significantly reduced barrier integrity to similar levels of those found under NH conditions. This suggests that p53 may play a role in altering barrier function of VK2s. With the discrepancy in results showing no change barrier function after p53 activation as compared to NH, and a reduction in barrier function after p53 inhibition in E2-treated cells, it could possibly be a result of off-target effects of the PFT-α small molecule inhibitor. To validate these findings, a better option would be to use VK2 cells with p53 knocked down to examine whether barrier function is altered. However, since these TER measurements were taken on the 7th day, p53 knock down effects may not persist in the VK2s for a long time since siRNA treatment effects are often transient.

Maintenance of a robust epithelial barrier is important to preventing entry of pathogens. Pro-inflammatory cytokines such as TNF-α and IL-1β are known to disrupt tight junctions and reduce barrier integrity.[187] Since we showed that E2 increased barrier integrity while suppressing inflammation, we pursued our investigation by examining effects on tight junctions. We decided to examine the ZO-1 protein since Zonula occludens serve as regulatory proteins to the tight

junction and is required for their assembly. Results of ZO-1 staining showed a similar trend as seen in TER measurements, where E2 treatment resulted in greater E2 resulted in significant induction of ZO-1 protein expression compared to NH in both LLI and ALI cultures (Figure 40), while addition of inhibiting p53 in E2-treated VK2s resulted in significant reduction in ZO-1 expression when compared to E2 alone. Although this may suggest that blocking p53 in addition to E2 reduces ZO-1 tight junction expression, since we do not see any drastic differences in ZO-1 after p53 activation, this could possibly be an effect of off-target effects of PFT-α. Indeed, the effects of E2 on ZO-1 expression align with a study that shows downregulation of various tight junctions, including ZO-1, in rat vaginas after ovariectomies and their upregulation after estradiol treatment compared to control.[230] Overall, we see a consistent pattern of p53 activator and p53 inhibitor effects on inflammation and barrier integrity as compared to E2 alone. With these patterns, our results imply that E2 is able to increase barrier function and integrity, but further examination is required to conclude whether it is mediated specifically through p53. Although the increase in barrier integrity after E2 treatment most likely does not contribute to the reduction in HSV-2 when examining LLI cultures, it suggests that E2 plays an important role in reducing paracellular movement of virions through spaces between adjacent epithelial cells. Therefore, E2 is able to not only alter cellular mechanisms intercellularly but is also able to influence the intracellular environment and thus contribute to possible reducing HSV-2 transmission.

5.2 Strengths of the study

The utilization of the VK2 ALI culture system is a major strength in our investigation. As discussed previously, the VK2 ALI culture system is more physiologically similar to the structure and function of the lower FRT epithelium.[78] VK2 cells grown in ALI cultures form stratified layers which is more representative of squamous epithelial cells growth of the vaginal tract. Although LLI cultures were sometimes used to perform mechanistic experiments, the initial transcriptome data was extracted from an ALI culture system. As a result, this study and the transcriptomic data associated with it is likely to provide a more accurate insight when compared to other studies. When using female sex hormones in culture, we used physiological levels of hormones in our study, which is something that many other similar studies overlook. Moreover, we also only provided hormonal supplementation on the basolateral side of cultures since that is the side that cells in the *in vivo* environment absorb nutrients from. Furthermore, many studies have previously shown the protective effects of estradiol on HSV-2, however, none have shown the cellular mechanism through which this occurs. Therefore, the prospects and findings of this study are novel to date and demonstrate a protective cellular antiviral mechanism of estradiol that has not been shown before.

5.3 Limitations and Future Directions

One of the major limitations of our study was the timeline of studying the response of VK2s to HSV-2 infection. After inoculation of HSV-2, the virus enters the cells during first few hours of infection, reaches its peak replication phase at approximately 16 hours after infection, and begins to lyse cells near the 24 hours time point as part of the lytic cycle. The transcriptomic analysis of this project was performed on VK2s that had been infected with HSV-2 for 24 hours, a period when most pathways would not be as highly expressed as what would be seen during the replicative phase of the virus. Hence, it would be more informative to examine transcriptome results of cells infected with HSV-2 between 14 and 18 hours of infection to examine the effects of the virus in its most metabolically active form.

With the VK2 cell line being immortalized due to addition of E6/E7 sequences from Human papillomavirus (HPV), it also raised concerns whether this could be a factor of interference in the effects we see on p53 expression. For example, the E6 protein has been found to associate with p53 as a mechanism by which HPV induces tumors, and in some cases target p53 for proteosome-dependent degradation.[169] Thus, to address this concern and to confirm that the effects of treatments seen in VK2s are not affected by E6/E7 interference, we performed immunofluorescent staining of p53 and ER-α in primary genital epithelial cells, particularly endometrial and ectocervical cells, (Figure 20 and 19). Although endometrial cells are from the upper FRT, ectocervical cells are closest representation of how vaginal cells would behave due to their similarity in morphology. Results showed that primary GECs show similar results as those seen under VK2s, thus confirming that E6/E7 genes do not interfere as a variable in the modulation of p53 in response to E2 treatment, as well as p53 inhibitor and activator reagents. Nevertheless, these results also suggested that the E2-mediated induction of p53 may not be specific to just the

lower FRT, but rather, similar in various cell types of the FRT. Further investigation is needed to examine the mechanistic differences of estradiol in various areas of the FRT. For example, it would be interesting to investigate whether the same antiviral and anti-inflammatory effects of estradiol are employed in different areas of the FRT and whether these are sufficient to provide similar protection as seen in VK2s. Moreover, since estradiol has also been shown to provide protective effects against various other STIs, it would be highly intriguing to evaluate whether the the antiviral and anti-inflammatory effects that it employs against HSV-2 would be sufficient against other viral or bacterial STIs.

Using an ALI and LLI system provides physiologically similar structural growth of VK2 cells such that it allows a foundational analysis of how HSV-2 would interact with them. While this provides insights into the mechanism of how HSV-2 infects and replicates in VK2 cells, there are various factors that influence susceptibility in the lower FRT which were absent from out system. For example, the presence of mucus, bacterial populations, hormones, lipids, electrolytes, and various proteins in the lower FRT also play a role in immune defence function, and thus, affect susceptibility to STIs.[45] Moreover, the presence of other cells such as immune cells and fibroblasts also contribute to interacting with epithelial cells in the FRT. Future efforts should aim to include these elements to comprehensively represent the conditions of the FRT.

Since there are various bioinformatic approaches that exist, our existing transcriptomic data and heatmaps can be reused the phenomena of other P4 and MPA, or further elucidate effects of E2. For example, the heatmap generated with DEGs between E2 and P4 (Figure 9) shows various clusters of genes on the coloured panel to the left of the heatmap. Most of these clusters of genes are clearly oppositely regulated by E2 compared to NH and P4. These are striking differences, and with the help of enrichment tools could help identify what pathways they represent.

Although our study mainly focuses on the mechanism of estradiol, the FRT is under the influence of combination of multiple hormones that vary in concentrations and ratios throughout the menstrual cycle. Future studies should study the effect of combination of estrogen and progesterone at various stages of the menstruation cycle and examine whether estradiol is still able to induce its protective mechanism and thus, prevent viral infection. Overall, our model system lays a strong foundation for future research into a variety of domains, advancing our knowledge and understanding of HSV-2 transmission in the FRT.

Another limitation in this study was the use of small-molecule inhibitors, Nutlin-3 and PFT-α. Performing experiments with small-molecule inhibitors have caveats and caution needs to be exercised in interpreting results without controls. For example, many experiments used the condition of PFT-α addition after E2 treatment, however, addition of PFT-α after NH treatment should be used as a control in all experiments prior to making interpretations of data. Although we used siRNA to validate the specific effects of p53 inhibition, it would be beneficial to perform a similarly validation of the specific effects of p53 activation. One way to possibly address this is through the use of p53 overexpressed cell lines.

Lastly, it is important to consider the role of p53 in tumor suppression and cancers in humans. Estrogen has commonly been reported in literature to have cancerous properties due to its ability to stimulate growth of breast and endometrial cancers.[231] Although we have found that estrogen stimulates p53 in various cell types in the FRT, this may not be enough to counteract other cancer-inducing effects of estrogen. With our study showing the novel antiviral effects of estrogen, along with existing evidence of estrogen's protumor activities, makes estrogen therapy a double edge sword. Interestingly, it has been found that adding progestins to estrogen therapy lowers the risk of endometrial and ovarian cancers.[232] One study found that patients with advanced

endometrial cancer that were treated with alternating weekly cycles of MPA demonstrated a 27% response rate.[233] This results in a conundrum where progestins, compounds found to increase susceptibility to infections helps with lowering progression of cancer, whereas E2 results in decreased susceptibility to infections but with increased cancer risk. It may be possible that an optimal ratio of estrogen to progesterone concentration exists, where the environment provides sufficient protection against infections without increasing vulnerability to cancers. However, further investigation is needed to address these concerns.

5.4 Significance

The findings from this study demonstrate the importance of sex-dependent factors such as hormones and their effect on susceptibility to pathogens. This study particularly highlights the role of E2 in exerting anti-viral and anti-inflammatory effects in the vaginal epithelium of the lower female reproductive tract, which in turn contribute to reducing susceptibility to HSV-2. Moreover, this is the first study to highlight the mechanism through which estradiol mediates protective effects in vaginal epithelial cells in response to infection. With various studies suggesting the increased risk of STI transmission being related to the use of hormonal contraceptives, particularly progestin-based ones such as MPA,[192, 234, 235] more research is needed to offer safer reproductive options for women globally. Our findings suggest that estradiol-based hormonal contraceptives may be a safer option for women to protect against STIs, however, further research is needed in clinical contexts to confirm. Overall, this study successfully lays the foundational assessment of protective estrogen effects against HSV-2 and provides the groundwork of considering estradiol-based options in the design of more optimal contraceptive techniques and strategies that have major consequences against various pathogens.

CHAPTER 6: CONCLUSION

Women are at increased risk of HSV-2 acquisition, especially in the region of sub-Saharan Africa, making it imperative to understand factors that contribute to transmission events in the FRT to develop better prevention strategies. The vaginal tract is a primary and essential barrier against STIs and is strongly under the influence of female sex hormones which alter its susceptibility to STIs such as HSV-2. The goal of this project was to investigate the effects of the female sex hormone estradiol on vaginal epithelial cells and determine the mechanism of action through which it provides its known protective effects. To do this, we first performed a bioinformatic transcriptomic analysis using an optimized *in vitro* VK2 ALI cell culture system. We found the p53 pathway to be an important part of the E2 response.

The second part of our study then used functional analyses confirm these results and prove whether they contribute to antiviral effects and thus, protection against HSV-2. E2 was found to increase p53 expression, thus confirming our hypothesis from our bioinformatic analysis. We also discovered that the E2-mediated p53 pathway contributes significantly in suppressing HSV-2 replication. It was found that E2 also modulates an interferon-stimulated gene, BST2, through the p53 pathway. Examination of antiviral effects of BST2 proved that it is a important in suppressing HSV-2 replication similar to p53. We showed that E2 is able to induce BST2 to tether onto HSV-2 virions to prevent their release, and thus transmission to neighbouring cells. Finally, this study also demonstrated that E2 has anti-inflammatory effects on VK2s and found this to be correlational with strengthening barrier integrity through increased tight junction protein expression.

Therefore, this study elucidates the cellular mechanisms through which estradiol provides protection against HSV-2 infection in human vaginal epithelial cells. Although the role of E2 in

providing protective effects against infections has been reported multiple times in literature, this study is the first to demonstrate the novel findings of antiviral effects that E2 modulates.

CHAPTER 7: MATERIALS AND METHODS

7.1 Propagation of VK2 cells

The vaginal epithelial cell line VK2/E6E7 (ATCC® CRL-2616™) was grown and maintained in keratinocyte serum-free medium (Thermo Fisher Scientific, Cat. 17005042) containing 0.1 ng/mL of human recombinant epidermal growth factor, 0.05 mg/mL of bovine pituitary extract, 100 units/mL of penicillin-streptomycin (Sigma Aldrich, Oakville, ON, Canada), supplemented with 0.4 mM CaCl2. All prepared media was stored at 4°C. When flasks containing VK2 cells reached 80% confluency, they were washed with phosphate buffered saline (PBS) and subsequently trypsinized with 1X trypsin-EDTA (McMaster Media Centre). Dulbecco's modified Eagle's medium and Ham's F12 (DMEM/F12) medium containing 10% fetal bovine serum (FBS) was added to trypsizined cells to neutralize acidic the effects of trypsin. The suspended VK2s in this mixture were vortexed at 1500 rpm for 5 minutes. The supernatant was then discarded, and the cell pellet was resuspended in fresh supplemented KSFM. Cells were incubated in a 5% CO_2 humidified atmosphere at 37°C. VK2 cells were grown up to a maximum passage number of 40.

7.2 Reagents and Compounds

7.2.1 Sex Hormones and Synthetic Hormone Compounds

Stocks of water-soluble E2 (Sigma-Aldrich, Cat. E4389), P4 (Sigma-Aldrich, Cat. P7556), MPA (Sigma-Aldrich, Cat. M1629) were aliquoted and stored in -4°C. Stocks were diluted with KSFM to create 10^{-9} M of E2 medium, 10^{-7} M of P4 medium and 10^{-7} M of MPA medium. Female sex hormone concentrations correspond to the highest serum levels during the menstrual cycle and

were used as described previously.[143, 144, 236] In ALI and LLI cultures, hormone-supplemented medium was provided only on the basolateral side.

7.2.2. P53 Activator Reagent

Nutlin-3 (Sigma-Aldrich, Cat. N6287), an activator of the p53 pathway, is a small-molecule and non-genotoxic activator of p53. Nutlin-3 is the most commonly used activator for p53, as well as for anti-cancer studies.[232] Nutlin-3 is known to prevent the p53-MDM2 interaction by binding to MDM2, an inhibitor of p53, with high specificity and thus, leading to stabilization of p53 and activation of the p53 pathway. Nutlin-3 was solubilized and stored in 10 mM stocks at -20°C. VK2 cells were grown in ALI or LLI cultures as described in 7.2 and 7.3, respectively, with NH or E2 (10^{-9} M) treatments. On the 5th day after initial seeding, stocks were diluted with KSFM to create a 5 µM Nutlin-3 solution, which was provided on both apical and basolateral sides for 48 hours until the 7th day for p53 activation. After completion of Nutlin-3 treatment, cultures were washed with PBS three times. For immunofluorescent staining, cell cultures were then either fixed directly after washing, or infected with HSV-2 at an MOI of one for various time points depending on the experimental requirement prior to being fixed. For viral titration experiment, HSV-2 infection at an MOI of one was performed directly after washing and supernatants collected after 24 hours, as described in section 7.7.1.

7.2.3 P53 Inhibitor Reagent

The p53 inhibitor, pifithrin-α-HBr (PFT-α) (Abcam, Cat. ab120478), is a small-molecule inhibitor compound that suppresses p53. However, there is no clearly defined molecular mechanism of action known for this agent. A recent study shows that PFT-α treatment results in

inhibition of total p53 protein suppression after Nutlin-3 induction, as well as suppression of various phosphorylated forms of p53, however; this effect is not observed consistently among different cell lines.[164] It was found that PFT-α treatment suppressed p53 which has been phosphorylated at either Ser15 or Ser33 sites, which are post-translational modifications, suggesting that PFT-α inhibits p53 post-translationally. Moreover, the same study found that PFT-α had a differential inhibitory effect on various genes downstream of p53, where some were partially inhibited, while others were not inhibited at all, suggesting that PFT-α does not function as a complete inhibitor of the p53 pathway and that it may have other unknown effects. PFT-α was solubilized and stored in 10 mM stocks at -20°C. VK2 cells were grown in ALI or LLI cultures as described in 7.2 and 7.3, respectively, with NH or E2 (10^{-9} M) treatments. Just before the completion of the 7th day after initial seeding, PFT-α stocks were diluted with KSFM to create a 10 µM solution, which was provided on both apical and basolateral sides for 1 hour for p53 inhibition. One study evaluated the characteristics of PFT-α to demonstrate its unstable nature when used *in vitro* and shows that the stability of PFT-α remains high at room temperature, but significantly drops at a rapid rate within the first few hours of incubation at 37°C.[168] Within the first three hours of incubation, the fraction of PFT-α remaining drops from 100% to less than 10%. Therefore, this is why 1 hour of PFT-α treatment was used as it has previously been reported to show effective p53 inhibition. After completion of PFT-α treatment, cultures were washed with PBS three times. For immunofluorescent staining, cell cultures were then either fixed directly after washing, or infected with HSV-2 at an MOI for various time points depending on the experimental requirement prior to being fixed. For viral titration experiment, HSV-2 infection at an MOI of one was performed directly after washing and supernatants collected after 24 hours, as described in section 7.7.1.

7.3 VK2 ALI Cultures

After trypsinizing and resuspending VK2 cells from the subculturing process, cells were enumerated using a trypan blue exclusion assay with the hemocytometer. To grow cells in an air liquid culture (ALI), 60,000 VK2/E6E7 (VK2) cells were seeded and cultured on the apical side of 0.4 μm pore-sized transwell polystyrene inserts (VWR, Cat. 82050-022) in 24 well plates.[78] Cells were supplemented with 200 μL and 700 μL of KSFM on the apical and basolateral sides of the transwell culture, respectively. Only the basolateral compartment contained KSFM with either no hormone, E2 (10^{-9}), P4 (10^{-7}) or MPA (10^{-9}). The 24 well plates were briefly rocked to ensure cells are distributed evenly in each transwell. Cells were incubated in a 5% CO_2 humidified atmosphere at 37°C. After 24 hours of seeding, medium was removed from the apical side to mimic *in vivo* conditions of the epithelial cell layers of the female genital tract where cells are exposes to air on the apical side and nutrients supplied from the basolateral side. Medium from the basolateral side was replenished every 48 hours for 7 days of culture.

7.4 VK2 LLI Cultures

After trypsinizing and resuspending VK2 cells from the subculturing process, cells were enumerated using a trypan blue exclusion assay with the hemocytometer. To grow cells in a liquid-liquid culture (LLI), 2,000 – 7000 VK2/E6E7 (VK2) cells were seeded and cultured on the apical side of 0.4 μm pore-sized transwell polystyrene inserts (VWR, Cat. 82050-022) in 24 well plates, depending on how confluent they were needed for confocal imaging.[78] Cells were supplemented with 200 μL and 700 μL of KSFM on the apical and basolateral sides of the transwell culture, respectively. Only the basolateral compartment contained KSFM with either no hormone, E2 (10^{-9}), P4 (10^{-7}) or MPA (10^{-9}). The 24 well plates were briefly rocked to ensure cells are

distributed evenly in each transwell. Cells were incubated in a 5% CO_2 humidified atmosphere at 37°C. After 24 hours of seeding, apical medium was replenished with fresh KSFM containing no hormones every 48 hours, and medium from the basolateral side was replenished with KSFM containing either no hormone, E2 (10^{-9}), P4 (10^{-7}) or MPA (10^{-9}) every 48 hours for 7 days of culture.

7.5 Transepithelial Resistance Measurements

VK2 cells were grown in ALI cultures as described above in section 7.2. Prior to measuring transepithelial resistance (TER), 100 µL of KSFM was added onto the apical side of ALI cultures and incubated for 1 hour in a 5% CO_2 humidified atmosphere at 37°C. TER measurements were taken using a volt-ohm meter (World Precision Instruments), after which the KSFM on the apical side was aspirated. To examine the effect of hormones and p53 activator/inhibitor on TERs of VK2 cells, TER values measured on day 7 (prior to infection with HSV-2) were used to examine the state of barrier integrity after full treatment. Cells were first grown in ALI cultures for 7 days in the presence of NH, E2 (10^{-9}) or P4 (10^{-7}) alone. Nutlin-3 (5 µM) was added for 48 hours in NH-treated cells on day 5, allowing cells to be ready for TER measurement on day 7. PFT-α (10 µM) was added to cells with E2 pre-treatment for one hour prior to measuring TERs on day 7.

7.6 Tissue processing and primary genital epithelial cell culture

Isolation of genital epithelial cells (GECs) from endometrial and endocervical tissues of women aged 30-59 years was obtained after hysterectomy for benign gynecological reasons at the McMaster Hamilton Health Sciences Hospital. Purpose of research was explained to all patients and written informed consent was obtained in accordance with approval of Hamilton Health

Sciences Research Ethics Board. Surgically removed tissues were examined by clinical pathologists for screening of any malignant or other clinically observed diseases prior to processing. Small pieces of endometrial or cervical tissue free of the aforementioned issues were provided for isolation of cells. Tissues were immediately submerged and placed in cold 1X Hanks Balanced Salt Solution (Invitrogen, Burlington, ON, Canada) and 100 U/mL of penicillin/streptomycin (Sigma-Aldrich, Cat. P4333) within 2-3 hours of surgery to maintain tissue viability. Tissues obtained from hysterectomy patients were received and processed for isolation cells within 24 h of surgery. Briefly, tissues were minced into small pieces and digested a mixed solution of HBSS and enzymes for 1 hour at 37°C. The enzyme mixture used for digestion was made up of 1.5 mg/mL collagenase D (Roche Diagnostics, Cat. 11-088-882-001), 3.45 mg/mL pancreatin (Sigma–Aldrich, Cat. P3292), 0.1 mg/mL hyaluronidase (Roche Diagnostics, Cat No. H6254) and 2.0 mg/mL D-glucose (EMD Chemicals Inc., Cat. DX0145-1). Following digestion, the mixture was passed through nylon mesh filters of different pore sizes for isolation of GECs. Once isolated, GECs were resuspended in primary tissue culture media (Dulbecco modified Eagle medium [DMEM]/F12; Invitrogen, Canada) supplemented with 10 µM HEPES (Invitrogen, Cat.15630-080), 2 µM L-glutamine (Invitrogen, Cat. 21051-024), 100 U/ml penicillin/streptomycin (Sigma–Aldrich, Oakville, Canada), 2.5% Nu Serum culture supplement (Becton Dickinson and Co., Cat. 355104), and 2.5% Hyclone defined fetal bovine serum (Thermo Fisher Scientific, Ottawa, Canada). The cells were then seeded on Matrigel™-coated (Becton, Dickinson and Co., Cat. 356235), 0.4-µm pore-size polycarbonate membrane tissue culture inserts (BD Falcon, Cat. 353095) in 24-well plates. Cells were supplemented with 300 µL and 700 µL of primary culture medium on the apical and basolateral sides of the transwell, respectively. Only the basolateral compartment contained primary culture medium with no hormone or E2 (10^{-9})

treatment, whereas the apical side contained medium with no hormone. The 24 well plates were briefly rocked to ensure cells are distributed evenly in each transwell. Cells were incubated in a 5% CO_2 humidified atmosphere at 37°C. After 24 hours of seeding, apical medium was replenished with fresh primary medium containing no hormones every 48 hours, and medium from the basolateral side was replenished with primary medium containing either no hormone or E2 (10^{-9}) every 48 hours for 7 days of culture. Nutlin-3 treatment was provided on the fifth day of treatment for 48 hours, as described in section 7.2.2, and PFT-α treatment was provided for one hour prior to fixing the cultures, as described in 7.2.3.

7.7 HSV-2 Infection of VK2s

7.7.1 HSV-2 Infection in VK2s ALI cultures

VK2 cells were grown in ALI culture as described above in 7.2, and subsequently infected with wild-type HSV-2 (strain 333) at a multiplicity of infection (MOI) of 1 as previously described by Lee et al.[78] After 2 hours, the cells were washed three times with PBS and replaced with 100 μL of KSFM media. The cells were incubated at 37°C in a 5% CO_2 humidified atmosphere. For quantification of viral replication, VK2s were incubated for 24 hours before collecting the supernatants from the apical side for viral titration and Vero plaque assay, as described below in 7.9. For RT-qPCR, VK2s were incubated for various amounts of times (2, 8, 16 and 24 hours) after infection and then subjected to RNA extraction as described below in section 7.12.

7.7.2 HSV-2-GFP Infection

VK2 cells were grown in monolayers in 24 wells until 70-80% confluent. Cells were then overlayed with GFP-tagged HSV-2 virus at an MOI of one and kept on ice for 2 hours to allow

virions to settle down and attach to VK2 cells.[34] This is done to allow all cells to undergo HSV-2 viral entry at the exact same time, since the virus is already attached to most cells, thus ensuring that the viral lifecycle is synchronized in all cells across the culture.[34] After 2 hours, the cells were washed three times with PBS and replaced with 500 μL of KSFM media. VK2 cells were then incubated at 37°C in a 5% CO_2 humidified atmosphere for 16 h and fixed with 4% paraformaldehyde. Cells were imaged using an EVOS™ FL digital inverted fluorescence microscope (Thermo Fisher Scientific, Burlington, ON, Canada).

7.7.3 HSV-2 Infection of VK2 LLI cultures

VK2 cells were grown in LLI culture as described above in section 7.3, and subsequently infected with wild-type HSV-2 (strain 333) at a multiplicity of infection (MOI) of 1 as previously described by Lee et al.[78] Cells were then kept on ice for 2 hours to allow virions to settle down and attach to VK2 cells.[34] This is done to allow all cells to undergo HSV-2 viral entry at the exact same time, since the virus is already attached to most cells, thus ensuring that the viral lifecycle is synchronized in all cells across the culture.[34] This is particularly important for measuring viral gene expression which is separated into immediate early, early and late genes, as well as imaging proteins after infection to ensure all cells show similar results based on treatment. After 2 hours of being kept on ice, the cells were washed three times with PBS and replaced with 100 μL of KSFM media. The cells were then incubated at 37°C in a 5% CO_2 humidified atmosphere. For the purpose of immunofluorescent staining, VK2s were incubated for various times, depending on the experiments, and fixed at the respective time point after infection with 4% paraformaldehyde. For RT-qPCR of viral genes, VK2s were incubated for various amounts of times (2, 8, and 24 hours) after infection and then subjected to RNA extraction as described below in section 7.12.

7.8 Vero Cell Culture

African green monkey kidney epithelial cells (Vero; ATCC CCL81) were cultured in T-150 flasks with minimum essential medium Eagle-Alpha Modification (α-MEM) supplemented with 10% fetal bovine serum (FBS), 1% penicillin-streptomycin (Sigma-Aldrich, Oakville, ON, Canada), L-glutamate (BioShop Canada Inc., Burlington, Canada), and 1% HEPES (Invitrogen, Burlington, Canada). Once the cells in flask were 100% confluent, they were washed with phosphate buffered saline (PBS) and subsequently trypsinized with 1X trypsin-EDTA (McMaster Media Centre). α-MEM with all supplementations listed above was added to trypsizined cells to neutralize acidic the effects of trypsin. More α-MEM medium with supplementations was added based on the amount needed to seed into 12-well plates, where one fully confluent flask contains enough cells for eight 12-well plates. Cells were incubated in a 5% CO_2 humidified atmosphere at 37°C for one day prior to performing a plaque assay.

7.9 Viral Titration and Plaque Assay

VK2 cells were grown in ALI cultures for 7 days and infected with wild-type HSV-2 directly for 2 hours. The cultures are then washed with PBS three times and overlayed with KSFM media for the next 22 hours to allow HSV-2 viral shedding into the media. The culture supernatants were then collected on ice. Monolayers of Vero cells were pre-seeded in 12-well plates one day prior to infection, as described in section 7.8 above. Supernatant samples were then serially diluted in serum-free α-MEM, added to the Vero cells, and incubated for 2 h at 37 °C and rocked every 15 minutes in order to facilitate viral absorption. The infected monolayers of Veros were then overlaid with α-MEM containing 10% FBS and subsequently incubated for 48 h at 37 °C. After

incubation, the cells were fixed and stained with crystal violet. Crystal violet was prepared by mixing 280 mL of 100% ethanol, 40 mL of 37% formaldehyde, 20 mL of glacial acetic acid, 120 mL of reverse osmosis filtered water and 4 grams of crystal violet powder (Sigma-Aldrich, Oakville, Canada). Viral plaques were quantified using an inverted microscope, and PFU per milliliter was calculated by taking account dilution factors. Accounting the number of plaques with the dilution factor allows calculation of the number of plaque forming units per millilitre (PFU/mL), also known as the viral titre.

7.10 Microarray Analysis (by Dr. Chris Verschoor)

VK2 cells were lysed and RNA was isolated after 24 hours of HSV-2 infection using RNAeasy kit (Qiagen, Toronto, ON, Canada), as described in section 7.12. The experimental design consisted of triplicates of each of the four treatment groups: VK2 cells in ALI cultures without hormones or treated with E2, P4 or MPA for 7 days followed by HSV-2 infection for 24 hours. Purified RNA was resuspended in RNase-free water and quantified using a Nanodrop spectrophotometer (NanoDrop Technologies Inc., Wilmington, DE). RNA sample bio-analysis, microarray chip hybridization and processing were performed by the Center for Applied Genomics facility at the Hospital for Sick Kids (Toronto, Ontario, Canada) for microarray analysis using the Affymetrix Human Genome ST 2.0 array gene chip. For data analysis, all pre-processing steps and differential expression analysis were performed using "R" v3.3.2 software (The R Foundation for Statistical Computing). Raw data were loaded using the package 'oligo' and background correction as well as normalization procedures were performed using Robust Multi-array Average (RMA) as described.[237] Although not a main component of the investigation, MPA was included as a factor for background subtraction in the processing of the array. This was done since all array conditions

were submitted and analyzed simultaneously, and so consistency should be maintained while including all original treatments as factors. Furthermore, inclusion of MPA in the background provides more input information for "limma", an "R" software extension used for differential expression analysis, thus reducing error and p-values.[238] Array batch and donor effects were removed sequentially using the ComBat function in the package 'sva', and the following probes were removed: spike-in, positive or negative housekeeping and background control, reporter probes (n=5,473); and those probes whose intensity was below the 95th percentile of both anti-genomic and intronic probes of housekeeping genes in more than 75% of chips analyzed (n=37,837). The final probe count was 10,307. Multidimensional scaling (MDS) was performed on background corrected and normalized probes following ComBat but prior to probe removal using the package 'minfi', and differential expression analysis was performed with the "limma" package. Adjusted *p*-values account for multiple testing using Benjamini-Hochberg's procedure for controlling false discovery rate (FDR).

7.11 Gene set enrichment analysis

A ranked list (RNK file) was generated by adjusting for both the p-value and the log fold change (log FC), using the formula sign(logFC)*-$\log_{10}$(p value). The RNK file including gene names and their ranked values, comparing SE2 vs SNH, SP4 vs SNH, SE2 vs SP4, SMPA vs SNH and SE2 vs SMPA, was used as an input for GSEA pre-ranked algorithm using the java GSEA 4.0.3 desktop program.[239] The GSEA java software was used with the Hallmark database from MSigDB to generate pathways that are enriched between various comparisons. The GSEA 4.0.3 java program applies an FDR cut-off of 0.25 as a suggested value for initial phases of hypothesis generation of novel data. However, since our data has provided adequate significance, we were

interested in pathways with an FDR < 0.05. A weighted enrichment scoring statistic was applied and the number of permutations was set to 5000. Default settings were used for all other parameters. Selection of pathways with low FDR values from GSEA has been demonstrated to be a strong tool for potential hypothesis generation, as stated by the software.

7.12 RNA Extraction and Quantitative Real-Time Polymerase Chain Reaction

VK2 cells were either grown in ALI or LLI cultures for 7 days as described in 7.2 and 7.3, respectively. The only time LLI cultures were used for qPCR was when viral genes needed to be analyzed; since they need to be analyzed shortly after entry (15 minutes post-infection), it was important that the LLI cultures be used and placed on ice to allow viral attachment and synchronous entry in all cells, as described in 7.7.3. VK2 cultures were either left uninfected (mock) or infected with HSV-2 (strain 333) at a MOI of one for 15 min, 2h, 8h, 16h or 24 h and total RNA was isolated using the RNAeasy kit (Qiagen, Toronto, ON, Canada). Total RNA was isolated from VK2 cultures using the RNAeasy kit (Qiagen, Cat 74104) according to the manufacturer's protocol. Purified RNA in RNAse-free water was quantified using a Nanodrop spectrophotometer (NanoDrop Technologoies, Inc, Wilmington, DE, USA). RNA was converted to cDNA using a high-capacity cDNA reverse transcription kit (Thermo Fisher Scientific, Cat. 4368814). Remaining RNA was stored in -80°C, and cDNA in -20°C. Real-time qPCR was performed using 2 µL of 1:20 diluted cDNA, 6 µL of RNAse-free water, 10 µL of RT^2 Real-Time^{TM} SYBR$^{®}$ Green/ROX PCR master mix (Qiagen, Cat. 330523) and 1 µL of each forward and reverse gene-specific primers (Table 1), according to the manufacturer's manual (Qiagen). The StepOne^{TM} Real-Time PCR system (Thermo Fisher Scientific, Canada) was used with settings as followed: Hot start 95°C; followed by 40 cycles 95°C 3 seconds, 60°C 30 seconds, and 1 cycle

at 72°C for 2 minutes. Hold at 4°C. Samples were run in triplicates and all data were normalized to GAPDH mRNA expression as an internal control. Fold change in gene expression of all genes was calculated in comparison to mock uninfected NH controls.

Table 1: Primers used for real-time quantitative polymerase chain reaction

Name	Forward Primer Sequence	Reverse Primer Sequence
ERα	TCGACGCCAGGGTGGCAGAG	TGGTGCACTGGTTGGTGGCTGG
GAPDH	ACAGTCAGCCGCATCTTCTTTTGC	TTGAGGTCAATGAAGGGGTC
p53	GTC CAG ATG AAG CTC CCA GA	CAA GAA GCC CAG ACG GAA AC
HSV-2 Genes		
gD	CCAAATACGCCTTAGCAGACC	CACAGTGATCGGATGCTGG
ICP0	GTGCATGAAGACCTGGATTCC	GGTCACGCCCACTATCAGGTA
ICP4	TAGCATGCGGAACGGAAGC	CGCATGGCATCTCATTACCG
ICP27	CCCTTTCTGCAGT	CCTTAATGTCCGA
VP16	AATGTGGTTTAGCTCCCGCA	CCAGTTGGCGTGTCTGTTTC
Interferons and Interferon Receptors		
IFN-α	CTG GCA CAA ATG GGA AGA AT	CTT GAG CCT TCT GGA ACT GG
IFN-β	CGCCGCAGTGACCATCTA	CCAGGAGGTTCTCAACAATAGTC
IFN-γ	TGC AGA GCC AAA TTG TCT CC	TGC TTT GCG TTG GAC ATT CA
IFN-λ1	CAC AGG AGC TAG CGA GCT TCA	TTT TCA GCT TGA GTG ACT CTT CCA
IFN-λ2/3	GCC AAA GAT GCC TTA GAA GAG	CAG AAC CTT CAG CGT CAG G
IFNAR1	GGT GCT CCA AAA CAG TCT GG	TCA TCC ATG GTG TGT GCT CT
Interferon Stimulated Genes		
BST2	GGGAGGAGCCTAGGTGAATC	GTGGCATTTGCCTTGTTTTT
IFIT1	GCAGCCAAGTTTTACCGAAG	GCCCTATCTGGTGATGCAGT
IFI44L	GTATAGCATATGTGGCCTTGCTTACT	ATGACCCGCCTTTGAGAAGTC
ISG15	ACTCATCTTTGCCAGTACAGGAG	CAGCATCTTCACCGTCAGGTC
OAS1	CAGGCAGAAGAGGACTGGAC	TAGAAGGCCAGGAGTCAGGA

OAS2	CTTTCTGCCTTTGGCTTTTG	GGAAGAAAATTTGCGGATGA
OAS3	GTCAAACCCAAGCCACAAGT	CTCCTTCCACAACCCCTGTA
RSAD2	AGGTTCTGCAAAGTAGAGTTGC	GATCAGGCTTCCATTGCTC
MX1	CAGCACCTGATGGCCTATCA	ACGTCTGGAGCATGAAGAACTG
GSEA Leading-edge subset genes		
ALOX15B	CTG CCC ACT GAT GAC AAG TG	CGA TGC CTG TGG ACT TGA AG
BAX	TGG ATC CAA GAC CAG GGT G	GGA GGT CAG CAG GGT AGA TG
BTG2	AGA ACT GTT GCG TGC TTG AG	ATC CCG ACC TCT CTG TTC AC
IER3	CAG CAC TTT CCT CCA GCA AC	TCC GCT GTA GTG TTC TGA GT
PCNA	AGG CAC TCA AGG ACC TCA TC	GCC AAG GTA TCC GCG TTA TC
RAB2B	AGA AGT ACG ACC CGA CCA TC	CTG GTT GAC GAG GCT GTA GA
RAP40C	ACG GCA TCA GAA CCA TCC TG	ATG GCT TCA GGA GAG AGG TG
SPHK1	TGA CCA ACT GCA CGC TAT TG	CCA GAC GCC GAT ACT TCT CA
TGFβ1	GCT GTA CAT TGA CTT CCG CA	CCG GGT TAT GCT GGT TGT AC
TRAFD1	TGC AAC CAA CCA TGT GAC AG	GGC CCA TTA GCT GTT TCC TG
VAMP8	AGA ATG CTG CTC GGT CCT C	AAC AGT TTC CCA GCC ACA TG
Cytokines and Chemokines		
IL-1β	GGG CCT CAA GGA AAA GAA TC	TTC TGC TTG AGA GGT GCT GA
IL-8	AGG GTT GCC AGA TGC AAT AC	CCT TGG CCT CAA TTT TGC TA
TNF-α	ATC AGA GGG CCT GTA CCT CA	GGA AGA CCC CTC CCA GAT AG

7.13 Cell Viability Assay

VK2 cells were seeded at a cell density of 10,000 cells per well in 24 well plates. Every 24 h for 8 days, a set of wells were trypsinized with 1X trypsin-EDTA (McMaster Media Centre) and neutralized with Dulbecco's modified Eagle's medium and Ham's F12 (DMEM/F12) medium containing 10% fetal bovine serum (FBS). This was done since hormone treatments, Nutlin-3, and

PFT-α treatments are added at different times, thus allowing monitoring of cell viability over time after addition of treatments. Cells were monitored up until 8 days to ensure that the treatments have no effect on cell viability on the 8th day as well, since that is the day when HSV-2 is infected into our cultures based on our timeline. Measuring cell viability on this day will help rule out the variable of cell death which has the potential to influence viral replication. After neutralization, 10 µL suspended cells were then mixed with 90 µL of 0.4% trypan blue solution (Thermo Fisher Scientific, Cat. 15250061) and counted with the trypan blue exclusion assay by light microscopy using a hemocytometer. Percent of viable cells were identified as those that are unstained, whereas stained cells were identified as nonviable. The following equation was used to calculate cell viability over time for 7 days:

$$Viable\ Cells\ (\%) = \frac{total\ number\ of\ viable\ cells\ per\ mL\ of\ aliquot}{total\ number\ of\ cells\ per\ mL\ of\ aliquot} \times 100$$

7.14 Lactate Dehydrogenase (LDH) Assay

VK2 cells were prepared in ALI cultures by seeding 60,000 VK2 cells on the apical side in the transwell (VWR, Cat. 82050-022). After 24 h, the apical medium was removed to mimic ALI conditions. For each of the eight days after seeding the cells, KSFM medium was added to the apical side for 1 h, incubated at 37°C in a 5% CO_2 humidified atmosphere and then collected for LDH assay, where LDH in culture supernatants was used as a marker of cell stress. This was done since hormone treatments, Nutlin-3, and PFT-α treatments are added at different times, thus allowing monitoring of cell viability over time after addition of treatments. Cells were monitored up until 8 days to ensure that the treatments have no effect on cell stress on the 8th day as well, since that is the day when HSV-2 is infected into our cultures based on our timeline. Measuring cell stress on this day will help rule out the variable of cell death which has the potential to

influence viral replication. Collected samples were used to measure LDH using the CyQUANT™ LDH Cytotoxicity Assay kit according to manufacturer's instructions (Thermo Fisher Scientific, Cat. C20300). One 8-day old ALI VK2 culture was lysed with 10X lysis buffer supplied with the LDH assay kit to use as a positive control for maximum cellular LDH. LDH activity was calculated by subtracting the 690 nm absorbance value (background) from the 490 nm absorbance value.

7.15 IFN-β ELISA

Supernatants collected from VK2 cells after HSV-2 infection were analyzed for IFN-β production using human IFN-β ELISA kit (R&D Systems, Cat. DIFNB0) according to manufacturer's instructions. The minimum detectable limit of IFN-β ELISA kit ranges from 0.269–0.781pg/ml and assay is specific to natural and recombinant human IFN-β.

7.16 Knockdown of p53 in VK2s with siRNA treatment

To block the expression of p53, two different silencer^{TM} select siRNAs for TP53 (Ambion Silencer Select 439824 siRNA IDs #s606 and #s607; Thermo Fisher Scientific; Massachusetts, USA) were used since they have both been validated by the company. We examined both siRNAs, with each siRNA targeting different exons of the p53 genome, since it allowed selection of one that inhibits p53 more efficiently for future experiments. Efficacy of siRNAs targeting p53 was tested in the vaginal epithelial cell line (VK2s) expressing endogenous p53. For negative control, silencer^{TM} negative control siRNA was used (Thermo Fisher Scientific, Cat. AM4611). This product is known not target any gene product, allowing us to determine the effects of siRNA delivery and act as a baseline to compare siRNA-treated samples. To find the most optimal siRNA concentration to completely block p53 gene expression, different doses of siRNAs were tested (1,

10, 30 and 50 nM). siRNA treatments of all aforementioned doses were used with VK2s grown in either no hormone (to observe blocking of basal level of P53) or after 48 hours of Nutlin-3 (5 μM) treatment (to observe blocking of induced level of P53). We found that 30 nM of s607 was optimal at suppressing expression of P53, so this concentration was used in further experiments with various treatments. Before siRNA transfections, KSFM medium was removed from the apical side. Transfection of siRNA was performed by diluting Lipofectamine^{TM} RNAiMax (Invitrogen, Cat. 13778075) in Opti-MEM medium (Thermo Fisher Scientific, Cat. 31985062) and mixing it with respective concentrations of siRNA diluted with Opti-MEM medium, creating a final mix to be overlayed for 6 hours on VK2s for transfection, according to the manufacturer's instructions. After 6 hours, the siRNA-transfected cells were overlaid with 10% FBS-containing DMEM/F12 medium. 24 – 48 hours after transfections, cells were left uninfected or infected with HSV-2, as described in section 7.7.3, prior to being fixed with 4% paraformaldehyde and stained for immunofluorescent microscopy, as described in section 7.17.

7.17 Immunofluorescent Staining and Confocal Microscopy

VK2 cells were either grown in ALI or LLI cultures. LLI cultures were often used instead of ALI cultures to allow optimal visualization of single-layered cells, as well as to prevent antibody cluttering between multilayers of cells. The only time ALI cultures were used for immunofluorescent staining was during analysis of ZO-1 due to the nature of the protein and its involvement in barrier integrity. To grow cells in a LLI culture, 2,000 – 5000 VK2 cells were seeded and cultured for 7 days on the apical side of 0.4 μm pore-sized transwell polystyrene inserts (VWR, Cat. 82050-022) in 24 well plates, depending on how confluent they were needed for confocal imaging.[78] For example, 5000 cells were needed to examine ZO-1 since a high level of

confluence provides optimal imaging of the protein at the junctions of cells. After completion of cultures, treatments or HSV-2 infection, VK2 cell cultures were briefly permeabilized and fixed in 4% paraformaldehyde before being stored in -4°C until needed. Fixed cultures were then treated with a blocking solution of 5% Bovine serum albumin (Millipore-Sigma, Oakville, ON, Canada) and 5% normal goat serum (Millipore-Sigma) in 0.1% Triton X-100 (Bio-Rad Laboratories, Mississauga, ON, Canada) with primary antibody (Table 2) together for one hour at room temperature. Following incubation with primary antibodies, the cells were washed three times with PBS. Blocking solution mixed with the secondary antibody was then added for 1 hour at room temperature. Following incubation with secondary antibodies, the cells were washed three times with PBS. After extensive washing, filters were excised from the polystyrene inserts and mounted on glass slides in VectaShield mounting medium containing DAPI (Vector Labs, Burlingame, CA, USA) and left to set overnight. All samples were imaged on an inverted confocal laser-scanning microscope (Nikon Eclipse Ti2) using standard operating conditions (63× objective, optical laser thickness of 1μm, image dimension of 512 × 512, lasers: green 488 nm and red 594 nm laser lines). For each experiment, confocal microscope settings for image acquisition and processing were identical between control and treated cells and three separate, random images were acquired for analysis with each replicate well for each experimental condition.

Table 2: Reagents used for immunofluorescence staining

Antibody	Dilution	Company (Catalogue Number)
Primary Antibodies		
Mouse anti-Human p53 monoclonal antibody	1:100	Abcam (ab26)
Rabbit anti-Human ERα	1:100	Santa Cruz Biotechnology (sc-542)
Rabbit anti-Human phospho-p53 (Ser15) polyclonal antibody	1:200	Cell Signaling Technology (9284)
Rabbit purified anti-HSV	1:50	Biolegend (clone: Poly29138)
Rabbit anti-Human EEA1	1:100	Abcam (ab2900)
Mouse anti-Human BST2	1:100	Abcam (ab88523)
Mouse anti-Human ZO-1 monoclonal antibody	1:200	Thermo Fisher Scientific (33-9100)
Rabbit anti-human NFκB (p65)	1:100	Santa Cruz Biotechnology (sc-372)
Secondary Antibodies		
Alexa Fluor 488 Goat anti-Mouse IgG	1:1000	Life Technology (A11001)
Alexa Fluor 594 Goat anti-Mouse IgG	1:1000	Invitrogen, Thermo Fisher Scientific (A11032)
Alexa Fluor 488 Goat anti-Rabbit IgG	1:1000	Invitrogen, Thermo Fisher Scientific (A-11008)
Alexa Fluor 594 Goat anti-Rabbit IgG	1:1000	Abcam (ab-150080)
Isotype Controls		
Normal rabbit IgG	1:100	Santa Cruz Biotechnology (sc-2027)
Normal mouse IgG	1:100	Santa Cruz Biotechnology (sc-2025)

7.18 Statistical Analysis

Statistical analysis and graphical representation were performed using GraphPad Prism version 9.1.0 (GraphPad Software, San Diego, CA, USA). One-way analysis of variance (ANOVA) and Bonferroni's multiple comparisons were used, unless otherwise stated, and $p < 0.05$ was considered statistically significant.

REFERENCES

1. Looker KJ, Magaret AS, Turner KM, Vickerman P, Gottlieb SL, Newman LM. Global estimates of prevalent and incident herpes simplex virus type 2 infections in 2012. PLoS One. 2015;10(1):e114989.
2. Looker KJ, Elmes JAR, Gottlieb SL, Schiffer JT, Vickerman P, Turner KME, et al. Effect of HSV-2 infection on subsequent HIV acquisition: an updated systematic review and meta-analysis. Lancet Infect Dis. 2017;17(12):1303-16.
3. Johnston C, Corey L. Current Concepts for Genital Herpes Simplex Virus Infection: Diagnostics and Pathogenesis of Genital Tract Shedding. Clin Microbiol Rev. 2016;29(1):149-61.
4. Agelidis AM, Shukla D. Cell entry mechanisms of HSV: what we have learned in recent years. Future Virol. 2015;10(10):1145-54.
5. Grinde B. Herpesviruses: latency and reactivation - viral strategies and host response. J Oral Microbiol. 2013;5.
6. Jaishankar D, Shukla D. Genital Herpes: Insights into Sexually Transmitted Infectious Disease. Microb Cell. 2016;3(9):438-50.
7. Ibanez FJ, Farias MA, Gonzalez-Troncoso MP, Corrales N, Duarte LF, Retamal-Diaz A, et al. Experimental Dissection of the Lytic Replication Cycles of Herpes Simplex Viruses in vitro. Front Microbiol. 2018;9:2406.
8. Birkenheuer CH, Baines JD. RNA Polymerase II Promoter-Proximal Pausing and Release to Elongation Are Key Steps Regulating Herpes Simplex Virus 1 Transcription. J Virol. 2020;94(5).
9. Oh HS, Neuhausser WM, Eggan P, Angelova M, Kirchner R, Eggan KC, et al. Herpesviral lytic gene functions render the viral genome susceptible to novel editing by CRISPR/Cas9. Elife. 2019;8.
10. Paludan SR, Bowie AG, Horan KA, Fitzgerald KA. Recognition of herpesviruses by the innate immune system. Nat Rev Immunol. 2011;11(2):143-54.
11. LeGoff J, Pere H, Belec L. Diagnosis of genital herpes simplex virus infection in the clinical laboratory. Virol J. 2014;11:83.
12. Spear PG, Eisenberg RJ, Cohen GH. Three classes of cell surface receptors for alphaherpesvirus entry. Virology. 2000;275(1):1-8.
13. Spear PG, Longnecker R. Herpesvirus entry: an update. J Virol. 2003;77(19):10179-85.
14. Steven AC, Roberts CR, Hay J, Bisher ME, Pun T, Trus BL. Hexavalent capsomers of herpes simplex virus type 2: symmetry, shape, dimensions, and oligomeric status. J Virol. 1986;57(2):578-84.
15. Dolan A, Jamieson FE, Cunningham C, Barnett BC, McGeoch DJ. The genome sequence of herpes simplex virus type 2. J Virol. 1998;72(3):2010-21.
16. Rosato PC, Leib DA. Neurons versus herpes simplex virus: the innate immune interactions that contribute to a host-pathogen standoff. Future Virol. 2015;10(6):699-714.
17. Shahnazaryan D, Khalil R, Wynne C, Jefferies CA, Ní Gabhann-Dromgoole J, Murphy CC. Herpes simplex virus 1 targets IRF7 via ICP0 to limit type I IFN induction. Scientific Reports. 2020;10(1):22216.
18. Boutell C, Everett RD. The herpes simplex virus type 1 (HSV-1) regulatory protein ICP0 interacts with and Ubiquitinates p53. J Biol Chem. 2003;278(38):36596-602.
19. Roizman B, Zhou G. The 3 facets of regulation of herpes simplex virus gene expression: A critical inquiry. Virology. 2015;479-480:562-7.
20. Weller SK, Coen DM. Herpes simplex viruses: mechanisms of DNA replication. Cold Spring Harb Perspect Biol. 2012;4(9):a013011-a.
21. Weerasooriya S, DiScipio KA, Darwish AS, Bai P, Weller SK. Herpes simplex virus 1 ICP8 mutant lacking annealing activity is deficient for viral DNA replication. Proceedings of the National Academy of Sciences. 2019;116(3):1033.

22. Hay J, Ruyechan WT. Alphaherpesvirus DNA replication. In: Arvin A, Campadelli-Fiume G, Mocarski E, Moore PS, Roizman B, Whitley R, et al., editors. Human Herpesviruses: Biology, Therapy, and Immunoprophylaxis. Cambridge2007.
23. Honess RW, Roizman B. Regulation of herpesvirus macromolecular synthesis: sequential transition of polypeptide synthesis requires functional viral polypeptides. Proceedings of the National Academy of Sciences. 1975;72(4):1276.
24. Gruffat H, Marchione R, Manet E. Herpesvirus Late Gene Expression: A Viral-Specific Pre-initiation Complex Is Key. Frontiers in microbiology. 2016;7:869-.
25. Kukhanova MK, Korovina AN, Kochetkov SN. Human herpes simplex virus: life cycle and development of inhibitors. Biochemistry (Mosc). 2014;79(13):1635-52.
26. Cossart P, Helenius A. Endocytosis of viruses and bacteria. Cold Spring Harb Perspect Biol. 2014;6(8):a016972.
27. Schwake M, Schröder B, Saftig P. Lysosomal membrane proteins and their central role in physiology. Traffic. 2013;14(7):739-48.
28. Mercer J, Schelhaas M, Helenius A. Virus entry by endocytosis. Annu Rev Biochem. 2010;79:803-33.
29. Akhtar J, Shukla D. Viral entry mechanisms: cellular and viral mediators of herpes simplex virus entry. The FEBS Journal. 2009;276(24):7228-36.
30. Spearman P. Viral interactions with host cell Rab GTPases. Small GTPases. 2018;9(1-2):192-201.
31. Hutagalung AH, Novick PJ. Role of Rab GTPases in membrane traffic and cell physiology. Physiol Rev. 2011;91(1):119-49.
32. Tebaldi G, Pritchard SM, Nicola AV. Herpes Simplex Virus Entry by a Nonconventional Endocytic Pathway. Journal of virology. 2020;94(24):e01910-20.
33. Nicola AV, Straus SE. Cellular and viral requirements for rapid endocytic entry of herpes simplex virus. J Virol. 2004;78(14):7508-17.
34. Devadas D, Koithan T, Diestel R, Prank U, Sodeik B, Döhner K. Herpes simplex virus internalization into epithelial cells requires Na+/H+ exchangers and p21-activated kinases but neither clathrin- nor caveolin-mediated endocytosis. J Virol. 2014;88(22):13378-95.
35. Amjadi F, Salehi E, Mehdizadeh M, Aflatoonian R. Role of the innate immunity in female reproductive tract. Adv Biomed Res. 2014;3:1.
36. Wira CR, Rodriguez-Garcia M, Patel MV. The role of sex hormones in immune protection of the female reproductive tract. Nat Rev Immunol. 2015;15(4):217-30.
37. Ochiel DO, Fahey JV, Ghosh M, Haddad SN, Wira CR. Innate Immunity in the Female Reproductive Tract: Role of Sex Hormones in Regulating Uterine Epithelial Cell Protection Against Pathogens. Curr Womens Health Rev. 2008;4(2):102-17.
38. Hickey DK, Patel MV, Fahey JV, Wira CR. Innate and adaptive immunity at mucosal surfaces of the female reproductive tract: stratification and integration of immune protection against the transmission of sexually transmitted infections. J Reprod Immunol. 2011;88(2):185-94.
39. Petrova MI, van den Broek M, Balzarini J, Vanderleyden J, Lebeer S. Vaginal microbiota and its role in HIV transmission and infection. FEMS Microbiol Rev. 2013;37(5):762-92.
40. Rodriguez-Garcia M, Patel MV, Wira CR. Innate and adaptive anti-HIV immune responses in the female reproductive tract. J Reprod Immunol. 2013;97(1):74-84.
41. Blaskewicz CD, Pudney J, Anderson DJ. Structure and function of intercellular junctions in human cervical and vaginal mucosal epithelia. Biol Reprod. 2011;85(1):97-104.
42. Nguyen PV, Kafka JK, Ferreira VH, Roth K, Kaushic C. Innate and adaptive immune responses in male and female reproductive tracts in homeostasis and following HIV infection. Cell Mol Immunol. 2014;11(5):410-27.

43. Wira CR, Patel MV, Ghosh M, Mukura L, Fahey JV. Innate immunity in the human female reproductive tract: endocrine regulation of endogenous antimicrobial protection against HIV and other sexually transmitted infections. Am J Reprod Immunol. 2011;65(3):196-211.
44. Chantler E. Structure and function of cervical mucus. Adv Exp Med Biol. 1982;144:251-63.
45. Lacroix G, Gouyer V, Gottrand F, Desseyn J-L. The Cervicovaginal Mucus Barrier. Int J Mol Sci. 2020;21(21):8266.
46. Shin H, Iwasaki A. Generating protective immunity against genital herpes. Trends Immunol. 2013;34(10):487-94.
47. Koelle DM, Corey L. Herpes simplex: insights on pathogenesis and possible vaccines. Annu Rev Med. 2008;59:381-95.
48. Ferreira VH, Nazli A, Mossman KL, Kaushic C. Proinflammatory cytokines and chemokines - but not interferon-beta - produced in response to HSV-2 in primary human genital epithelial cells are associated with viral replication and the presence of the virion host shutoff protein. Am J Reprod Immunol. 2013;70(3):199-212.
49. Wira CR, Fahey JV, Sentman CL, Pioli PA, Shen L. Innate and adaptive immunity in female genital tract: cellular responses and interactions. Immunol Rev. 2005;206:306-35.
50. Chew T, Taylor KE, Mossman KL. Innate and adaptive immune responses to herpes simplex virus. Viruses. 2009;1(3):979-1002.
51. Zahid A, Ismail H, Li B, Jin T. Molecular and Structural Basis of DNA Sensors in Antiviral Innate Immunity. Frontiers in Immunology. 2020;11(3094).
52. Fazeli A, Bruce C, Anumba DO. Characterization of Toll-like receptors in the female reproductive tract in humans. Human Reproduction. 2005;20(5):1372-8.
53. Lv X, Wang H, Su A, Xu S, Chu Y. Herpes simplex virus type 2 infection triggers AP-1 transcription activity through TLR4 signaling in genital epithelial cells. Virology journal. 2018;15(1):173-.
54. Nazli A, Yao XD, Smieja M, Rosenthal KL, Ashkar AA, Kaushic C. Differential induction of innate anti-viral responses by TLR ligands against Herpes simplex virus, type 2, infection in primary genital epithelium of women. Antiviral Res. 2009;81(2):103-12.
55. Chan T, Barra NG, Lee AJ, Ashkar AA. Innate and adaptive immunity against herpes simplex virus type 2 in the genital mucosa. J Reprod Immunol. 2011;88(2):210-8.
56. van Gent M, Sparrer KMJ, Gack MU. TRIM Proteins and Their Roles in Antiviral Host Defenses. Annu Rev Virol. 2018;5(1):385-405.
57. Tanaka Y, Chen ZJ. STING specifies IRF3 phosphorylation by TBK1 in the cytosolic DNA signaling pathway. Sci Signal. 2012;5(214):ra20.
58. Helgason E, Phung QT, Dueber EC. Recent insights into the complexity of Tank-binding kinase 1 signaling networks: the emerging role of cellular localization in the activation and substrate specificity of TBK1. FEBS Lett. 2013;587(8):1230-7.
59. Ning S, Pagano JS, Barber GN. IRF7: activation, regulation, modification and function. Genes Immun. 2011;12(6):399-414.
60. Akira S, Takeda K. Toll-like receptor signalling. Nat Rev Immunol. 2004;4(7):499-511.
61. Farrell PJ, Sen GC, Dubois MF, Ratner L, Slattery E, Lengyel P. Interferon action: two distinct pathways for inhibition of protein synthesis by double-stranded RNA. Proc Natl Acad Sci U S A. 1978;75(12):5893-7.
62. Everett H, McFadden G. Apoptosis: an innate immune response to virus infection. Trends in Microbiology. 1999;7(4):160-5.
63. Givan AL, White HD, Stern JE, Colby E, Gosselin EJ, Guyre PM, et al. Flow cytometric analysis of leukocytes in the human female reproductive tract: comparison of fallopian tube, uterus, cervix, and vagina. Am J Reprod Immunol. 1997;38(5):350-9.

64. Rodriguez-Garcia M, Barr FD, Crist SG, Fahey JV, Wira CR. Phenotype and susceptibility to HIV infection of CD4+ Th17 cells in the human female reproductive tract. Mucosal Immunol. 2014;7(6):1375-85.
65. Zhu J, Hladik F, Woodward A, Klock A, Peng T, Johnston C, et al. Persistence of HIV-1 receptor-positive cells after HSV-2 reactivation is a potential mechanism for increased HIV-1 acquisition. Nat Med. 2009;15(8):886-92.
66. Milligan GN, Bernstein DI, Bourne N. T lymphocytes are required for protection of the vaginal mucosae and sensory ganglia of immune mice against reinfection with herpes simplex virus type 2. J Immunol. 1998;160(12):6093-100.
67. Dobbs ME, Strasser JE, Chu CF, Chalk C, Milligan GN. Clearance of herpes simplex virus type 2 by CD8+ T cells requires gamma interferon and either perforin- or Fas-mediated cytolytic mechanisms. J Virol. 2005;79(23):14546-54.
68. Harandi AM, Svennerholm B, Holmgren J, Eriksson K. Differential roles of B cells and IFN-gamma-secreting CD4(+) T cells in innate and adaptive immune control of genital herpes simplex virus type 2 infection in mice. J Gen Virol. 2001;82(Pt 4):845-53.
69. Nakanishi Y, Lu B, Gerard C, Iwasaki A. CD8+ T lymphocyte mobilization to virus-infected tissue requires CD4+ T-cell help. Nature. 2009;462(7272):510-3.
70. Cone RA. Handbook of Mucosal Immunology: Academic Press; 2005 2005. 49-72 p.
71. Kaushic C, Wira C.R. IgA and Reproductive Tract Immunity. In: C.S K, editor. Mucosal Immune Defense: Immunoglobulin A. Boston, MA: Springer; 2007.
72. McDermott MR, Brais LJ, Evelegh MJ. Mucosal and systemic antiviral antibodies in mice inoculated intravaginally with herpes simplex virus type 2. J Gen Virol. 1990;71 (Pt 7):1497-504.
73. Iijima N, Iwasaki A. Access of protective antiviral antibody to neuronal tissues requires CD4 T-cell help. Nature. 2016;533(7604):552-6.
74. Parr MB, Parr EL. Immunity to vaginal herpes simplex virus-2 infection in B-cell knockout mice. Immunology. 2000;101(1):126-31.
75. Dudley KL, Bourne N, Milligan GN. Immune protection against HSV-2 in B-cell-deficient mice. Virology. 2000;270(2):454-63.
76. Gillgrass AE, Tang VA, Towarnicki KM, Rosenthal KL, Kaushic C. Protection against genital herpes infection in mice immunized under different hormonal conditions correlates with induction of vagina-associated lymphoid tissue. J Virol. 2005;79(5):3117-26.
77. Bhavanam S, Snider DP, Kaushic C. Intranasal and subcutaneous immunization under the effect of estradiol leads to better protection against genital HSV-2 challenge compared to progesterone. Vaccine. 2008;26(48):6165-72.
78. Lee Y, Dizzell SE, Leung V, Nazli A, Zahoor MA, Fichorova RN, et al. Effects of Female Sex Hormones on Susceptibility to HSV-2 in Vaginal Cells Grown in Air-Liquid Interface. Viruses. 2016;8(9).
79. Gillgrass AE, Fernandez SA, Rosenthal KL, Kaushic C. Estradiol regulates susceptibility following primary exposure to genital herpes simplex virus type 2, while progesterone induces inflammation. J Virol. 2005;79(5):3107-16.
80. Gillgrass AE, Ashkar AA, Rosenthal KL, Kaushic C. Prolonged exposure to progesterone prevents induction of protective mucosal responses following intravaginal immunization with attenuated herpes simplex virus type 2. J Virol. 2003;77(18):9845-51.
81. Gillgrass A, Chege D, Bhavanam S, Kaushic C. Estradiol limits viral replication following intravaginal immunization leading to diminished mucosal IgG response and non-sterile protection against genital herpes challenge. Am J Reprod Immunol. 2010;63(4):299-309.
82. Rodriguez-Garcia M, Biswas N, Patel MV, Barr FD, Crist SG, Ochsenbauer C, et al. Estradiol reduces susceptibility of CD4+ T cells and macrophages to HIV-infection. PLoS One. 2013;8(4):e62069.

83. Wira CR, Fahey JV, Rodriguez-Garcia M, Shen Z, Patel MV. Regulation of mucosal immunity in the female reproductive tract: the role of sex hormones in immune protection against sexually transmitted pathogens. Am J Reprod Immunol. 2014;72(2):236-58.
84. Smith SM, Mefford M, Sodora D, Klase Z, Singh M, Alexander N, et al. Topical estrogen protects against SIV vaginal transmission without evidence of systemic effect. AIDS. 2004;18(12):1637-43.
85. Stanton A, Mowbray C, Lanz M, Brown K, Hilton P, Tyson-Capper A, et al. Topical Estrogen Treatment Augments the Vaginal Response to Escherichia coli Flagellin. Scientific reports. 2020;10(1):8473-.
86. Cui J, Shen Y, Li R. Estrogen synthesis and signaling pathways during aging: from periphery to brain. Trends Mol Med. 2013;19(3):197-209.
87. Paterni I, Granchi C, Katzenellenbogen JA, Minutolo F. Estrogen receptors alpha (ERα) and beta (ERβ): subtype-selective ligands and clinical potential. Steroids. 2014;90:13-29.
88. The Human Protein Atlas. ESR1 2021 [Available from: https://www.proteinatlas.org/ENSG00000091831-ESR1/summary/rna]
89. Fish EN. The X-files in immunity: sex-based differences predispose immune responses. Nat Rev Immunol. 2008;8(9):737-44.
90. Galand P, Leroy F, Chretien J. Effect of oestradiol on cell proliferation and histological changes in the uterus and vagina of mice. J Endocrinol. 1971;49(2):243-52.
91. Zhu L, Pollard JW. Estradiol-17beta regulates mouse uterine epithelial cell proliferation through insulin-like growth factor 1 signaling. Proc Natl Acad Sci U S A. 2007;104(40):15847-51.
92. Kaushic C, Ashkar AA, Reid LA, Rosenthal KL. Progesterone increases susceptibility and decreases immune responses to genital herpes infection. J Virol. 2003;77(8):4558-65.
93. Marx PA, Spira AI, Gettie A, Dailey PJ, Veazey RS, Lackner AA, et al. Progesterone implants enhance SIV vaginal transmission and early virus load. Nat Med. 1996;2(10):1084-9.
94. Gorodeski GI. Aging and estrogen effects on transcervical-transvaginal epithelial permeability. J Clin Endocrinol Metab. 2005;90(1):345-51.
95. Zeng R, Li X, Gorodeski GI. Estrogen abrogates transcervical tight junctional resistance by acceleration of occludin modulation. J Clin Endocrinol Metab. 2004;89(10):5145-55.
96. Gipson IK, Ho SB, Spurr-Michaud SJ, Tisdale AS, Zhan Q, Torlakovic E, et al. Mucin genes expressed by human female reproductive tract epithelia. Biol Reprod. 1997;56(4):999-1011.
97. Elstein M. Functions and physical properties of mucus in the female genital tract. Br Med Bull. 1978;34(1):83-8.
98. Wessels JM, Felker AM, Dupont HA, Kaushic C. The relationship between sex hormones, the vaginal microbiome and immunity in HIV-1 susceptibility in women. Dis Model Mech. 2018;11(9).
99. Wagner RD, Johnson SJ. Probiotic lactobacillus and estrogen effects on vaginal epithelial gene expression responses to Candida albicans. J Biomed Sci. 2012;19:58.
100. Schaefer TM, Wright JA, Pioli PA, Wira CR. IL-1beta-mediated proinflammatory responses are inhibited by estradiol via down-regulation of IL-1 receptor type I in uterine epithelial cells. J Immunol. 2005;175(10):6509-16.
101. Fahey JV, Wright JA, Shen L, Smith JM, Ghosh M, Rossoll RM, et al. Estradiol selectively regulates innate immune function by polarized human uterine epithelial cells in culture. Mucosal Immunol. 2008;1(4):317-25.
102. Murphy AJ, Guyre PM, Pioli PA. Estradiol suppresses NF-kappa B activation through coordinated regulation of let-7a and miR-125b in primary human macrophages. J Immunol. 2010;184(9):5029-37.
103. Ghisletti S, Meda C, Maggi A, Vegeto E. 17beta-estradiol inhibits inflammatory gene expression by controlling NF-kappaB intracellular localization. Mol Cell Biol. 2005;25(8):2957-68.

104. Kaushic C, Roth KL, Anipindi V, Xiu F. Increased prevalence of sexually transmitted viral infections in women: the role of female sex hormones in regulating susceptibility and immune responses. J Reprod Immunol. 2011;88(2):204-9.
105. Wira CR, Fahey JV. A new strategy to understand how HIV infects women: identification of a window of vulnerability during the menstrual cycle. AIDS. 2008;22(15):1909-17.
106. Birse K, Arnold KB, Novak RM, McCorrister S, Shaw S, Westmacott GR, et al. Molecular Signatures of Immune Activation and Epithelial Barrier Remodeling Are Enhanced during the Luteal Phase of the Menstrual Cycle: Implications for HIV Susceptibility. J Virol. 2015;89(17):8793-805.
107. Saba E, Origoni M, Taccagni G, Ferrari D, Doglioni C, Nava A, et al. Productive HIV-1 infection of human cervical tissue ex vivo is associated with the secretory phase of the menstrual cycle. Mucosal Immunol. 2013;6(6):1081-90.
108. Tasker C, Ding J, Schmolke M, Rivera-Medina A, Garcia-Sastre A, Chang TL. 17beta-estradiol protects primary macrophages against HIV infection through induction of interferon-alpha. Viral Immunol. 2014;27(4):140-50.
109. Sodora DL, Gettie A, Miller CJ, Marx PA. Vaginal transmission of SIV: assessing infectivity and hormonal influences in macaques inoculated with cell-free and cell-associated viral stocks. AIDS Res Hum Retroviruses. 1998;14 Suppl 1:S119-23.
110. Hearps AC, Tyssen D, Srbinovski D, Bayigga L, Diaz DJD, Aldunate M, et al. Vaginal lactic acid elicits an anti-inflammatory response from human cervicovaginal epithelial cells and inhibits production of pro-inflammatory mediators associated with HIV acquisition. Mucosal Immunol. 2017;10(6):1480-90.
111. Niu X-X, Li T, Zhang X, Wang S-X, Liu Z-H. Lactobacillus crispatus Modulates Vaginal Epithelial Cell Innate Response to Candida albicans. Chin Med J (Engl). 2017;130(3):273-9.
112. Dhawan T, Zahoor MA, Heryani N, Workenhe ST, Nazli A, Kaushic C. TRIM26 Facilitates HSV-2 Infection by Downregulating Antiviral Responses through the IRF3 Pathway. Viruses. 2021;13(1):70.
113. Fichorova RN, Rheinwald JG, Anderson DJ. Generation of papillomavirus-immortalized cell lines from normal human ectocervical, endocervical, and vaginal epithelium that maintain expression of tissue-specific differentiation proteins. Biol Reprod. 1997;57(4):847-55.
114. Marrs CN, Knobel SM, Zhu WQ, Sweet SD, Chaudhry AR, Alcendor DJ. Evidence for Gardnerella vaginalis uptake and internalization by squamous vaginal epithelial cells: implications for the pathogenesis of bacterial vaginosis. Microbes Infect. 2012;14(6):500-8.
115. Brady CA, Attardi LD. p53 at a glance. J Cell Sci. 2010;123(Pt 15):2527-32.
116. Liang SH, Clarke MF. Regulation of p53 localization. Eur J Biochem. 2001;268(10):2779-83.
117. Maclaine NJ, Hupp TR. The regulation of p53 by phosphorylation: a model for how distinct signals integrate into the p53 pathway. Aging (Albany NY). 2009;1(5):490-502.
118. Joerger AC, Fersht AR. The p53 Pathway: Origins, Inactivation in Cancer, and Emerging Therapeutic Approaches. Annual Review of Biochemistry. 2016;85(1):375-404.
119. Karimian A, Ahmadi Y, Yousefi B. Multiple functions of p21 in cell cycle, apoptosis and transcriptional regulation after DNA damage. DNA Repair (Amst). 2016;42:63-71.
120. Chène P. Inhibiting the p53–MDM2 interaction: an important target for cancer therapy. Nature Reviews Cancer. 2003;3(2):102-9.
121. Aloni-Grinstein R, Charni-Natan M, Solomon H, Rotter V. p53 and the Viral Connection: Back into the Future (double dagger). Cancers (Basel). 2018;10(6).
122. Brychtova V, Hrabal V, Vojtesek B. Oncogenic Viral Protein Interactions with p53 Family Proteins. Klin Onkol. 2019;32(Supplementum 3):72-7.
123. Turpin E, Luke K, Jones J, Tumpey T, Konan K, Schultz-Cherry S. Influenza virus infection increases p53 activity: role of p53 in cell death and viral replication. J Virol. 2005;79(14):8802-11.
124. Nailwal H, Sharma S, Mayank AK, Lal SK. The nucleoprotein of influenza A virus induces p53 signaling and apoptosis via attenuation of host ubiquitin ligase RNF43. Cell Death Dis. 2015;6:e1768.

125. Yan W, Wei J, Deng X, Shi Z, Zhu Z, Shao D, et al. Transcriptional analysis of immune-related gene expression in p53-deficient mice with increased susceptibility to influenza A virus infection. BMC Med Genomics. 2015;8:52.
126. Ma-Lauer Y, Carbajo-Lozoya J, Hein MY, Müller MA, Deng W, Lei J, et al. p53 down-regulates SARS coronavirus replication and is targeted by the SARS-unique domain and PL^{pro} via E3 ubiquitin ligase RCHY1. Proceedings of the National Academy of Sciences. 2016;113(35):E5192.
127. Cardozo CM, Hainaut P. Viral strategies for circumventing p53: the case of severe acute respiratory syndrome coronavirus. Curr Opin Oncol. 2021;33(2):149-58.
128. Munoz-Fontela C, Macip S, Martinez-Sobrido L, Brown L, Ashour J, Garcia-Sastre A, et al. Transcriptional role of p53 in interferon-mediated antiviral immunity. J Exp Med. 2008;205(8):1929-38.
129. Hao Z, Fu F, Cao L, Guo L, Liu J, Xue M, et al. Tumor suppressor p53 inhibits porcine epidemic diarrhea virus infection via interferon-mediated antiviral immunity. Mol Immunol. 2019;108:68-74.
130. Porta C, Hadj-Slimane R, Nejmeddine M, Pampin M, Tovey MG, Espert L, et al. Interferons alpha and gamma induce p53-dependent and p53-independent apoptosis, respectively. Oncogene. 2005;24(4):605-15.
131. Rivas C, Aaronson SA, Munoz-Fontela C. Dual Role of p53 in Innate Antiviral Immunity. Viruses. 2010;2(1):298-313.
132. The Human Protein Atlas. TP53 2021 [Available from: https://www.proteinatlas.org/ENSG00000141510-TP53]
133. Hurd C, Khattree N, Dinda S, Alban P, Moudgil VK. Regulation of tumor suppressor proteins, p53 and retinoblastoma, by estrogen and antiestrogens in breast cancer cells. Oncogene. 1997;15(8):991-5.
134. Hurd C, Khattree N, Alban P, Nag K, Jhanwar SC, Dinda S, et al. Hormonal regulation of the p53 tumor suppressor protein in T47D human breast carcinoma cell line. J Biol Chem. 1995;270(48):28507-10.
135. Fernandez-Cuesta L, Anaganti S, Hainaut P, Olivier M. p53 status influences response to tamoxifen but not to fulvestrant in breast cancer cell lines. Int J Cancer. 2011;128(8):1813-21.
136. Weige CC, Allred KF, Armstrong CM, Allred CD. P53 mediates estradiol induced activation of apoptosis and DNA repair in non-malignant colonocytes. J Steroid Biochem Mol Biol. 2012;128(3-5):113-20.
137. Song S, Wu S, Wang Y, Wang Z, Ye C, Song R, et al. 17beta-estradiol inhibits human umbilical vascular endothelial cell senescence by regulating autophagy via p53. Exp Gerontol. 2018;114:57-66.
138. Qin C, Nguyen T, Stewart J, Samudio I, Burghardt R, Safe S. Estrogen up-regulation of p53 gene expression in MCF-7 breast cancer cells is mediated by calmodulin kinase IV-dependent activation of a nuclear factor kappaB/CCAAT-binding transcription factor-1 complex. Mol Endocrinol. 2002;16(8):1793-809.
139. Hurd C, Dinda S, Khattree N, Moudgil VK. Estrogen-dependent and independent activation of the P1 promoter of the p53 gene in transiently transfected breast cancer cells. Oncogene. 1999;18(4):1067-72.
140. Gu G, Barone I, Gelsomino L, Giordano C, Bonofiglio D, Statti G, et al. Oldenlandia diffusa extracts exert antiproliferative and apoptotic effects on human breast cancer cells through ERalpha/Sp1-mediated p53 activation. J Cell Physiol. 2012;227(10):3363-72.
141. Berger CE, Qian Y, Liu G, Chen H, Chen X. p53, a target of estrogen receptor (ER) alpha, modulates DNA damage-induced growth suppression in ER-positive breast cancer cells. J Biol Chem. 2012;287(36):30117-27.
142. Berger C, Qian Y, Chen X. The p53-estrogen receptor loop in cancer. Curr Mol Med. 2013;13(8):1229-40.

143. Woods MW, Zahoor MA, Dizzell S, Verschoor CP, Kaushic C. Medroxyprogesterone acetate-treated human, primary endometrial epithelial cells reveal unique gene expression signature linked to innate immunity and HIV-1 susceptibility. Am J Reprod Immunol. 2018;79(1).
144. Zahoor MA, Woods MW, Dizzell S, Nazli A, Mueller KM, Nguyen PV, et al. Transcriptional profiling of primary endometrial epithelial cells following acute HIV-1 exposure reveals gene signatures related to innate immunity. Am J Reprod Immunol. 2018;79(4):e12822.
145. Woods MW, Zahoor MA, Lam J, Bagri P, Dupont H, Verschoor CP, et al. Transcriptional response of vaginal epithelial cells to medroxyprogesterone acetate treatment results in decreased barrier integrity. Journal of Reproductive Immunology. 2021;143:103253.
146. Jiang Z, Zhou X, Li R, Michal JJ, Zhang S, Dodson MV, et al. Whole transcriptome analysis with sequencing: methods, challenges and potential solutions. Cell Mol Life Sci. 2015;72(18):3425-39.
147. Altman RB, Raychaudhuri S. Whole-genome expression analysis: challenges beyond clustering. Curr Opin Struct Biol. 2001;11(3):340-7.
148. Celis JE, Kruhoffer M, Gromova I, Frederiksen C, Ostergaard M, Thykjaer T, et al. Gene expression profiling: monitoring transcription and translation products using DNA microarrays and proteomics. FEBS Lett. 2000;480(1):2-16.
149. Manger ID, Relman DA. How the host 'sees' pathogens: global gene expression responses to infection. Curr Opin Immunol. 2000;12(2):215-8.
150. Conesa A, Madrigal P, Tarazona S, Gomez-Cabrero D, Cervera A, McPherson A, et al. A survey of best practices for RNA-seq data analysis. Genome Biol. 2016;17:13.
151. Lytal N, Ran D, An L. Normalization Methods on Single-Cell RNA-seq Data: An Empirical Survey. Frontiers in Genetics. 2020;11(41).
152. Rapaport F, Khanin R, Liang Y, Pirun M, Krek A, Zumbo P, et al. Comprehensive evaluation of differential gene expression analysis methods for RNA-seq data. Genome Biol. 2013;14(9):R95.
153. Park T, Yi S-G, Kang S-H, Lee S, Lee Y-S, Simon R. Evaluation of normalization methods for microarray data. BMC Bioinformatics. 2003;4(1):33.
154. Tipney H, Hunter L. An introduction to effective use of enrichment analysis software. Hum Genomics. 2010;4(3):202-6.
155. Stricker R, Eberhart R, Chevailler MC, Quinn FA, Bischof P, Stricker R. Establishment of detailed reference values for luteinizing hormone, follicle stimulating hormone, estradiol, and progesterone during different phases of the menstrual cycle on the Abbott ARCHITECT analyzer. Clin Chem Lab Med. 2006;44(7):883-7.
156. Arya AK, El-Fert A, Devling T, Eccles RM, Aslam MA, Rubbi CP, et al. Nutlin-3, the small-molecule inhibitor of MDM2, promotes senescence and radiosensitises laryngeal carcinoma cells harbouring wild-type p53. British Journal of Cancer. 2010;103(2):186-95.
157. Kim S, You D, Jeong Y, Yu J, Kim SW, Nam SJ, et al. TP53 upregulates α-smooth muscle actin expression in tamoxifen-resistant breast cancer cells. Oncol Rep. 2019;41(2):1075-82.
158. Jiang X, Wang J. Knockdown of TFAM in Tumor Cells Retarded Autophagic Flux through Regulating p53 Acetylation and PISD Expression. Cancers. 2020;12(2):493.
159. Rong X, Rao J, Li D, Jing Q, Lu Y, Ji Y. TRIM69 inhibits cataractogenesis by negatively regulating p53. Redox Biol. 2019;22:101157-.
160. Li X, Qu Z, Jing S, Li X, Zhao C, Man S, et al. Dioscin-6'-O-acetate inhibits lung cancer cell proliferation via inducing cell cycle arrest and caspase-dependent apoptosis. Phytomedicine. 2019;53:124-33.
161. Fuentes N, Silveyra P. Estrogen receptor signaling mechanisms. Adv Protein Chem Struct Biol. 2019;116:135-70.
162. Liu G, Schwartz JA, Brooks SC. Estrogen receptor protects p53 from deactivation by human double minute-2. Cancer Res. 2000;60(7):1810-4.

163. Fernández-Cuesta L, Anaganti S, Hainaut P, Olivier M. Estrogen levels act as a rheostat on p53 levels and modulate p53-dependent responses in breast cancer cell lines. Breast Cancer Res Treat. 2011;125(1):35-42.
164. Zhu J, Singh M, Selivanova G, Peuget S. Pifithrin-α alters p53 post-translational modifications pattern and differentially inhibits p53 target genes. Scientific Reports. 2020;10(1):1049.
165. Tovar C, Rosinski J, Filipovic Z, Higgins B, Kolinsky K, Hilton H, et al. Small-molecule MDM2 antagonists reveal aberrant p53 signaling in cancer: implications for therapy. Proc Natl Acad Sci U S A. 2006;103(6):1888-93.
166. Vassilev LT, Vu BT, Graves B, Carvajal D, Podlaski F, Filipovic Z, et al. In vivo activation of the p53 pathway by small-molecule antagonists of MDM2. Science. 2004;303(5659):844-8.
167. Peper A. Aspects of the relationship between drug dose and drug effect. Dose Response. 2009;7(2):172-92.
168. Walton MI, Wilson SC, Hardcastle IR, Mirza AR, Workman P. An evaluation of the ability of pifithrin-α and -β to inhibit p53 function in two wild-type p53 human tumor cell lines. Molecular Cancer Therapeutics. 2005;4(9):1369-77.
169. Yim E-K, Park J-S. The role of HPV E6 and E7 oncoproteins in HPV-associated cervical carcinogenesis. Cancer Res Treat. 2005;37(6):319-24.
170. Daecke J, Fackler OT, Dittmar MT, Kräusslich HG. Involvement of clathrin-mediated endocytosis in human immunodeficiency virus type 1 entry. J Virol. 2005;79(3):1581-94.
171. Yasen A, Herrera R, Rosbe K, Lien K, Tugizov SM. HIV internalization into oral and genital epithelial cells by endocytosis and macropinocytosis leads to viral sequestration in the vesicles. Virology. 2018;515:92-107.
172. Tognarelli EI, Reyes A, Corrales N, Carreño LJ, Bueno SM, Kalergis AM, et al. Modulation of Endosome Function, Vesicle Trafficking and Autophagy by Human Herpesviruses. Cells. 2021;10(3):542.
173. Ashley CL, Abendroth A, McSharry BP, Slobedman B. Interferon-Independent Upregulation of Interferon-Stimulated Genes during Human Cytomegalovirus Infection is Dependent on IRF3 Expression. Viruses. 2019;11(3):246.
174. Thomas E, Saito T. Special Issue "IFN-Independent ISG Expression and its Role in Antiviral Cell-Intrinsic Innate Immunity". Viruses. 2019;11(11):981.
175. Ru J, Sun H, Fan H, Wang C, Li Y, Liu M, et al. MiR-23a facilitates the replication of HSV-1 through the suppression of interferon regulatory factor 1. PLoS One. 2014;9(12):e114021.
176. Danastas K, Miranda-Saksena M, Cunningham AL. Herpes Simplex Virus Type 1 Interactions with the Interferon System. Int J Mol Sci. 2020;21(14):5150.
177. Gonzalez-Perez AC, Stempel M, Chan B, Brinkmann MM. One Step Ahead: Herpesviruses Light the Way to Understanding Interferon-Stimulated Genes (ISGs). Frontiers in Microbiology. 2020;11(124).
178. Hao Z, Tao L. Microarray analysis of novel genes involved in HSV-2 infection. Research Square. 2021.
179. Madjo U, Leymarie O, Frémont S, Kuster A, Nehlich M, Gallois-Montbrun S, et al. LC3C Contributes to Vpu-Mediated Antagonism of BST2/Tetherin Restriction on HIV-1 Release through a Non-canonical Autophagy Pathway. Cell Reports. 2016;17(9):2221-33.
180. Akhtar J, Shukla D. Viral entry mechanisms: cellular and viral mediators of herpes simplex virus entry. Febs j. 2009;276(24):7228-36.
181. Dizzell S, Nazli A, Reid G, Kaushic C. Protective Effect of Probiotic Bacteria and Estrogen in Preventing HIV-1-Mediated Impairment of Epithelial Barrier Integrity in Female Genital Tract. Cells. 2019;8(10):1120.
182. Cooks T, Harris CC, Oren M. Caught in the cross fire: p53 in inflammation. Carcinogenesis. 2014;35(8):1680-90.

183. Gudkov AV, Gurova KV, Komarova EA. Inflammation and p53: A Tale of Two Stresses. Genes Cancer. 2011;2(4):503-16.
184. Murphy SH, Suzuki K, Downes M, Welch GL, De Jesus P, Miraglia LJ, et al. Tumor suppressor protein (p)53, is a regulator of NF-kappaB repression by the glucocorticoid receptor. Proc Natl Acad Sci U S A. 2011;108(41):17117-22.
185. Schneider G, Henrich A, Greiner G, Wolf V, Lovas A, Wieczorek M, et al. Cross talk between stimulated NF-κB and the tumor suppressor p53. Oncogene. 2010;29(19):2795-806.
186. Webster GA, Perkins ND. Transcriptional cross talk between NF-kappaB and p53. Mol Cell Biol. 1999;19(5):3485-95.
187. Al-Sadi R, Boivin M, Ma T. Mechanism of cytokine modulation of epithelial tight junction barrier. Front Biosci (Landmark Ed). 2009;14:2765-78.
188. Rodgers LS, Beam MT, Anderson JM, Fanning AS. Epithelial barrier assembly requires coordinated activity of multiple domains of the tight junction protein ZO-1. Journal of Cell Science. 2013;126(7):1565-75.
189. Panchanadeswaran S, Johnson SC, Mayer KH, Srikrishnan AK, Sivaran S, Zelaya CE, et al. Gender differences in the prevalence of sexually transmitted infections and genital symptoms in an urban setting in southern India. Sex Transm Infect. 2006;82(6):491-5.
190. UNAIDS. Global HIV & AIDS statistics - Fact sheet 2021 [cited 2021 September 5]. Available from: https://www.unaids.org/en/resources/fact-sheet
191. Hapgood JP, Kaushic C, Hel Z. Hormonal Contraception and HIV-1 Acquisition: Biological Mechanisms. Endocrine Reviews. 2018;39(1):36-78.
192. Ralph LJ, McCoy SI, Shiu K, Padian NS. Hormonal contraceptive use and women's risk of HIV acquisition: a meta-analysis of observational studies. The Lancet Infectious diseases. 2015;15(2):181-9.
193. Jackson B, Tilli CM, Hardman MJ, Avilion AA, MacLeod MC, Ashcroft GS, et al. Late cornified envelope family in differentiating epithelia--response to calcium and ultraviolet irradiation. J Invest Dermatol. 2005;124(5):1062-70.
194. Bamberger CM, Else T, Bamberger AM, Beil FU, Schulte HM. Dissociative glucocorticoid activity of medroxyprogesterone acetate in normal human lymphocytes. J Clin Endocrinol Metab. 1999;84(11):4055-61.
195. Govender Y, Avenant C, Verhoog NJ, Ray RM, Grantham NJ, Africander D, et al. The injectable-only contraceptive medroxyprogesterone acetate, unlike norethisterone acetate and progesterone, regulates inflammatory genes in endocervical cells via the glucocorticoid receptor. PLoS One. 2014;9(5):e96497.
196. Anderson DJ, Marathe J, Pudney J. The structure of the human vaginal stratum corneum and its role in immune defense. American journal of reproductive immunology (New York, NY : 1989). 2014;71(6):618-23.
197. Cone RA. Vaginal microbiota and sexually transmitted infections that may influence transmission of cell-associated HIV. The Journal of infectious diseases. 2014;210 Suppl 3(Suppl 3):S616-S21.
198. Jackson B, Tilli CMLJ, Hardman MJ, Avilion AA, MacLeod MC, Ashcroft GS, et al. Late Cornified Envelope Family in Differentiating Epithelia—Response to Calcium and Ultraviolet Irradiation. Journal of Investigative Dermatology. 2005;124(5):1062-70.
199. Shen H, Maki CG. Pharmacologic activation of p53 by small-molecule MDM2 antagonists. Curr Pharm Des. 2011;17(6):560-8.
200. Sanz G, Singh M, Peuget S, Selivanova G. Inhibition of p53 inhibitors: progress, challenges and perspectives. Journal of Molecular Cell Biology. 2019;11(7):586-99.
201. Lloyd V, Morse M, Purakal B, Parker J, Benard P, Crone M, et al. Hormone-Like Effects of Bisphenol A on p53 and Estrogen Receptor Alpha in Breast Cancer Cells. BioResearch Open Access. 2019;8(1):169-84.

202. Muñoz-Fontela C, Angel Garcia M, Garcia-Cao I, Collado M, Arroyo J, Esteban M, et al. Resistance to viral infection of super p53 mice. Oncogene. 2005;24(18):3059-62.
203. Kamentseva R, Kosheverova V, Kharchenko M, Zlobina M, Salova A, Belyaeva T, et al. Functional cycle of EEA1-positive early endosome: Direct evidence for pre-existing compartment of degradative pathway. PloS one. 2020;15(5):e0232532-e.
204. Thorn P, Gaisano H. Molecular control of compound Exocytosis. Communicative & Integrative Biology. 2012;5(1):61-3.
205. Cornick S, Kumar M, Moreau F, Gaisano H, Chadee K. VAMP8-mediated MUC2 mucin exocytosis from colonic goblet cells maintains innate intestinal homeostasis. Nature Communications. 2019;10(1):4306.
206. Caine EA, Scheaffer SM, Arora N, Zaitsev K, Artyomov MN, Coyne CB, et al. Interferon lambda protects the female reproductive tract against Zika virus infection. Nature Communications. 2019;10(1):280.
207. Li Z, Lu X, Zhu Y, Cheng P, Liu S, Zhang Y, et al. Lambda-Interferons Inhibit Herpes Simplex Virus Type 2 Replication in Human Cervical Epithelial Cells by Activating the JAK/STAT Pathway. Japanese Journal of Infectious Diseases. 2017;70(4):416-22.
208. Haller O, Staeheli P, Kochs G. Interferon-induced Mx proteins in antiviral host defense. Biochimie. 2007;89(6-7):812-8.
209. Haller O, Frese M, Kochs G. Mx proteins: mediators of innate resistance to RNA viruses. Rev Sci Tech. 1998;17(1):220-30.
210. Blondeau C, Pelchen-Matthews A, Mlcochova P, Marsh M, Milne Richard SB, Towers Greg J. Tetherin Restricts Herpes Simplex Virus 1 and Is Antagonized by Glycoprotein M. Journal of Virology. 2013;87(24):13124-33.
211. Liu Y, Luo S, He S, Zhang M, Wang P, Li C, et al. Tetherin restricts HSV-2 release and is counteracted by multiple viral glycoproteins. Virology. 2015;475:96-109.
212. Liu Y, Li M, Zhang D, Zhang M, Hu Q. HSV-2 glycoprotein gD targets the CC domain of tetherin and promotes tetherin degradation via lysosomal pathway. Virology Journal. 2016;13(1):154.
213. Zenner HL, Mauricio R, Banting G, Crump CM. Herpes simplex virus 1 counteracts tetherin restriction via its virion host shutoff activity. Journal of virology. 2013;87(24):13115-23.
214. Tokarev A, Skasko M, Fitzpatrick K, Guatelli J. Antiviral activity of the interferon-induced cellular protein BST-2/tetherin. AIDS Res Hum Retroviruses. 2009;25(12):1197-210.
215. Arias JF, Iwabu Y, Tokunaga K. Structural Basis for the Antiviral Activity of BST-2/Tetherin and Its Viral Antagonism. Front Microbiol. 2011;2:250.
216. Zhang J, Liang C. BST-2 diminishes HIV-1 infectivity. J Virol. 2010;84(23):12336-43.
217. Neil SJ, Zang T, Bieniasz PD. Tetherin inhibits retrovirus release and is antagonized by HIV-1 Vpu. Nature. 2008;451(7177):425-30.
218. Van Damme N, Goff D, Katsura C, Jorgenson RL, Mitchell R, Johnson MC, et al. The interferon-induced protein BST-2 restricts HIV-1 release and is downregulated from the cell surface by the viral Vpu protein. Cell Host Microbe. 2008;3(4):245-52.
219. Jouvenet N, Neil SJ, Zhadina M, Zang T, Kratovac Z, Lee Y, et al. Broad-spectrum inhibition of retroviral and filoviral particle release by tetherin. J Virol. 2009;83(4):1837-44.
220. Kaletsky RL, Francica JR, Agrawal-Gamse C, Bates P. Tetherin-mediated restriction of filovirus budding is antagonized by the Ebola glycoprotein. Proceedings of the National Academy of Sciences. 2009;106(8):2886.
221. Le Tortorec A, Willey S, Neil SJD. Antiviral Inhibition of Enveloped Virus Release by Tetherin/BST-2: Action and Counteraction. Viruses. 2011;3(5).

222. Mansouri M, Viswanathan K, Douglas JL, Hines J, Gustin J, Moses AV, et al. Molecular mechanism of BST2/tetherin downregulation by K5/MIR2 of Kaposi's sarcoma-associated herpesvirus. J Virol. 2009;83(19):9672-81.
223. Pan XB, Han JC, Cong X, Wei L. BST2/tetherin inhibits dengue virus release from human hepatoma cells. PLoS One. 2012;7(12):e51033.
224. Sakuma T, Noda T, Urata S, Kawaoka Y, Yasuda J. Inhibition of Lassa and Marburg virus production by tetherin. J Virol. 2009;83(5):2382-5.
225. Beyond Tethering the Viral Particles: Immunomodulatory Functions of Tetherin (BST-2). DNA and Cell Biology. 2019;38(11):1170-7.
226. Ferreira VH, Nazli A, Dizzell SE, Mueller K, Kaushic C. The anti-inflammatory activity of curcumin protects the genital mucosal epithelial barrier from disruption and blocks replication of HIV-1 and HSV-2. PloS one. 2015;10(4):e0124903-e.
227. Masson L, Passmore JA, Liebenberg LJ, Werner L, Baxter C, Arnold KB, et al. Genital inflammation and the risk of HIV acquisition in women. Clin Infect Dis. 2015;61(2):260-9.
228. Nazli A, Chan O, Dobson-Belaire WN, Ouellet M, Tremblay MJ, Gray-Owen SD, et al. Exposure to HIV-1 directly impairs mucosal epithelial barrier integrity allowing microbial translocation. PLoS Pathog. 2010;6(4):e1000852.
229. Nazli A, Kafka JK, Ferreira VH, Anipindi V, Mueller K, Osborne BJ, et al. HIV-1 gp120 induces TLR2- and TLR4-mediated innate immune activation in human female genital epithelium. J Immunol. 2013;191(8):4246-58.
230. Oh K-J, Lee H-S, Ahn K, Park K. Estrogen Modulates Expression of Tight Junction Proteins in Rat Vagina. BioMed Research International. 2016;2016:4394702.
231. Rothenberger NJ, Somasundaram A, Stabile LP. The Role of the Estrogen Pathway in the Tumor Microenvironment. Int J Mol Sci. 2018;19(2):611.
232. Kim JJ, Kurita T, Bulun SE. Progesterone action in endometrial cancer, endometriosis, uterine fibroids, and breast cancer. Endocrine reviews. 2013;34(1):130-62.
233. Rodriguez GC, Rimel BJ, Watkin W, Turbov JM, Barry C, Du H, et al. Progestin treatment induces apoptosis and modulates transforming growth factor-beta in the uterine endometrium. Cancer Epidemiol Biomarkers Prev. 2008;17(3):578-84.
234. Socías ME, Duff P, Shoveller J, Montaner JSG, Nguyen P, Ogilvie G, et al. Use of injectable hormonal contraception and HSV-2 acquisition in a cohort of female sex workers in Vancouver, Canada. Sex Transm Infect. 2017;93(4):284-9.
235. Grabowski MK, Gray RH, Makumbi F, Kagaayi J, Redd AD, Kigozi G, et al. Use of injectable hormonal contraception and women's risk of herpes simplex virus type 2 acquisition: a prospective study of couples in Rakai, Uganda. Lancet Glob Health. 2015;3(8):e478-e86.
236. Ferreira VH, Dizzell S, Nazli A, Kafka JK, Mueller K, Nguyen PV, et al. Medroxyprogesterone Acetate Regulates HIV-1 Uptake and Transcytosis but Not Replication in Primary Genital Epithelial Cells, Resulting in Enhanced T-Cell Infection. J Infect Dis. 2015;211(11):1745-56.
237. Bolstad BM, Irizarry RA, Astrand M, Speed TP. A comparison of normalization methods for high density oligonucleotide array data based on variance and bias. Bioinformatics. 2003;19(2):185-93.
238. Ritchie ME, Phipson B, Wu D, Hu Y, Law CW, Shi W, et al. limma powers differential expression analyses for RNA-sequencing and microarray studies. Nucleic Acids Res. 2015;43(7):e47.
239. Subramanian A, Tamayo P, Mootha VK, Mukherjee S, Ebert BL, Gillette MA, et al. Gene set enrichment analysis: a knowledge-based approach for interpreting genome-wide expression profiles. Proc Natl Acad Sci U S A. 2005;102(43):15545-50.